SUDAAR 486

STANFORD UNIVERSITY

CENTER FOR SYSTEMS RESEARCH

Selection of Sampling Rate for Digital Control of Aircrafts

by

Paul Katz

J. David Powell

Guidance and Control Laboratory

September 1974

Department of Aeronautics and Astronautics
STANFORD UNIVERSITY
Stanford, California 94305

PRICES SUBJECT TO CHANGE

This research was supported by

The Government of Israel

and partially supported by
NASA–Edwards Flight Research Center
NASA Grant NSG 4002

SUDAAR 486

SELECTION OF SAMPLING RATE FOR DIGITAL CONTROL OF AIRCRAFTS

by

Paul Katz

J. David Powell

Guidance and Control Laboratory
Department of Aeronautics and Astronautics
STANFORD UNIVERSITY
Stanford, California 94305

This research was supported by

The Government of Israel

and partially supported by
NASA—Edwards Flight Research Center,
NASA Grant NSG 4002

September 1974

ABSTRACT

The considerations in selecting the sampling rate for a digital control of aircrafts are identified and evaluated. The design method used in this analysis is the optimal discrete synthesis. Due to discretization of the continuous plant this method of design does not introduce an artificial limitation on the sampling rate. The principal example used is the short period mode of a hypothetical high performance aircraft. The assumed model includes a bending mode and wind gusts.

Four major factors which influence the selection of the sampling rate are identified: (a) the time response to control inputs; (b) the response to an external disturbance; (c) the sensitivity to variation of parameters; (d) the roughness of the response to control inputs. Each of these factors and its relation to the sampling rate was investigated. It was found that the limiting factors in the selection of the sampling rate for the example are the time response to a control input, and the response to an external disturbance. The sensitivity to variation of parameters is larger for lower sampling rates. However, the sensitivity can be reduced by modifying the design of the optimal linear compensator. Different roughness functions which measure the roughness to control inputs are suggested and demonstrated on the example.

The optimal discrete synthesis computer program, which is based on eigenvector decomposition of the state-costate Hamiltonian matrix, is a highly efficient program. This program calculates the optimal discrete regulator, the steady state Kalman filter, and the mean response to external disturbances.

ACKNOWLEDGMENTS

I wish to extend my gratitude to my advisor, Professor J. David Powell for his advice and guidance throughout the course of this research, and for his many helpful suggestions. I also wish to thank Professors Arthur Bryson and Dan DeBra for their thorough review and in particular, their constructive criticisms as readers.

My appreciation is extended to Ms. Ida M. Lee for her conscientious typing and editing, and also to Dovie R. Wylie for her editing assistance.

Particular gratitude is expressed to the Government of Israel who provided my financial support. Acknowledgment is extended the NASA Edwards Flight Research Center, NASA Grant NSG 4002.

Last but not least, special thanks go to my wife, Shelly, who gave me much support and encouragement during the period of this research.

This Dissertation is dedicated to the memory of my father, Zeew Wilhelm Katz.

TABLE OF CONTENTS

TABLE OF CONTENTS (Cont)

TABLE OF CONTENTS (Cont)

TABLE OF CONTENTS (Cont)

LIST OF FIGURES

LIST OF FIGURES (Cont)

LIST OF FIGURES (Cont)

LIST OF FIGURES (Cont)

LIST OF TABLES

LIST OF SYMBOLS

In the following list of symbols, the matrices will be represented by capital letters, and the vectors by small letters.

A	weighting matrix (states)
$\mathcal{A}$	$A_{11} - A_{12} A_{22}^{-1} A_{21}$ (Eq. 3.32)
B	weighting matrix (control)
$\mathcal{B}$	$B = A_{22}$ (Eq. 3.32)
C	control gain matrix
$C_w(\tau')$	correlation function
D	D(z) or D(w), discrete compensation (Fig. II-1)
E	def: $E \triangleq z^{-1}$, Ch. III
E	linear operator (average), Ch. VII
F	system matrix
F_e	force on the elevator
F_n	force on the nose
G	input distribution matrix
G_1	input distribution matrix (control)
G_2	input distribution matrix (noise)
H	measurement matrix
$\mathcal{H}$	defined in Eq. 3.89
$\mathcal{H}$	Hamiltonian
$\mathcal{K}$	defined in Eq. 3.80
h_r, h_a	rate gyro and accelerometer pickup

I	unity matrix
J	cost function
K	Kalman gains
K_q, K_n	pitch rate and acceleration gains
k	general parameter slope of first order hold, Ch. III and Ch. VII
ℓ_a	distance (elevator--center of mass)
ℓ_j	$j = 1, \ldots, n$; eigenvectors of Φ
M	moment
M	error covariance matrix (after measurment)
M_q, M_w M_{δ_e}, $M_{\dot{w}}$	aerodynamic moment coefficients
m	number of zeros
N	number of intervals (T)
n	number of states; acceleration
n_a	accelerometer's measurements
n_z	acceleration (z-direction)
P	error covariance matrix (before measurement)
$P_n(z)$	n-order characteristic polynomial
Q	power spectral density matrix
Q_d	discrete covariance matrix
q	pitch rate
q	$q \triangleq \sigma^2$

R	Ch VII	defined in Eq. 7.14
R		power spectral density matrix of the measurement noise
r_q, r_n		power spectral density of the measurement noise (rate gyro and accelerometer)
S		solution of the matrix Riccati equation
s		Laplace transform
T	Ch III	matrix of the eigenvectors
T		sampling interval
T_r		transformation
$T_r(\ )$		trace of matrix
t		time
U		control covariance matrix
$\mathfrak{U}$	Ch III	defined in Eq. 3.32
u		input
u_o		velocity
v		measurement (white noise)
v_q, v_n		measurement white noise of the rate gyro and the accelerometer
W		weighting matrix for roughness function
w	II, III	w-transform
w		vertical wind (white noise)
w		external disturbance (white noise)
w_d		discrete disturbance
w_g		vertical wind gusts (correlated)

LIST OF SYMBOLS (Cont)

X	covariance matrix of the states
X_E Ch III	defined in Eq. 3.59 and 3.88
x	state variable vector
x_3, x_4	bending mode states
y	measurements and/or output of a system
Z_w	aerodynamic lift coefficient
z	z-transform
$\bar{z}$	bending mode deflection
z'	bending mode slope
$\mathfrak{Z}$	transformation to z-plane

Greek Symbols

α	angle of attack
Γ	discrete input distribution matrix
Γ_1	discrete input distribution matrix (control)
Γ_2	discrete input distribution matrix (noise)
γ	$\gamma \triangleq zx$, (see Eq. 3.57)
Δt	subdivision of T
δ_ℓ	elevator angle
δ_{s_o}	pilot stick input (Fig. IV-11)
δ_{s_1}	see Fig. IV-11
ϵ	interval of time
ζ	damping ratio
ζ^*	equivalent damping

η	white noise
η_o	unstable mode
θ	angle (Fig. VII-14)
$\Lambda_{E,z}$	defined in Eq. (3.59) and (3.88)
λ	Lagrange undetermined multiplier
ξ_o	stable mode as defined in Eq. 3.64
$\bar{\xi}_o$	defined in Eq. 3.70
σ	standard deviation
τ	time, time constant, correlation time
Φ	transition matrix
ω	angular frequency

Superscripts

k	corresponds to one of the n states
T	transposition of matrix
$\sim$	estimation error
$-$	mean value
$\hat{}$	best estimate

Subscripts

a	corresponds to enlarged system (Section VI-F)
b	corresponding to bending modes
c	corresponding to closed loop
d	discrete
E	unstable eigenvalues (z-plane)

i	sampling instant
p	corresponding to plant
ss	steady state
T	total
w	relative to wind
z	relative to stable eigenvalues (z-plane)

Abbreviations

A/D	analog to digital
cps	cycles per second
E-L	Euler-Lagrange
F-H	hypothetical aircraft
FOH	first order hold
LPF	low pass filter
N(O,Q)	normal distribution with a zero mean and a power spectral density matrix Q
RF	roughness function
rms	root mean square
RSL	root square locus
SAS	stability augmentation system
SP	short period
SPS	samples per second
TRP	time response parameter
ZOH	zero order hold

I. INTRODUCTION

A. PROBLEM STATEMENT

During the last ten years, the aerospace industry has shown a tendency to replace the analog components of closed loop systems with digital computers. The advantages of using a digital computer instead of a specially built analog system are numerous. Among them are greater accuracy, the ability to change parameters during the control operation, and flexibility of the control logic. On the other hand, the principal disadvantage of a digital computer in a closed loop control system is its discrete mode of operation. The computer processes numbers generated in real time by sampling continuous signals. The computer outputs, which are sequences of numbers, have to be reconstructed into analog signals (commands to actuators). Therefore, in the process of designing a digital autopilot, careful selection of the rate of sampling and the processing of commands are important.

Selecting an appropriate sampling rate for an aircraft digital controller necessitates a compromise. Cost and accuracy are factors which argue for lowering the rate, ω_s. A low ω_s directly reduces the cost of A/D and D/A equipment. Using less central processing unit percentage time can either free the system for other functions, or result in reduced central processor costs. The increased accuracy obtained by slower sampling is well documented [BO-1] and can be translated into additional cost savings by reducing the word size. Economically speaking, the best engineering choice is the slowest possible sampling rate meeting all performance specifications.

Factors which may constitute an incentive to increase the sampling rate are, e.g., (1) closed-loop bandwidth, or time response requirements; (2) sensitivity to parameter variations; (3) effect of random disturbances; and (4) roughness of control.

Our objective will be to identify and analyze the important factors which influence the selection of a sampling rate for a closed-loop aircraft discrete control system. After discussing the factors and their properties, we will propose methods which will help the designer choose a sampling rate which will not violate given criteria of performance or given properties of the system.

As an example, we chose a hypothetical, Mach 3 aircraft [BO-1, SU-1], flying in a highly turbulent atmosphere. This choice, which we shall term F-H, was made because the requirements of a high-performance military aircraft impose a limit on the minimal sampling rate.

B. PREVIOUS RELATED RESULTS

Aircraft digital control systems have now been implemented [DE-1, MA-1], and many more have been studied [BE-1, BO-1, DS-1, LE-1, SU-1]. The pertinent literature discusses various methods for selecting the sampling rate.

Sampling rate selection is sometimes based on a specific multiple of the highest important bending mode. An appropriate value for this multiple was reported by Lee [LE-1] to be four. Others [JO-1, SI-1, ST-1] have also selected sampling rate to be about four times the highest important bending mode; however, it is perhaps more typical to select sample rates at approximately six to ten times the highest bending mode [see, for example, Refs. BO-1, DE-1, ED-1, OS-1, SU-1]. Recently, Berman [BE-1] introduced the concept that the proper sampling rate is independent of the bending modes and should be based solely on disturbance effects. This was applied to a V/STOL example and yielded a sampling rate which was slower than the highest bending mode. According to some discussions [LE-1], such a slow sampling rate violates the sampling theorem [RA-1], which is said to state that the sampling rate must be at least twice the highest bending mode frequency. Our interpretation of the sampling theorem will be discussed in Chapter IV.

A completely different approach to selection of sampling rates

was taken by Mrazek [MR-1]. His selection process was dominated by the time constants of the measuring instruments' analog prefilters. This consideration resulted in sampling rates of 100 to 200 cps. However, flying experience with digital autopilots [MA-1] shows that such high sampling rates as suggested by Mrazek are unnecessary.

The design technique used in the analysis often influences the sampling rate selection and, in some cases, causes the sampling rate to be significantly faster than required. Although many variations exist, we prefer to divide the design methods into two broad categories: (1) those whose design is done in the continuous domain (or s-plane), and (2) those whose design is done in the discrete domain (z or w-plane). Designs of the first category are attractive since they utilize the experience gained over many years of continuous autopilot designing. The authors using this method [BO-1, ED-1, OS-1, SU-1] choose one or a combination of discrete approximation techniques (reviewed recently by Edwards [ED-2] and Slater [SL-1]) to transform the resulting continuous compensation into a discrete compensation. The effect of the approximation in the design is typically checked by a precise simulation.

Designs of the second category include the w-plane techniques [LE-1, ST-1], z-plane Nyquist techniques [SI-1], and the discrete state space techniques of Berman [BE-1], Johnson [JO-1], and the author of this work.

The approximations inherent in category 1 (s-plane) methods introduce an additional constraint which may be important in sampling rate selection. It is interesting to note that all authors reporting the use of a category 1 design method selected a sample rate which was a higher multiple of the bending modes of interest than those authors using a category 2 method.

An attempt was made to relate the sampling rate to overall performance for the case of optimally controlled systems. Lewis and Athans [LEW-1], and Astrom [AS-1] developed a method which investigated the change in the quadratic index of the continuous plant for different sampling intervals. Their results, which are essentially experimental

(on computer), show that for larger sampling intervals, the general tendency of the quadratic index is to increase.

C. NEW RESULTS

Four major factors which influence the selection of the sampling rate for the discrete control of a continuous system were identified and analyzed. These factors are:

1. the time response,
2. the response to an external noise,
3. the sensitivity to variations of parameters,
4. the roughness of control.

By using an optimal discrete design, we eliminated the time lags introduced into the control loop by the discretization of a continuous design. Hence, the sampling rate is no longer limited by discretization approximations and we can concentrate on the analysis of the four factors listed above.

1. The time response to a step input is directly related to the length of the sampling interval. For a given criterion in the time domain, the time response deteriorates for longer sampling intervals. From simulation of the F-H short period mode, we found that the discretized low pass filter and the discretization of the pilot's analog input introduce a considerable delay. This delay is as long as two sampling intervals and limits the choice of the sampling rate. For the F-H short period example, the lower limit of the sampling rate, imposed by the time response, was found to be in the vicinity of 10 cps.
2. The response to external disturbances is a function of closed loop dynamics, the disturbance correlation time, and the sampling interval. It was found that for any available (discrete) control, there is a well-defined limit to noise alleviation. This limit is a function of the sampling rate. For higher

sampling rates, the noise alleviation by the closed loop system is greater.

By analyzing the external disturbance as a Gauss-Markov process, and by using an optimal discrete control, greater noise alleviation for the same sampling rates can be achieved.

3. Sensitivity to variation of parameters was reduced by proper modeling of the discrete compensator. The optimal discrete compensator assumes a perfect knowledge of the system and the noise. However, if some of the system's parameters vary from their nominal value, the filtering and controling action of the optimal compensator is distorted. This distortion was shown to be worse at lower sampling rates.

   In the F-H short period example, a 10 percent uncertainty in the bending frequency causes instability of the closed loop system. By remodeling the discrete observer, essentially by increasing the damping of the observer's error poles corresponding to the bending mode, the closed loop system was stabilized. The same could be done for larger sampling intervals.

   Further restriction in sensitivity to variations of the bending frequency can be achieved by a damping augmentation of the bending mode.

4. Roughness of control is caused by the quantization of the input signal by the zero order reconstruction hold. Intuitively, it is obvious that for very high sampling rates, this roughness is negligible. But for lower sampling rates, the phenomenon cannot be ignored. This is more than a theoretical speculation. It was also reported by Mathew [MA-1], who detected an undesirable jittery action on the digitally-controlled Saab actuators.

   To put the concept on an analytical basis, different roughness functions (RF) were defined. Basically, the RF is defined as a sum (for an impulse response), or as a mean value (for rms response)

of the squares of the control discontinuities. Algorithms for calculating the RF are given and the RF concept is demonstrated for the F-H short period mode configuration. An interesting result came out: if the quadratic cost function is kept constant, the roughness of control may decrease for larger sampling intervals. This phenomenon is fully explained in Chapter VII.

D. THESIS OUTLINE

In Chapter II, various discrete control techniques will be surveyed.

In Chapter III, the fundamentals of a continuous system's discretization and of the optimal discrete theory will be outlined. The author's approach to an optimal discrete synthesis, by eigenvector decomposition, will be given. Various numerical algorithms, useful in discrete analysis, will be described.

In Chapter IV, the limit on the sampling rate, imposed by a time response, will be investigated. An example, which illustrates the basic concepts and is used in other chapters, will be described.

In Chapter V, we will investigate the relation between the sampling rate and the response to an external disturbance. A theoretical proof of the limit of noise reduction as a function of the sampling rate will be given.

In Chapter VI, the sensitivity to variations of parameters will be described. We will investigate the behavior of a closed loop system which includes unwanted frequencies, in our case, the bending mode. We will show how sensitive the system is to an imperfect knowledge of unwanted frequencies and what can be done to reduce this sensitivity.

An interesting relation between sensitivity and the stability of the compensator will conclude this chapter.

In Chapter VII, a new criterion (the roughness function), will be explained and methods for calculating the function will be given. This new concept will be demonstrated in the design of the control loop of the F-H short period mode example.

In Appendix A, an instruction manual and a program DISC are given. This program, for the synthesis of an optimal regulator and an optimal steady state observer for discrete linear systems, has various options. The discretization procedure and the calculation of the response to an external disturbance are included. An illustrative example is given at the end of Appendix A.

In Appendix B, the simulation algorithm of the principal example's behavior will be explained. This simulation, based on a specially built computer program, simulates the behavior of a discretely controlled continuous system. An imperfect knowledge of various parameters of the simulated system is included as an option in the program. Most of our results regarding the time response of our principal example are deduced from this simulation.

E. SUMMARY OF CONTRIBUTIONS

1. The first investigation of sampling rates, considering all effects and identifying what is important.

2. The factors which influence the selection of the sampling rate were evaluated for an F-H example. It was shown that a proper time response and gust alleviation were the two major factors determining the sampling rate.

3. Demonstration of a technique that eliminates bending modes and uncertainty of their exact frequencies as an important constraint on many aircraft autopilot designs. All cases are easier than that of an F-H flying at Mach 1.2 and at zero altitude.

4. A relation between the stability of the compensator and the sensitivity was described.

5. It was found that there is a definite limit on the alleviation of an external noise by a discrete controller. This limit is a function of the sampling rate.

6. A new criterion, the roughness function, was defined. Methods for calculating the function by using existing algorithms are given and

demonstrated for the F-H example.

7. A new algorithm is given for calculating the Liapunov equation using eigenvector decomposition.

8. A computer program was developed for the synthesis of an optimal discrete regulator and an optimal discrete steady state observer based on eigenvector decomposition.

II. SURVEY OF TECHNIQUES FOR DESIGNING DISCRETE CONTROLLERS FOR CONTINUOUS SYSTEMS

The method of design, divided in the previous chapter into two major categories, can be further divided into the following categories:

A. A classical continuous design and a discretization,

B. A continuous design and an optimal discretization,

C. A classical discrete design,

D. Discretization and optimal discrete design.

A. CLASSICAL CONTINUOUS DESIGN AND DISCRETIZATION

Design on the s-plane and discretization of the compensation network is a widely used method. Borow et al [BO-1], Edwards [ED-1], Osder [OS-1], and Sutton et al [SU-1] use this method of design. Their fundamental approach is to duplicate the analog filters by digital filters.

Edwards [ED-2] and Slater [SL-1] investigated various methods which are used to design digital filters having properties similar to the corresponding analog filters. The transformations used in converting the filters from the s-plane to the z-plane are: the standard z-transform, the bilinear transformation, z-forms, and the matched z-transform. These transformations yield digital filters of the same order as the original analog filter. Edward's conclusion is that the z-matched transform has proved to be a good technique for generating all the standard filter forms. McGough [McG-1] analyzed this design method and suggested using the frequency response characteristics of a zero order reconstruction hold to filter out the unwanted bending frequencies, which usually consist of the highest frequency component. We will show in Chapter VI that in practice, sampling at the bending frequency may cause instability.

B. CONTINUOUS DESIGN AND AN OPTIMAL DISCRETIZATION

Designing a discrete controller in the continuous domain is attractive to any designer because the required characteristics and the closed loop properties are usually given in the time domain (or s-plane). Most designers have a better understanding of the physical quantities expressed in the s-plane. Hence, several attempts were made to transform the continuous design to a discrete domain in some optimal way.

Melzer and Kuo [ME-1] use Taylor's approximation for the solution of an optimal regulator as a function of the sampling interval. Once a sampling interval is chosen and an optimal continuous design is done, the feedback matrix is obtained by Taylor's series approximation. As the authors claim, this method can be verified only by numerical experiments. The method was later improved by Kuo and Peterson [KU-1]. Using Taylor's expansions of the feedback matrix and the solution of the Riccati equation, they modified the feedback gains so that the response of the sampled-data model was as close to that of the original continuous system as possible.

Yet the most promising approach of this kind is given by Yackel, Kuo, and Singh [YA-1]. Their method, based on Kuo's previous results, is a complete digital redesign of continuous systems by matching states in multiple sampling periods. Their method is essentially based on the controllability theorem, which states that an n-order discrete system can be brought to an arbitrary state in no more than n-steps. The desired state is the solution of the continuous system during the interval $n \times T$. (T is the sampling interval.) The main disadvantage of their method lies in the fact that the gains have to be changed for every sampling period. This adds to the complexity of the numerical calculation in the real time computer.

C. CLASSICAL DISCRETE DESIGN

This is an exact method based on z-transformation of the continuous plant F(s). The plant F(s) is transformed to a discrete plant F(z)

(via a zero order hold) on the z-plane, see Fig. II-1. F(z) includes the zero order hold (ZOH).

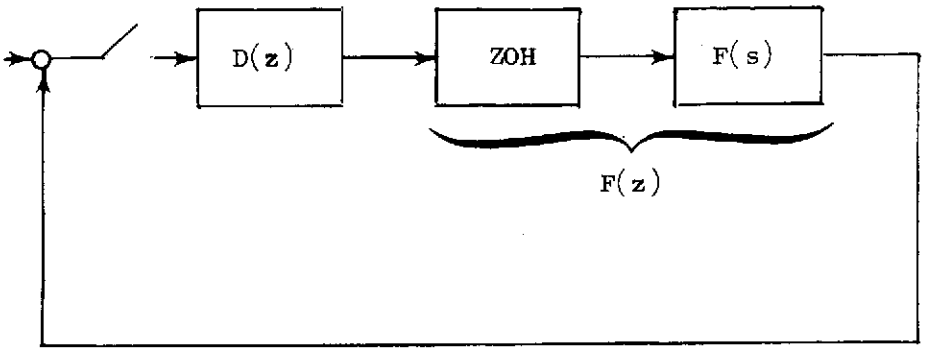

FIG. II-1 DESCRIPTION OF THE DISCRETE PLANT

Methods of design on the z-plane are well documented [e.g., CA-1, CA-2, RA-1]. However, designers who are accustomed to s-plane formulations prefer to transform the F(z) plant to the w-plane. The F(z) plant is transformed to a w-plane by the bilinear transformation $z = (1+w)/(1-w)$.

F(w) has many properties similar to the continuous plant, F(s) [e.g., RA-1]. Therefore, a compensator design can be done by classical methods (Bode plot, root locus).

After determining a proper compensation D(w), D(w) is transformed back to the z-plane, $w = (z-1)/(z+1)$. D(z) immediately gives the recursive compensating equations.

Analytical expressions for $\mathcal{Z}[F(s)]$ are only known for very simple transfer functions. However, computer algorithms which transform F(s) to F(z) are available. The main disadvantage of this method is its inability to design properly multi-input, multi-output systems.

D. DISCRETIZATION AND OPTIMAL DISCRETE DESIGN

The optimal discrete design is based on fundamental work done by Kalman [KA-1]. He pointed out the equivalence between the optimal linear discrete regulator and the optimal linear discrete observer,

and proposed algorithms for computing them. This is an exact method since no discretization approximations are made. Franklin [GU-1] has shown that the optimal discrete compensator can be designed by first designing the optimal controller and then the optimal observer. We can separate this approach into a set of two distinct problems: the transformation of a continuous system into an equivalent discrete system, and the numerical solution of the matrix Riccati difference equation.

The discretization of the continuous system is done by a numerical calculation of the state transition matrix and its integral. This subject, seemingly elementary, has not been exhausted. New efficient algorithms are discovered and rediscovered all the time. For example, Hansen [HA-1] rediscovered the algorithm devised nearly 25 years ago by Frame [FRA-1] and Fadeev.

Numerical methods for calculation of the discrete regulator and the steady state filter are extensively documented [e.g., BR-1, and KW-1]. Those methods are based on recursive computation of the matrix Riccati difference equation until a steady state solution is reached. Following Potter [PO-1], who solved the matrix Riccati differential equation by a nonrecursive method, Vaughan [VA-1] found a nonrecursive solution for the matrix Riccati difference equation. His method involves the calculation of the eigenvalues and eigenvectors of the canonical state-costate equations. Using the QR transformation--a highly efficient algorithm for calculating eigenvectors [FR-1], Bryson and Hall [BR-2] constructed a computer program for steady-state optimal control and filter synthesis of a continuous system. Independently of Vaughan's results, the author of this work constructed a method and a computer program for a steady state optimal discrete control and filter synthesis by eigenvector decomposition.

The Vaughan solution is further explored by Howerton [HO-1], who shows that further simplification of the discrete algebraic Riccati equation can be achieved by transforming the system to a Luenberger canonical form.

III. OPTIMAL DISCRETE SYNTHESIS

There are different methods of designing a discrete compensator for a continuous system. These methods can be divided into two basic categories as explained in Chapter I. They are: (1) those in which the design is done in the continuous domain/s-plane; (2) those in which the design is done in the discrete domain/z or w-plane.

The methods of the second category result in no artificial sampling rate constraints due to discretization procedure. Therefore, these methods are more suitable for our major objective in this work; i.e., to investigate the various factors which influence the sampling rate selection. The author of this work preferred the discrete state approach (instead of the w-plane approach) for the following reasons: (a) the state space approach easily handles multi-input multi-output systems; (b) the w-plane design method, essentially a classical method of design, does not have convenient computational means for the minimization of disturbance influences.

It will be shown in further chapters that the optimal discrete approach, which is used in this work, is a valuable design tool.

In this chapter we will describe the procedure for synthesis of an optimal linear regulator based on minimization of a quadratic cost function for a linear, time-invariant discrete system. The procedure for synthesis of a discrete optimal filter will be described by using the Kalman analogy between an optimal regulator and an optimal steady state filter.

The calculation of the regulator and the filter is based on eigenvector decomposition of the related state-costate Hamiltonian matrix.

A discretization procedure will be described for the case in which the controlled system is continuous and the control input, generated by a digital computer, is reconstructed by a reconstruction hold.

Various useful numerical algorithms will be given.

A. DISCRETIZATION PROCEDURE

A-1 Reconstruction Holds

Most of the practical cases of designing a discrete controller are those in which the controlled system is an analog plant. A special hardware element, called the "reconstruction hold", is inserted between the computer and the controlled plant. The purpose of the reconstruction hold is to convert a sequence of numbers, usually equally spaced in time, to a continuous signal. See Fig. III-1.

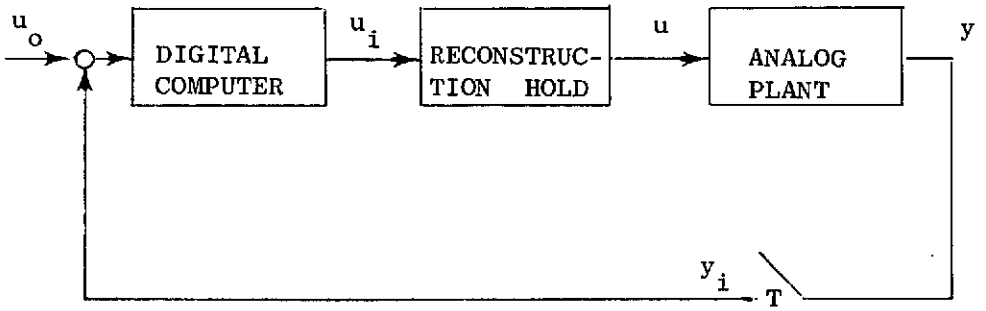

FIG. III-1 DISCRETE CONTROL OF AN ANALOG PLANT. u = control signal, u_i = sequence of numbers, T = sampling interval.

For real time in closed loop control systems, the reconstruction hold generates signal $u(t)$ (for $t \geq nT$), based on u_i for $i \leq n$. Basically, the reconstruction scheme is an extrapolation. The zero order hold (ZOH), generates a constant signal $u(t) = u_i$ for $iT \leq t < (i+1)T$. This reconstruction hold is widely used. Higher order holds are used primarily as examples in literature. The first order hold (FOH) is based on the last two control vectors--u_i, and u_{i-1}, and generates a signal varying linearly with time:

$$u(t) = u_i + \frac{u_i - u_{i-1}}{T}\tau$$

$$iT \leq t < (i+1)T \qquad 0 \leq \tau \leq T \,. \tag{3.1}$$

This formulation of the first order reconstruction hold originates in sample data theory. The sample data approach usually considers a single input control channel and sequentially processed scalar quantities. If a state space approach and a digital computer are used, the FOH can be reformulated. The new FOH can be defined as

$$u(t) \triangleq u_i + k_i\tau$$

$$iT \leq t \leq (i+1)T \qquad 0 \leq \tau \leq T \tag{3.2}$$

where u_i and k_i are quantities calculated simultaneously in the digital computer. Recall that the FOH is a hardware device, which generates the step u_i and the linear rate k_i of the continuous control signal $u(t)$, during the interval T. The vector k_i (a scalar for a single input system), can be calculated with respect to some specific criteria and does not necessarily have to be equal to $(u_i - u_{i-1})/T$.

A-2 Formulation and Algorithms For Discretization Procedure

a. The transition matrix and its first integral.

The discrete formulation of a linear continuous, differential system is essentially the solution in the time domain from sample point to sample point. The solution of

$$\dot{x} = Fx + G_1 u \tag{3.3}$$

is given by [KW-1]

$$x_{i+1} = \Phi(T)x_i + \int_{iT}^{(i+1)T} \Phi[(i+1)T - \tau]G_1 u(\tau)d\tau \,. \tag{3.4}$$

For a time invariant system, the matrices F and G_1 are constants; therefore, (3.4) may be rewritten as

$$x_{i+1} = \Phi(T)x_i + \int_o^T \Phi(\tau)G_1 u(\tau)d\tau \tag{3.5}$$

where the transition matrix $\Phi(\tau)$ is given as

$$\Phi(\tau) = e^{F\tau} = I + F\tau + \frac{F^2\tau^2}{2!} + \ldots . \tag{3.6}$$

If $u(\tau)$ is a constant during the interval T, then the second term on the right hand side of (3.5) is defined as $\Gamma_1(T)u_i$, where $\Gamma_1(T)$ is

$$\Gamma_1(T) \triangleq \int_o^T \Phi(\tau)G_1 d\tau . \tag{3.7}$$

b. Discretization of a continuous system driven by a white noise.

The disturbed system:

$$\dot{x} = Fx + G_2 w \qquad [w \to N(O, Q)]^{\dagger} \tag{3.8}$$

may be represented at sampling points [BR-1] by:

$$x_{i+1} = \Phi x_i + \Gamma_2 w_{d_i} \qquad w_{d_i} \to N(O, Q_d) \tag{3.9}$$

where

$$Q_d = \int_o^T \Phi(\tau)Q\Phi^T(\tau)d\tau^{\ddagger}$$

$$\Gamma_2 = \int_o^T \Phi(\tau)Gd\tau .$$

---

† We will use the following notation: $w \to N(O,Q)$, where w is a random disturbance, normally distributed, with a zero mean and a power spectral density matrix Q.

‡ The reader's attention is directed to the fact that the symbol T is used for the sampling interval and also for a transposition of matrices.

We are interested in the covariance matrix Q_d for a statistical analysis of system behavior, whereas Γ_w and w_d would only be needed for a complete stochastic simulation. Therefore, (3.9) will be replaced by

$$x_{i+1} = \Phi x_i + I w_{d_i} \qquad w_{d_i} \rightarrow N(0, Q_d)$$

$$I = \begin{bmatrix} 1 & & 0 \\ & \ddots & \\ 0 & & 1 \end{bmatrix} \tag{3.10}$$

$$Q_d = \int_0^T \Phi(\tau) G_2 Q G^T \Phi^T(\tau) d\tau \ .$$

c. Discretization of a continuous cost function.

A continuous quadratic cost function $J(x, u, t)$:

$$J = \int_0^t (x^T A x + u^T B u) d\tau \tag{3.11}$$

can be transformed to a discrete version

$$J = \sum_{i=0}^{N-1} [x_i^T \ u_i^T] \begin{bmatrix} A_{11} & A_{12} \\ A_{21} & A_{22} \end{bmatrix} \begin{bmatrix} x_i \\ u_i \end{bmatrix} \tag{3.12}$$

where $N = t/T$; by the following procedure, (3.11) can be rewritten as

$$J = \sum_{i=0}^{N-1} \int_{iT}^{(i+1)T} (x^T A x + u^T B u) d\tau \ . \tag{3.13}$$

The interval $0 - t$ was subdivided into N intervals T. The integrals inside the summation expression of (3.13) can be expressed as functions of x_i and u_i instead of x and u. Using (3.5)

$$x(\tau) = \Phi(\tau)x_i + \Gamma_1(\tau)u_i$$

$$iT \leq \tau < (i+1)T ,$$

therefore,

$$\int_{iT}^{(i+1)T} (x^T Ax + u^T Bu)dt = [x_i^T u_i^T] \begin{bmatrix} A_{11} & A_{12} \\ A_{21} & A_{22} \end{bmatrix} \begin{bmatrix} x_i \\ u_i \end{bmatrix} \qquad (3.14)$$

where

$$\begin{aligned} A_{11} &= \int_0^T \Phi^T(\tau)A\Phi(\tau)d\tau \\ A_{22} &= \int_0^T [\Gamma_1(\tau)A\Gamma_1(\tau) + B]d\tau \\ A_{12} &= \int_0^T \Phi^T(\tau)A\Gamma_1(\tau)d\tau \\ A_{12} &= A_{21}^T . \end{aligned} \qquad (3.15)$$

d. Numerical algorithms for calculating the matrices Φ, Γ_1, Q_d, A_{11}, A_{12}, A_{22}.

There are various methods for calculating the transition matrix $\Phi(\tau)$ and its first integral $\Gamma_1(\tau)$. Most of them are included in computer libraries. Efficient and simple algorithms for calculating the matrices Q_d, A_{11}, A_{21}, A_{22}, however, are not found. A highly complicated method for evaluating the expressions for A_{11}, A_{12}, and A_{22} is described in Reference AS-1. This method requires about 250 FORTRAN statements. We will describe a relatively simple method for solving (3.15) without a numerical integration, which involves about 80 FORTRAN statements. This solution is accomplished in two steps: first, we transform all the A's to a simpler form; second, we subdivide the sampling interval T into 2^k subintervals $\Delta T[\Delta T = (T)/(2^k)]$. Then

we show that if the various A's are known for ΔT [$A = A(\Delta T)$], then A(T) is obtained in k recursive computations. We will explain exactly how it is done and how k is chosen.

The A's are transformed first because the integrands in the integral expressions of these matrices are highly complicated; e.g, the complete expression for A_{21} is:

$$A_{21} = \int_0^T \left\{ \left[\int_0^T \Phi(\tau') G_1 d\tau' \right]^T \left[A \int_0^\tau (\tau') G d\tau' \right] + B \right\} d\tau . \qquad (3.16)$$

In order to simplify the calculation of A_{22} and A_{21}, we will reformulate the cost function of (3.11) by augmenting the state vector x with input u. The cost function J will be

$$J = \sum_{i=0}^{N-1} \int_0^T [x_i^T \; u_i^T] \, \Phi'^T(\tau) \begin{bmatrix} A & 0 \\ 0 & B \end{bmatrix} \Phi'(\tau) \begin{bmatrix} x_i \\ u_i \end{bmatrix} d\tau \qquad (3.17)$$

where $\Phi'(\tau)$ is defined as

$$\Phi'(\tau) = \begin{bmatrix} \Phi(\tau) & \Gamma_1(\tau) \\ 0 & I \end{bmatrix} = \exp \begin{bmatrix} F & G_1 \\ 0 & 0 \end{bmatrix} \tau \; . \qquad (3.18)$$

The expressions for A_{11}, A_{12}, and A_{22} are given by evaluating

$$\int_0^T \Phi'^T(\tau) \begin{bmatrix} A & 0 \\ 0 & B \end{bmatrix} \Phi'(\tau) d\tau = \begin{bmatrix} A_{11} & A_{12} \\ A_{21} & A_{22} \end{bmatrix} . \qquad (3.19)$$

By using this formulation we have transformed the problem to one of evaluating an integral of the type

$$Q_d = \int_o^T \Phi(\tau) Q \Phi(\tau)^T d\tau . \tag{3.20}$$

It is not necessary to calculate integral (3.20) by a numerical integration. As in Johnson [JOH-1], we will use the property of the transition matrix $\Phi(T)$.

$$\Phi(T + \tau) = \Phi(T)\Phi(\tau) = \Phi(\tau)\Phi(T) . \tag{3.21}$$

T will be subdivided into 2^k parts ΔT. If $Q_d(\Delta T)$ and $\Phi(\Delta T)$ are known, then $Q(2\Delta T)$ and $\Phi(2\Delta T)$ are given by

$$\Phi(2\Delta T) = \Phi(\Delta T)\Phi(\Delta T) \tag{3.22}$$

$$\begin{aligned} Q_d(2\Delta T) &= \int_o^{2\Delta T} \Phi(\tau) Q \Phi^T(\tau) d\tau \\ &= \int_o^{\Delta T} \Phi(\tau) Q \Phi(\tau)^T + \int_o^{\Delta T} \Phi(\Delta T + \tau) Q \Phi^T(\Delta T + \tau) d\tau \end{aligned} \tag{3.23}$$

$$Q_d(2\Delta T) = Q_d(\Delta T) + \Phi(\Delta T) Q_d(\Delta T) \Phi^T(\Delta T) . \tag{3.24}$$

Recall that $\Delta T = T/2^k$, $\Phi(T)$ and $Q_d(T)$ are obtained by k recursive computations of (3.22) and (3.24), which are relatively simple expressions.

In order to calculate initial values of $\Phi(\Delta T)$ and $Q_d(\Delta T)$, a constant is selected (say, k = 3) and the following approximations are evaluated:

$$\begin{aligned} Q_d(\Delta T)_1 &= Q\Delta T \\ Q_d(\Delta T)_2 &= Q\Delta T + FQ \frac{\Delta T^2}{2} + QF^T \frac{\Delta T^2}{2} + FQF^T \frac{\Delta T^3}{3} \end{aligned} \tag{3.25}$$

$$\begin{aligned} \Phi(\Delta T)_1 &= I + F\Delta T \\ \Phi(\Delta T)_2 &= I + F\Delta T + F \frac{\Delta T^2}{2} . \end{aligned} \tag{3.26}$$

If every term of $|Q_{d_1} - Q_{d_2}|$ and $|\Phi_1 - \Phi_2|$ is smaller than some predetermined number ε, then $Q_d(\Delta T)_2$ and $\Phi(\Delta T)_2$ are the initial values. If not, k is increased by 1. Throughout our computation (short period example), k was never larger than 4. Therefore the sampling interval T was divided into 16 parts ΔT. The predetermined number ε depends on the engineering judgment of the user who will have the time constants of the system which interests him.

B. OPTIMAL DISCRETE REGULATOR

In the previous section we described how a continuous system, control via a ZOH, can be formulated as a discrete system on the sampling points. In this section we will develop the theory of an optimal regulator of a discrete system which minimizes a quadratic cost function. Using the discretization procedure, the theory and results of the discrete regulator can be applied directly to a continuous system controlled by a digital computer.

B-1 The General Formulation of the Discrete Regulator Problem

In the last section, it was shown that a continuous system controlled by a ZOH with an associated continuous cost function J can be reformulated into a discrete form:

$$\begin{aligned} x_{i+1} &= \Phi x_i + \Gamma_1 u_i \\ J &= \frac{1}{2} \sum_{i=0}^{N-1} [x_i^T \; u_i^T] \begin{bmatrix} A_{11} & A_{12} \\ A_{21} & A_{22} \end{bmatrix} \begin{bmatrix} x_i \\ u_i \end{bmatrix}. \end{aligned} \tag{3.29}$$

System (3.29) can be transformed into a simpler form. The cost function J will be rewritten as

$$J = \frac{1}{2}\sum_{i=o}^{N-1}\Big[(u_i^T + x_i^T A_{12}A_{22}^{-1})\, A_{22}(u_i + A_{22}^{-1}A_{21}x_i) + x_i^T(A_{11} - A_{12}A_{22}^{-1}A_{21})x_i\Big] \tag{3.30}$$

or

$$J = \frac{1}{2}\sum_{i=o}^{N-1} x_i^T \mathcal{A} x_i + \mathcal{U}_i^T \mathcal{B} \mathcal{U}_i \tag{3.31}$$

where

$$\begin{aligned} \mathcal{A} &= A_{11} - A_{12}\, A_{22}^{-1}\, A_{21} \\ \mathcal{B} &= A_{22} \\ \mathcal{U}_i &= u_i + A_{22}\, A_{21}\, x_i . \end{aligned} \tag{3.32}$$

Using the last expression of (3.32), (3.29) can be reformulated as

$$\begin{aligned} x_{i+1} &= (\Phi - \Gamma_1\, A_{22}^{-1}\, A_{21})_{\ i} + \Gamma_1\, \mathcal{U}_i \\ J &= \frac{1}{2}\sum_{i=o}^{N-1} x_i^T\, \mathcal{A} x_i + \mathcal{U}_i^T \mathcal{B} \mathcal{U}_i . \end{aligned} \tag{3.33}$$

If a linear, full state feedback is determined for the system (3.33), i.e.,

$$\mathcal{U}_i = C x_i \tag{3.34}$$

then the control u_i for system (3.29) will be

$$u_i = (C - A_{22}^{-1}\, A_{21}) x_i . \tag{3.35}$$

This transformation is necessary because the theory of the optimal discrete regulator is solved for the system (3.33), while a discretization of the continuous system yields cost function (3.29).

For the same reason we can transform a continuous system with an FOH to an equivalent form of (3.33). Using our new formulation of FOH, (3.2) yields

$$x_{i+1} = \Phi x_i + [\Gamma_1 \ \Gamma_k] \begin{bmatrix} u \\ k \end{bmatrix}_i \tag{3.36}$$

where Γ_k is

$$\Gamma_k \triangleq \int_o^T \Phi(\tau) G \tau d\tau \ . \tag{3.37}$$

B-2 The Solution of the Optimal Regulator

It was shown that most of the control configurations which interest us can be rewritten in the simple form of (3.33) repeated here:

$$x_{i+1} = \Phi x_i + \Gamma u_i$$

$$J = \frac{1}{2} \sum_{i=o}^{N} x_i^T A x_i + u_i^T B u_i \ .$$

The optimal linear controller is a control law

$$u_i = C(i) x_i \tag{3.38}$$

that minimizes the cost function J, for any initial conditions. If N increases to infinity and a steady state is reached, then $C(i) = C$ = constant, and the controller is called a regulator.

The solution of the optimal linear controller was given by Kalman [KA-1] who used the dynamic programming approach. We will use Bryson's approach [BR-1] which solves the system (3.33) via the calculus of variation.

For a finite N, the last control u_N is meaningless. It will influence only the state x_{n+1}, which does not interest us. Therefore

the cost function J obtains the form

$$J = \frac{1}{2} x_N^T A x_N + \frac{1}{2} \sum_{i=o}^{N-1} (x_i^T A x_i + u_i^T B u_i). \tag{3.39}$$

In the minimization procedure used in the calculus of variation, we will augment the cost function J by the constraints multiplied by a Lagrange undetermined multiplier λ_i^T (vector). The constraints are the equations of motion for (3.33). The augmented cost function J is

$$J = \frac{1}{2} x_N^T A x_N - \lambda_N^T x_N + \sum_{i=1}^{N-1} (\mathcal{H}_i - \lambda_i x_i) + \mathcal{H}_o \tag{3.40}$$

where $\mathcal{H}_i$ is defined as the Hamiltonian sequence:

$$\mathcal{H}_i = \frac{1}{2} x_i^T A x_i + \frac{1}{2} u_i^T B u_i + \lambda_{i+1}^T (\Phi x_i + \Gamma u_i). \tag{3.41}$$

Using the methods of the calculus of variation, the condition for a stationary value of J is that dJ is zero for arbitrary du_i:

$$\begin{aligned} dJ = (x_N^T A_N - \lambda_N^T) dx_N + \sum_{i=1}^{N-1} \left\{ \left[\frac{\partial \mathcal{H}_i}{\partial x_i} - \lambda_i^T \right] dx_i + \frac{\partial \mathcal{H}}{\partial u_i} du_i \right\} \\ + \frac{\partial \mathcal{H}_o}{\partial x_o} dx_o + \frac{\partial \mathcal{H}_o}{\partial u_o} du_o . \end{aligned} \tag{3.42}$$

We choose λ_i such that

$$\frac{\partial \mathcal{H}_i}{\partial x_i} - \lambda_i^T = 0 \qquad i = 0, \ldots, N-1 \tag{3.43}$$

$$x_N^T A_N - \lambda_N^T = 0 . \tag{3.44}$$

For an extremum:

$$\frac{\partial \mathcal{H}_i}{\partial u_i} = 0 \tag{3.45}$$

yields

$$\frac{\partial \mathcal{H}_i}{\partial u_i} = u_i^T B + \lambda_{i+1}^T \Gamma = 0 \tag{3.46}$$

$$u_i = -B^{-1}\Gamma^T \lambda_{i+1} . \tag{3.47}$$

Combining (3.33) and (3.47), we obtain

$$x_{i+1} = \Phi x_i - \Gamma B^{-1}\Gamma^T \lambda_{i+1} \tag{3.48}$$

and from (3.42) and (2.40), we obtain

$$\lambda_i = \Phi^T \lambda_{i+1} + Ax_i . \tag{3.49}$$

Equations (3.48) and (3.49), called the "Euler-Lagrange difference equations" formulated in state space notation are:

$$\begin{bmatrix} x \\ \lambda \end{bmatrix}_{i+1} = \begin{bmatrix} \Phi + \Gamma B^{-1}\Gamma^T \Phi^{-T} A & -\Gamma B^{-1}\Gamma^T \Phi^{-T} \\ -\Phi^{-T} A & \Phi^{-T} \end{bmatrix} \begin{bmatrix} x \\ \lambda \end{bmatrix}_i . \tag{3.50}$$

This is a two-point boundary value problem: x_o is given at $i = 0$. From (3.43) we get the boundary condition for $i = N$:

$$\lambda_N = Ax_N . \tag{3.51}$$

The solution to this problem was accomplished by Bryson using the "sweep method" [BR-1]. The sweep method assumes a solution for λ_i of the form:

$$\lambda_i = S_i x_i . \tag{3.52}$$

This solution leads to a matrix Riccati difference equation in S_j:

$$S_j = \Phi^T(S_{j+1} + \Gamma B^{-1}\Gamma^T)^{-1}\Phi + A \qquad j = N-1, \ldots, 0$$
$$S_N = A \ . \tag{3.53}$$

Determining S_j from the backward recursive relations (3.53), and using (3.57) and (3.42), the optimal control u_i is expressed as a linear combination of the state x_i. If certain conditions are satisfied as N increases, S_j reaches a steady state S_{ss}, and the controller is reduced to a regulator:

$$u_i = -B^{-1}\Gamma\Phi^{-T}(S_{ss} - A)x_i \tag{3.54}$$

which is obtained by combining (3.47), (3.49), and (3.52). In the steady state, the matrix Riccati difference equation is reduced to a second-order matrix algebraic equation

$$S_{ss} = \Phi^T(S_{ss}^{-1} + \Gamma B^{-1}\Gamma^T)^{-1}\Phi + A. \tag{3.55}$$

During the last two decades, a considerable effort has been made to find an efficient solution of the Riccati equation and the steady state matrix equation. The usual method of solution for (3.55) is a recursive computation of (3.53) until S reaches a steady state S_{ss}. A completely different approach to solving for S_{ss} is to use the eigenvector decomposition of the transition matrix (3.50).

3. Solution of S_{ss} by Eigenvector Decomposition

In 1966, Potter [PO-1] described a method for the steady state solution of the matrix Riccati differential equation by eigenvector decomposition. Bryson and Hall [BR-2], using efficient QR algorithm for eigenvector calculation, constructed a computer program for linear regulators and Kalman filter syntheses. Vaughan [VA-1] extended the Potter method for discrete system control synthesis. The authors solved the eigenvector

decomposition problem independently of Vaughan, and also applied it to the discrete filter synthesis problem. Our interpretation and our proof will be given here.

The Euler-Lagrange equation (3.50) will be repeated here, but on the z-plane:

$$\begin{bmatrix} zx \\ z\lambda \end{bmatrix} = \begin{bmatrix} \Phi+\Gamma B^{-1}\Gamma^T\Phi^{-T}A & -\Gamma B^{-1}\Gamma^T\Phi^{-T} \\ -\Phi^{-T}A & \Phi^{-T} \end{bmatrix} \begin{bmatrix} x \\ \lambda \end{bmatrix}.$$

The following theorems will be proved.

Theorem 1: If z is an eigenvalue of the system (3.51), the $1/z$ is also an eigenvalue.

Proof: (a) defining E: $E \triangleq z^{-1}$; (b) defining a new variable: $\gamma \triangleq z\lambda$ and directly using (3.48) and (3.49), the system (3.56) can be transformed to an equivalent form:

$$\begin{bmatrix} \Phi - Iz & -\Gamma B^{-1}\Gamma^T \\ A & \Phi^T - Iz^{-1} \end{bmatrix} \begin{bmatrix} x \\ \gamma \end{bmatrix} = 0 \qquad (3.57)$$

$\Gamma B^{-1}\Gamma^T$ and A are symmetric; therefore, (3.57) may be rewritten as

$$[\gamma^T x^T] \begin{bmatrix} \Phi - IE & -\Gamma B^{-1}\Gamma^T \\ A & \Phi^T - IE^{-1} \end{bmatrix} = 0. \qquad (3.58)$$

Systems (3.57) and (3.58) have the same transition matrix. Therefore, if z is the solution of the characteristic equation of (3.57), then E is a solution also.

Conclusion: The eigenvalues of the Euler-Lagrange equations (3.56) are reflected symmetrically across the unit circle on the z-plane. See Fig. III-2.

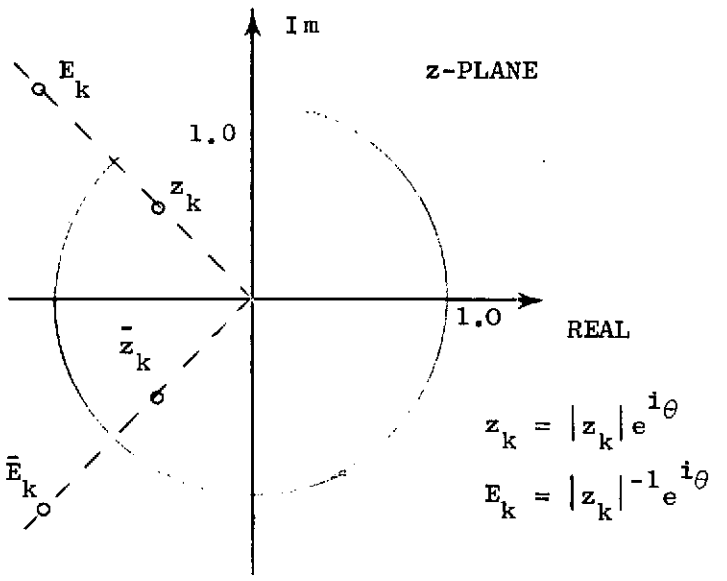

FIG. III-2 ROOTS LOCATION OF EULER-LAGRANGE (E-L) EQUATIONS

Definition:

$$T \triangleq \begin{bmatrix} X_z & X_E \\ \Lambda_z & \Lambda_E \end{bmatrix} \triangleq [T_z \quad T_E]. \tag{3.59}$$

Matrices T_z and T_E are the eigenvectors of the E-L equations, (3.56), associated with z and E respectively.

Before formulating and proving Theorem 2, a well-known result from linear systems theory will be presented [e.g., KW-1].

A homogeneous, linear time-invariant discrete system

$$x_{i+1} = \Phi x_i \tag{3.60}$$

with the initial conditions x_o, has the solution

$$x_i = \Phi^i x_o . \tag{3.61}$$

The solution x_i can be expressed in terms of the individual eigenvector modes as follows: the initial condition x_o is resolved along the modes of the eigenvectors by the transformation T_r^{-1}:

$$\xi_o = T_r^{-1} x_o \tag{3.62}$$

where T_r is the matrix of the eigenvectors of Φ

$$T_r = [\ell_1, \ldots, \ell_j, \ldots, \ell_n] . \tag{3.63}$$

The solution x_i is a linear combination of the particular excited modes, i.e.,

$$x_i = \sum_{j=1}^{n} z_j^i \ell_j \xi_o . \tag{3.64}$$

Using this result, we can formulate Theorem 2.

Theorem 2: The steady state solution S_{ss} at the matrix Riccati difference equation (repeated from Eq. 3.55)

$$S = \Phi^T (zS^{-1} + \Gamma B^{-1} \Gamma^T)^{-1} \Phi + A \tag{3.65}$$

is

$$S_{ss} = \Lambda_E X_E^{-1} . \tag{3.66}$$

Proof: The homogeneous solution of the E-L equations (3.56) is

$$\begin{bmatrix} x \\ \lambda \end{bmatrix}_i = \sum_{i=1}^{n} \xi_{o_k} \begin{pmatrix} x_z^{(k)} \\ \lambda_z^{(k)} \end{pmatrix} z_k^i + \sum_{k=1}^{n} \eta_{o_k} \begin{pmatrix} x_E^{(k)} \\ \lambda_E^{(k)} \end{pmatrix} z_k^{N-i} \tag{3.67}$$

where n = the order of the system,

$\begin{cases} \xi_{o_k} \\ \eta_{o_k} \end{cases}$ = constants expressing boundary conditions

$\begin{cases} z_k \\ E_k \end{cases}$ = eigenvalues of (3.51)

and $\begin{pmatrix} x_z(k) \\ \lambda_z(k) \end{pmatrix}$ and $\begin{pmatrix} x_E(k) \\ \lambda_E(k) \end{pmatrix}$

are the eigenvectors of (3.56) corresponding to z_k and E_k. Equation (3.67) may be formulated in a matrix notation

$$\begin{bmatrix} x \\ \lambda \end{bmatrix}_i = \begin{bmatrix} x_z^{(1)} & x_z^{(n)} \\ \lambda_z^{(4)} & \lambda_z^{(n)} \end{bmatrix} \begin{bmatrix} \xi_{o1} z_1^i \\ \vdots \\ \xi_{on} z_n^i \end{bmatrix} + \begin{bmatrix} x_E^{(1)} & x_E^{(n)} \\ \lambda_E^{(1)} & \lambda_E^{(n)} \end{bmatrix} \begin{bmatrix} \eta_{o1} E_1^{-(N-i)} \\ \vdots \\ \xi_{on} E_n^{-(N-i)} \end{bmatrix}, \tag{3.68}$$

defining Z as

$$Z = \begin{bmatrix} z_1 & & 0 \\ & \ddots & \\ 0 & & z_n \end{bmatrix}. \tag{3.69}$$

Equation (3.68) can be further reduced to

$$x_i = X_z Z^i \bar{\xi}_o + X_E Z^{N-i} \bar{\eta}_o$$

$$\lambda_i = \Lambda_z Z_1^i \bar{\xi}_o + \Lambda_E Z^{N-i} \bar{\eta}_o .$$

As i increases, the stable modes multiplied by the vector $\bar{\xi}_o$

attenuate so that equations (3.70) become

$$\begin{aligned} x_i &= X_E Z^{N-i} \bar{\eta}_o \\ \lambda_i &= \Lambda_E Z_1^{N-i} \bar{\eta}_o \, . \end{aligned} \tag{3.71}$$

Solving (3.71), we get

$$\lambda_i = \Lambda_E X_E^{-1} x_i \, . \tag{3.72}$$

But $\lambda_i = S_i x_i$ was the assumed solution of the matrix Riccati difference equation (3.53). Therefore (repeat of Eq. 3.66)

$$S_{ss} = \Lambda_E X_E^{-1} .$$

This concludes the proof of (3.66).

Having these results, the optimal feedback control of the linear discrete regulator is

$$u_i = -B^{-1}\Gamma\Phi^{-T}(\Lambda_E X_E^{-1} - A)x_i = Cx_i \, . \tag{3.73}$$

This solution requires nonsingularity of the transition matrix Φ. Made discrete, the linear continuous system always has the property that $|\Phi| \neq 0$. This stems from the fact that a continuous linear system has a unique solution for a given initial conditions [e.g., KW-1]; however, this property ($|\Phi| \neq 0$) is not obvious for a pure discrete system. If, in a pure discrete system Φ is singular, it indicates that some of the states (or the modes) can be expressed as a linear combination of the remaining states (or modes). Hence, if a state variable feedback is required, the singular system representation can be reduced in dimension until regularity is achieved and the feedback matrix C can be calculated.

Two more results will be given:

a) The stable eigenvalues of the E-1 equations (3.56) are identical with the eigenvalues of the closed loop optimal system. This useful property can be proven by analogy to continuous systems [e.g., BR-2].

b) The expression for S_{ss}, Eq. (3.66), repeated

$$S_{ss} = X_E \Lambda_E^{-1}$$

is independent of any rearrangement of the individual eigenvectors in

$$\begin{bmatrix} X_E \\ \Lambda_E \end{bmatrix} .$$

The proof is obvious if (3.66) is rewritten as

$$S_{ss} \Lambda_E = X_E . \tag{3.74}$$

Assuming S_{ss} is fixed, then any column j of X_E is a linear combination of S_{ss} and column j of Λ_E. Its values are independent of its relative position with respect to other columns.

The computer program, DISC, listed and explained in Appendix A, is based on these results.

C. THE OPTIMAL LINEAR DISCRETE FILTER

C-1 The Measurement Timing

The purpose of the filter is to reconstruct the states which are not measured, and to minimize the process and measurement noise influence. For the physical system,

$$\begin{aligned} x_{i+1} &= \Phi x_i + \Gamma_1 u_i + \Gamma_2 w_i \qquad & w_i \rightarrow N(0, Q_d) \\ y_i &= H x_i + v_i \qquad & v_i \rightarrow N(0,R) . \end{aligned} \tag{3.75}$$

The optimal steady state filter is given by

$$\bar{x}_{i+1} = \Phi\hat{x}_i + \Gamma_i u_i \tag{3.76}$$

$$\hat{x}_{i+1} = \bar{x}_{i+1} + K(y_{i+1} - H\bar{x}_{i+1}) \tag{3.77}$$

$$\begin{aligned} K &= PH^T R^{-1} \\ P &= \Phi^{-1}(M - \Gamma_2 Q_d \Gamma_2^T)\Phi^{-T} \end{aligned} \tag{3.78}$$

where M is the error covariance matrix before measurements, and P is the error covariance matrix after the measurements y_{i+1} were done. How M is computed will be explained later. Relation (3.77) is the one which is used by Bryson and Ho [BR-1], and throughout this work. Here, we assume a zero computation time between the measurements y_{i+1} and the output of the filter x_{i+1}. Borow [B -1] shows that the delay for the short period mode calculation is of the order of one millisecond. The other possibility is to use the approach of Kwakernaak [KW-1]:

$$\hat{x}_{i+1} = \bar{x}_{i+1} + K(y_i - H\hat{x}_i)\,. \tag{3.79}$$

These two approaches could be summarized on the time axis in Fig. III-3.

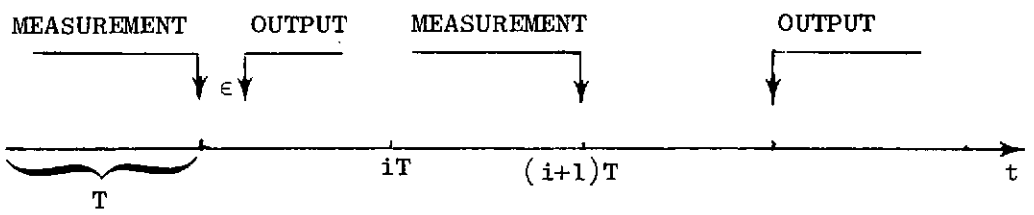

FIG. III-3 MEASUREMENT AND SAMPLING INTERVAL

In (3.77) we assume $\epsilon \to 0$. Both of the formulations have advantages and disadvantages. The main feature is that (3.77) is an approximation only as ϵ is finite. On the other hand, (3.69) uses 'obsolete' information. The compromise will be to use a third method; for example, the one shown in Fig. III-4.

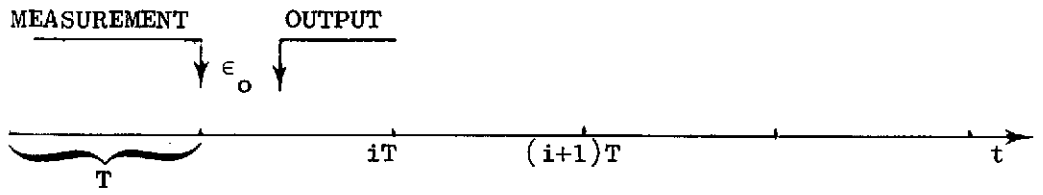

FIG. III-4 INTERSAMPLE MEASUREMENTS

ϵ_o is the fixed time interval, longer than the maximum computation time needed to generate the states $\hat{x}_{i+1}$ from y_{i+1} measurements. As is shown by Kwakernaak et al [KW-1], the calculation of the optimal filter is highly complicated. We will use the first approach which assumes that the delay time between the measurements and the output of the filter $\hat{x}$ is much smaller than the sampling. From an inspection of (3.76) and (3.77), we can see that most of the updating of the filter can be done before the measurements y_{i+1} are received. Actually, the only calculation which has to be done during the delay interval is to multiply K by y_{i+1} and to add this quantity to the rest of (3.77).

C-2 Calculation of the Steady State Optimal Filter by Eigenvector Decomposition

The steady state optimal (Kalman) filter is an observer which minimizes the steady state error covariance matrix P. The recursive equation for M obtained from the minimization process has the same structure as those for S for the optimal control problem. The equations are identical if we consider the following equivalence first recognized by Kalman [KA-1]:

Control		Filter
Φ	$\longleftrightarrow$	Φ^T
H	$\longleftrightarrow$	Γ_2^T
Γ_1	$\longleftrightarrow$	H^T
A	$\longleftrightarrow$	Q_d
B	$\longleftrightarrow$	R

Thus we will replace the matrices of the optimal control problem by the matrices of the filter in E-L equation (3.56) which yields the matrix $\mathcal{H}$:

$$\mathcal{H} = \begin{bmatrix} \Phi^T + H^T R^{-1} H \Phi^{-1} \Gamma_2^T Q_d \Gamma_2 & -H^T B^{-1} + 1\Phi^{-1} \\ -\Phi^{-1} \Gamma_2 Q_d \Gamma_2^T & \Phi^{-1} \end{bmatrix}. \qquad (3.80)$$

Making direct use of the results from the optimal regulator calculation, the error covariance matrix M is given by

$$M = X_E \Lambda_E^{-1} \qquad (3.81)$$

where X_E and Λ_E are defined from

$$T = \begin{bmatrix} x & X_E \\ \Lambda_z & \Lambda_E \end{bmatrix}, \qquad (3.82)$$

T is a matrix of the eigenvectors of the $2n \times 2n$ matrix $\mathcal{H}$,

$$\begin{bmatrix} X_z \\ \Lambda_z \end{bmatrix}$$

are the eigenvectors of $\mathcal{H}$ corresponding to the stable eigenvalues of $\mathcal{H}$, and

$$\begin{bmatrix} X_E \\ \Lambda_E \end{bmatrix}$$

are the eigenvectors corresponding to the eigenvalues of $\mathcal{H}$ located outside the unit circle.

Similar to the optimal control problem, the stable eigenvalues of $\mathcal{H}$ (inside the unit circle) are identical with the eigenvalues of the observer error system defined from (3.76) and (3.77) as

$$\tilde{x} \triangleq \hat{x} - x \tag{3.83}$$

$$\tilde{x}_{i+1} = (\Phi - KH\Phi)x_i + (KH\Gamma_2 - \Gamma_2)w_i + Kv_{i+1}. \tag{3.84}$$

D. ALGORITHM FOR AN EVALUATION OF THE STEADY STATE RESPONSE TO AN EXTERNAL NOISE

A stable discrete system Φ, disturbed by an external noise with a covariance matrix Q_d reaches a steady state. The average behavior of its states is characterized by a covariance matrix X which is the solution of Bryson and Ho [BR-1]:

$$X = \Phi X \Phi^T + Q_d . \tag{3.85}$$

Following Bryson, the average behavior of an optimally controlled discrete system, with an external noise disturbance and measurement noise, is characterized by the state covariance matrix X. This is the solution of

$$X - M = (\Phi + \Gamma C)(X - P)(\Gamma + \Gamma C)^T \tag{3.86}$$

where C is the optimal gain (3.73), M and P are the observer error

and covariance matrices defined in (3.78). Equation (3.87) will be re-written as

$$X - P = (\Phi + \Gamma C)(X - P)(\Phi + \Gamma C)^T + M - P \,. \tag{3.87}$$

Equation (3.87) is now in the form of (3.85). Equation (3.85) is essentially a linear equation of X. New algorithms for solving (3.85) appear frequently in the numerical method literature [e.g., BER-1]. We will present a new numerical solution of (3.85) which utilizes the algorithm for eigenvector decomposition.

Claim 1:

$$X = \Lambda_E X_E^{-1} \tag{3.88}$$

where

$$\begin{bmatrix} X_Z & X_E \\ \Lambda_Z & \Lambda_E \end{bmatrix}$$

is a matrix of eigenvectors of the $2n \times 2n$ system of $\acute{H}$:

$$\acute{H} = \begin{bmatrix} \Phi^{-T} & 0 \\ Q_d \Phi^{-T} & \Phi \end{bmatrix} , \tag{3.89}$$

$$\begin{bmatrix} X_E \\ \Lambda_E \end{bmatrix}$$

is the eigenvectors submatrix corresponding to the eigenvalues of $\acute{H}$ outside the unit circle.

Claim 2: If z_k is an eigenvalue of $\acute{H}$, then $z_k^{-1} = E_k$ is also an eigenvalue of $\acute{H}$.

Proofs: Claim 2 is obvious from inspection. To prove Claim 1, we let

$$\acute{H}\begin{pmatrix} X_E \\ \Lambda_E \end{pmatrix} = \begin{pmatrix} X_E \\ \Lambda_E \end{pmatrix} D_E \tag{3.90}$$

where

$$D = \begin{bmatrix} D_E & \\ & D_z \end{bmatrix} = \begin{bmatrix} E_1 \ddots E_n & \bigcirc \\ \bigcirc & z_1 \ddots z_n \end{bmatrix} \qquad |E_k| > 1 . \tag{3.91}$$

Using (3.90) and (3.91)

$$\begin{aligned} \Phi^{-T} X_E &= X_E D_E \\ Q_d \Phi^{-T} X_E + \Phi \Lambda_E &= \Lambda_E D_E \end{aligned} \tag{3.92}$$

yields

$$Q_d + \Phi \Lambda_E X_E^{-1} \Phi^T = \Lambda_E X_E^{-1} . \tag{3.93}$$

Define

$$X = \Lambda_E X_E^{-1} . \tag{3.94}$$

Equation (3.93) is identical to (3.85), thus proving Claim 1.

Using this result, the average behavior X of the optimally controlled discrete system, including process noise and measurement noise, is given as the solution of (3.81), which is

$$X = \Lambda_E X_E^{-1} + P , \tag{3.95}$$

where

$$\begin{bmatrix} X_z & X_E \\ \Lambda_z & \Lambda_E \end{bmatrix}$$

is a matrix of eigenvectors corresponding to $2n \times 2n$ matrix $\acute{H}$:

$$\acute{H} = \begin{bmatrix} (\Phi + \Gamma c)^T & 0 \\ (M - P)(\Phi + \Gamma c)^{-T} & \Phi + \Gamma c \end{bmatrix} . \tag{3.96}$$

E. SUMMARY

1. A linear continuous system, controlled by a discrete controller via a zero order hold (ZOH) or a first order hold (FOH) can be formulated as simple linear discrete systems (3.97). We have shown that if a digital computer generates the control sequence, the information needed for the FOH can be generated simultaneously, and not by extrapolating the last two control inputs.

If a continuous cost function is assumed and a continuous white noise acts on the system, the whole controlled system can be represented by equations of the form

$$\begin{aligned} x_{i+1} &= \Phi x_i + \Gamma_1 u_i + \Gamma_2 w_i \qquad w_i \to N(0,\ Q_d) \\ J &= \sum_{i=0}^{N-1} x_i^T A x_i + u_i^T B u_i \\ y_i &= H x_i + v_i \qquad\qquad v_i \to N(0,\ R) \ . \end{aligned} \tag{3.97}$$

Converting to the formulation (3.97) enables us to calculate the optimal regulator and the optimal steady state observer using discrete algorithms.

2. We have developed an eigenvector decomposition computer program for solving the discrete steady state matrix Riccati differential equation. It is highly efficient compared to recursive methods, due to the use of the QR algorithm [FR-1], which finds eigenvalues and eigenvectors of a matrix with widely dispersed eigenvalues very rapidly and accurately.

Our eigenvector decomposition program calculates the optimal regulator gains and the optimal steady state filter gains, and as a by-product, it provides the closed loop eigenvalues and the observer error poles [App. A].

3. Calculation of the root mean square response of the closed loop system involves the solution of a linear matrix equation of the form

$$X = \Phi X \Phi^T + Q_d. \tag{3.98}$$

A new algorithm for solving (3.98) was found. This algorithm is based on eigenvector decomposition of a system associated with (3.98). We do not claim that this algorithm is more efficient than algorithms already in the literature. Its main advantage is that it uses the existing program for eigenvector decomposition of a matrix.

IV. SAMPLING TIME AND TIME RESPONSE

The time response of a controlled system is determined by its closed loop dynamics and by the input signals. A system has a proper time response if for a specific input, some combination of the states follows approximately a predetermined pattern. In the case of a pilot's commands, the input is a continuous signal, e.g., an output of a potentiometer. This continuous signal has to be sampled and fed to the digital computer which further processes it. The questions now are: how well does the digital processor interpret the sampled signal, and how well do the states follow the desired pattern?

The theoretical basis for the reconstruction of a continuous signal from sampled data is given in the sampling theorem developed by Shannon [e.g., RA-1]. The sampling theorem states that in order to reconstruct an unknown continuous signal from samples of that signal, one must use a sample rate which is twice as high as the highest frequency contained in the unknown signal. This theorem is not directly applicable to a reconstruction of an input signal in a real time digital system. This is true for the following reasons: (a) for causal systems, the reconstructed signal has a phase shift with respect to the input signal. The theorem states that it is possible to reconstruct the signal but it doesn't say that it will be done in the same time. Actually, any reconstruction scheme has to accumulate a minimal amount of data points in order to start the reconstruction of the sampled signal. (b) For aircraft applications, the proper time response is formulated as a response to the pilot's step input. However, from a theoretical point of view, a step input has an infinitely large frequency spectrum. (c) In the feedback path, the sampling theorem doesn't hold since we have knowledge of the plant. Therefore, insteady of applying the sampling theorem, we will investigate the time response of a realistic example using a simulation scheme.

The key question of how to get a proper time response can be reformulated as a problem of what the input signal should be in order to

obtain some predetermined pattern of the states. Extensive research dealing with this complicated problem is currently being done by Holley and Bryson [HOL-1]. Their approach, called "a nonzero set point regulator design", consists of an analytical basis for the time response synthesis, and can be extended to discrete control systems. Meanwhile, we will use the time response specification given by Borow et al [BO-1] and Sutton et al [SU-1], which is based on the accumulated experience of the U.S. Navy. A complete description of this specification will be given in Section IV-B.

The outline of this chapter is as follows. In Section IV-A we will define the example, "F-H", which will be used in this work. It includes the short period mode, a bending mode, and wind gusts.

In Section IV-B we will describe the various design objectives, including the time response.

In Section IV-C the inner control loop design will be described. The classical approach will only be outlined, but the optimal discrete design will be explained in detail.

In Section IV-D the main objectives of this chapter will be investigated. It will be shown that, for the F-H short period example, a proper time response imposes a definite limit on the sampling interval.

A. EXAMPLE DEFINITION

In order to be able to illustrate the various factors which influence the sampling rate selection, our investigation into aircraft discrete controls should be related to a definite and relevant technical system. We chose a controlled short period mode configuration of a hypothetical type aircraft, which we term F-H. This type of aircraft is described by Borow [BO-1] and Sutton [SU-1] as the future aircraft of the U.S. Navy. Our choice was made for the following reasons:

1. The time constants and the time responses in the longitudinal mode are short and they constrain the sampling rate.
2. The influence of bending modes on the stability and sensitivity of the control loop must be taken into account. A considerable effort must be made to include these effects in the control design.

3. Only a military aircraft flies in such difficult flight conditions as Mach 1.2 at ground level. The strongest wind gust amplitudes are found at zero altitude. A high velocity flight through such gusts generates a short correlation time of the external disturbance, which makes the gust alleviation more difficult. During landing conditions (Mach 0.19), this type of aircraft has an extremely slow time response (ω = 0.5 rad/sec). Therefore a strong bandwidth augmentation is necessary. It will be shown that this behavior imposes serious limitations on the sampling rate.

The geometry of this aircraft as a flexible body is described in Fig. IV-1a and Fig. IV-1b. References BO-1, ED-1, and SU-1 use this model.

The equation of motion, based on body axes and dimensional stability derivatives are

$$\begin{aligned}
\dot{q} &= (M_q)q + (M_\alpha)\alpha_T + (M_{\dot{\alpha}})\dot{\alpha}_T + (M_{\delta_e})\delta_e \\
\dot{\alpha}_T &= q + \frac{Z_\alpha}{U_o}\alpha_T + \frac{w_g}{U_o\tau_w} + \frac{Z_{\delta_e}}{U_o}\delta_e - \frac{\sqrt{2\tau_w}\,\sigma_w}{\tau_w U_o}\eta_g \\
\dot{w}_g &= -\frac{w_g}{\tau_w} + \frac{\sqrt{2\tau_w}\,\sigma_w}{\tau_w}\eta_g
\end{aligned} \tag{4.1}$$

These are the short period mode equations; they include a vertical gust, modeled as a first order Gauss-Markov process.

$$\alpha_T \triangleq \alpha - \frac{1}{V_o} w_g \tag{4.2}$$

is defined as the total angle of attack. The reason for preferring the state variable α_T instead of α (as used by Borow [BO-1] and Sutton [SU-1]) is that α_T is an important variable in the gust alleviation study. The vertical acceleration is directly related to α_T.

The bending mode is modeled as a second order system driven by the elevator input and the rate of the angle of attack--$\dot{\alpha}$. The bending mode

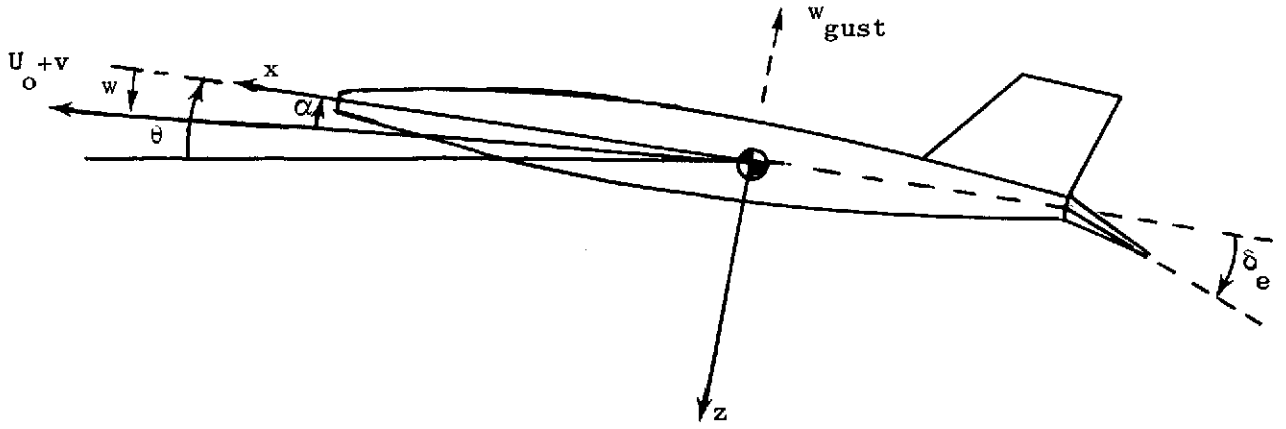

FIG. IV-1a RIGID BODY CONFIGURATION. Note: $w = \alpha_x U_o$.

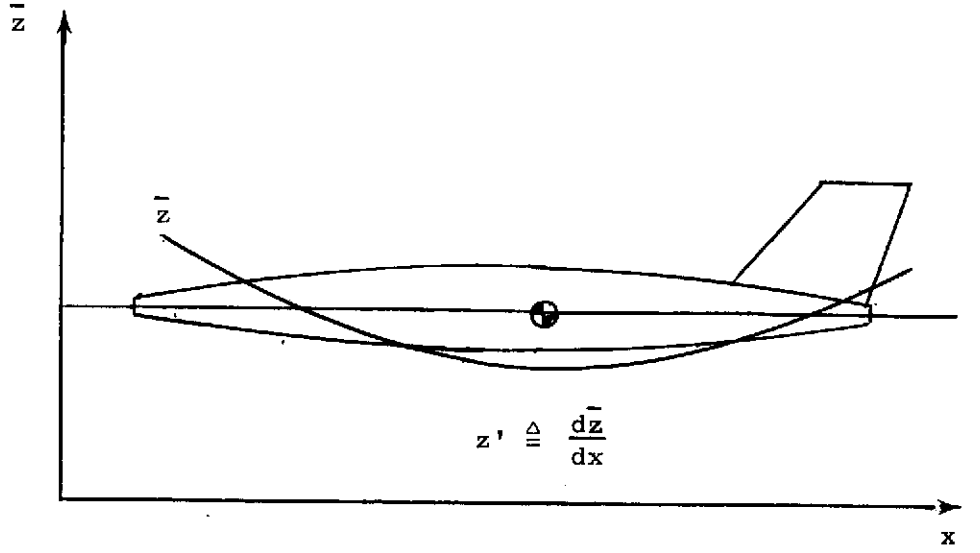

FIG. IV-1b BENDING MODE DEFLECTION

is slightly damped ($\zeta_b = 0.01$). The bending equations are

$$\begin{aligned} \dot{x}_3 &= \omega_b x_4 \\ \dot{x}_4 &= -\omega_b x_3 - 2\zeta_b \omega_b x_4 + \omega_b k_1 Z_{\delta_e} \delta_e + k_2 \omega_b Z_{\dot{\alpha}} \dot{\alpha} \,. \end{aligned} \tag{4.3}$$

The actual acceleration and rotation of any point on the body axis x_1 due to bending, is

$$\begin{aligned} q_b &= \frac{z_1'}{\omega_b} x_4 \\ \ddot{z}_b &= \frac{\bar{z}_1}{\omega_b} \dot{x}_4 \end{aligned} \tag{4.4}$$

where k_1, k_2, are quantities depending on the airplane shape and mass distribution, and $\bar{z}_1(x)$ is the first mode shape. The wind gust influences the bending mode primarily through $\dot{\alpha}_T$ (see Eqs. 4.1 and 4.2). Sutton [SU-1] and Blakelock [BL-1] disregard this influence.

An accelerometer and a rate gyro are the measuring instruments. The measurement signals are combined from the rigid body motion, the bending mode motion, and additive white noises:

$$\begin{aligned} q_T &= q + \frac{z_1'}{\omega_b} x_4 + v_q \\ n_T &= U_o(q - \dot{\alpha}) + \ell_a \dot{q} + \frac{\bar{z}_1}{\omega_b} \dot{x}_4 + v_n . \end{aligned} \tag{3.5}$$

where $v_q = N(0, r_q)$, $v_n = N(0, r_n)$. For a numerical example, we chose two difficult flight conditions of the F-H aircraft [BO-1, SU-1]:

a) Flight condition No. 1 is a flight at zero altitude and Mach 0.19. As mentioned in the beginning of this section, a considerable increase in the bandwidth (acceleration feedback) is necessary in order to improve the time response. It will be shown later that this flight condition limits the selection of the sampling rate.

b) Flight condition No. 8 is a flight at zero altitude and Mach 1.2. High velocity flight at zero altitude generates strong wind gusts. The maximum available gust alleviation is necessary for several reasons, including improved aiming and minimizing the fatigue of the pilot.

The corresponding numerical data are summarized in Table IV-1.

Table IV-1

NUMERICAL DATA OF THE F-H SHORT PERIOD (SP) MODE

	Condition No. 1	Condition No. 8
U_o(ft/sec)	212.0	1340
M_q(1/sec)	-0.44	-1.91
M_w(1/ft sec)	-0.0017	-0.13
M_{δ_e}(1/sec^2)	-1.23	-69.1
$M_{\dot{w}}$(1/ft)	-0.62×10^{-3}	0.52×10^{-3}
Z_w(1/sec)	-0.57	-4.03
Z_{δ_e}(ft/sec^2)	-13.2	-399.0
τ_w(sec)	3.0	0.5
σ_w(ft/sec)	12.0	12.0
ζ_b	0.01	0.01
ω_b(rad/sec)	25.0	25.0
$\delta_{e_{max}}$(rad)	0.4	0.4
$\bar{z}_1$ of accelerometer	0.07	0.07
z_1' of rate gyro	-0.005	-0.005
k_1	4.0	4.0
k_2	0.06	0.06
ℓ_a(f)	14.0	14.0
SP freq (rad/sec)	0.60	13.2
period of SP (sec)	10.5	0.476

A-1 Open Loop Coupling Between the Bending Mode and the Rigid Body Motion

Borow et al, Blakelock, and Sutton et al [BO-1, BL-1, SU-1] disregard any direct influence of the bending mode on the rigid body motion. However, in flight condition No. 8, the supersonic velocity in a high density atmosphere generates a considerable restoring moment (M_α). Consequently, the short period mode oscillation is high (~ 13.6 rad/sec) and has the same order of magnitude as the bending mode frequency (25 rad/sec).

To estimate the influence of the bending mode on the rigid body motion, we will assume a simplified configuration which generates a moment around the center of mass, see Fig. IV-2.

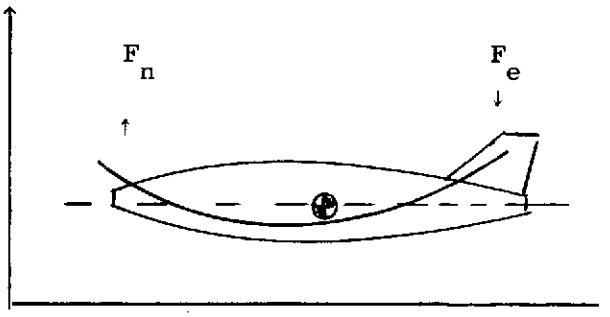

FIG. IV-2 MOMENT AROUND THE CENTER OF MASS AS GENERATED BY THE BENDING MODE.

The force F_e and the corresponding moment around the center of mass are proportional to $z'(x)$. . We may consider the rotation of the tail as an additional angle of attack of the elevator. In supersonic aircrafts, the whole elevator surface is moving and thus the moment caused by F_e is approximately equal to $-M_{\delta_e}(z'_e x_3)/(\omega_b^2)$ where $(z'_e x_3)/(\omega_b^2)$ is the additional angle of the elevator due to the bending rotation.

We will use another assumption: the sum of the moments generated by the deflection of other parts of the body (including F_n) is equal or lower than 50% of the moment generated by the bending rotation of the elevator.

By using these approximations, the additional term of the first equation of (4.1) will be

$$-k_b M_{\delta_e} \frac{z'_e x_3}{\omega_b^2}$$

where $0 \leq k_b \leq 1.5$.

The poles of the coupled system, combined from the rigid body and the bending mode are summarized in Table IV-2.

Table IV-2

THE OPEN LOOP POLES OF THE COUPLED SYSTEM

	Rigid Body	Bending Mode
$k_b = 0$	$s = -2.5 \pm j13.6$	$s = -0.5 \pm j25.0$
$k_b = 1$	$s = -0.9 \pm j13.5$	$s = -1.9 \pm j24.8$
$k_b = 1.5$	$s = -0.3 \pm j13.4$	$s = -2.4 \pm j24.7$

From Table IV-2 we see that for a detailed design, the coupling between the short period mode and the bending mode cannot be neglected. Although the stability augmentation system stabilizes the system, the open loop configuration is only marginally stable.

B. DESIGN OBJECTIVES

There are several different objectives required of an inner loop longitudinal autopilot. The most important may be summarized as follows: (1) A proper time response to various inputs; (2) A proper dynamic behavior based on the pilot's experience; (3) Wind gust alleviation.

The crucial constraint on the actual design is the condition that for one definite flight condition, there should be only one control configuration which will meet all the objectives.

For the conventional aircraft where the elevator is behind the center of the mass, the objectives 1, 2, and 3 are conflicting; thus, a suitable compromise will be suggested in Section IV-3.

The various design objectives will now be explained in more detail.
Objective 1: The proper time response requirement varies for different aircrafts. Essentially, the requirement is for a fast response, but one which is not too sensitive and has a sufficient stability margin. The exact formulation will be given with Objective 2.

Objective 2: A desirable dynamic behavior, expressed as a location of the augmented short period poles, is described in Kolk [KO-1]. The shaded area in Fig. IV-3 is the location of poles which is preferred by pilots.

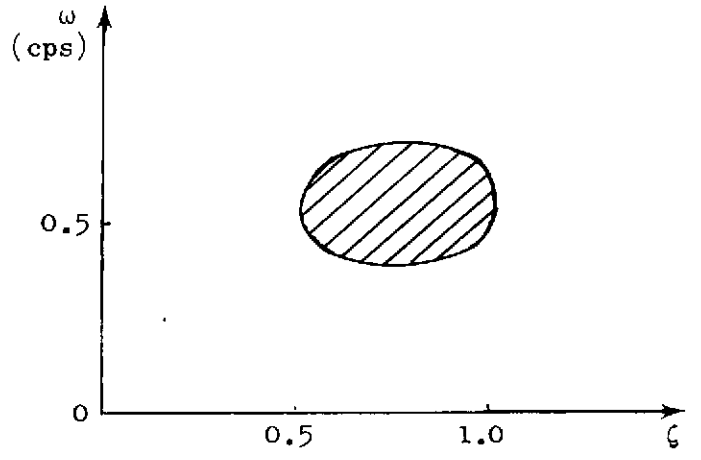

FIG. IV-3 SHORT PERIOD POLES LOCATION; PREFERRED BY MOST PILOTS.

Combining Objectives 1 and 2, we may say that a high performance military aircraft is expected to have a fast response in order to be able to execute properly different maneuvers. It must also dampen adequately for precise weapons release. An attempt to give a quantitative formulation to these requirements was made by the Navy, as described by Borow [BO-1] and Sutton [SU-1] under the name TRP (time response parameter).

The TRP is defined by the quantities in Fig. IV-4 and the relation,

$$TRP = \left(\frac{t_d}{t_c}\right)_q + 0.08\,(A_q - 1) + 0.05\,(t_{d_{nz}} - 0.7) + 0.3(A_{nz} - 0.3) \tag{4.6}$$

where A_q is the pitch rate overshoot, and A_{nz} is the vertical acceleration overshoot. The objective is to keep $TRP < 0.25$. All parenthesized terms, if negative, are assumed to be zero for the TRP calculation.

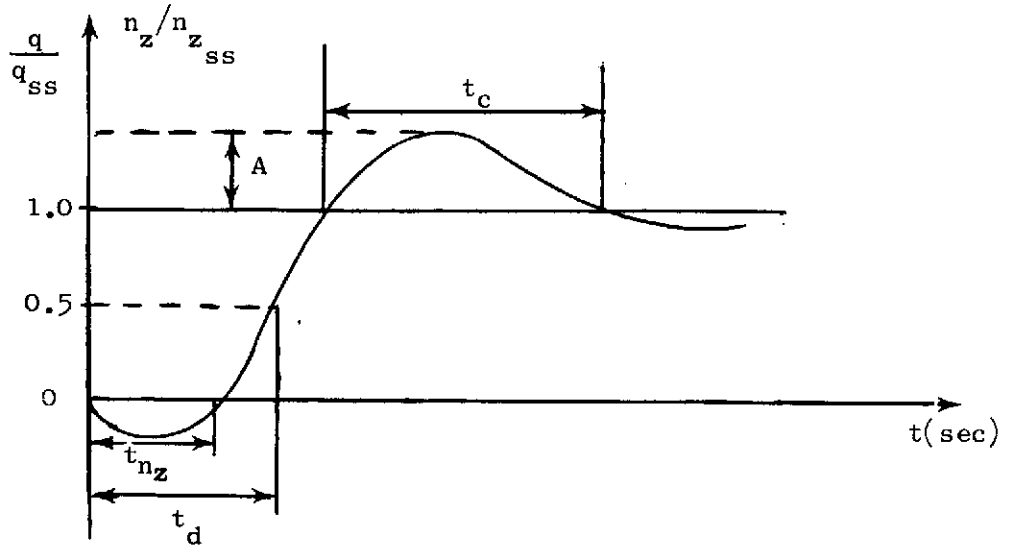

FIG. IV-4 THE TIME RESPONSE PARAMETER (TRP) DESCRIPTION

We will interpret the meaning of the different terms in the TRP specification: TRP is zero (the 'best' response) if: (a) the overshoot of q is not larger than 1; (b) the time to reach half final value of the vertical acceleration is less than 0.7s; (c) the maximum overshoot of the vertical acceleration is less than 0.3; (d) the undershoot (the non-minimum phase property) is shorter than 0.2 sec; (e) the system is well damped. Therefore, $(t_c)_q$ should be as large as possible, but not lower than $(t_c)_q = 4(td)$.

Generally speaking, the TRP specification indicates that the vertical acceleration time constant should be less than ~ 1 sec.

Objective 3. Gust alleviation is achieved by a proper control. The optimal controller, which minimizes a quadratic cost function for an impulse response, minimizes also the mean response to white noise disturbance (Parseval Theorem [KW-1]). Further alleviation can be achieved if the external disturbance has a finite correlation time and if the average wind gust behavior can be predicted. In Chapter V, a detailed description of relations between gust alleviation and the sampling time will be given.

C. INNER CONTROL LOOP DESIGN

The main purpose of this section is to point out the assumptions and the basic differences between a classical design and the modern control approach. Only a brief description will be given.

C-1 Summary of Classical Control Design

The classical control design of the inner loop can be subdivided into two basic methods: (a) A continuous design on the s-plane and discretization; (b) A design in the z or w-plane. Both of these methods use the transfer function approach. This classical design is summarized in Fig. IV-5.

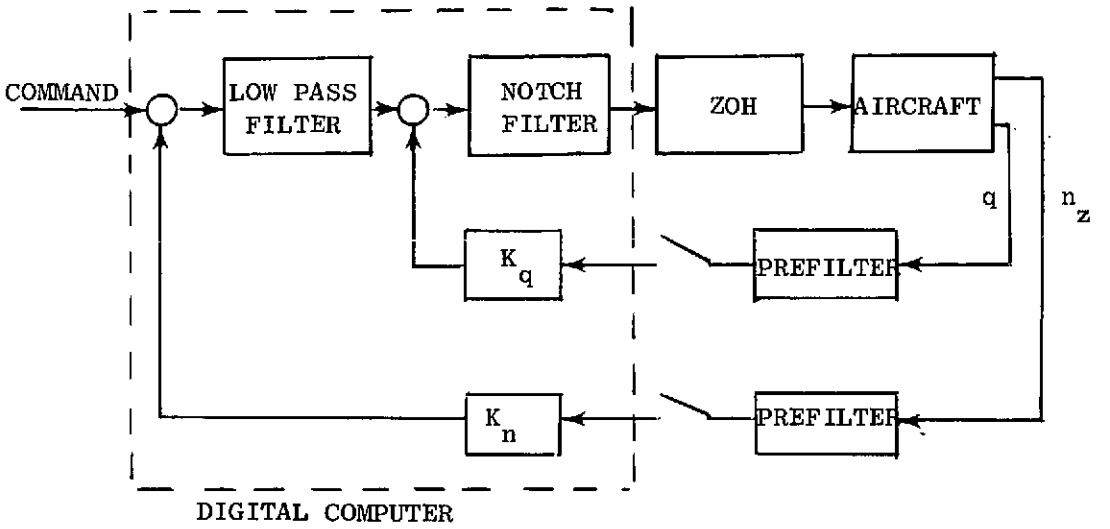

Fig. IV-5 CLASSICAL DESIGN OF THE CONTROLLED SHORT PERIOD MODE

The first method consists of three basic steps:

1. A continuous design of the inner loop based on previous experience.

2. Discretization of the compensation, using digital filter approximations;

3. Modification of the different gains and parameters, in order to diminish the unwanted properties of the sampling (e.g. time lags).

Step 3 can be omitted if the sampling rate is fast enough for the digital filter approximations to cause negligible error. It often results in ω_s 5 to 10 times faster than the bending modes.

Different elements, mechanized on the digital computer, are designed on the s-plane by classical techniques. Discretization is achieved by the Tustin Transform [BO-1, ED-1, and OS-1] or, in rare cases, by z-transform [SU-1]. This design, which works quite well with analog elements, has the following disadvantages: (a) Gust alleviation can only be achieved by a trial and error computation and simulation. (b) The sensitivity behavior on the s-plane doesn't coincide with the sensitivity of the discrete controller. (c) Approximations in digital filters lead to undesired properties of the closed loop system (as aliasing).

The second method consists of two basic steps:

1. Transformation (discretization) to z- or w-plane.
2. Classical design of the digital compensator based on previous experience.

The compensation network is usually designed on the w-plane [ST-1, LE-1] because of its similarity to the s-plane (c.f., Chapter II). This is an exact design and therefore the problem of digital approximations is eliminated.

The main disadvantage of the classical approach is its inability to handle multi-input, multi-output design problems. Even Lee [LE-1], who is currently developing a w-plane automatic synthesis program, says, "The use of a classical approach is limited. Sooner or later, we will have to start design in the state space."

C-2 Optimal Discrete Design

An optimal discrete synthesis, based on quadratic criteria, includes a full state-variable feedback and an optimal steady-state observer. This is an exact design; no approximations are made as in the first classical design, where the continuous compensation was made discrete.

The discrete compensator, calculated for a predetermined sampling interval, always yields a stable system which minimizes given quadratic criteria. However, these properties are only correct if the assumptions about the controlled system are perfect; i.e., the system is linear, there are no limitations on actuator bandwidths, the designer has a good knowledge of the systems parameters, etc.

Furthermore, for a real system, the designer has to face a whole new set of problems: (a) What model to use; (b) How to determine the cost function; (c) How to achieve a proper time response; (d) How to handle nearly undisturbable states; (e) How to reduce the sensitivity to parameter variation; (f) What sampling rates to choose in order to obtain a minimum response to external disturbances; (g) How the system behaves for longer sampling intervals (roughness). The last three problems will be answered in Chapters V, VI, and VII. The first four

problems will be partially answered by outlining the optimal discrete design of the principal example. The optimal design is based on the Separation Theorem [GU-1] which shows that the controller and the observer can be designed separately.

a. The controller design.

The main difficulty in an optimal control design is to find the numerical value of the weighting matrix A of the quadratic criteria. This problem is further complicated by the nonminimum phase property of the F-H short period mode.

The necessity for a fast response conflicts with the effort to alleviate the wind gusts. Therefore, the root square locus approach was used [BR-4]. The short period poles are relocated to an acceptable region, while in the meantime the gust response is minimized. No weight is given to the bending states x_3 and x_4, since no attempt will be made to control the bending mode (during the first design). Similarly, no weight will be given to w_g.

The root square locus of the short period mode, based on Eq. (4.1) is: (a) for a continuous system

$$1 + \frac{A_q}{B}\, y_q(-s)y_q(s) + \frac{A_\alpha}{B}\, y_\alpha(-s)y_\alpha(s) = 0 \; ; \tag{4.9}$$

(b) for a discrete system:

$$1 + \frac{A_q}{B}\, y_q(z^{-1})y_q(z) + \frac{A_\alpha}{B}\, y_\alpha(z^{-1})y_\alpha(z) = 0 \tag{4.10}$$

where

$$y_q = \frac{q}{\delta_e}$$

$$y_\alpha = \frac{\alpha}{\delta_e} \; . \tag{4.11}$$

A_q and A_α are the weighting terms in the main diagonal of the weighting matrix A.

In order to obtain a better engineering insight, the root square locus was also traced on the s-plane. Note that the trace on the z-plane depends on the sampling interval.

The root square locus of the F-H short period mode for flight condition No. 8 is given in Fig. IV-7. As can be seen, the minimization of α increases the bandwidth, which is undesirable. Therefore, a combination of A_q and A_α was chosen as a nominal design.

The root square locus for flight condition No. 1 is given in Fig. IV-9. The major problem in this flight condition is the sluggish response to the pilot's commands. Therefore, a bandwidth increase was necessary. We will analyze the time response in more detail in Section IV-D.

The nominal pole design for flight condition No. 1 vs the sampling interval is traced in Fig. IV-9. The damping is nearly unchanged.

b. The observer design.

An observer design, which uses steady state optimal techniques, is straightforward if the power spectral density matrices of the noises are known. But the nearly undisturbable modes are a problem which needs further clarification. A nearly undisturbable mode, in our case, is the bending mode, which is primarily excited by the elevator's input [BL-1, BO-1, ED-1]. In this case, the observer error corresponding to the bending mode is virtually undamped. Only Sutton [SU-1] assumes a slight excitation of the bending mode by the external disturbance. Consequently, for this particular mode, the optimal filter yields a very low gain in the observer error equations. In order to avoid this situation, an artificial noise will be applied to the bending mode state. This is done only for computational purposes and it is equivalent to a pole placement of the observer error. Another method, which relocates the observer's error poles of the undisturbable modes and uses an optimality criteria, is currently being developed by Breza and Bryson [BRE-1]. This method can be extended to a discrete system.

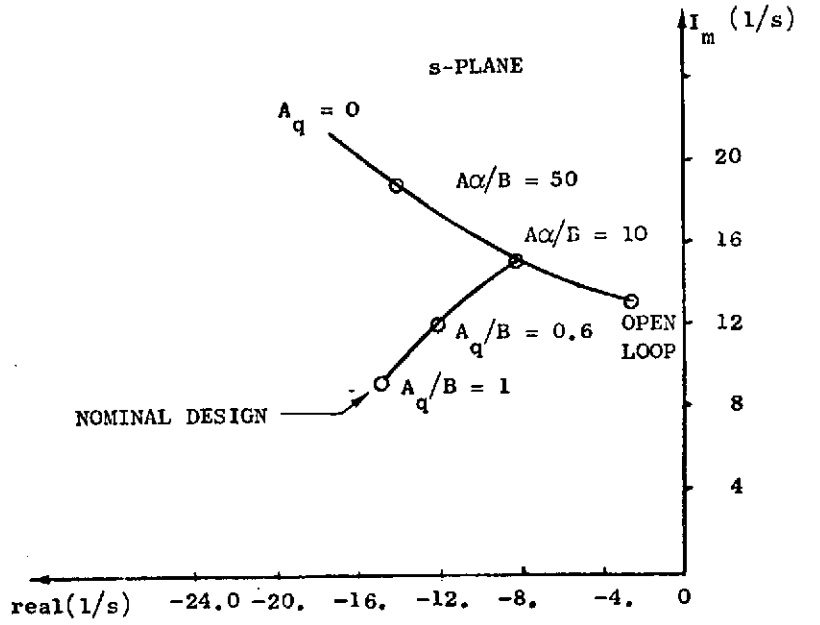

FIG. IV-6 POLES LOCATION VS WEIGHTS OF THE F-H SHORT PERIOD MODE. Flight Condition No. 8.

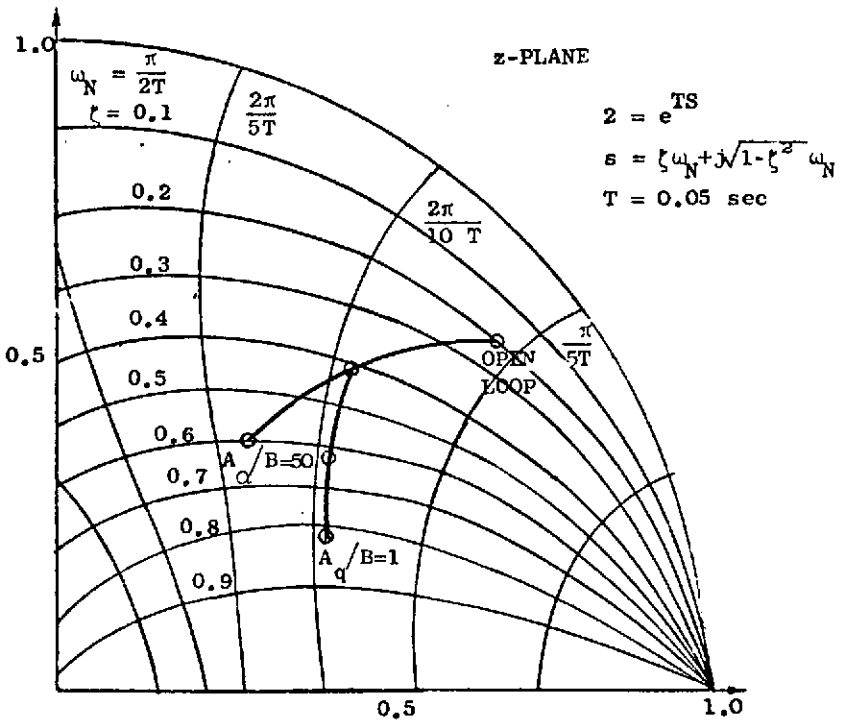

FIG. IV-7 POLES LOCATION VS WEIGHTS OF THE F-H SHORT PERIOD MODE. Flight Condition No. 8.

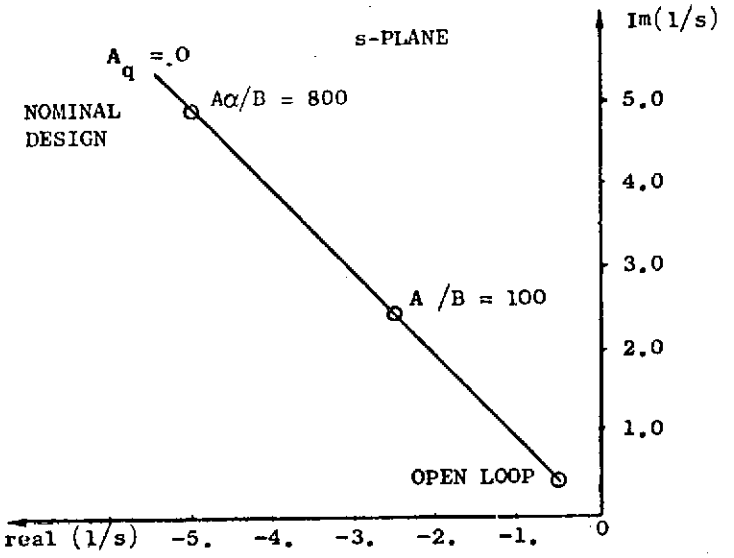

FIG. IV-8 POLES LOCATION VS WEIGHTS OF THE F-H SHORT PERIOD MODE. Flight Condition No. 1.

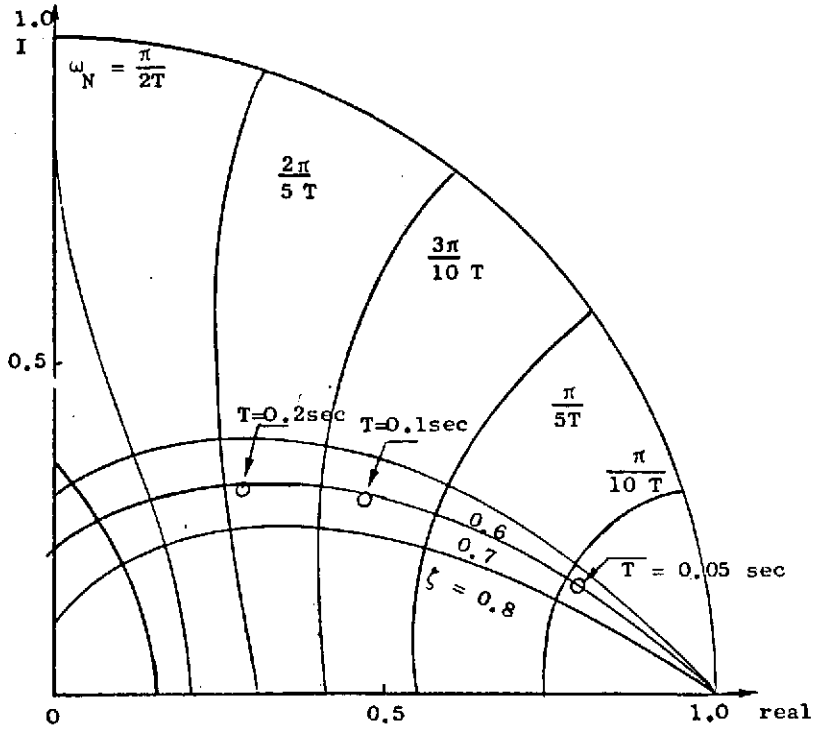

FIG. IV-9 THE POLES OF THE NOMINAL DESIGN OF THE F-H SHORT PERIOD MODE vs SAMPLING INTERVAL. Flight Condition No. 1.

In this chapter we are interested in the time response to the pilot's commands. Those commands are fed simultaneously to the plant and to the observer. Therefore, during the first seconds, the time response of the plant is unaffected by the observer error poles. In Chapter VI, where we deal with the sensitivity problem, the location of the observer error poles will be investigated in detail.

D. THE TIME RESPONSE OF THE F-H SHORT PERIOD MODE EXAMPLE

One of the objectives of the optimal discrete controller is to minimize the average pitch rate q and the average total angle of attack α_T. This is accomplished by determining a proper weight on the states in the quadratic cost function. But we are limited in our choice, depending on: (a) the bandwidth of the actuator (~ 45 rad/sec); (b) the maximum amplitude of the actuator (0.4 rad); (c) a proper time response.

The closed loop poles are far below the bandwidth of the actuator and the restriction is the time response. We will explain in detail how a proper time response is achieved and how the time response is related to the closed loop poles and to the sampling interval.

The link between the pilot and the behavior of the aircraft is described in Fig. IV-10.

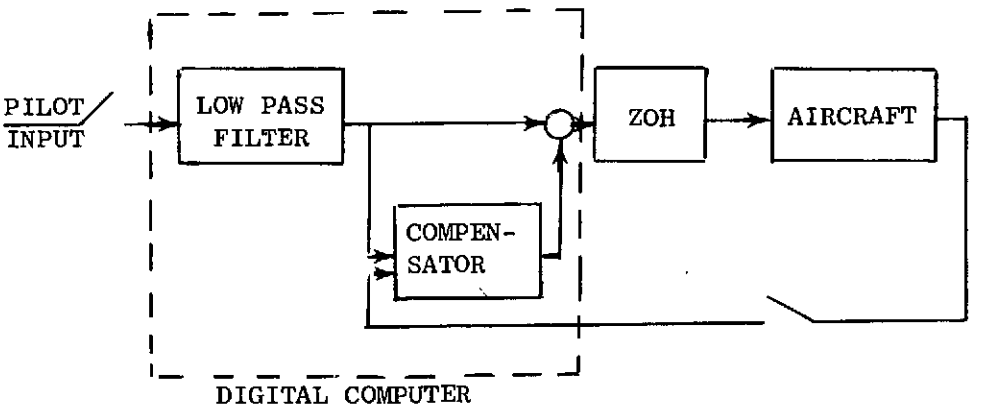

FIG. 4.10 THE CONTROL CONFIGURATION OF THE SHORT PERIOD MODE

The low pass filter is necessary and serves two purposes: (a) It is known from previous experience [BO-1, SU-1] that pilots favor a smoothed stick input with a time constant of 0.4 to 0.6 sec. (b) The low pass filter helps to reduce the pitch rate overshoot of the controlled configuration.

The only way to visualize the time response to the pilot input is to simulate it. Our results are based on a simulation scheme described in Appendix B.

We will now explain in detail how the pilot command is actually processed by the system. This detailed analysis is important.

The time $t = 0$ will be defined as the instant when the pilot executes the δ_{s_o} stick input (a step function). The information about this command will reach the computer within T time (T sampling interval). In order to be on the safe side, we have to assume a full delay $T_1 = T$ between the δ_{s_o} and the time the computer receives this command (δ_{s_1}). Some mechanization of the first order filter on the aircraft computer will generate one delay interval ($T = T_2$). See Fig. IV-11. u_{δ_e} is the output of the digital low pass filter.

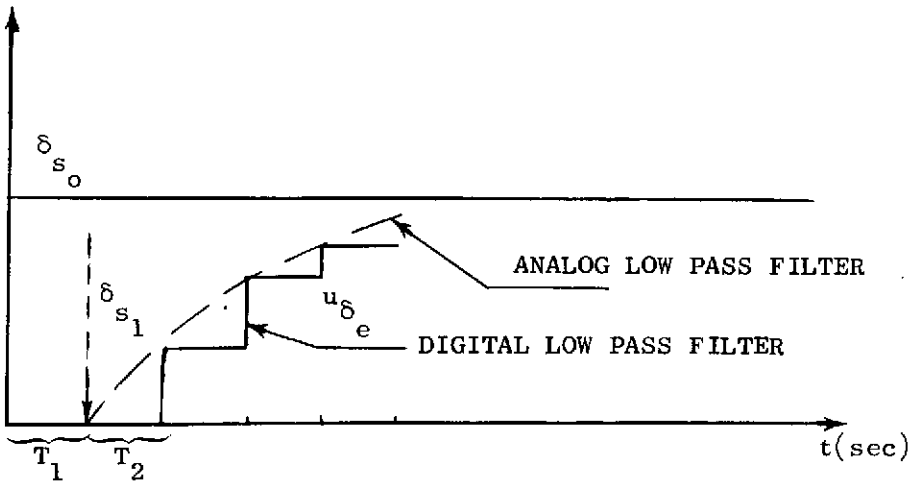

FIG. IV-11 THE INPUT TIMING

One of the delay intervals, T_2, can be eliminated if an analog low pass filter is implemented. However, in this case, we are losing the

option of changing the time constant of the low pass filter for different flight conditions in the digital computer. We assume that the low pass filter [as in BO-1 and SU-1] is mechanized on the digital computer and is a part of the discrete control system. The control configuration described in Fig. IV-10 is closed by an additional feedback loop--the pilot, who is sensing θ (the pitch angle). The pilot's transfer function includes a pure delay ($\Delta t \cong 0.3$ sec), and together with the delay caused by the digital system, this loop may be unstable. A current research done by Stapleford [STA-1] shows that by lowering the sampling rate to $\omega_s = 10$ to 15 cps, the pilot rejects this sampling rate before instability occurs. The reason for this rejection is the roughness of control.

The simulation results for different flight conditions and different sampling rates are analyzed and evaluated as follows:

(a) Flight condition No. 1 (zero altitude, Mach 0.19). The behavior of the aircraft is plotted in Fig. IV-12. The first plot is the response of the free (uncontrolled) aircraft to an elevator step-input. As shown, the response is slow and unsatisfactory (TRP $\cong$ 1.0). Fig. IV-12 shows that after the closed loop pole relocation, the response to δ_e is fast but with an excessive pitch overshoot (TRP $\cong$ 0.27). By filtering the pilot stick input, a good time response was obtained (TRP $\cong$ 0.1).

The time response for lower sampling rates is plotted in Fig. IV-13 and Fig. IV-14. As far as the TRP criterion is considered, the limit on the sampling interval is in the vicinity of $T = 0.1$ (Fig. IV-13). As seen in Fig. IV-14, the slow response (TRP > 0.25) is caused by the two delay intervals, T_1 and T_2.

(b) Flight conditions No. 8 (zero altitude, Mach 1.2). The free flight behavior of the F-H aircraft, in this flight condition,

is characterized by a fast, short period oscillation with a low damping. The time response of the controlled aircraft to a filtered stick input for different sampling rates is described in Figs. IV-15, IV-16, and IV-17.

The time response parameter is within its specifications, but the TRP is not a suitable criterion for this discrete case. As seen in Fig. IV-17, the time response of the pitch rate between the sampling points is essentially a free oscillation. Therefore we may conclude that, for this flight condition too, the acceptable limit on the sampling rate is in the vicinity of $T = 0.1$ sec.

E. SUMMARY

1. To preserve acceptable time response, there is a minimum value of the sampling rate due to the delays introduced by the sampling of the pilot's filtered input. This minimum sampling rate depends on the required speed of response and on the time constant of the pilot's stick filter.

2. A sampling rate selection study was made for controlling the short period motion of the F-H airplane. The maximal sampling interval, T, was found to be in the vicinity of $T = 0.1$ sec; the rigid body short period was 10.5 sec and 0.476 sec for Flight Condition No. 1 and No. 8 respectively, and the first bending mode period was 0.2 sec.

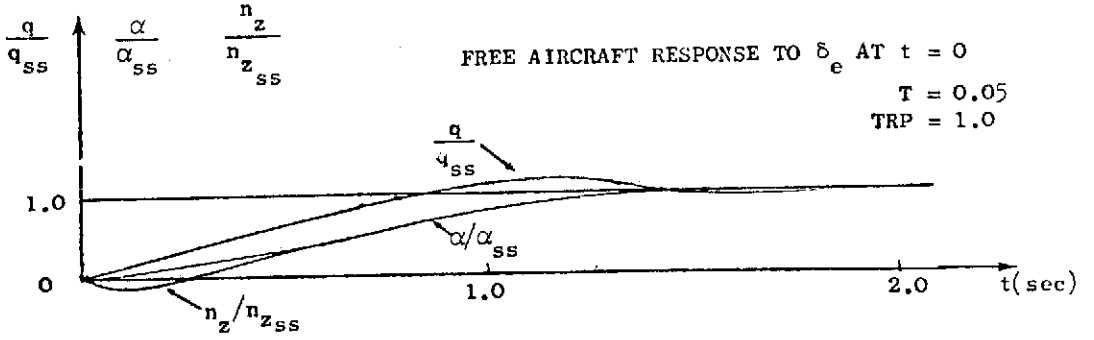

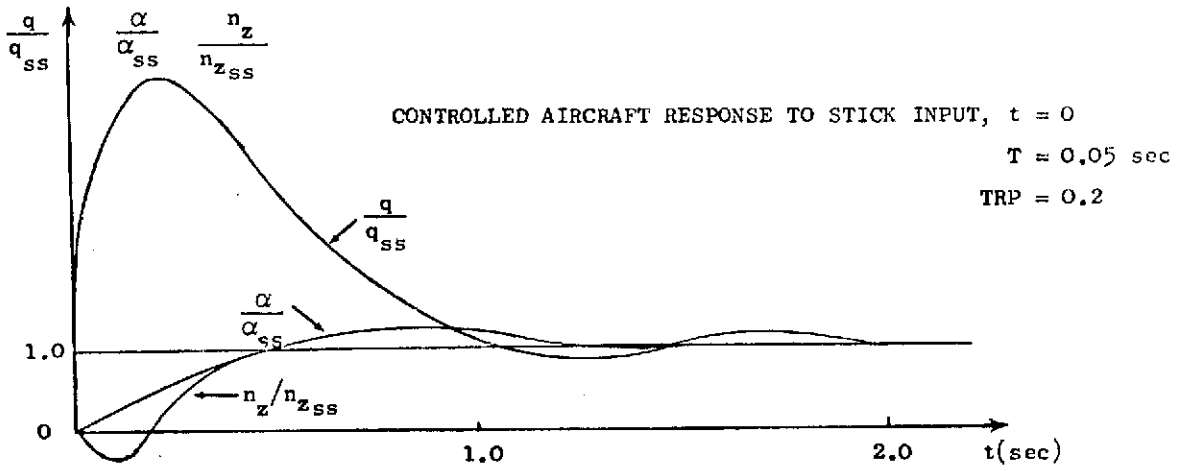

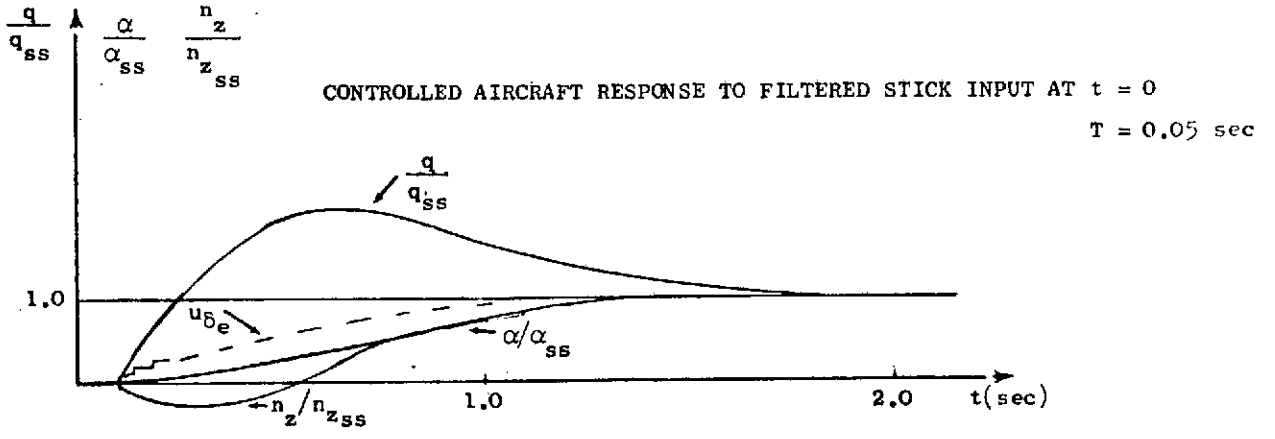

FIG. IV-12 THE F-H SHORT PERIOD TIME RESPONSE TO A STEP INPUT. Flight Condition No. 1.

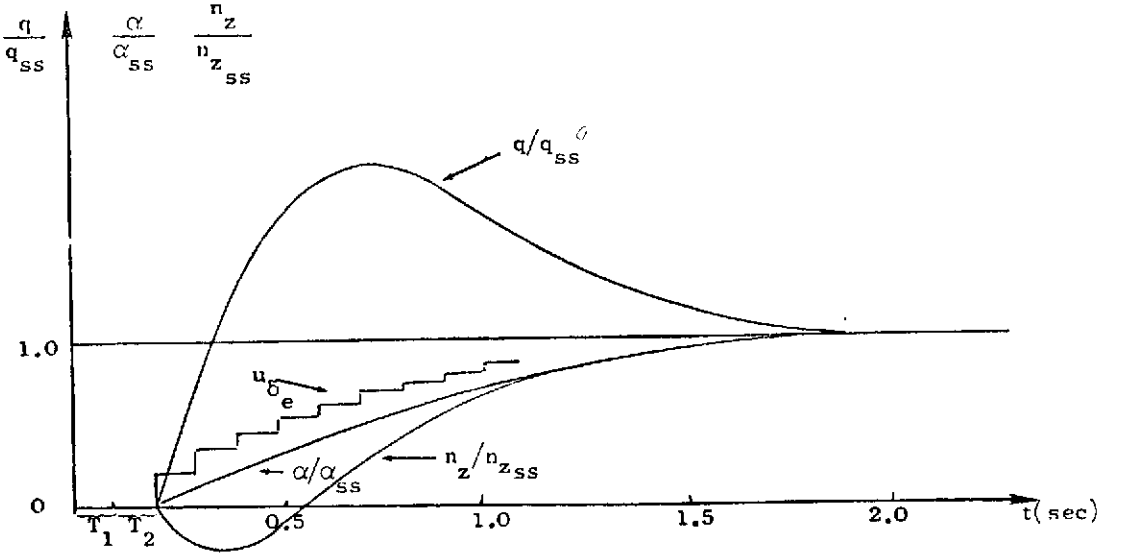

FIG. IV-13 THE TIME RESPONSE OF THE F-H SHORT PERIOD TO A FILTERED STICK INPUT. Flight Condition No. 1. T = 0.1 sec; TRP = 0.18.

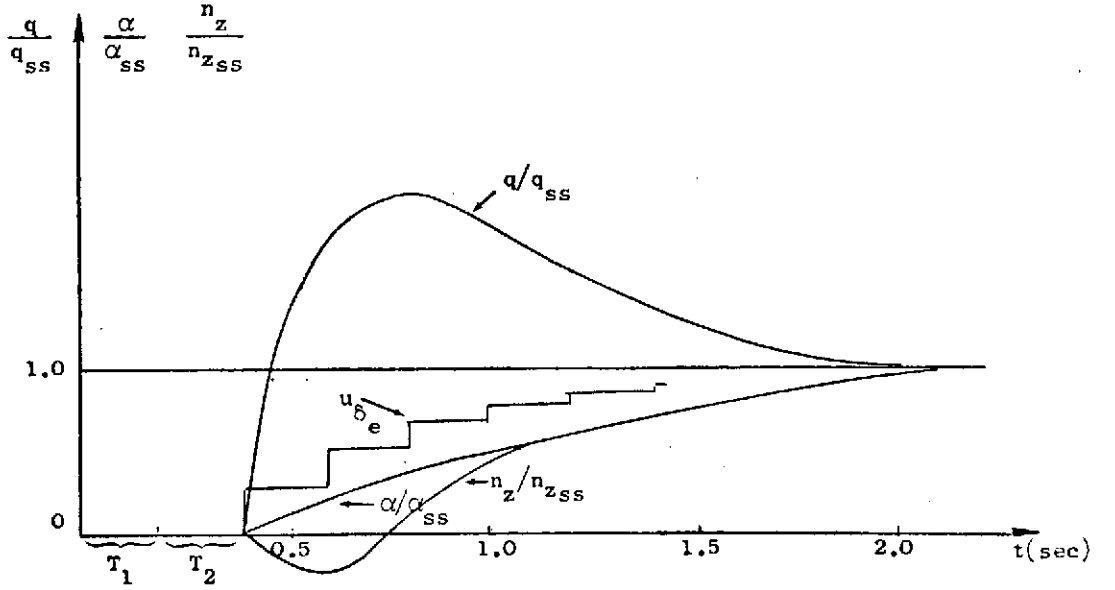

FIG. IV-14 THE TIME RESPONSE OF THE F-H SHORT PERIOD TO A FILTERED STICK INPUT. Flight Condition No. 1. T = 0.2 sec; TRP = 0.3.

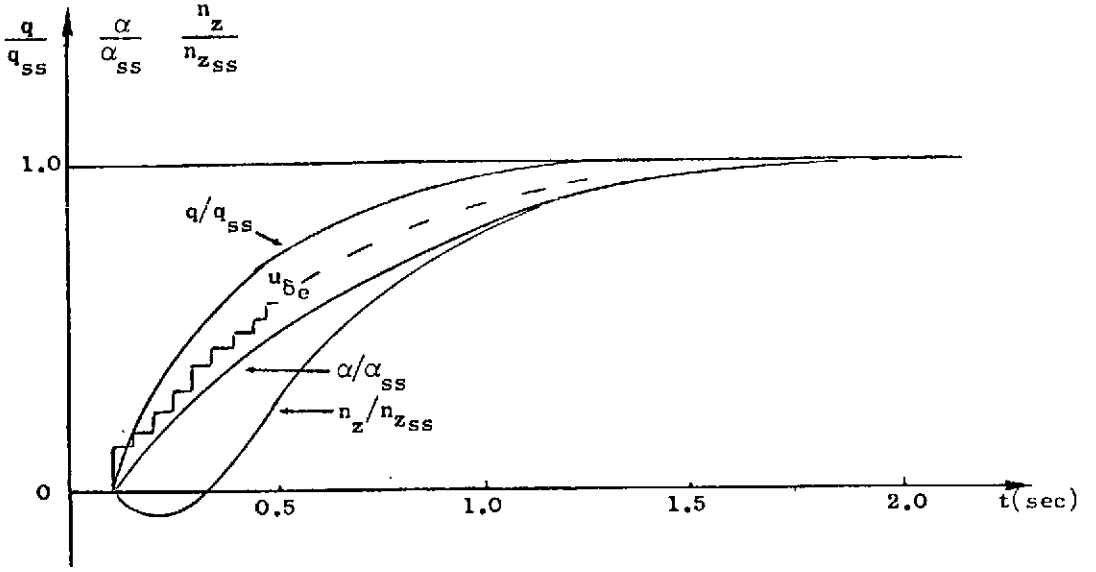

FIG. IV-15 TIME RESPONSE OF THE F-H SHORT PERIOD TO A FILTERED STICK INPUT. Flight Condition No. 8. T = 0.05; TRP = 0.02.

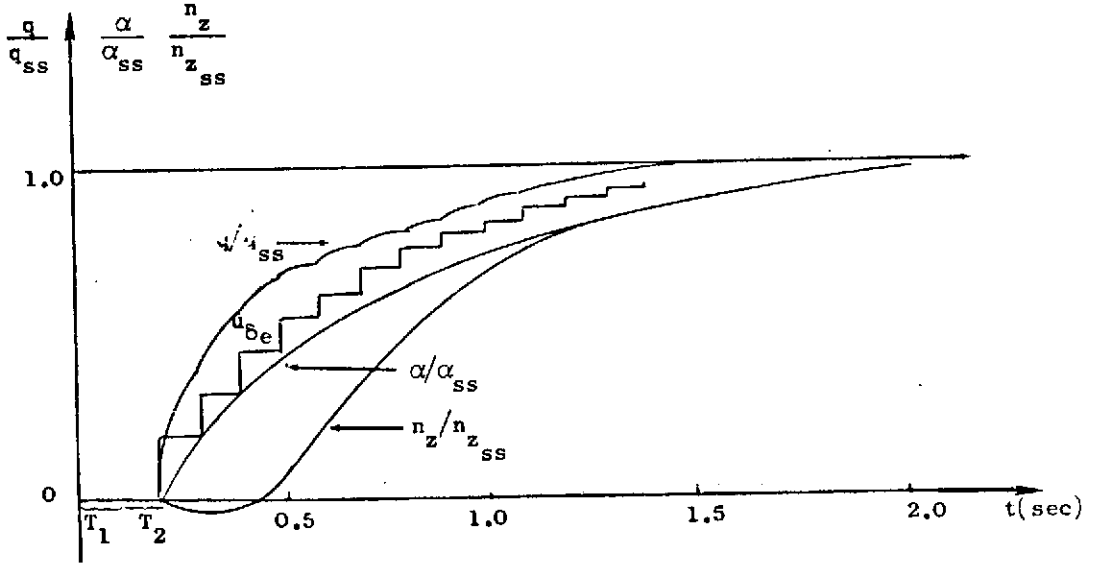

FIG. IV-16 TIME RESPONSE OF THE F-H SHORT PERIOD TO A FILTERED STICK INPUT. Flight Condition No. 8. T = 0.1 sec; TRP = 0.11.

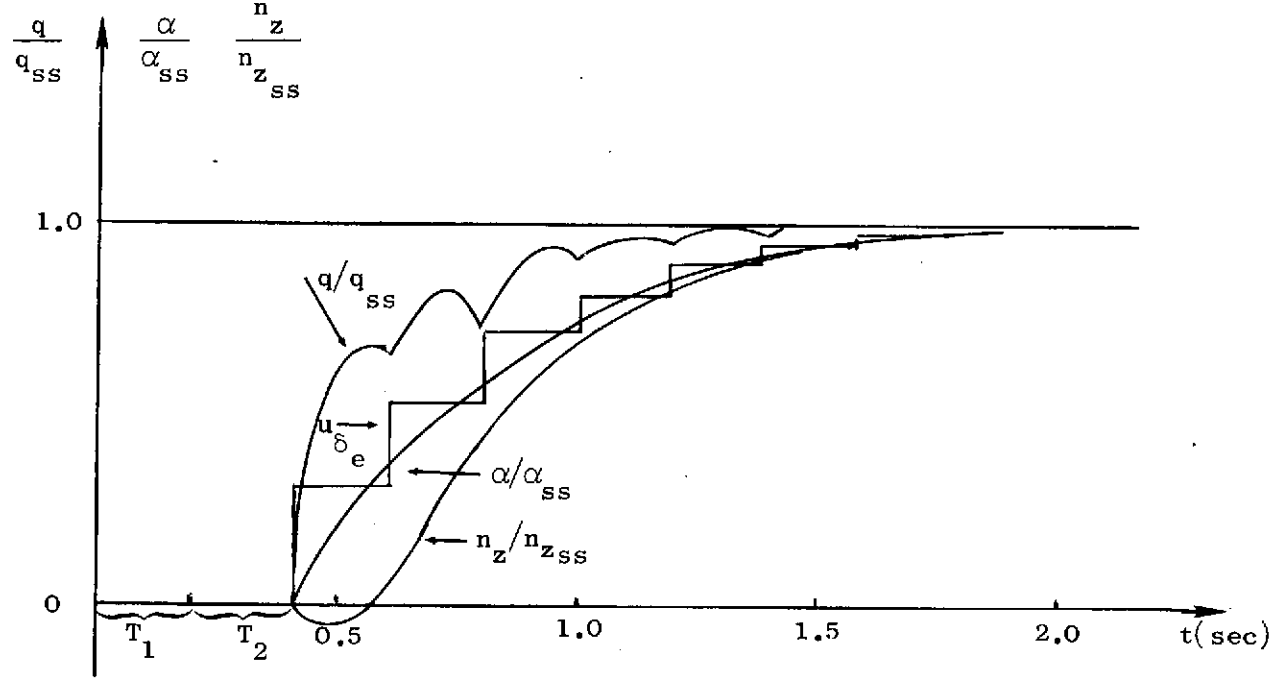

FIG. IV-17 TIME RESPONSE OF THE F-H SHORT PERIOD MODE TO A FILTERED STICK INPUT. FLIGHT CONDITION NO. 8. T = 0.2 SEC. Time response parameter (TRP) = 0.18.

V. SAMPLING AND ROOT MEAN SQUARE RESPONSE TO NOISE

One of the principal objectives of the aircraft autopilot is to reduce the influence of random gusts of wind. The problem of gust alleviation is especially severe during high speed flights at low altitudes. If a discrete control is used, there is a finite time interval between corrective commands. During this time interval, the aircraft's average random motion due to external noise is increasing. If the time interval is too long, i.e., the sampling rate is too low, the rms value of some of the aircraft states may exceed acceptable boundaries. This places an upper limit on the sampling interval.

The first systematic approach to sampling rate selection as it relates to rms response was devised by Berman [BE-1] in 1973. Berman discusses measurements contaminated by white noise at the sampling instant. Then he propagates the state covariance matrix of an aircraft disturbed by white noise until one of the covariants goes beyond a predetermined limit. The elapsed time is the sampling interval. Using this interval, Berman calculates the optimal (Kalman) observer. Controls are predetermined by a pole placement.

However, the purpose of an optimal observer is not only to reconstruct the unmeasured states. In addition, it makes a better estimate of the states than could be obtained from noisy measurements alone. The uncertainty of the measurement taken at the beginning of the sampling interval is only known after the optimal observer has been determined. But the optimal observer can be calculated only if the sampling interval is given. For this reason, Berman's approach would yield a higher value of the covariance than would result from using an optimal observer.

We will show a systematic way to select a maximal sampling interval related to the rms response.

A. PRELIMINARIES

The behavior of a continuous system driven by white or colored noise is well understood and is described in various sources [BR-1, BR-4, KW-1]. A closed loop system, with a perfect observer and a fast controller, may reduce the influence of an external colored noise to any degree of acceptable rms response provided that a proper (quadratic) criteria is assumed and that no restriction is imposed on time response.

In the case of nonminimum phase systems, or systems with a limited amount of control available, the rms response will depend on dynamic characteristics of the closed loop system and on correlation times of the colored noise. Discretely controlled continuous systems, driven by a continuous noise, white or colored, are more complicated. It will be proven that if an unlimited control were available, there is a well defined limit on the noise alleviation. This limit depends on the sampling time.

The objectives of this section are as follows: (1) to outline the basic relationships; (2) to demonstrate the limitation on noise reduction due to sampling.

A-1 Basic Relationships

A continuous plant, F, driven by a colored noise w, may be formulated as

$$\begin{bmatrix} \dot{x} \\ \dot{w} \end{bmatrix} = \begin{bmatrix} \overbrace{F}^{n_1} & \overbrace{G_3}^{n_2} \\ 0 & F_w \end{bmatrix} \begin{bmatrix} x \\ w \end{bmatrix} + \begin{bmatrix} G_1 \\ 0 \end{bmatrix} u + \begin{bmatrix} 0 \\ G_2 \end{bmatrix} \eta \qquad (5.1)$$

where $\eta \rightarrow N(0, Q)$, white noise, and w is n_2 order Gauss-Markov process for the case of a discrete control; the equations are:

$$\begin{bmatrix} x \\ w \end{bmatrix}_{i+1} = [\Phi] \begin{bmatrix} x \\ w \end{bmatrix}_i + [\Gamma_1] u_i + [\Gamma_2] \eta_i , \qquad (5.2)$$

where $\eta_i \rightarrow N(0, Q_d)$.

As described in Chapter III, for practical reasons, we shall choose

$$\Gamma_2 = I = \begin{bmatrix} 1 & & 0 \\ & \ddots & \\ 0 & & 1 \end{bmatrix}$$

and consequently, $Q_d(T)$ will be given as

$$Q_d(T) = \Phi(T)X(0)\Phi(T)^T + \int_0^T \Phi(T-\tau)G_2 Q C_2^T \Phi^T(T-\tau)\,d\tau \,. \tag{5.3}$$

Assuming $X(0) = 0$, $u_i = Cx_i$, the rms response (or the steady state of the Gauss-Markov sequence) is the solution of Bryson and Ho [BR-1],

$$X = (\Phi + \Gamma_1 C)X(\Phi + \Gamma_1 C)^T + Q_d \tag{5.4}$$

where X is the covariance matrix of the states; the square roots of the main diagonal are the rms responses of the states. $\Phi + \Gamma_1 C$ is the closed loop transition matrix, but not necessarily the optimal one. In this case the state of the wind w is not fed back. Equation 5.4 assumes a perfect knowledge of the states of the plant.

If the measurements are highly contaminated by noise, the rms response of the system can be calculated by augmenting the plant equations, (5.1), by observer equations and solving for X from (5.4) for the augmented system.

In Section V-2, we will use the optimal control and optimal filtering approach which was described in detail in Chapter III.

A-2 Basic Limitation on Noise Alleviation Due to Sampling

Contrary to the continuous control systems, the discrete commands are executed at discrete intervals. During these intervals, the system

is exposed to disturbances. The best way to reduce the noise influence is to try to use inputs which will bring the system to zero as quickly as possible. But there is a limit to the noise alleviation no matter what control we use. This will now be shown. First, some general results will be derived.

(a) A linear discrete system controlled by a state variable feedback, can be reduced to a zero state at most in n steps (n-order of the system). A complete proof, using the Caley-Hamilton theorem, is given in Kwakernaak [KW-1].

If Φ_c is the closed loop transition matrix, and

$$x_{i+1} = \Phi_c x_i \tag{5.5}$$

then the results are that (1) Φ_c is a nilpotent matrix ($\Phi_c^n = 0$), and (2) all eigenvalues of Φ_c are located at the origin. In classical control literature, this system is named a "deadbeat" system, or a "finite settling" time design.

(b) Claim: Given a continuous system with zeros at the origin, controlled by an optimal discrete controller, then if all $A_i/B \to \infty$ (unlimited amount of control available), the system is equivalent to a deadbeat system, where A_i is the weight on the state x_i; B is the weight on the control, assuming a single input system.

Proof: Using root square locus, the system (5-5) can be formulated as [KW-1]

$$B + y(z^{-1})^T A y(z) = 0 \tag{5.6}$$

where $y(z)$ is the vector of the transfer functions, $x(z) = y(z)u(z)$, (u scalar), and A is the weighting matrix of the states in the quadratic criteria. The transfer functions $y_j(z)$, where $x_j(z) = y_j(z)\, u(z)$ have the following structure

$$y_j(z) = \frac{z^{m_j}}{P_n(z)} \tag{5.7}$$

where z^{m_j} are the zeros corresponding to the state j, and $P_n(z)$ is the n-order characteristic polynomial of the open loop system. For physical systems, $m_j \leq n$. Using (5.7), Eq. (5.6) can be formulated as

$$\sum_j^n \left(B + \frac{z^{-m_j}}{P_n(z^{-1})} A_j \frac{z^{m_j}}{P_n(z)} \right) = 0 \tag{5.8}$$

or, by multiplying the numerators and denominators by z^{m_j} and rearranging

$$\sum_j^n \left[BP_n(z^{m_j-1})P_n(z) + A_j z^{m_j} \right] = 0$$

as $A_i/B \to \infty$, the poles of (5.7), which are the poles of the closed loop system, approach the zeros of the open loop system (located at the origin), and therefore become a deadbeat system.

Using these results, we can formulate the following theorem.

Theorem: For a discretely controlled continuous system, the rms response to white noise, for any control, is equal to or greater than:

$$X = \Phi^{n-1} Q_d \Phi^{n-1^T} + \ldots + \Phi_c Q_d \Phi_c^T + Q_d \,. \tag{5.10}$$

If all the closed loop zeros are located at the origin, the equality holds.

Proof: The closed loop system, (5.5), driven by white noise, is

$$x_{i+1} = \Phi_c x_i + \Gamma w_i \,. \tag{5.11}$$

From (5.11) we obtain

$$x_{i+n} = \Phi_c^n x_i + \Phi_c^{n-1}\Gamma w_i + \ldots + \Gamma w_i \tag{5.12}$$

but $\Phi_c^n = 0$. Multiplying (5.12) by x_{i+n}^T and averaging yields

$$E(x_i x_i^T)_{i>n} = X \triangleq \Phi^{n-1} Q_d \Phi^{n-1^T} + \ldots + Q_d \,. \tag{5.13}$$

Equation (5.13) gives the lower limit on X. Note: (1) $\Phi_c = \Phi_c(T)$; (2) $X = X(T,Q)$; (3) If not all the closed loop zeros are located at the origin, or A_i/B is limited, then $\Phi^n \neq 0$, in this case, $\Phi^n X_i X_i^T \Phi^{nT} > 0$ and the rms response to white noise is greater than (5.13).

Example: A first order system, driven by a continuous white noise and controlled by a discrete controller, e.g., the following system

$$\begin{aligned} \dot{x} &= ax + gu + w && w \to N(0,\ q) \\ x_{i+1} &= e^{aT} x_i + \gamma u_i + w_i && w_i \to N(0,\ q_d) \qquad (5.14) \\ q_d &= \int_0^T e^{a\tau} q e^{a\tau} d\tau = \frac{q}{2a}\left(e^{2aT} - 1\right). \end{aligned}$$

Closing the loop of (5.14) by $\gamma u = bx_i$ yields

$$x_{i+1} = (e^{aT} + b)x_i + w_i \qquad w_i \to N\left[0,\ \frac{q}{2a}\left(e^{2aT} - 1\right)\right]. \tag{5.15}$$

The rms response of the closed loop system to white noise is the steady state solution of the Gauss-Markov sequence (5.13).

Definition: $\sigma_{x_i}^2 = q_{x_i}$. The steady state value of q_{x_i} is given by the solution of (5.4)

$$q_{x_i}{}_{ss} = \frac{\frac{q}{2a}\left(e^{2aT} - 1\right)}{1 - \left(e^{aT} + b\right)^2} . \tag{5.16}$$

Note: for $T = 0$ (continuous control), $q_{ss} = q/-2(a+b)$, $a + b < 0$. Some properties of (5.16) are: (a) for $b = 0$ or $T \to \infty$, $q_{x_i} \to -q/2a$ which is the open loop steady state covariance of x. (b) for a given T, the deadbeat b is

$$e^{aT} + b = 0 \rightarrow \boxed{b = -e^{aT}}$$

or

$$q_{x_i}{}_{min} = -\frac{q}{2a}\left(1 - e^{-2aT}\right). \tag{5.17}$$

Equation (5.17) shows that even for any control available, $q_{x_i}{}_{min}$ is always finite, and zero response to external noise can be achieved by limiting $T \to 0$ only, $T \to 0 \Rightarrow q_{x_i} \to 0$.

This analysis is strictly valid on sampling points only. If the open loop is stable and the output of the controller is a deadbeat system, then this analysis could be extended to intersample points also.

B. DETERMINATION OF THE MAXIMUM ALLOWABLE SAMPLING INTERVAL

We will analyze in detail the influence of various factors which determine the rms response of a discretely controlled continuous system. Using the expression for rms response calculation derived in Chapter III, we will consider the influence of

1. Different correlation times of external disturbance;
2. Optimal control vs pole placement;
3. Varying accuracy of measuring instrument.

A clearer understanding of these factors will help us to select the proper sampling rate. Our calculation will be carried out for the F-H aircraft example, flying in the most gusty environment.

After detailed analysis in Sections V-B-1, V-B-2, and V-B-3, we will summarize the method of selection of the sampling rate in Section V-B-4.

B-1 Relation Between Correlation Time of The Colored Noise Disturbance and the Sampling Time

For the rms calculations we will use a simplified model of the short period dynamics:

$$\begin{bmatrix} \dot{q} \\ \dot{\alpha}_T \\ \dot{w}_g \end{bmatrix} = \begin{bmatrix} M_q + M_{\dot{\alpha}} & M_\alpha + M_{\dot{\alpha}} \frac{Z_{\alpha_T}}{U} & 0 \\ 1 & Z_{\alpha_T} & 1/U\tau_w \\ 0 & 0 & 1/\tau_w \end{bmatrix} \begin{bmatrix} q \\ \alpha_T \\ w_g \end{bmatrix}$$

$$+ \begin{bmatrix} M_{\delta_e} + M_{\dot{\alpha}} \frac{Z_{\delta_e}}{U} \\ Z_{\delta_e}/U \\ 0 \end{bmatrix} \delta_e + \begin{bmatrix} 0 \\ -\frac{\sqrt{2\tau_w}}{\tau_w U}\sigma \\ \frac{\sqrt{2\tau_w}}{\tau_w}\sigma \end{bmatrix} \eta, \quad \eta \to N(0, 1). \tag{5.18}$$

The wind gusts are modeled as a colored noise disturbance. "Colored" means that the power at the wind gusts is not equally distributed over all frequencies. If, as in our case, a first order Gauss-Markov process is used for the stochastic wind gust model, then the correlation time τ_w determines the spectrum of the wind gust. More power is concentrated in the lower frequencies than in the higher frequencies. The rms value of the wind is related to the integral of the power spectrum and is designated by σ. The mathematical process which

generates this colored noise is based on a first order filter, with the time constant τ_w, which filters a white noise with a power spectral density $2\sigma^2/\tau_w$.

Modeling the disturbance as a colored noise instead of as a white noise has three advantages:

(a) It is a more realistic model from an engineering point of view;

(b) The white noise has a weak mathematical definition [KW-1]; moreover, its total power is infinitely great.

(c) In the short period example, one of the measurements is the acceleration. The acceleration is related to α_T which is combined from the angle-of-attack and wind gusts. If a white noise is used as a model of the wind disturbance, then the measurements are contaminated, not only by the measurement noise, but also by the process noise. This makes the calculation of the optimal observer much more difficult [BR-1].

The colored noise can be characterized by its spectral distribution, or by its correlation function. The correlation function $C_w(\tau')$ indicates how the disturbance at time t relates to a disturbance at time $t \pm \tau'$. The various relationships can be visualized in Figs. V-1 and V-2.

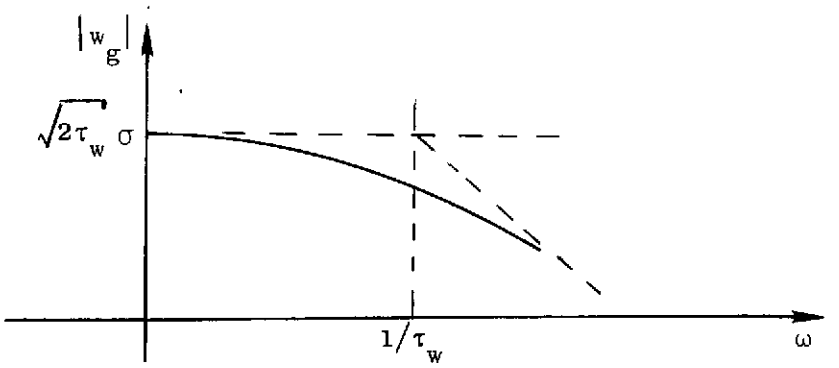

FIG. V-1 THE SPECTRUM OF $|w_g|$.

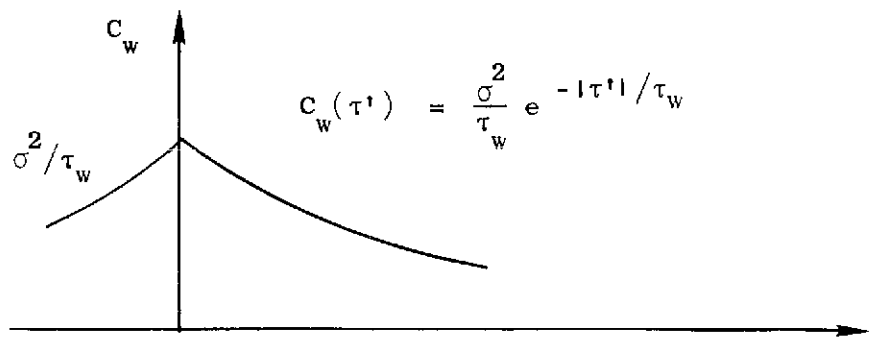

FIG. V-2 THE CORRELATION FUNCTION OF w_g .

To calculate the rms response to a vertical gust, we will compare the influence of different sampling rates and different correlation times. The most meaningful comparison can be made if the gusts have the same intensity, i.e., σ^2 = constant. In this case, σ^2, which is the variance of the wind gust, is related to the intensity of the wind. The energy distribution is schematically described in Fig. V-3 (log scale).

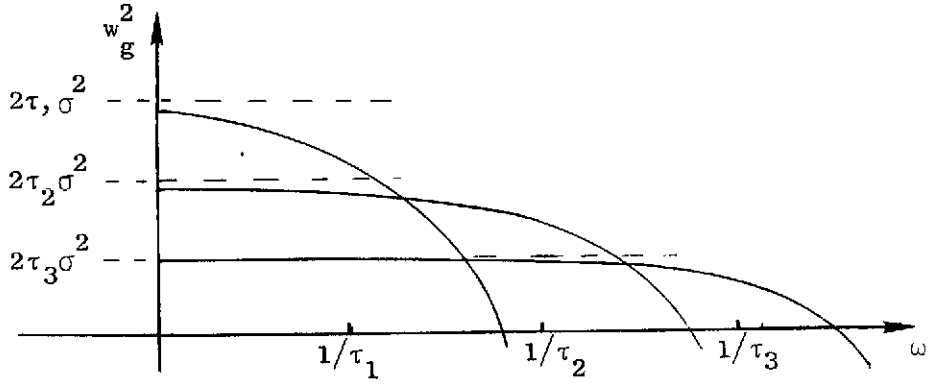

FIG. V-3 ENERGY DISTRIBUTION OF WIND WITH THE SAME INTENSITY AND DIFFERENT CORRELATION TIMES.

The area under each curve is related to the total kinetic energy of the wind and is constant.

Using the methods from Chapter III, the rms response of q and α_T were calculated for different sampling times and different correlation times.

The numerical example we are investigating in this Chapter is the flight condition No. 8. of the F-H aircraft described by Borow [BO-1] and Sutton [SU-1]. This is a flight in zero altitude and at Mach 1.2. It is usually assumed [cf ET-1] that the wind disturbance is "frozen" in space and the velocity of flight determines the correlation time τ_w. Furthermore, τ_w depends on various other factors such as the terrain over which the aircraft is flown (zero altitude). Borow and Sutton each give the average values of σ and τ_w as $\sigma = 12$ ft/sec and $\tau_w = 0.5$ sec. During our investigation, we will vary τ_w only. The total rms response is directly related to σ and therefore it will not be necessary to analyze the influence of various σ's on α_T and q. The rms response depends also on the weighting matrices in the quadratic cost function. In Chapter IV we described how the weights on the states are chosen. It was shown that the selection of the weights represents a compromise among such factors as rms response, time response to a pilot input, bandwidth of the actuators, and of the closed loop system. Taking into account these considerations, the selected weights and the corresponding closed loop roots are summarized in Table V-1:

Table V-1

LOCATION OF THE CLOSED LOOP ROOTS, FLIGHT CONDITION No. 8

Closed Loop Roots \ Sampling Time	T = 0.005 sec	T = 0.05 sec	T = 0.1 sec
z-plane	0.929±j0.045	0.41 ± j0.22	0.065±j0.15
s-plane	-14.5±j9.6	-16 ± 12.0	-17±j12.5

Open Loop Roots: $s = -2.5 \pm 13.5$

Weights: $A_q/B = 0.12\ (\text{sec}^{-1})$, $A_{\alpha_{T/B}} = 11.0$ [0].

The results of the rms response calculations are plotted in Figs. V-4 and V-5 as a function of various sampling times and various correlation times. $\bar{q}$ is the rms response of the pitch rate. Reduction of the pitch rate of the F-H example when the aircraft is flying at zero altitude, is important for precise aiming. $\bar{\alpha}_T$ is the rms value of the total angle of attack, and includes the angle of attack generated by the vertical gust. α_T is directly related to the lift and therefore to the vertical acceleration, which in turn determines the pilot's comfort. Figure V-4 demonstrates how the rms response increases as the sampling interval increases. Figure V-5 demonstrates that a system disturbed by colored noise is better able to alleviate noise with a longer correlation time and identical intensity.

Certainly the designer cannot choose the correlation time of the vertical noise; this is an empirical, measured quantity. But these figures show that it is important to identify the correlation time of the disturbance and not only the rms value of the gust. For the same intensity of the vertical gust, the designer can choose a longer sampling interval if he knows the correlation time of the external noise.

B-2 Reduction of RMS Response by Optimal Control Compared to the Classical Approach.

As explained in the previous section, there is a definite relationship between sampling time, correlation time, and rms response. Gust alleviation can be achieved by classical control methods, essentially by pole relocation, but maximal reduction can be obtained by using existing knowledge of noise characteristics. Colored noise is characterized by its correlation time constant. For longer correlation times, we may make a more accurate prediction of future behavior of the disturbance and consequently we may apply better feedback control in order to reduce the disturbance influence. We will describe in more detail how the optimal controller uses the information on behavior of w_g in the following equation, repeated from Eq. (5.2):

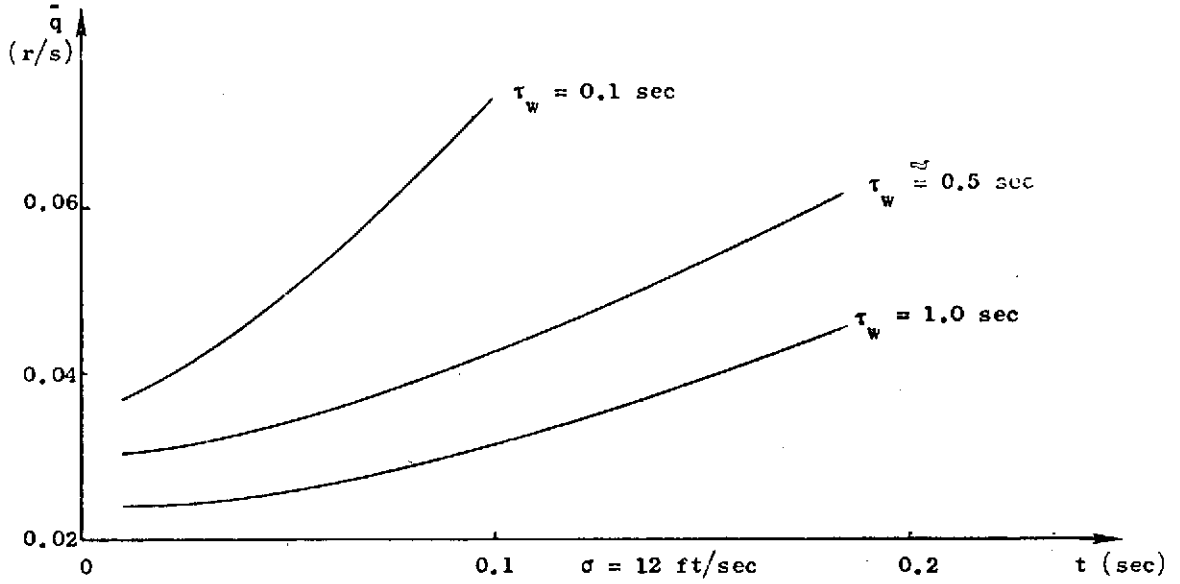

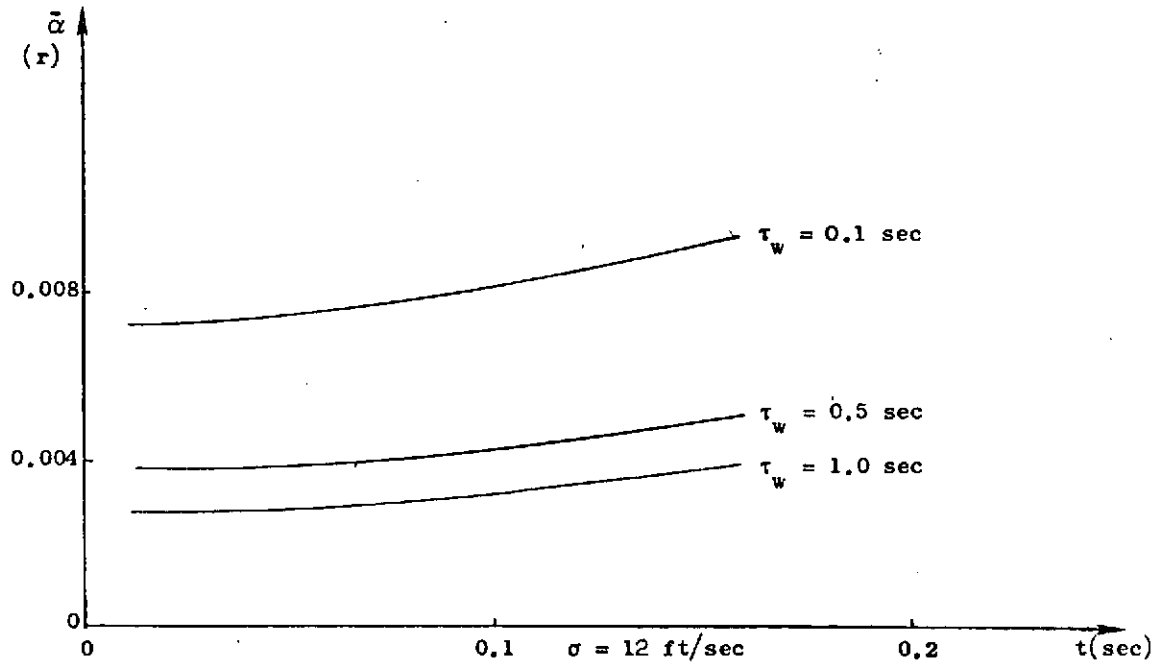

FIG. V-4 RMS RESPONSE OF THE F-H SHORT PERIOD MODE AS A FUNCTION OF SAMPLING TIME, T.

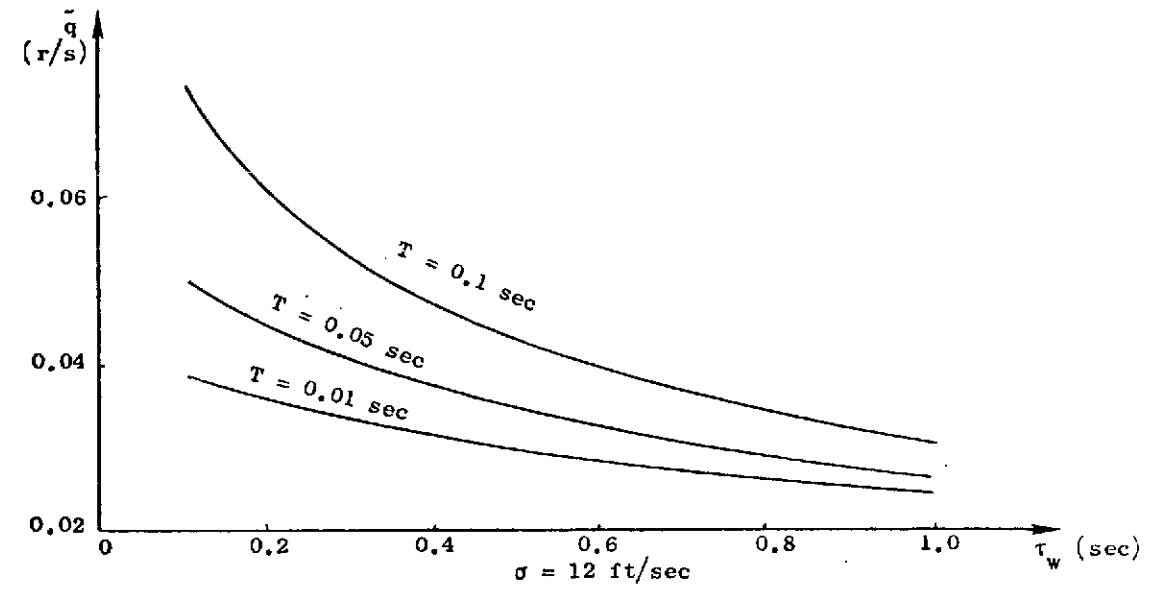

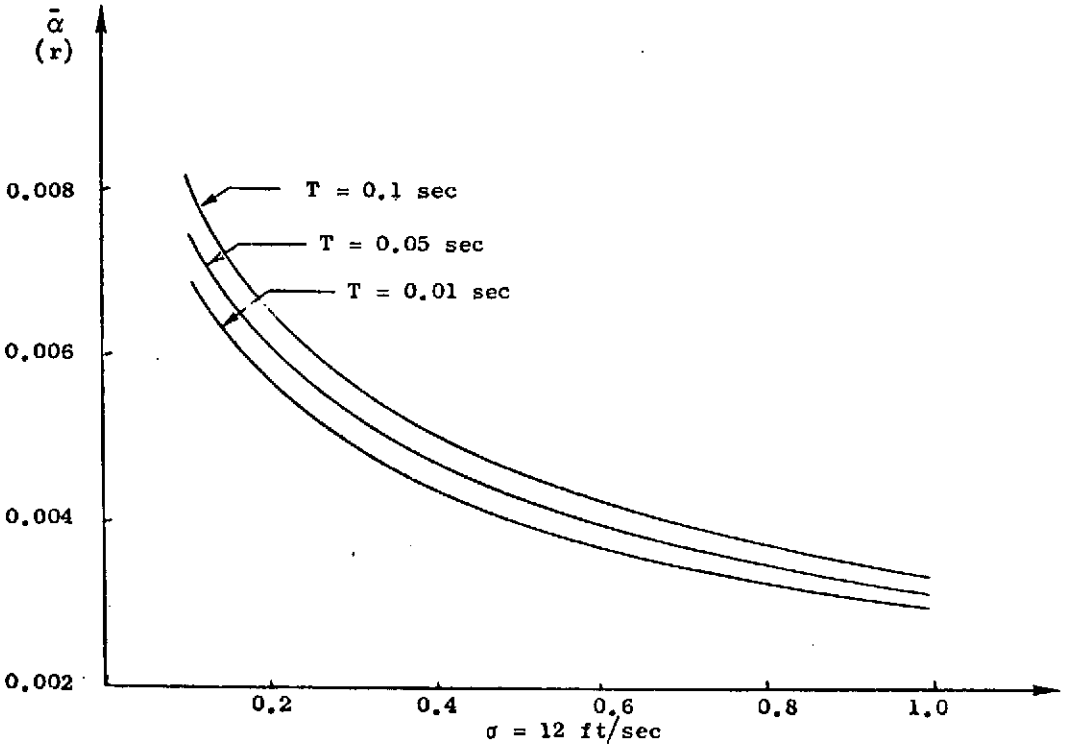

FIG. V-5 RMS RESPONSE OF THE F-H SHORT PERIOD MODE AS A FUNCTION OF CORRELATION TIME τ_w. σ = 12 ft/sec.

C - 2

$$\begin{bmatrix} x \\ w_g \end{bmatrix}_{i+1} = [\Phi] \begin{bmatrix} x \\ w_g \end{bmatrix} + \Gamma_1 \; u_i + [\Gamma_2] \; \eta_i \qquad \eta_i \rightarrow N(0, \; Q_d).$$

The matrices Φ, Γ_1, Γ_2 and the covariance matrix Q_d have the following form:

$$\Phi = \begin{bmatrix} \Phi_1 & \Phi_{12} \\ 0 & \Phi_{22} \end{bmatrix}$$

$$\Gamma = \begin{bmatrix} \Gamma_1 \\ 0 \end{bmatrix}$$

$$Q_d = \begin{bmatrix} Q_{d_{11}} & Q_{d_{12}} \\ Q_{d_{21}} & Q_{d_{22}} \end{bmatrix} \tag{5.19}$$

$$\Gamma_3 = I = \begin{bmatrix} 1 & & 0 \\ & \ddots & \\ 0 & & 1 \end{bmatrix}.$$

Using the separation theorem, the optimal controller

$$u_i = [C_x \quad C_w] \begin{bmatrix} x \\ w \end{bmatrix}_i$$

is calculated from the deterministic part of (5.2). Furthermore, it could be proven that C_x is unaffected by the extended state of the external disturbance w_g [HAL-1], i.e., C_x is not a function of Φ_{12} and Φ_{22}. In other words, C_x feedback gains of the system states are unaffected by the state of the disturbance, but not vice versa. The feedback gain C_w of the external disturbance depends on the

structure of the system. This indicates the main advantage of the optimal design. Even if the closed loop roots are relocated by other methods to the same position, the feedback gain C_w always reduces the rms response.

The rms response for the augmented short period mode, including wind as a feedback state, was calculated for different sampling times and different correlation times and is summarized in Fig. V-6. Figure V-6 describes the rms response at the pitch rate to a vertical gust for two different designs: (a) $C_w \neq 0$ is the optimal control approach; (b) $C_w = 0$ is equivalent to a pole placement design, the state of the disturbance is not fed back. Figure V-6 clearly shows that the optimal approach will be preferred, especially at low sampling rates and for shorter correlation times of the external disturbance.

B-3 RMS Response for Imprecise Measurements

In this section we will analyze the influence of measurement noise on the rms response to the vertical gust with reference to the F-H example. We have no precise knowledge of the states. Only q (pitch rate) is measured directly. The other two states, α_T (angle of attack) and w_g (wind gust) are estimated by an observer. For our illustrative example, we will not use a reduced order observer even if q is directly measured.

The measurements are made by an accelerometer (n_a), and a rate gyro, q.

$$y = \begin{bmatrix} q \\ n_a \end{bmatrix} \cong \begin{bmatrix} 1 & 0 & 0 \\ \ell_a M_q & (\ell_a M_w - z_w)U & 0 \end{bmatrix} \begin{bmatrix} q \\ \alpha_T \\ w_g \end{bmatrix} + \begin{bmatrix} v_g \\ v_n \end{bmatrix} \qquad (5.20)$$

where

$$\begin{bmatrix} v_q \\ v_n \end{bmatrix} \rightarrow N(0, R) .$$

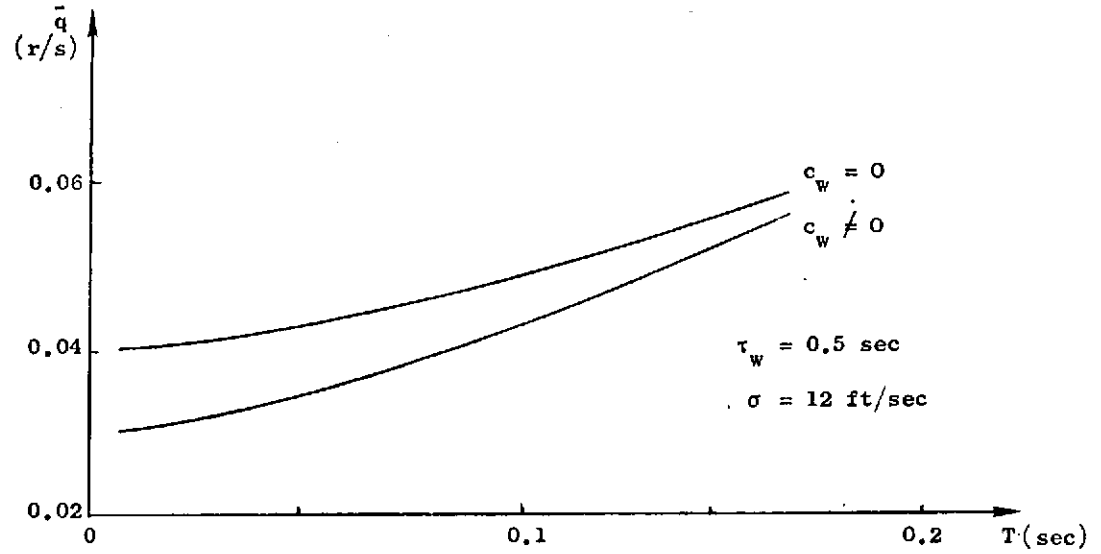

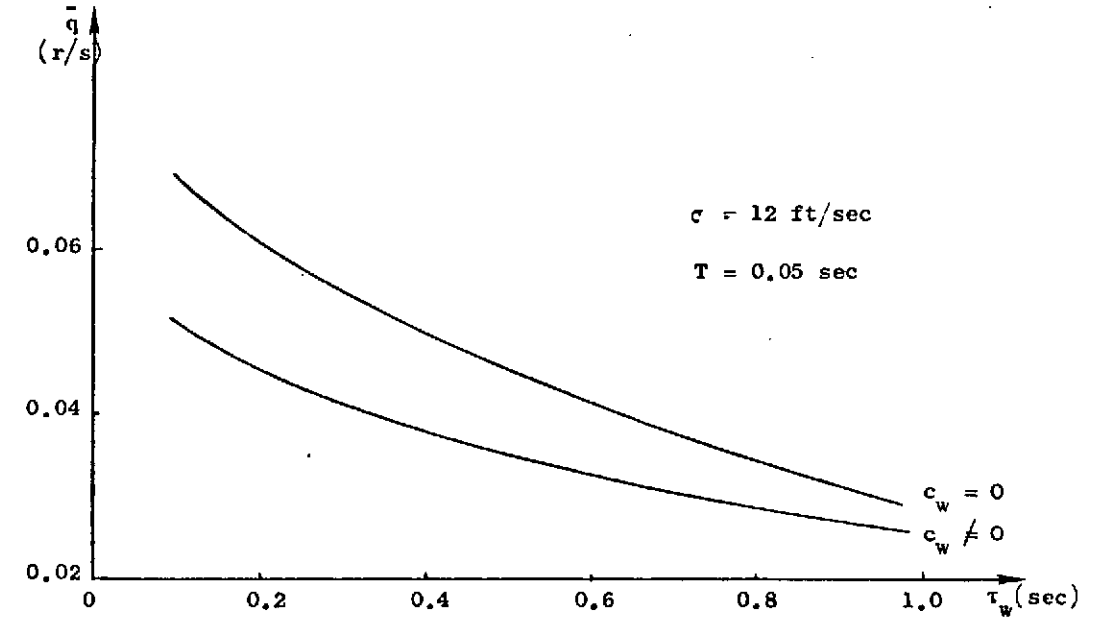

FIG. V-6 COMPARISON OF THE SHORT PERIOD RESPONSE FOR OPTIMAL CONTROL AND POLE PLACEMENT DESIGN.

The power spectral density matrix R of the additive white noise is calculated by the following method. There are two major sources of measurement noise.

1. The A/D converter resolution inaccuracy. This error is regarded as a white noise independent of the sampling rate. Borow [BO-1] assumes the power spectral density of this noise to be 0.1% of the full range of the measuring instrument.

2. The instrument noise. Borow considers this noise to be colored, with a correlation time of about $\tau = 0.01$ sec and an rms level of 0.25% of the full range of the measuring instrument. This continuous colored noise can be approximated as a discrete white noise by a procedure suggested by Bucy and Joseph [BU-1], where the discrete covariance of the sampled noise is given by

$$R = \sigma^2 \frac{1 + e^{-T/\tau}}{1 - e^{-T/\tau}} .$$

The full range of the instruments is approximated in Borow, for the accelerometer $n_{max} \cong 10g$, and for the rate gyro, $q_{max} \cong 1$ rad/sec.

The total measurement noise is derived from these two sources. The equivalent power spectral density matrix of the discrete noise is given in Table V-2.

Table V-2

THE POWER SPECTRAL DENSITY OF THE MEASUREMENT NOISE

T	R_n	R_q
0.005 sec	2.6 ft^2/sec^4	2.6×10^{-5} rad^2/sec^2
0.05 sec	0.8 ft^2/sec^4	8.0×10^{-6} rad^2/sec^2
0.1 sec	0.8 ft^2/sec^4	8.0×10^{-6} rad^2/sec^2

The rms response of the closed loop system was derived in Chapter 3, Eq. (3.86). We repeat it here as a solution X of

$$X - M = (\Phi + \Gamma C)(X - P)(\Phi + \Gamma C)^T.$$

Obviously for larger R, the rms response of the closed loop system will be larger.

In Fig. V-7 the rms response of the pitch rate and the total angle of attack are plotted for different levels of the power spectral densities of the measurement white noise. The price of the measuring instrument is related to its accuracy. Precalculated figures, such as Fig. V-7, can help the designer trade off between the sampling rate, the external noise reduction, and the cost of the measuring instruments.

B-4 Selection of Sampling Rate for the F-H Example

The properties of the external disturbance were given in Section V-B-1. They are $\sigma = 12$ ft/sec, $\tau_w = 0.5$ sec. In Borow and Sutton, no limits were given on the acceptable rms response. The general requirement is to reduce the gust influence as much as possible.

Using the optimal control and the optimal filtering approaches, the rms responses were calculated and plotted in Fig. V-8. The dynamic properties of the closed loop are achieved by proper weightings in the quadratic cost function (Ch. IV), keeping in mind the bandwidth of the actuator and the time response to a step input. From Fig. V-8 we can see that for sampling rates higher than $\omega_s = 20$ cps ($T = 0.05$ sec), little improvement in gust alleviation is realized. Therefore, when gust response is considered, the sampling rate of the F-H short period mode should be in the vicinity of $\omega_s = 20$ cps.

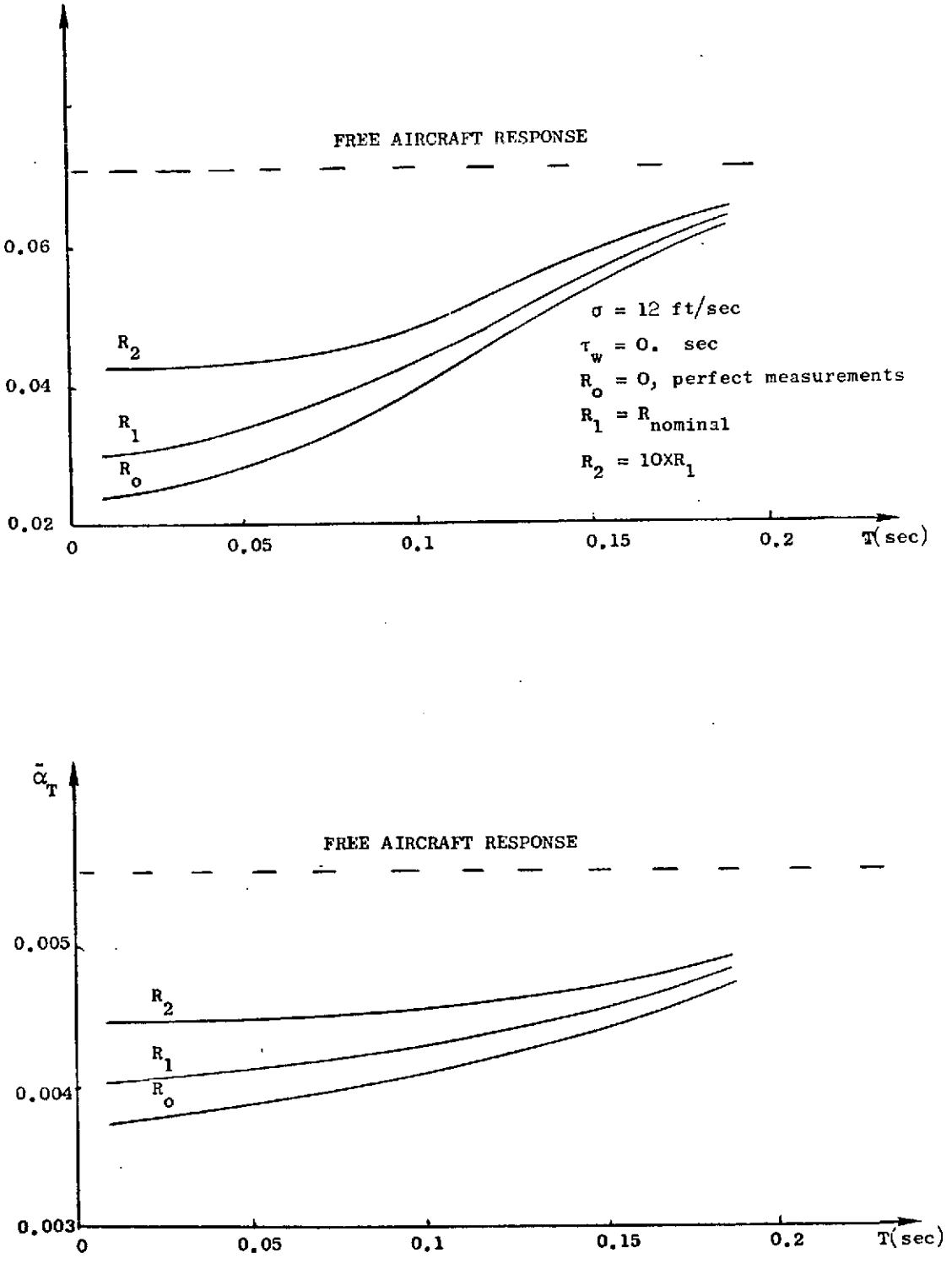

FIG. V-7 RMS RESPONSE OF THE F-H SHORT PERIOD EXAMPLE FOR DIFFERENT MEASUREMENT NOISES.

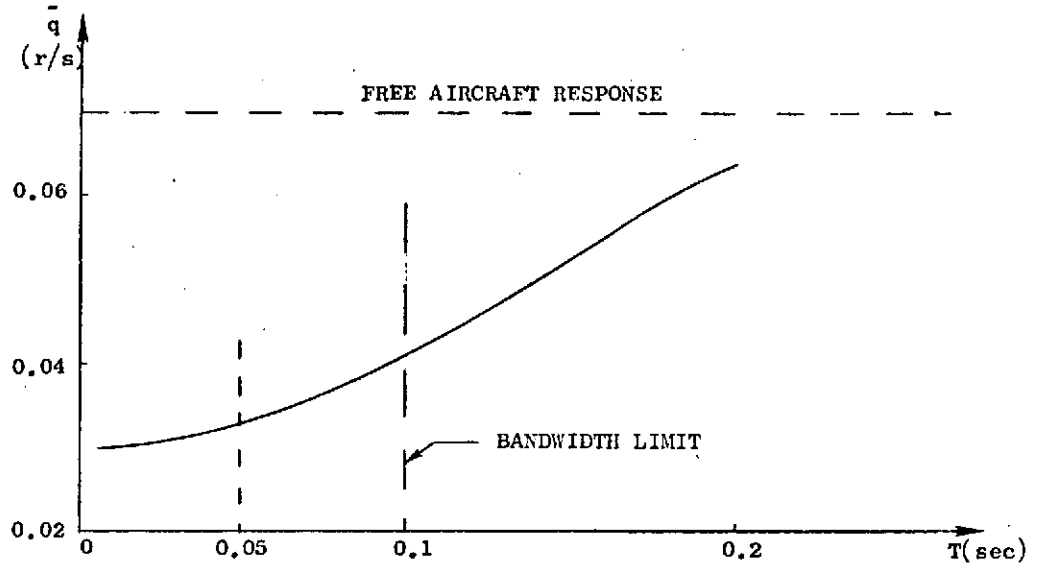

CLOSED LOOP

ω = 10 rad/sec
ξ = 0.8
σ_w = 12 ft/sec
τ_w = 0.5 sec

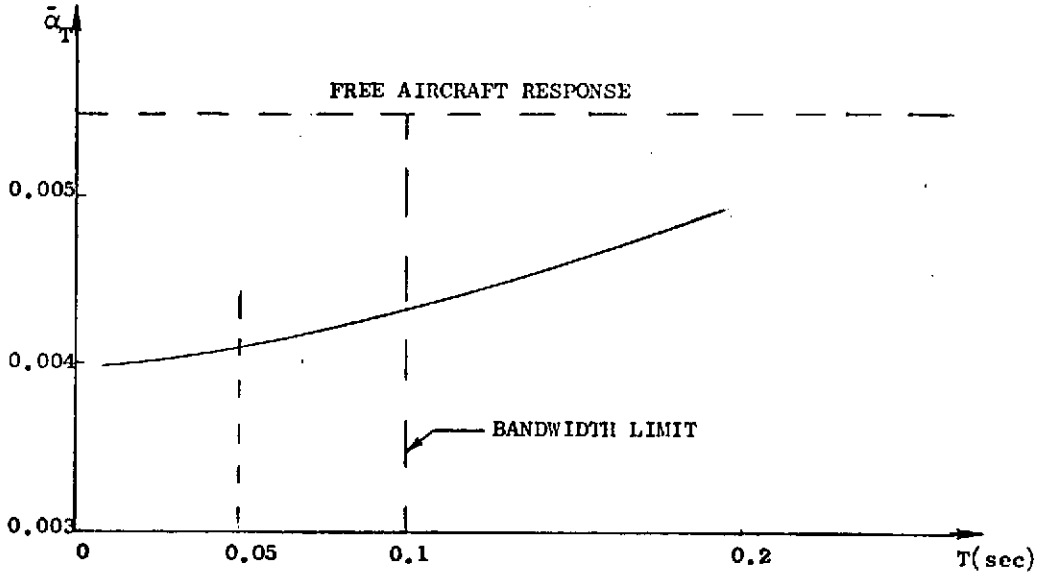

FIG. V-8 SELECTION OF SAMPLING RATE FOR THE F-H SHORT PERIOD MODE.

C. SUMMARY

1. For a discrete controller, the lower limit on the rms response to a random disturbance is a function of the sampling frequency, the rms disturbance level, and the correlation time of the disturbance.

2. By using a simplified model, and a stochastic model of the external disturbances, the designer may determine the lowest sampling rate which will yield an acceptable rms response.

3. Furthermore, by plotting graphs such as Fig. V-7, the designer may choose measurement instruments, which are economical with respect to rms response.

4. We conclude that for our principal example, F-H flight condition No. 8, the sampling rate should be between 10 and 20 cps, in order to reduce effectively the rms response to gust. Any increase in the sampling rate past 20 cps results in a very small improvement.

5. An important consideration is that we are using linear models and therefore the weights on the states should be chosen, keeping in mind the bandwidth of the actuator.

VI. SAMPLING TIME AND SENSITIVITY

In the linear discrete system theory, if a perfect linear model is given, there is no lower limit on the sampling rate, i.e., one can obtain closed loop roots in an arbitrary location in the z-plane for any ω_s (sampling rate). A completely different problem is the sensitivity of the closed loop poles to variations of different parameters of the assumed model. For example, in the F-H short period extended model with the nearly undamped bending mode, the measured signals of the accelerometer and of the rate gyro are contaminated by the bending oscillation. Those combined measurements are fed to the observer which reconstructs the desired states of the system. As shown later, the optimal compensator generates a notch filter which filters the unwanted bending frequency. But if the actual bending frequency differs from the assumed model, the incoming bending frequency misses the notch and is fed back to the elevator as a positive feedback. Potentially, this mechanism can destroy the stability determined using a perfect model of the system. The purpose of this chapter is to analyze this situation and to find a way to reduce the sensitivity to bending frequency variation. We will investigate the following aspects of this problem.

In Section VI-A we will show that in a linear control system, which includes a nearly undamped and uncontrolled frequency, the optimal compensator generates a notch filter. The depth of the notch is directly proportional to the amount of the sensor pickup of the unwanted frequency.

In Section VI-B we will investigate the sensitivity of the short period example to the bending frequency variation. We will show that the sensitivity increases for lower sampling rates.

In Section VI-C a method which desensitizes the system will be shown. The method is based on relocation of the observer error poles and of the closed loop bending poles. The primary goal is to increase the width of the notch filter rather than to control the bending mode.

In Section VI-D we will show how the rms response was changed after the desensitization of the optimal system (as described in VI-C). It will be shown that in this case, the rms response will increase slightly. This is the penalty we have to pay for a less sensitive system.

In Section VI-E we will show that there is a definite relation between the location of the compensator poles and the sensitivity of the closed loop system. A system with a more stable compensator is less sensitive to variations of parameters. A theoretical proof will be given.

In Section VI-F we will look into the possibility of filtering the the bending frequency by sampling at the same rate as the bending oscillation. It will be shown that this approach may cause a hidden excitation of the bending mode. This instability cannot be detected by a regular analysis in the z-plane.

A. FORMULATION OF THE PROBLEM

A-1 Basic Configuration

The basic configuration being investigated is described in Fig. VI-1.

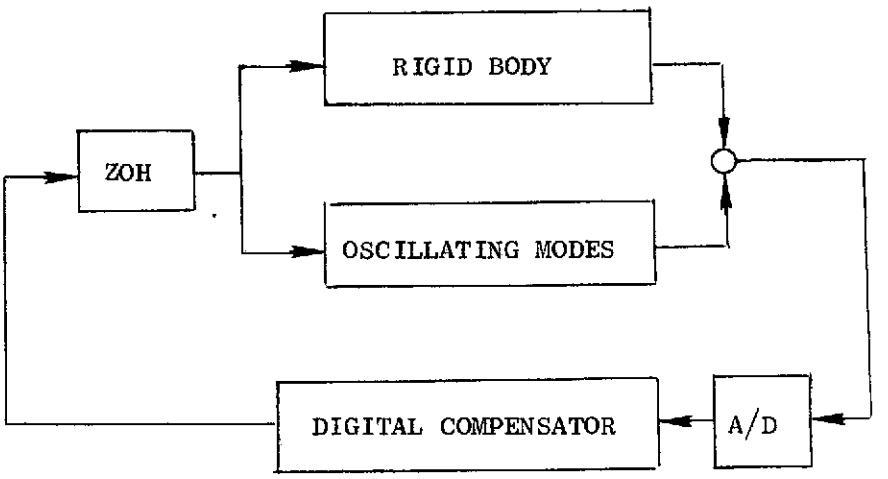

FIG. VI-1 THE BASIC SYSTEM FOR SENSITIVITY INVESTIGATION

The oscillating modes, in our case the structural dynamics, are part of the system. The primary purpose of the compensator is to control the rigid body dynamics, but it must be done in such a way that the bending modes are adequately damped. In the basic system (Fig. VI-1), we assumed that there is no direct coupling between the plant and the oscillating modes. This is the usual approximation found in several sources [BO-1], [BL-1], [SU-1], for modeling the rigid body dynamics and the structural modes. There will certainly be an important coupling if the closed loop bandwidth of the plant will be too near to the bending mode frequency. However, usually the bending mode frequency is higher than the closed loop frequencies. In our short period example, the first bending mode (the slowest), is located at $\omega_b = 25$ rad/sec, while the fastest short period open loop frequency is 13.5 rad/sec. The closed loop short period mode frequency is about 10 rad/sec (flight condition No. 8, see Ch. IV).

Using the results from Chapter III, the different blocks of Fig. VI-1 will be described in more detail in Fig. VI-2, where the following definitions have been made:

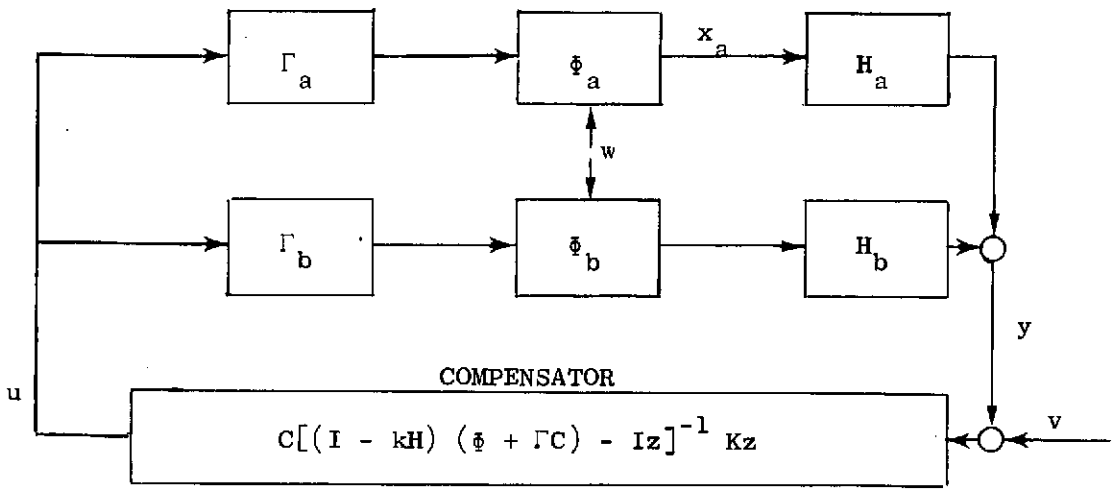

FIG. VI-2 THE UNCOUPLED SYSTEM

$$\Phi = \begin{bmatrix} \Phi_a & 0 \\ 0 & \Phi_b \end{bmatrix}$$

$$H = [H_a \quad H_b]$$

$$\Gamma = \begin{bmatrix} \Gamma_a \\ \Gamma_b \end{bmatrix} \tag{6.1}$$

$$C = [C_a \quad C_b] .$$

As described in Chapter III, the compensator transfer function is based on

$$\left.\begin{aligned} \hat{x}_i &= \bar{x}_i + K(y_i - H\bar{x}_i) \\ x_{i+1} &= \Phi\hat{x}_i + \Gamma u_i \end{aligned}\right\} \text{observer}$$

$$u_i = C\hat{x}_i \qquad \text{controller} \tag{6.2}$$

therefore,

$$u_i = C[(I-KH)(\Phi+\Gamma C)-Iz]^{-1}Kzy_i \qquad \text{compensator.}$$

In this simplified system, the oscillating bending modes are separated from the system, and are only slightly influenced by external disturbances. Sutton [SU-1] and Blakelock [BL-1] assume that the bending modes are not directly influenced by the external disturbance. Their assumption is that the bending mode is excited by the elevator input only. Borow [BO-1] uses a more elaborate model and assumes some direct influence of the external disturbance on the bending mode. We are using the approach of Borow, which is more realistic.

A-2 Optimal Compensator as a Notch Filter

The compensator transfer function (6.3) can be more explicitly written as

$$u(z) = \frac{C\ \mathrm{adj}^{T}[(I-KH)(\Phi+\Gamma C)-Iz]Kz}{\left|[(I-KH)(\Phi+\Gamma C)-Iz]\right|}\ \cdot \qquad (6.4)$$

Using a well known theorem from linear systems theory (e.g., [CH-1]), the zeros of a linear system are unaffected by a state variable feedback and therefore (6.4) can be simplified to:

$$u(z) = \frac{C_1\ \mathrm{adj}^{T}[\Phi - Iz]Kz}{\left|[(I-KH)(\Phi+\Gamma C) - Iz]\right|}\ y(z)\ . \qquad (6.5)$$

Note that in the case of the compensator, the state variable feedback is derived from gains of the observer and of the controller. Furthermore, using the model of (6.1), where Φ_a and Φ_b are uncoupled, and assuming that no attempt is made to control the bending modes, i.e., $C_b = 0$, the numerator of Eq. (6.5) obtains the form:

$$[C_a \quad 0]\left\{\begin{bmatrix}(\Phi_a-Iz)^{-1} & 0\\ 0 & (\Phi_b-Iz)^{-1}\end{bmatrix}\left|\Phi_a-Iz\right|\ \left|\Phi_b-Iz\right|\right\}\begin{bmatrix}K_a\\ K_b\end{bmatrix} z \qquad (6.6)$$

and the simplified compensator transfer function will be

---

† where adj[ ] = cofactor matrix of [ ].

$$u(z) = \frac{\left|\Phi_b - Iz\right| \; C_a \; \mathrm{adj}^T \left[\Phi_a - Iz\right] K_{az}}{\left| \left\{ \begin{bmatrix} I - K_a H_a & K_a H_b \\ K_b H_a & J - K_b H_b \end{bmatrix} \begin{bmatrix} \Phi_a + \Gamma_a C_a & 0 \\ \Gamma_b C_a & \Phi_b \end{bmatrix} - \begin{bmatrix} Iz & 0 \\ 0 & Iz \end{bmatrix} \right\} \right|} \; y(z) \qquad (6.7)$$

Johnson [JO-1], using the relation of (6.6), points out that the zeros of the compensator (represented by $|\Phi_b - Iz|$), consist of a notch filter which is located exactly at the bending frequency. But a proper notch filter is a combination of second order zeros and second order poles [CA-2], as

$$\text{notch filter} = \frac{(z - r_1 e^{j\omega_1 T})(z - r_1 e^{-j\omega_1 T})}{(z - r_2 e^{j\omega_2 T})(z - r_2 e^{-j\omega_2 T})} . \qquad (6.8)$$

Here, ω_2 is as near as possible to ω_1 (ω_1, the tuned frequency). The sharpness of the notch is related to the ratio r_2/r_1. r_1 is related to the damping of the open loop bending mode and cannot be changed. By manipulating the controller gains C and the observer gains K, the notch filter poles can be shifted to a suitable position. However, Johnson, who uses a pole placement approach, considers a completely different criterion when observer error gains are chosen. Their criterion is a proper time response of the whole closed loop system. Usually the time response of a controller-observer design is unaffected by the observer error gains. However, Johnson doesn't feed the input commands to the observer; therefore the system response is significantly influenced by observer gains. As indicated by Eq. (6.2), the pilot input and the measurements are fed to the compensator. Except for sensitivity problems, the observer error gains are chosen by the optimal design from the standpoint of noise statistics. To obtain a better understanding of the filtering action of the compensator, we will investigate the behavior of the compensator for the extended model of the short period example.

As pointed out at the end of Section VI-A-1, several references assume no direct influence at the external disturbance on the bending mode. From a sensitivity point of view, that is a highly undesirable model. The optimal design procedure in this case considers the bending mode to be an undisturbable mode and generates zero gains for the observer's error. Consequently, the damping at the observer's error of the bending mode is nearly zero. We are using the approach of Borow [BO-1], which assumes a direct influence of the external disturbance on the bending mode. Hence, the optimal procedure generates a higher damping of the observer error of the bending mode. See Table VI-1.

Table VI-1

NOTCH FILTER POLES-ZEROS LOCATION. NOMINAL CONFIGURATION, FLIGHT CONDITION No. 8

Open loop bending mode: (notch filters, zeros), T = 0.05 sec)	z = 0.33 ± j0.94
s-plane equivalent:	s = -0.5 ± j25
Observer error bending mode poles, T = 0.05s:	z = 0.32 ±j0.91
s-plane equivalent:	s = -0.98 ± j24.6
Compensator bending mode poles, T = 0.05s: (notch filter poles)	z = 0.25 ± j0.91
s-plane equivalent:	s = -1.3 ± j26.5

The filtering properties of the notch are characterized by the ratio of the open loop bending poles which are the notch zeros, and the compensator bending mode poles. As we can see from Fig. VI-3, the notch is generated by superimposing the frequency response of the poles and the zeros of the notch filter.

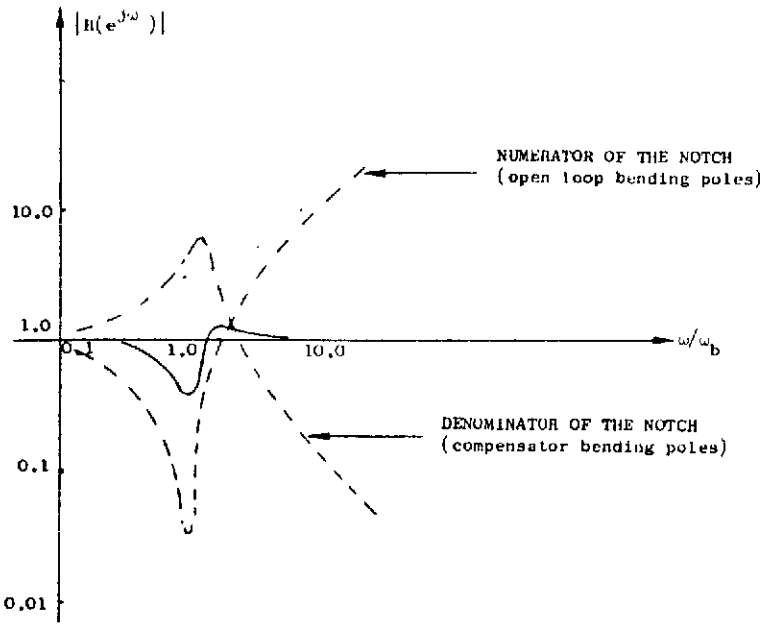

FIG. VI-3 NOTCH FILTER GENERATED BY THE OPTIMAL COMPENSATOR.

The amount of the bending mode pickup, H_b, depends on the location of the measuring instruments with respect to the bending mode. If the accelerometer and the rate gyro are located exactly on their neutral points as per Fig. VI-4, then there is no direct measurement of the bending mode ($H_b = 0$), and the numerator bending zeros (in Eq. 6.7) are cancelled by the denominator bending poles.

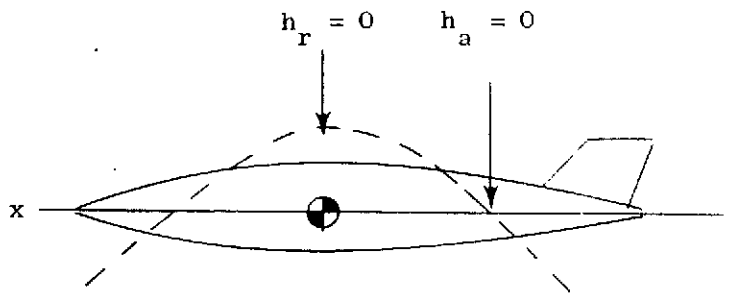

FIG. VI-4 THE NEUTRAL POSITION OF THE ACCELEROMETER (h_a) AND OF THE RATE GYRO (h_r) WITH RESPECT TO THE BENDING MODE.

It is highly impractical to assume that the measuring instruments can be allocated to the neutral points. The neutral points ($H_b = 0$) are changing during the flight. Moreover, the neutral points for higher order bending modes (not considered here) are not in the same positions. Therefore, we will analyze the behavior of the notch as a function of H_b. In Fig. VI-5 the compensator bending pole location is traced as a function of the accelerometer position, assuming that the rate gyro is in a neutral position ($h_r = 0$). As can be seen, the frequency increases, but the damping of the poles is nearly unchanged. Looking at Fig. VI-3, as the frequency increases, the frequency pattern of the poles moves to the right hand side and the depth of the notch increases.

It should be emphasized that in Fig. VI-3, only the notch response is plotted. The total frequency response of the optimal compensator includes all other factors of (6.7).

B. SENSITIVITY OF THE SHORT PERIOD MODE

Based on the previous section, which shows how the optimal compensator filters the unwanted frequency, we will investigate the sensitivity of the system to a variation of this frequency.

B-1 Sensitivity Definition

The sensitivity of the closed loop system is defined as a change in the location of the poles due to the parameter variations of the system. The closed loop system includes the plant:

$$\begin{aligned} x_{i+1} &= \Phi_p x_i + \Gamma_p u_i + w_i \\ y_i &= Hx_i + v_i \quad , \end{aligned} \tag{6.9}$$

and the compensator: (repeated from Eq. 6.2)

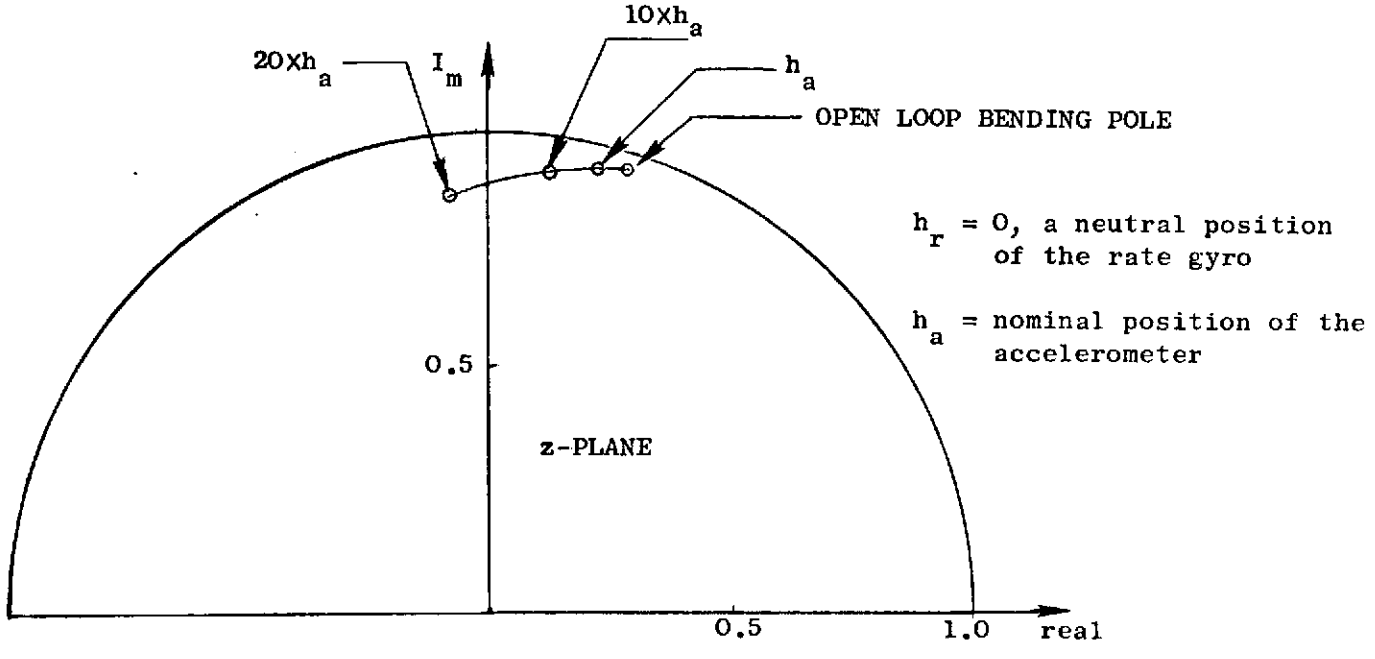

FIG. VI-5 RELOCATION OF THE COMPENSATOR BENDING POLES AS A FUNCTION OF THE ACCELEROMETER PICKUP.

$$\hat{x}_i = \bar{x}_i + K(y_i - Hx_i)$$

$$\bar{x}_{i+1} = \Phi\hat{x}_i + \Gamma u_i$$

$$u_i = C\hat{x}_i \ .$$

If $\Phi = \Phi_p$ and $\Gamma = \Gamma_p$, the assumed model in the observer, is completely identical to the plant, then we will define the observer's error x as $\tilde{x} = \hat{x} - x$.

Combining the compensator equations with the plant equations of state, we get

$$\begin{aligned} \bar{x}_{i+1} &= (\Phi + \Gamma C)(\bar{x}_i - KH\tilde{x}_i - Kv_i) \\ \tilde{x}_{i+1} &= \Phi(I - KH)\tilde{x}_i + \Phi Kv_i - w_i \ . \end{aligned} \tag{6.10}$$

The characteristic equation of the system (6.10) is:

$$\begin{vmatrix} \Phi+\Gamma C-Iz & -(\Phi+\Gamma C)KH \\ 0 & \Phi(I-KH)-Iz \end{vmatrix} = 0. \tag{6.11}$$

The closed loop poles, for a perfect knowledge of the plant parameters, are the poles of the closed loop plant and the observer error system:

$$|\Phi+\Gamma C-Iz| \ |\Phi(I-KH)-Iz| = 0. \tag{6.12}$$

The zeros of expression (6.12) are the poles of the total closed loop system, (6.10). But by inspecting (6.2) and (6.10, we see that the time response of the closed loop is only influenced by the zeros of $|\Phi+\Gamma C-Iz| = 0$. These are the poles of the transfer function $u_i \rightarrow y_i$. It could be shown that the zeros of (6.12) are the poles of the transfer function $v_i \rightarrow y_i$.

If $\Phi_p \neq \Phi$ and $\Gamma_p \neq \Gamma$, then the plant-compensator system becomes:

$$\begin{aligned} x_{i+1} &= \Phi_p x_i + \Gamma_p C\hat{x}_i + w_i \\ y_i &= Hx_i + v_i \\ \hat{x}_{i+1} &= (I - KH)(\Phi + \Gamma C)\hat{x}_i + Ky_{i+1}. \end{aligned} \tag{6.13}$$

The last equation can be rewriten as

$$\hat{x}_{i+1} = (I-KH)(\Phi+\Gamma C)\hat{x}_i + KH(\Phi_p x_i + \Gamma_p C\hat{x}_i + w_i) + Kv_i . \tag{6.14}$$

The characteristic equation, for the case of an imperfect knowledge of the plant, will be

$$\begin{vmatrix} \Phi_p - I_z & \Gamma_p C \\ KH\Gamma_p & (I-KH)(\Phi+\Gamma C)+KH\Gamma_p C - I_z \end{vmatrix} = 0 . \tag{6.15}$$

We may still define $\tilde{x}$, the observer error, but separation of the poles no longer exists. The poles of the closed loop system are the eigenvalues of (6.15).

The sensitivity can be defined as the relocation of the eigenvalues of the system (6.15) with respect to the perfect system, (6.11).

The pole's location on the z-plane does not provide us with a clear physical interpretation of the behavior of the system; particularly for poles located near point 1 on the real axis of the z-plane. Therefore, as an aid to evaluating the performance of the closed loop system, an equivalent damping, ζ^*, based on sampling of a continuous system will be defined. See Fig. VI-6.

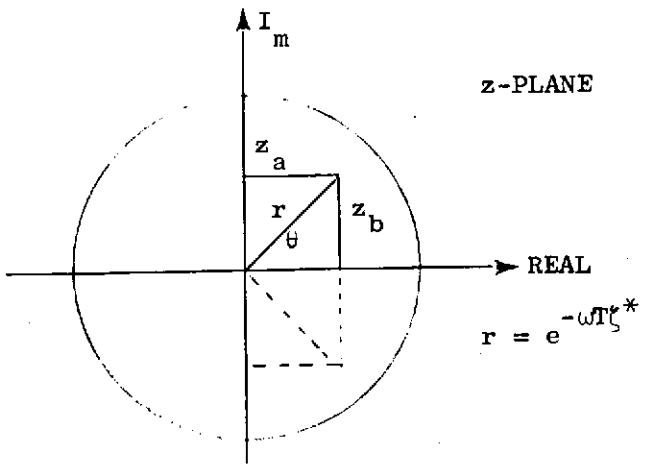

FIG. VI-6 z-PLANE DESCRIPTION OF ζ^*.

$$z = z_a + iz_b$$

$$r = e^{-\omega T\zeta^*}$$

$$\theta = \omega T\sqrt{1 - \zeta^{*2}} = \tan^{-1}\frac{z_b}{z_a} \qquad (6.16)$$

$$\zeta^* \triangleq \frac{-\log\left(\sqrt{z_a^2 + z_b^2}\right)}{\left\{\left[\tan^{-1}\left(\frac{z_b}{z_a}\right)\right]^2 + \log^2\left(\sqrt{z_a^2+z_b^2}\right)\right\}^{\frac{1}{2}}} .$$

We may consider the equivalent damping ratio ζ^* as a damping ratio of a continuous sampled second order system. This definition is necessary since the discrete system, controlled by a zero order hold, behaves differently between the sampling points.

B-2 Sensitivity of the Extended Short Period Mode to a Bending Frequency Variation

Because of the deep and sharp notch generated by the optimal compensator, we assumed that the system is highly sensitive to the bending frequency variation. We will investigate the sensitivity by varying the actual bending frequency by 10% from its nominal value, i.e., from 25 rad/sec to 22.5 rad/sec.

The model of the extended short period mode (flight condition No. 8) was described in Chapter IV. Using the controller and observer design of Chapter IV, the sensitivity was calculated by solving (6.15) and (6.16). The behavior of the equivalent damping ζ^* of the bending mode as a function of the sampling rate is plotted in Fig. VI-7. We can see how the sensitivity increases for lower sampling rates.

The time response of the normalized bending mode, x_4, to a wind gust impulse is plotted in Fig. VI-8 for $\omega_b/\omega_s = 0.02, 0.44$. The simulation scheme is described in Appendix B. Note that, contrary to an input command, the impulse is applied only to the plant and not to the observer. Therefore, correcting commands are only activated after one sampling period. The main reason for the instability of the case $\omega_b/\omega_s = 0.44$ (T = 0.1 sec) is the undamped behavior of the observer error bending mode. In other words, the observer is unable to follow the plant.

In the next section, we will describe a method for filtering the bending mode, even for an imperfect knowledge of the bending frequency.

C. REDUCTION OF SENSITIVITY TO BENDING FREQUENCY VARIATION

To reduce the sensitivity to the bending frequency variation, we have to increase the width of the notch filter which is generated by the compensator. As explained in Section VI-A, the width of the notch filter is related to the damping of the bending mode in the compensator. The damping may be increased by a modification in the control loop, or in both. This modification can be achieved by three basic methods:

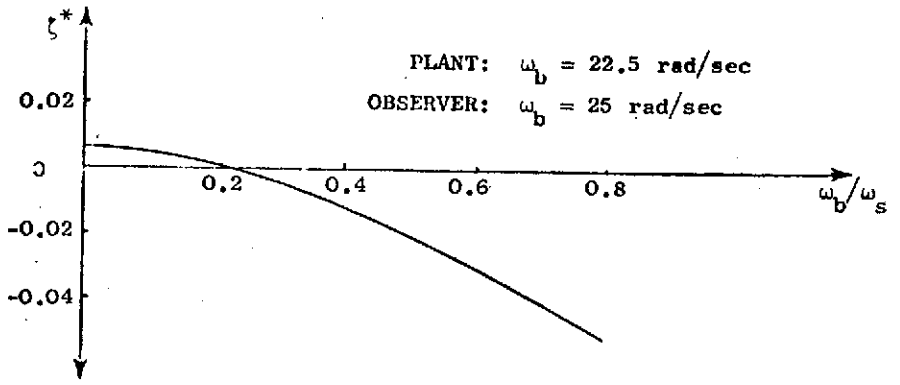

FIG. VI-7 THE SHORT PERIOD MODE. Imperfect knowledge of the bending frequency. ζ^* vs ω_b/ω_s.

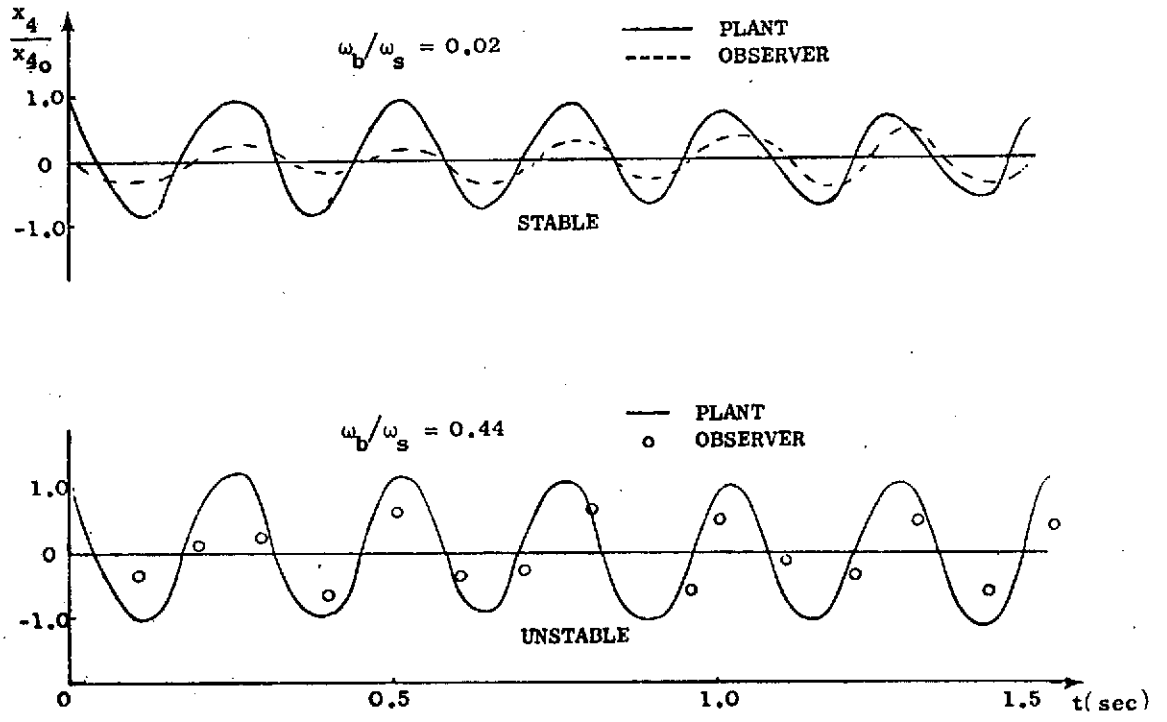

FIG. VI-8 BENDING MODE TIME HISTORY. 10% error in ω_b.

(a) By a pole placement.

(b) By using an automatic synthesis procedure, which will satisfy the quadratic criteria and will reduce the sensitivity. An appropriate computer program exists for continuous linear systems [HAD-1] but it is not yet available for discrete systems.

(c) By a modification of the optimal discrete system.

In our synthesis, we used the third approach. Stabilization of the perturbed closed loop system was achieved by weighting the bending mode state, x_4. The gain of the observer was changed by assuming that more noise would act directly on the bending mode. This modification might have changed the dynamic properties of the system, but we will show that no significant change took place.

C-1 Desensitivity by Increasing the Damping of the Bending Mode

We are investigating the nominal design of the short period mode described in Chapter IV and in Section VI-B. In this design, no weight was given to the bending mode in the quadratic criteria. For desensitization of the system, we will damp the bending mode by weighting it The relocation of the poles as a function of the bending mode weight (A_{x_4}) is given in Table VI-2.

Table VI-2

CLOSED LOOP EIGENVALUES AS A FUNCTION OF WEIGHT ON THE BENDING MODE (T = 0.1 sec).

A_{x_4}	Short Period Mode	Bending Mode
0	$z = 0.137 \pm j0.280$	$z = -0.781 \pm j0.584$
10^{-6}	$z = 0.14 \pm j0.275$	$z = -0.669 \pm j0.485$
10^{-5}	$z = 0.16 \pm j0.24$	$z = -0.516 \pm j0.29$

Rigid body weights: $A_{q/B} = 0.12$, $A_{\alpha/B} = 11$.

Flight Condition No. 8.

From the results in Table VI-2, we conclude that when A_{x_4} varies from zero to 10^{-5}, the dynamic properties of the rigid body are not significantly changed. The influence of this modification on the stability of the closed loop bending modes is described in Fig. VI-9, where ξ^* has been plotted vs A_{x_4}. As seen in Fig. VI-9, it is possible to stabilize the bending mode for an assumed 10 percent error in the bending frequency. The time response of the bending mode to a wind gust impulse is shown in Fig. V-10. The gust impulse was translated via the initial value theorem to initial conditions formulation. The calculation of this time response was done by a digital simulation scheme described in Appendix B. Note that the impulse is applied only to the plant and not to the observer; therefore, the first observer's states and the first command appear only after one sampling interval. We can see that $A_{x4} > 10^{-6}$ stabilized the system. Further stabilization, especially that of the observer error, will be made in the next section.

C-2 Desensitivity by Increasing the Sampling of the Observer Error Bending Mode

The observer error gains can be increased by introducing an artificial external noise on the bending mode. This artificial noise is not included in the total rms response to external disturbances of the system. But the dynamic and filtering properties of the observer is no longer optimal in the sense that it minimizes the influence of all the noises acting on the system. This change in the total rms response for the modified system will be treated in detail in Section VI-D.

By varying the factor G_4 in the noise distribution matrix Γ_2, the observer error gains were changed. The observer error poles corresponding to the bending mode vs the factor G_4 are given in Table VI-3. The equivalent damping of the closed loop bending mode (10% error on ω_b) is plotted in Fig. VI-11. As seen for $G_4 > 100$, the bending modes are stabilized. The time history of the bending mode is traced in Fig. VI-12. The primary stabilization effect is achieved by a damping of the observer's error. When these phenomena are understood, it is possible to desensitize the perturbed short period mode.

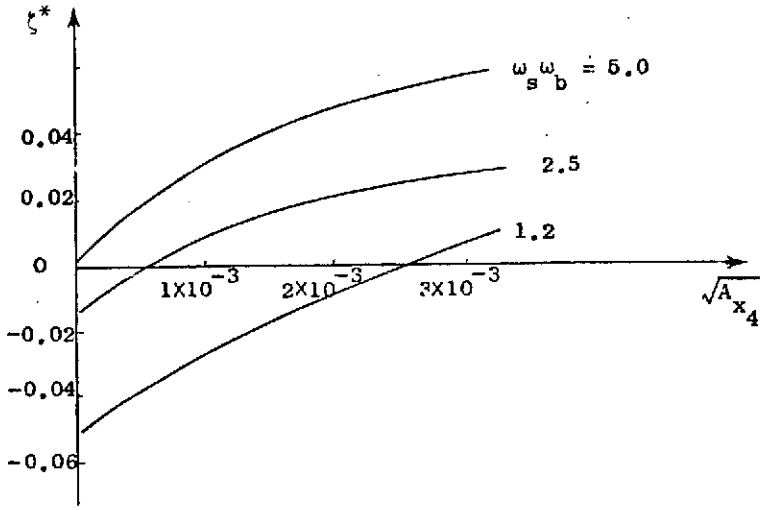

FIG. VI-9 CLOSED LOOP BENDING MODE DAMPING VS A_{x_4} WEIGHTING FACTOR. 10% error in ω_b. Flight Condition No. 8.

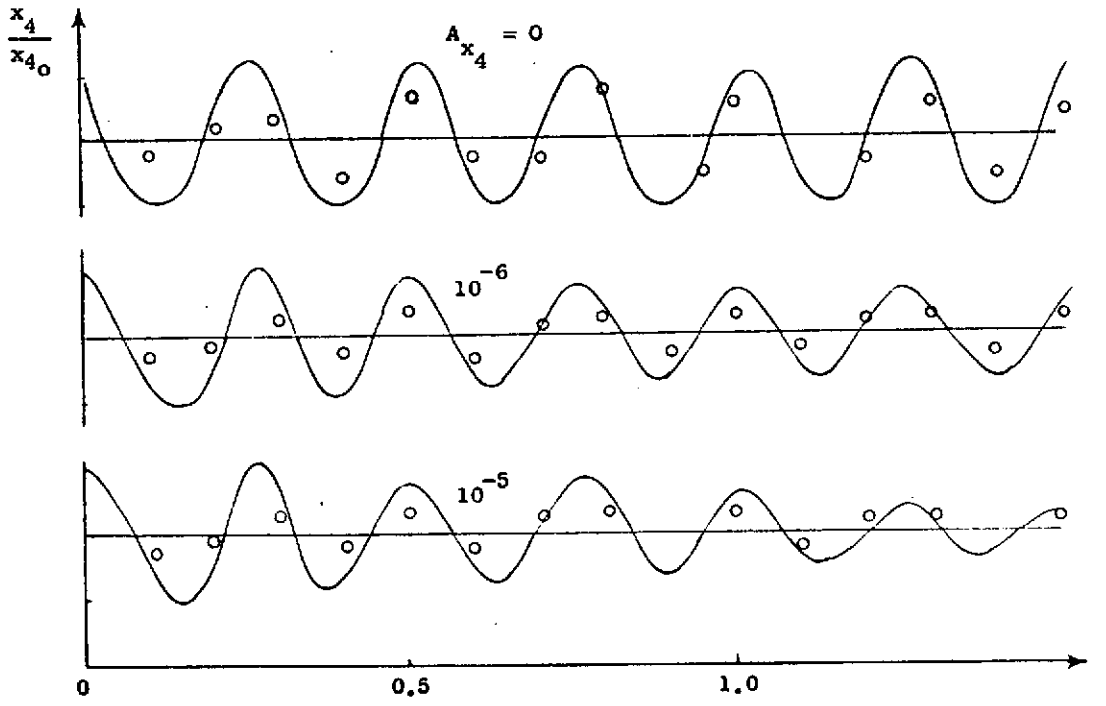

FIG. VI-10 BENDING MODE TIME HISTORY FOR VARIOUS WEIGHT FACTORS. 10% error in ω_b. Flight Condition No. 8. ω_s/ω_b = 2.5; T = 0.1 sec.

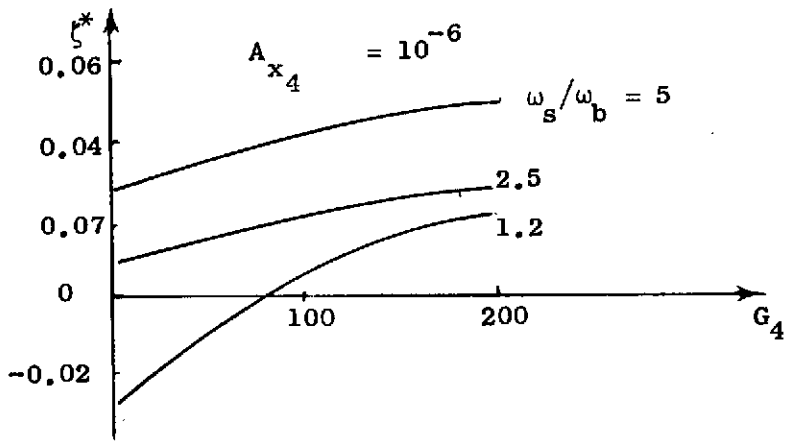

FIG. VI-11 CLOSED LOOP BENDING MODE DAMPING VS NOISE MAGNITUDE, G_4. 10% Error in ω_b. Flight Condition No. 8.

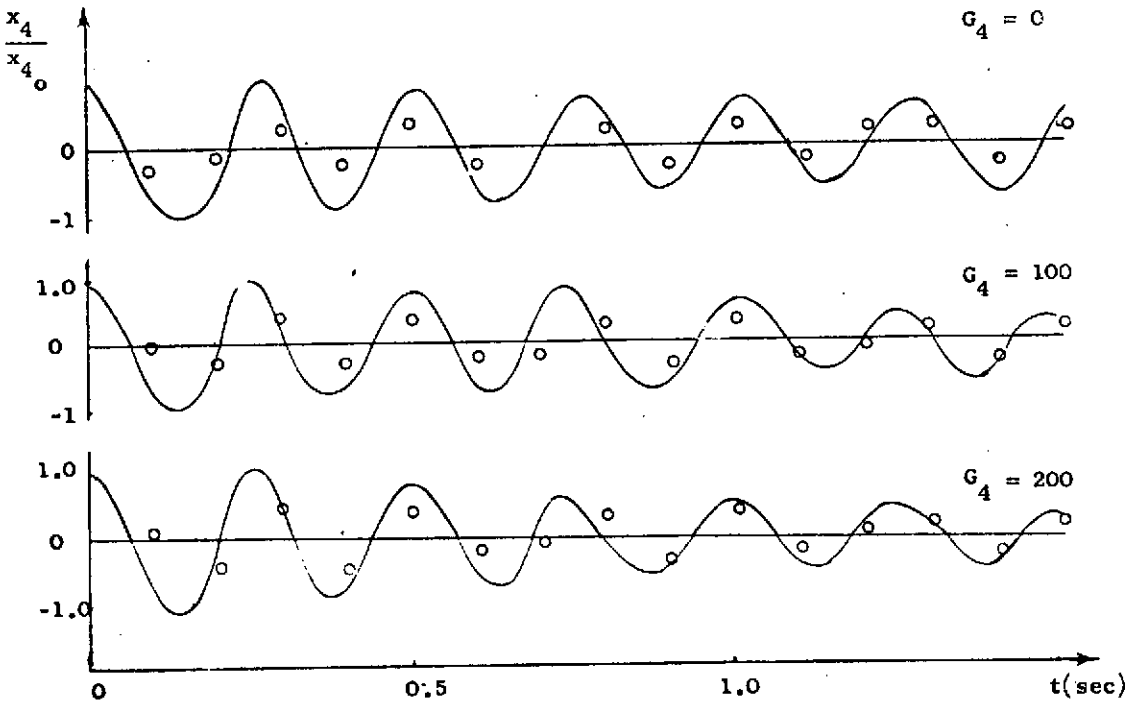

FIG. VI-12 BENDING MODE TIME HISTORY FOR VARIOUS NOISE MAGNITUDES. 10% error in ω_b. ω_s/ω_b = 0.5, T = 0.1 sec, A_{x4} = 10^{-6}.

Table VI-3

OBSERVER ERROR BENDING MODE EIGENVALUES AS A FUNCTION OF G_4, THE ARTIFICIAL NOISE (T = 0.1 sec).

G_4	z-plane Observer Error Poles	s-plane Equivalent
0	-0.725 ± j0.572	-1.0 ± j25
100	-0.6736 ± j0.508	-1.5 ± j24.8
200	-0.622 ± j0.452	-2.5 ± j24.5

D. THE EVALUATION OF THE PERFORMANCE OF THE DESENSITIZED CLOSED LOOP SYSTEM

The rms response of the optimal system was evaluated in Chapter V. In this chapter, Section VI-C, we desensitize the optimal design by changing the weights in the cost function and by introducing an artificial noise on the bending mode. As a consequence of this modification, the control and the observer error gains were changed. The modified closed loop system is not optimal in the sense that it minimizes the rms response when the noise statistics and the original weight in the quadratic cost function are given. Yet, from a more general point of view, this modification would be a better engineering solution if the performance of the system didn't greatly change. The performance criteria are mostly characterized by the closed pole location and the rms response.

As has been shown in Table VI-2, the rigid body poles of the short period example were only slightly relocated. The modification we used ($A_{x_4} = 10^{-6}$) negligibly influenced the time response to a pilot input. The filtered pilot commands (Ch. III) are fed simultaneously to the aircraft and to the observer. During the first second, the time response is dominated by the closed loop rigid body poles and not by the observer error poles of the bending mode. However, the observer error poles and

gains of the bending mode were changed (Table VI-3), and thus the steady state rms response properties were also changed. Therefore, it is necessary to find out how the modification of the closed loop system influences the rms response to external disturbances. This investigation will be conducted by considering the total rms response of the modified closed loop system to all noises acting on the system.

The relation for the states covariance matrix calculation used in Chapter III is repeated here as: (repeated from Eq. 3.86)

$$X - M = (\Phi + \Gamma c)(X - p)(\Phi + \Gamma c)^T$$

is not more applicable because it assumes an optimal observer. The covariance matrices M and p of the observer error before and after measurement do not represent the modified system. M and p now include the additional artificial noise which was applied to the system to obtain a better damping of the observer error of the bending mode poles. Thus the rms response will be calculated by the following method:

The state equations of the plant will be augmented by the equations of the compensator system to a $2n \times 2n$ open loop representation. The external noise, combined with the measurement noise, act simultaneously on the enlarged system. The equations of the augmented system are, first, the controlled plant:

$$x_{i+1} = \Phi_p x_i + \Gamma_p C\hat{x}_i + \Gamma_2 w_i \qquad w_i \to N(0, Q_d) \tag{6.17}$$

and the observer,

$$\hat{x}_{i+1} = KH\Phi_p x_i + [(I-KH)(\phi+\Gamma C) + KH\Gamma_p C]\hat{x}_i + Kv_i, \qquad v_i \to N(0,R) \tag{6.18}$$

These equations were derived in Section VI-B.

The steady state covariance matrix X_a of the augmented states is the solution of

$$X_a = \Phi_a X_a \Phi_a^T + \Gamma_a Q_a \Gamma_a^T , \tag{6.19}$$

where

$$\Phi_a = \left[\begin{array}{c|c} \Phi_p & \Gamma_p C \\ \hline K H \Phi_p & (I-KH)(\Phi+\Gamma C)+KH\Gamma_p C \end{array}\right] \tag{6.20}$$

$$Q_a = \left[\begin{array}{c|c} Q_d & \begin{matrix} 0 & \ddots \\ & 0 \end{matrix} \\ \hline \begin{matrix} 0 & \ddots \\ & 0 \end{matrix} & R \end{array}\right] \tag{6.21}$$

$$\Gamma_a = \left[\begin{array}{c|c} \Gamma_2 & \begin{matrix} 0 & \ddots \\ & 0 \end{matrix} \\ \hline \begin{matrix} 0 & \ddots \\ & 0 \end{matrix} & K \end{array}\right] . \tag{6.22}$$

The observer error gains K, and the state variable feedback gains C were calculated in Section VI-C. Φ_p and Γ_p include the uncertainty for the short period example, and the variation on the bending mode frequency. The rms response of the plat states are the square roots of the first n terms on the main diagonal of X_a.

The results of the foregoing method for the rms response of the modified system ($Ax_y = 10^{-6}$, $G_4 = 200$) is compared to the original optimal design, Fig. VI-13. There is a certain increase of the rms response of the states.

E. RELATIONSHIP BETWEEN THE COMPENSATOR POLES AND SENSITIVITY

In this section we will generalize the results of Section VI-A. It will be shown that there is a definite relationship between the location of the compensator's poles and the sensitivity of the closed loop system.

The compensator poles are not necessarily well damped or even stable

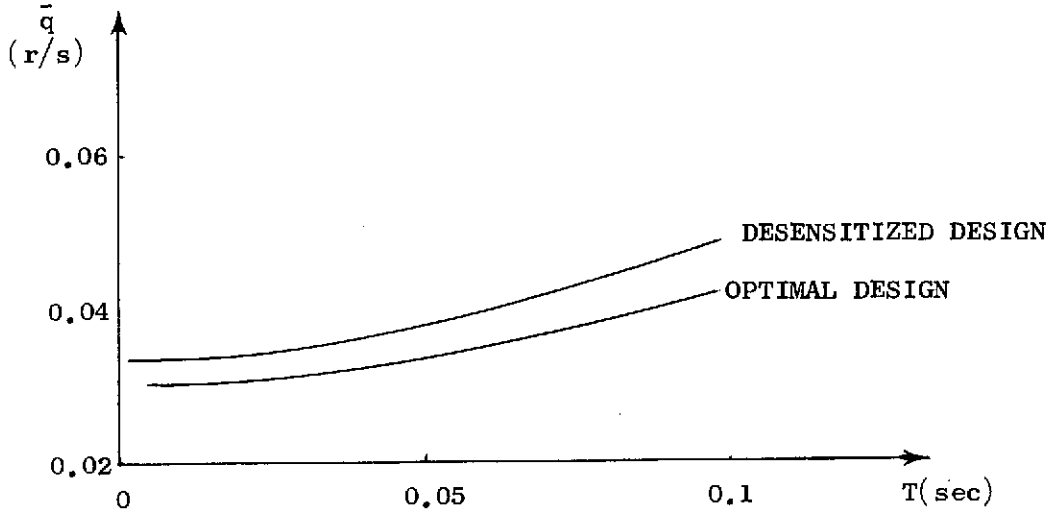

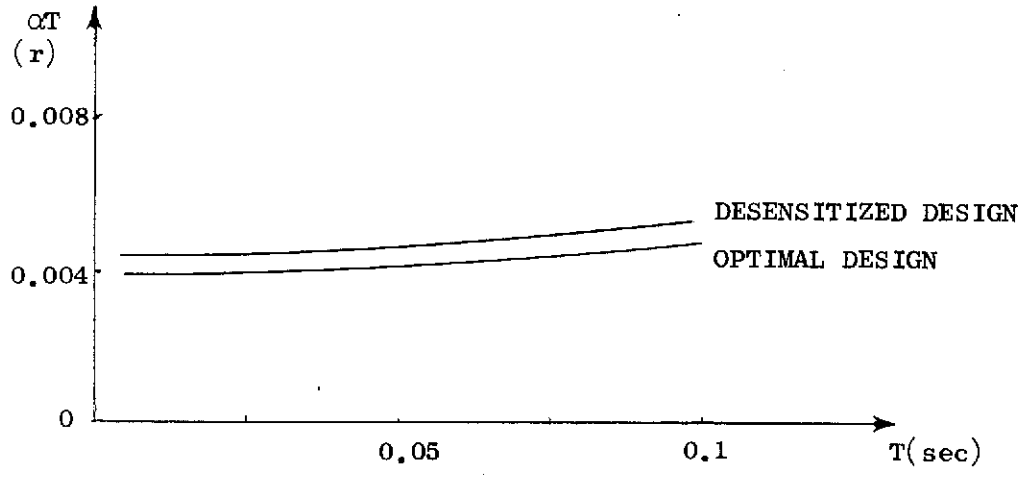

FIG. VI-13 A COMPARISON OF THE RMS RESPONSE BETWEEN THE OPTIMAL DESIGN AND THE DESENSITIZED DESIGN. FLIGHT CONDITION No. 8. Wind gust: σ = 12 ft/sec; τ_w = 0.5 sec.

for a stable closed loop system. However, our analysis will show that if the coefficients of the plant are perturbed, the closed loop ples have the tendency to migrate toward the compensator poles. Therefore, if the compensator poles are stable and well damped, the closed loop system is less sensitive to variations of the plant's parameters. This interesting property of the perturbed closed loop system will be proven as follows: The characteristic equation of the closed loop system (from Section VI-2, Eq. 6.15) is

$$\begin{bmatrix} \Phi - Iz & \Gamma_p C \\ KH\Phi_p & (I-KH)(\Phi+\Gamma c)+KH\Gamma_p C - Iz \end{bmatrix} = 0 .$$

By using (6.13) we will reformulate (6.15),

$$\begin{aligned} x_{i+1} &= \Phi_p x_i + \Gamma_p C\hat{x}_i \\ \hat{x}_{i+1} &= A\hat{x}_i + Ky_{i+1} \end{aligned} \qquad (6.23)$$

where $y_{i+1} = Hx_{i+1}$

and $A = (I - KH)(\Phi + \Gamma C)$

which yields a different formulation of the characteristic equation

$$\begin{vmatrix} \Phi_p - Iz & \Gamma_p C \\ KHz & A - Iz \end{vmatrix} = 0 . \qquad (6.24)$$

Using the well known relationship,

$$\det \begin{bmatrix} A_1 & A_2 \\ A_3 & A_4 \end{bmatrix} = \det A_4 \det[A_1 - A_2 A_4^{-1} A_3] .$$

Equation (6.24) will obtain the following form:

$$P_c(z)\ \det[(\Phi_p - Iz) - \Gamma_p C\ \frac{B(z)}{P_c(z)} KHz\ ] \ = \ 0 \qquad (6.25)$$

where $P_c(z) \triangleq |A - Iz|$ are the poles of the compensator. $B(z)$ are zeros of $(A - Iz)^{-1}$. Let $\Phi_p = \Phi + \Delta\Phi$, $\Gamma_p = \Gamma$. The characteristic equation will be

$$P_c(z)\ \det\left[(\Phi + \Delta\Phi - Iz) - \Gamma C\ \frac{B(z)}{P_c(z)}\ KHz\right] \ = \ 0 \qquad (6.26)$$

or

$$P_c(z)\left[\det\ (\Phi - Iz) - \Gamma C\ \frac{B(z)}{P_c(z)}\ KHz + \Delta\Phi\right] \ = \ 0. \qquad (6.27)$$

Assuming

$$\Delta\Phi \ = \begin{bmatrix} 0 & \cdots & \cdots & \cdots \\ \vdots & & & \\ \vdots & & \Delta\Phi_{ij} & \\ \vdots & & & \\ & & & 0 \end{bmatrix}$$

Equation (6.27) will become

$$P_c(z)\left\{\underbrace{\det[(\Phi - I_z) - \Gamma\ \frac{CB(z)}{P_c(z)}\ KHz\ ]}_{M(z)} + \Delta\Gamma_{ij}\ \det[M_{ij}]\right\} \qquad (6.28)$$

where M_{ij} is the cofactor of M. Now the characteristic equation obtains the following form:

$$P_c(z)\{\det\ M(z) + \Delta\Phi_{ij}\ \det\ M_{ij}\} \ = \ 0\ . \qquad (6.29)$$

However, $P_c(z)\det\ M(z)$ in (6.29) is the characteristic equation of the nominal system:

$$P_c(z) \det M(z) = \left|(\Phi+\Gamma C-Iz)[\Phi(I-KH)-Iz]\right| \triangleq NP(z). \qquad (6.30)$$

All zeros of the NP(z) (nominal poles) are inside the unit circle.

Finally, the characteristic equation of the perturbed system is

$$NP(z) + \Delta\Phi_{ij} P_c(z) \left|M_{ij}(z)\right| = 0 . \qquad (6.31)$$

Recall that $P_c(z)$ is the characteristic equation of the compensator. Equation (6.31) is now in a familiar form for a root locus analysis, where the perturbed coefficient Δ_{ij} replaces the gain. An increase in $\Delta\Phi_{ij}$ will move part of the closed loop poles [zeros of NP(z)] toward the poles of the compensator [zeros of $P_c(z)$]. Therefore, even if the observer error system is stable, it is important to check the location of the compensator poles. Unstable compensator poles may cause a greater sensitivity to variations in the parameters.

F. HIDDEN INSTABILITY DUE TO SAMPLING

In the previous sections we have defined the bending mode as an undesirable frequency. It has also been shown that the optimal compensator generates a notch filter which attenuates the unwanted frequency. Classical approaches, such as those given in Borow [BO-1] and Sutton [SU-1], design the notch filter directly into the feedback loop. The notch filter implementation requires mechanizing a second order system on the digital computer. Therefore, it seems promising to circumvent the necessity of using this filter by taking advantage of the filtering properties of the sampler. McGough [McG-1] in 1973 proposed sampling at the same rate as the bending frequency and he proved doing this would filter the unwanted frequency. The purpose of this section is to show that, for certain cases, the closed loop will diverge. This effect cannot be detected by the regular stability analysis used by McGough [McG-1].

In Section VI-F-1 we will show what the conditions are to generate the instability effect, and in VI-F-2 we will demonstrate it for the short period example.

F-1 Problem Statement and Theoretical Background

The transfer function of the ZOH is given as [RA-1]

$$ZOH = \frac{1 - e^{-sT}}{sT} .$$

The frequency response of the zero order hold is described in Fig. VI-14.

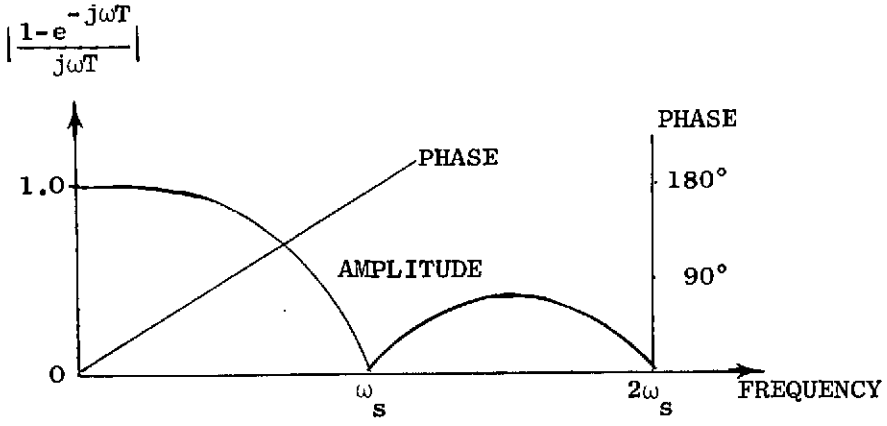

FIG. VI-14 FREQUENCY RESPONSE OF THE ZERO ORDER HOLD (ZOH)

Intuitively it is obvious that a signal with a frequency near the sampling rate or near the multiples of the sampling rates will pass the ZOH as a slow varying bias, or d-c. See Fig. VI-15. This idea is especially attractive for our principal example where the second bending mode is an integral multiple of the first bending mode (25 H, 50 H). Therefore,

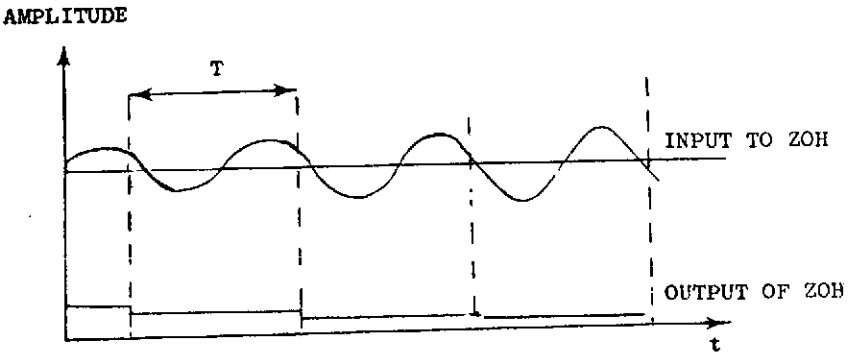

FIG. VI-15 FILTERING PROPERTIES OF THE ZERO ORDER HOLD

this approach is worth a more detailed analysis. For analyzing this situation, we shall use the formulation of Section VI-A-1. The system,

$$\begin{bmatrix} x_a \\ x_{b_1} \\ \vdots \\ x_{b_k} \end{bmatrix}_{i+1} = \begin{bmatrix} \Phi_a & 0 & & \\ 0 & \Phi_{b_1} & & \\ & & \ddots & 0 \\ & & 0 & \Phi_{b_k} \end{bmatrix} \begin{bmatrix} x_a \\ x_{b_1} \\ \vdots \\ x_{b_k} \end{bmatrix}_i + \begin{bmatrix} \Gamma_a \\ \Gamma_{b_1} \\ \vdots \\ \Gamma_{b_k} \end{bmatrix} u_i \qquad (6.32)$$

$$y_i = Hx_i$$

where x_{b_i} = ith bending mode state.

Using an optimal control and no weighting on $x_{b_1} \ldots x_{b_k}$, the control is

$$u_i = [C_a \quad 0] \begin{bmatrix} x_a \\ x_{b_1} \\ \vdots \\ x_{b_k} \end{bmatrix} = C_a x_{a_i}. \qquad (6.33)$$

The exact states x_a are not known. Any method of reconstruction of the states, using Φ_a only, will generate states "contaminated" by the unwanted frequencies

$$u_i = C_a x_{a_i} + k x_{b_i}; \qquad k = k(H). \tag{6.34}$$

By inspection we can show that the closed loop poles of the subsystems Φ_b are separated. Therefore it will be sufficient to analyze one of the second order subsystems. Explicitly written, the subsystem Φ_b is

$$\ddot{x}_b = -2\zeta_b \omega_b \dot{x}_b^2 - \omega_b x_b + gu \tag{6.35}$$

where u is a constant through the interval, T.

The system (6.35) will be rewritten in a state space form using an artificial state $\ddot{x}_b$. This is done in order to close the loop with an accelerometer feedback

$$\begin{bmatrix} \dot{x}_b \\ \ddot{x}_b \\ \dddot{x}_b \end{bmatrix} = \begin{bmatrix} 0 & 1 & 0 \\ -\omega_b^2 & -2\zeta_b\omega_b & 0 \\ 0 & -\omega_b^2 & -2\zeta_b\omega_b \end{bmatrix} \begin{bmatrix} x_b \\ \dot{x}_b \\ \ddot{x}_b \end{bmatrix} + \begin{bmatrix} 0 \\ g \\ 0 \end{bmatrix} u + \begin{bmatrix} 0 \\ 0 \\ g \end{bmatrix} \dot{u} . \tag{6.36}$$

Using a ZOH for u we get

$$\begin{bmatrix} x_b \\ \dot{x}_b \\ \ddot{x}_b \end{bmatrix}_{i+1} = \begin{bmatrix} \phi_1 & \phi_2 & 0 \\ \phi_3 & \phi_4 & 0 \\ \phi_5 & \phi_6 & \phi_7 \end{bmatrix} \begin{bmatrix} x_b \\ \dot{x}_b \\ \ddot{x}_b \end{bmatrix}_i + \begin{bmatrix} \gamma_1 \\ \gamma_2 \\ 0 \end{bmatrix} u_i + \begin{bmatrix} 0 \\ 0 \\ g \end{bmatrix} [u_i - u_{i-1}] \tag{6.37}$$

where u_i is a linear function of x_a and of the unwanted frequencies. If an acceleration or pickoff is used, then:

$$u_i = C_a x_a + k(\ddot{x}_b + \ddot{x}_a) \tag{6.38}$$

where k depends on the particular structure of the compensator. Thus the characteristic equation of (6.37) has the following form

$$\begin{vmatrix} \phi_1 z & \phi_2 & \gamma_1 k \\ \phi_3 & \phi_4 - z & \gamma_2 k \\ \phi_5 & \phi_6 & \phi_7 - z + gk(1-z^{-1}) \end{vmatrix} = 0 . \tag{6.39}$$

The bending modes are nearly undamped ($\zeta_b = 0.01$). To simplify, we will assume that $\zeta_b = 0$. The various terms ϕ and γ are:

$$\phi_1 = \cos \omega_b T \qquad \phi_6 = \omega_b \sin \omega_b T$$

$$\phi_2 = \frac{\sin \omega_b T}{\omega_b} \qquad \phi_7 = \cos \omega_b T$$

$$\phi_3 = \omega_b \sin \omega_b T \qquad \gamma_1 = \frac{g}{\omega_b}(\cos \omega_b T - 1)$$

$$\phi_4 = \cos \omega_b T \qquad \gamma_2 = \frac{g}{\omega_b} \sin \omega_b T .$$

$$\phi_5 = 0$$

If the sampling is done in the same frequency as ω_b, (6.39) reduces to

$$(1-z)(1-z)[1-z + gk(1-z^{-1})] = 0 . \tag{6.40}$$

The roots of (5.40) are $z_{1,2} = 1$, $z_{3,4} = \{\frac{1}{gk}\}$. If $|gk| > 1 \Rightarrow$ the subsystem will diverge. The physical interpretation is as follows. The modes x and $\dot{x}$ are constant at the sampling points, i.e., $x_i = x_{i-1}$, $\dot{x}_i = \dot{x}_{i-1}$. But if $|gk| > 1$, the acceleration will diverge and the closed loop system is unstable. This property can be visualized in Figs. VI-16

VI-17.

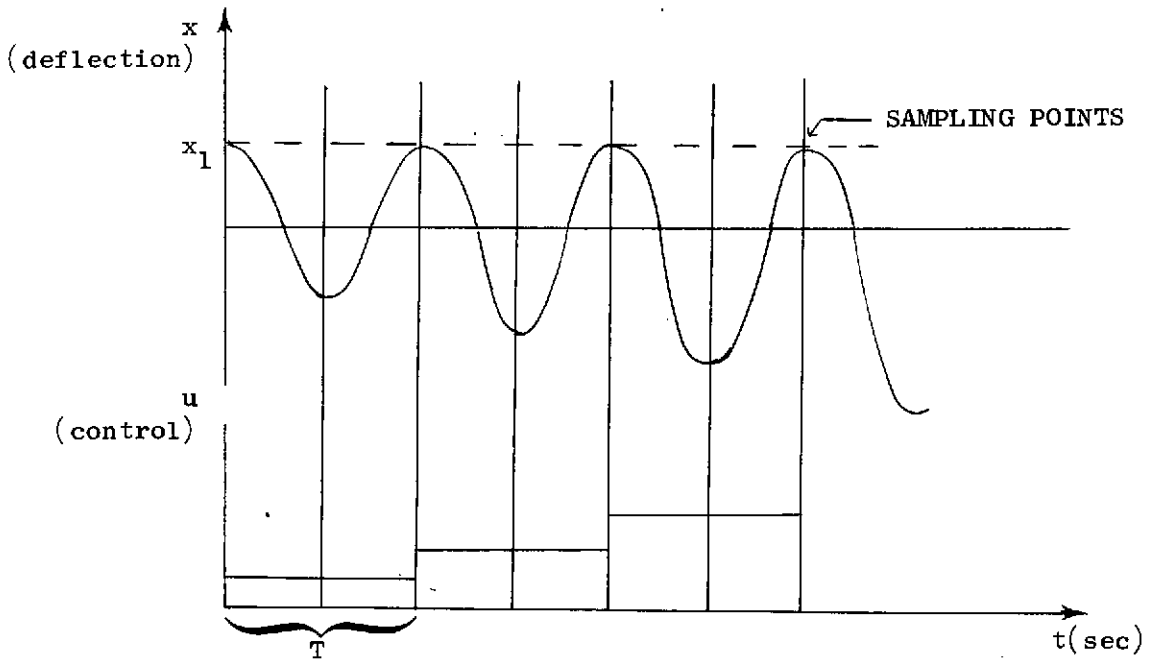

FIG. VI-16 HIDDEN INSTABILITY OF AN OSCILLATING MODE ($kg > 1$).

Diagrams similar to Figs. VI-16 and VI-17 can be traced for $-1 < kg < 0$ and $kg < -1$. Note: (a) For all four cases, x_b and $\dot{x}_b$ are constants at the sampling points. (b) Without using the third artificial state $\ddot{x}_b$ or an equivalent formulation, this behavior could not be detected.

F-2 Hidden Instability of the F-H Short Period Mode Example Due to Sampling

In order to investigate the effect of sampling at the same frequency as the bending frequency, we will use the simulation scheme described in Appendix B. The model we will use is the extended short period mode described in Chapter IV. That model represents the plant. Investigating

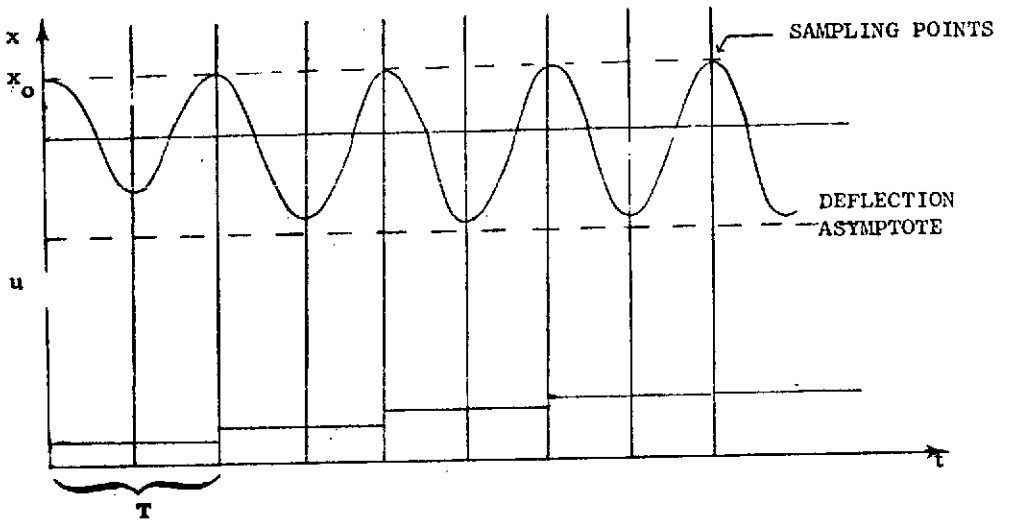

FIG. VI-17 ASYMPTOTIC STABILITY OF THE OSCILLATING MODE. ($|kg| < 1$)

the claim of McGough [McG-1] regarding the bending mode which generates the notch filter, will not be included in the compensator. The closed loop system we will simulate is described in Fig. VI-18.

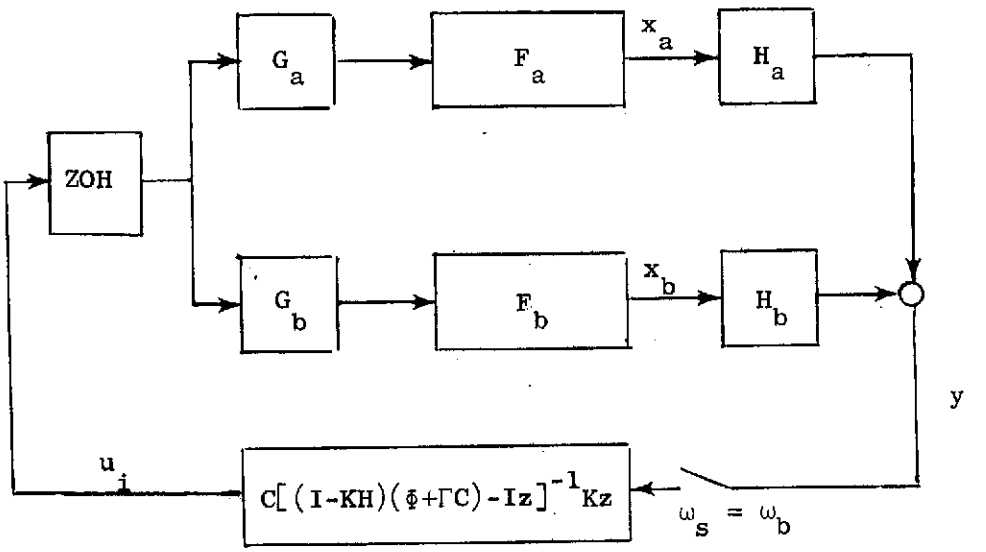

FIG. VI-18 SIMULATION SCHEME FOR THE HIDDEN INSTABILITY INVESTIGATION.

where

$$K = \begin{bmatrix} K_a \\ 0 \end{bmatrix}; \qquad H = [H_a \quad 0];$$

$$C = [C_a \quad 0];$$

$$\Phi = \begin{bmatrix} \omega_b & 0 \\ 0 & 0 \end{bmatrix};$$

$$\Gamma = \begin{bmatrix} \Gamma_a \\ 0 \end{bmatrix}.$$

Using this scheme, the influence of the bending mode is eliminated from the compensator. However, the measurements y are combined from the output of the whole plant.

The simulation results plotted in Fig. VI-19 and Fig. VI-20 confirm our analysis of Section VI-F-1. The behavior of the bending mode for nominal accelerometer pickup is plotted in Fig. VI-19. We can see that the bending mode is marginally stable.

Figure VI-20 plots the behavior of the bending mode for the case in which the accelerometer pickup was increased by a factor of 10. The system is unstable. The behavior of the bending mode and the input in Fig. VI-20 does not exactly match the schematic behavior charted in Fig. VI-17. The reason for this difference is that in Fig. VI-17 we plotted the schematic behavior of the homogeneous solution of the bending mode. In Fig. VI-20, the rigid body mode is also excited.

G. SUMMARY

1. An optimal compensator of a closed loop system having an unwanted frequency is essentially a notch filter. The depth of the notch depends on the amount of pickup of the unwanted frequency.

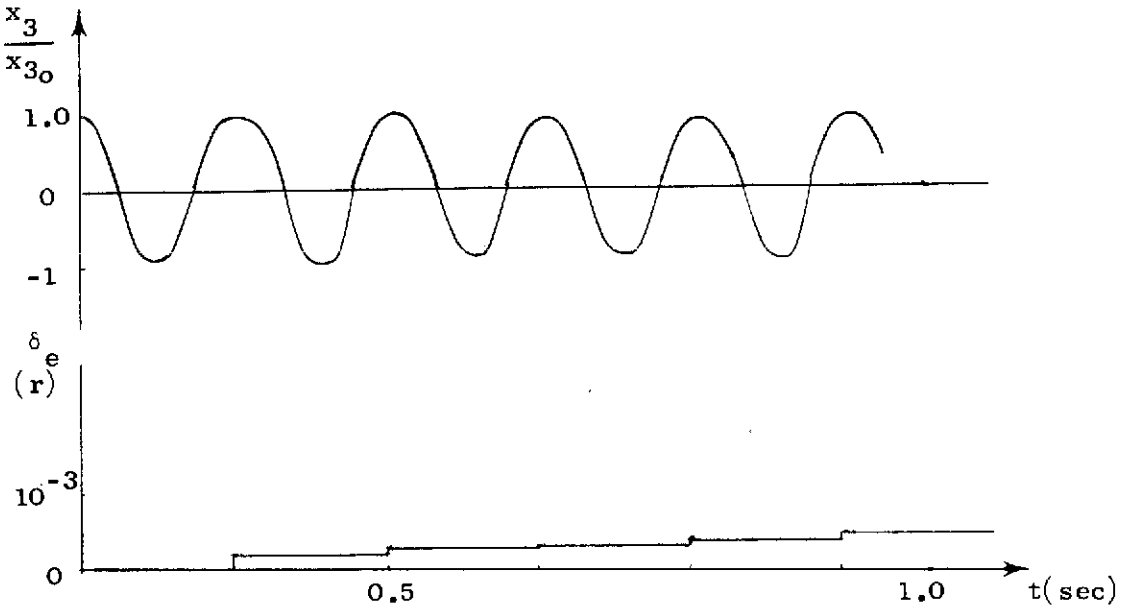

FIG. VI-19 MARGINAL STABILITY OF THE BENDING MODE DUE TO A SAMPLING IN THE BENDING FREQUENCY. $\omega_s = \omega_b = 31.4$ rad/sec; h_a = nominal; T = 0.2 sec.

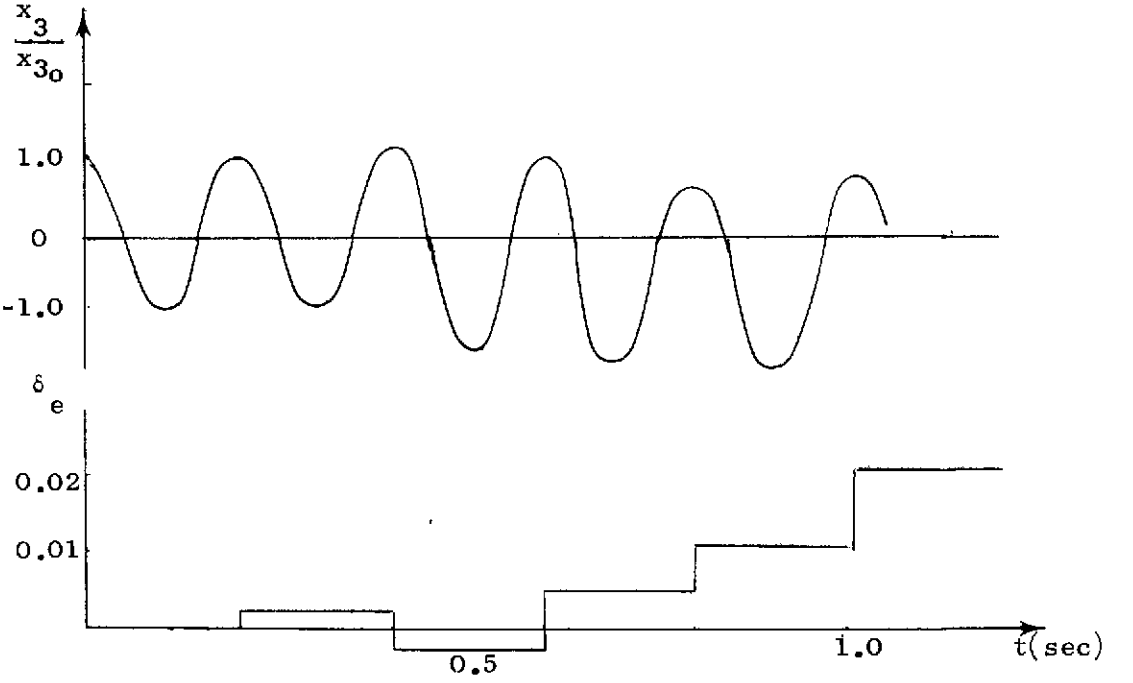

FIG. VI-20 EXCITATION OF THE BENDING MODE DUE TO SAMPLING IN THE BENDING FREQUENCY. $\omega_s = \omega_b = 31.4$ rad/sec; $h_a = 10 \times h_a$ nominal; T = 0.2 sec.

2. In the F-H short period example, the closed loop control system is sensitive to a bending frequency variation. The sensitivity increases for lower sampling rates.

3. The sensitivity to a bending frequency variation can be reduced by increasing the damping of the observer error poles.

4. Systems with more stable compensators are less sensitive to parameter variations.

5. Sampling at the bending mode frequency may cause an instability which contradicts the results given in McGough [McG-1]. The reason for the instability is that McGough didn't consider the intersample behavior.

6. The important parameters which cause the sensitivity are poorly damped, almost undisturbable modes, and low sampling rates.

VII. SAMPLING TIME AND ROUGHNESS OF CONTROL

Most of the digital systems which control analog (continuous) plants use the zero order hold (ZOH) as a reconstruction hold. The abrupt action of the ZOH for higher sampling rates is lessened and is further smoothed by the filtering properties of the various electro-mechanical actuators. The tendency is to shorten the actuator time constants as much as possible in order to satisfy various time response criteria. Therefore the action of the controls becomes more abrupt at lower sampling rates. However, there is no documented analytical approach to control roughness in the digital control literature. The purpose of this chapter is to formulate and analyze a criterion which will enable us to compare the roughness of control for different sampling rates and for different control laws.

The first experimental evidence of the necessity for such a roughness criteria appeared recently [MA-1]. In that paper, J. Mathews describes the Saab digital flight control system. This is a highly successful digital control impelmentation. The first flight test was made in March 1973. Upon installation of the system in the aircraft, it was discovered that the servo valves responded to the small steps in the output wave form. It was originally believed that the high sampling rates (40 cps in roll and 80 cps in pitch) would be above the bandpass of the servo valve. This turned out not to be the case and a lag had to be added to the servo preamp. The roll axis computation rate was changed to 80 cps to minimize the size of the lag filter. This example clearly shows the need for an analytical tool which will help the designer estimate roughness of control.

The basic concept in this chapter are the definitions of roughness functions (RF). The fundamental RF will be defined as the weighted sum of the squares of the abrupt changes in the states' derivatives or the control inputs.

In Section VII-A we will define the RF for an impulse response of a continuous system controlled by a digital controller. A method based

on eigenvector decomposition will be given for computing the RF. A simple first order example will illustrate the new concept. The RF of the F-H short period mode for different sampling rates will be investigated in detail. The surprising result is that if the dynamic properties of the closed loop are kept constant, the RF is not a monotonic function of the sampling interval. Actually, it will be shown that for this example, the RF has a maximum. The minimum RF is obviously zero (for T = 0).

In Section VII-B we will define the mean roughness function, (RF_m), for a continuous system, disturbed by an external noise and controlled by a digital controller. A direct solution of the RF_m wil be given. We will also investigate the RF_m of the short period example for different dynamic properties of the closed loop while keeping the sampling rate constant. An intuitively predicted phenomenon, that the RF_m increases for larger mean values of the control, will be verified. In Section VII-C we propose and investigate different RFs which enable us to compare roughness of systems controlled via different reconstruction holds and actuators.

A. THE ROUGHNESS FUNCTION/RF

A-1 Definition

A continuous linear system, controlled discretely, has the following form:

$$\dot{x} = Fx + Gu$$

where u = constant, $t_i \le t < t_i + T$. Written in a discrete form,

$$x_{i+1} = \Phi x_i + \Gamma u_i. \tag{7.2}$$

When a step function is applied to the system (7.1) at time t_i, some of the variables $\dot{x}$ abruptly change their magnitude from $\dot{x}_{-i}$ to $\dot{x}_{+i}$. These are all the variables (not states), which are directly influenced by the input u_i. In other words, the abruptly changed variables are the derivatives of the states for which the control distribution matrix G has nonzero elements. We shall limit our discussion to the case in

which the state variables x are not abruptly changed; i.e., $x_{+i} = x_{-i} = x_i$. This is the common case in mechanical systems, where a step input in forces changes the acceleration. The requirement that none of the states be abruptly changed is necessary in order to obtain an explicit expression for the RF.

If a full state variable feedback is implemented, the equations (7.1) and (7.2) can be combined as the following form:

$$\dot{x}_{+i+1} - \dot{x}_{-i+1} = GC[(\Phi + \Gamma C) - I]x_i . \tag{7.3}$$

Proof: The input u_i, through the time interval T, $t_i \le t \le t_i + T$ is

$$u_i = Cx_i \tag{7.4}$$

and

$$\begin{aligned} \dot{x}_{-i+1} &= Fx_{i+1} + Gu_{-i+1} \\ \dot{x}_{+i+1} &= Fx_{i+1} + Gu_{+i+1} . \end{aligned} \tag{7.5}$$

Combining (7.5) and (7.4)

$$\dot{x}_{+i+1} = \dot{x}_{-i+1} + GC(x_{i+1} - x_i) . \tag{7.6}$$

By using (7.2) we obtain the desired form (7.3). This concludes the proof.

The quantity $|\dot{x}_{t_i} - \dot{x}_{-i}|$ indicates the roughness of control in the instant t_i. We will define a RF of a closed loop system as a scalar non-negative number RF:

$$RF \triangleq \sum_{i=o}^{N} \Delta\dot{x}_i^T W \Delta\dot{x}_i , \tag{7.7}$$

where

$$\Delta\dot{x}_i \triangleq \dot{x}_{+i} - \dot{x}_{-i}$$

$$t = N \times T$$

$$W \geq 0 .$$

In the definition of (7.7), RF = RF(N). By using (7.3), we may express RF as a function of x_i:

$$RF = \sum_{i=o}^{N} x_i[(\Phi+\Gamma C) - I]^T C^T G^T WGC[(\Phi+\Gamma C) - I]x_i . \tag{7.8}$$

If x_o is given, the RF is a function of x_o and N:

$$RF = \sum_{i=o}^{N} x_o(\Phi+\Gamma C)^{iT} [(\Phi+\Gamma C)-I]^T C^T G^T WGC[\Phi+\Gamma C)-I](\Phi+\Gamma C)^i x_o . \tag{7.9}$$

Obviously, the expression (7.9) is rather difficult to calculate. However, a simple form for RF can be obtained for the limiting case $N \to \infty$. There are two methods for the calculation of $RF_{N\to\infty}$.

Method 1: Using z-transforms and Parseval's Theorem:

$$r \triangleq GC(x_{i+1} - x_i) \tag{7.10}$$

$$r(z) = GC(Iz - I)(Iz - \Phi-\Gamma C)x_o \tag{7.11}$$

$$RF = \frac{1}{2\pi j} \oint_{\gamma} r^T(a)Wr(z^{-1})dz . \tag{7.12}$$

where γ is the unit circle.

Method 2: By using a Liapunov function. From (7.2) and (7.8) we obtain the following set of equations:

$$x_{i+1} = (\Phi + \Gamma C)x_i$$

$$RF = \sum_{i=o}^{N} x_i^T R x_i = Tr(x_o x_o^T P_o) \tag{7.13}$$

where

$$x_o \text{ - given}$$

$$R \triangleq [(\Phi+\Gamma C) - I]^T C^T G^T W G C[(\Phi+\Gamma C) - I] \tag{7.14}$$

$$(R \geq 0)$$

and P_o is obtained by a backward sweep from (7.15):

$$P_j = (\Phi + \Gamma C)^T P_{j+1}(\Phi + \Gamma C) + R$$

$$P_N = R, \quad j = N - 1, \ldots, 0 . \tag{7.15}$$

For $N \to \infty$, the solution for the RF reduces to a simple form:

$$RF = \sum_{i=o}^{N} x_i^T R x_i = Tr(x_o x_o^T P), \quad N \to \infty \tag{7.16}$$

where P is the solution of

$$P = (\Phi + \Gamma C)^T P(\Phi + \Gamma C) + R . \tag{7.17}$$

A-2 Numerical Solution of the Roughness Function

The easiest way to obtain the limiting case $RF_{N\to\infty}$ is to use Method 2, which involves the solution of the linear matrix equation (7.17). This type of equation is extensively treated in Chapter II (Section B-4). The solution we proposed there was to use the eigenvector decomposition algorithm. This algorithm, directly applicable

for (7.17) solves for P. After that, the RF is immediately obtained from (7.16).

A-3 Example of Roughness Function

We will demonstrate the RF on a simple first order continuous system controlled discretely. The purpose of this example is to illustrate the new concept. A more realistic example will be worked out in Sections VII-A-3 and VII-B-1.

The first order system is

$$\begin{aligned} \dot{x} &= -ax + gu \\ x_{i+1} &= e^{-aT}x_i + \Gamma u_i \\ \Gamma &= \left(1 - e^{-aT}\right)\frac{g}{a} \\ u_i &= cx_i \ . \end{aligned} \tag{7.18}$$

Equation (7.18) combined together yields

$$x_{i+1} = \left[e^{-at} + \left(1 - e^{aT}\right)\frac{gc}{a}\right]x_i \ . \tag{7.19}$$

The behavior of the controlled system of (7.19) is schematically described in Fig. VII-1.

A-4 Roughness Function of the Controlled Short Period Mode for Different Sampling Rates

We will investigate the behavior of the RF for the short period mode example described in Chapter III. The open loop poles of the short period mode are located at $s = -2.6 \pm j13.5$ (flight condition No. 8). The closed loop poles have been relocated to $s = -15 \pm j10$. The simplified equation of motion is

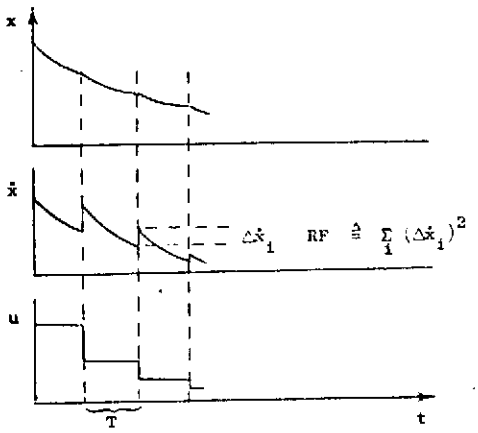

FIG. VII-1 SCHEMATIC DESCRIPTION OF THE ROUGHNESS FUNCTION

$$\begin{bmatrix} \dot{q} \\ \dot{\alpha} \end{bmatrix} = F \begin{bmatrix} q \\ \alpha \end{bmatrix} + Gu$$

where u is a discrete input, $u_i(\tau) = Cx_i$, $t_i < \tau < t_{i+1}$; u_i minimizes the cost function, J.

$$J = \int_0^\infty \left\{ [q \quad \alpha] \begin{bmatrix} A_q & 0 \\ 0 & A_\alpha \end{bmatrix} \begin{bmatrix} q \\ \alpha \end{bmatrix} + u^2 B \right\} dt . \qquad (7.21)$$

In our RF calculation we are assuming a perfect estimation of the states. This is assumed in order to make a parametric study. In this section we will investigate how the roughness changes at different sampling rates, while the dynamic properties are kept nearly constant. In the next section, we will keep the sampling rate constant but we will vary the dynamic properties.

The dynamic properties are characterized by the location of the closed loop poles on the z-plane. In Table VII-1 the closed loop poles of the short period example are summarized. In order to provide a better engineering insight, the equivalent s-plane poles are also listed. Furthermore, the trace of the poles on the z-plane is given

Table VII-1

POLE LOCATIONS OF THE SHORT PERIOD EXAMPLE FOR DIFFERENT SAMPLING RATES

	Pole Location		Control Gains	
Sampling Interval (sec)	z-plane	Equivalent s-plane	c_q	c_α
Open Loop	--	$-2.6 \pm j13.5$	0	0
T = 0	--	$-14.5 \pm j59.6$	0.3	0.6
T = 0.02	$0.73 \pm j0.14$	$-15.0 \pm j11$	0.273	-0.0101
T = 0.03	$0.63 \pm j0.68$	$-15.5 \pm j11.5$	0.245	-0.25
T = 0.05	$0.11 \pm j0.22$	$-16.0 \pm j12$	0.198	-0.603
T = 0.08	$0.18 \pm j0.2$	$-16.4 \pm j12.4$	0.143	-0.93
T = 0.1	$0.07 \pm j0.15$	$-17.0 \pm j12.5$	0.11	-1.06
T = 1.2	0.003 -0.06	$-17.5 \pm j12.7$	0.086	-1.1

in Fig. VII-2. All the z-plane poles and the feedback gains were calculated by the discrete synthesis program, keeping the weights in the quadratic cost function constant. The continuous case, T = 0, was calculated by a continuous synthesis program by Bryson et al [BR-2]. As seen in Table VII-1, the closed loop poles for different sampling interval were not significantly changed. The reason for the drastic change in the control gains will be explained later. The RF for this example was calculated for two different initial conditions: (a) $q_o \neq 0$, $\alpha_o = 0$; (b) $q = 0$, $\alpha_o \neq 0$.

For simplicity we assumed that the weigting matrix W has the simple form

$$W = \begin{bmatrix} 1 & 0 \\ 0 & 0 \end{bmatrix} . \qquad (7.22)$$

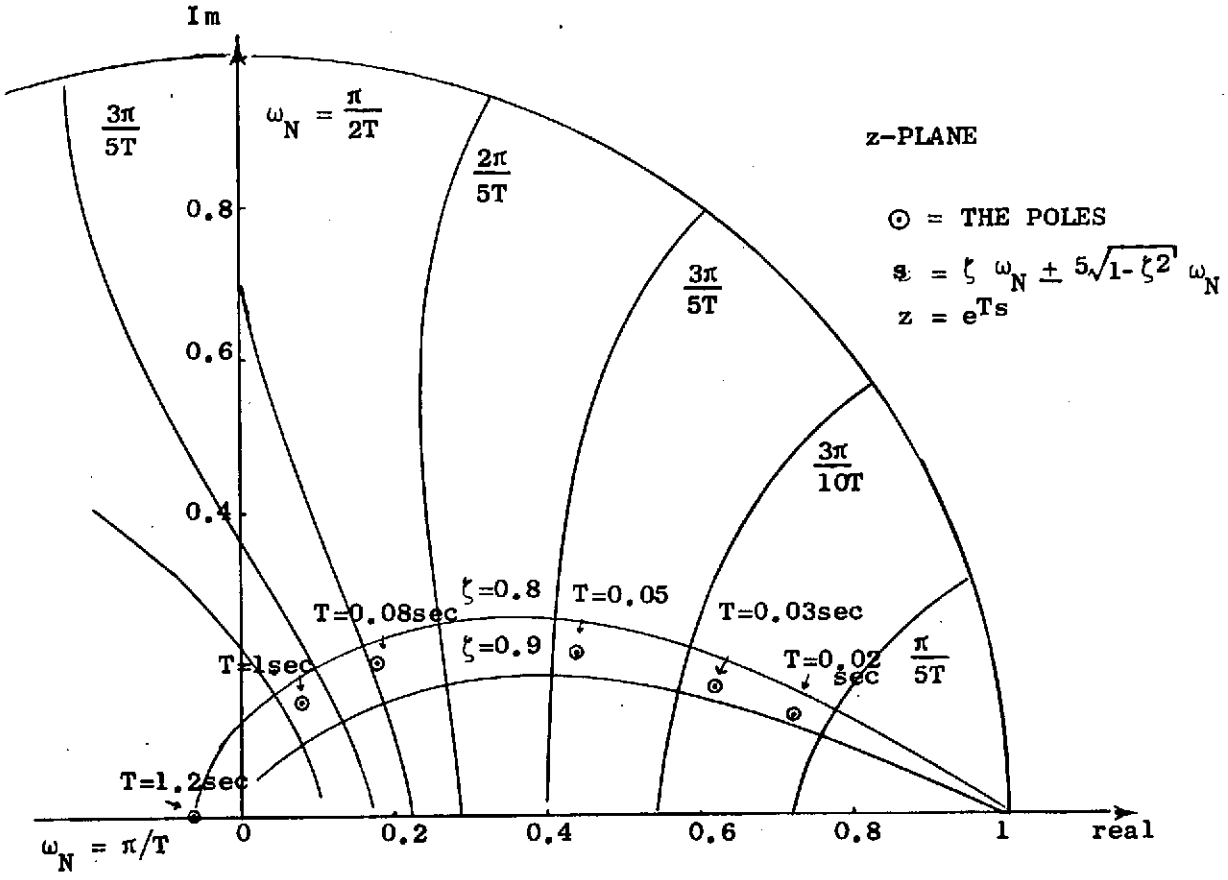

FIG. VII-2 THE CLOSED LOOP POLES OF THE SHORT PERIOD EXAMPLE

This is not a serious restriction as it can be easily proven that for a scalar input system, the time history of the roughness ($\Delta\dot{x}_i$) is similar to all the states (influenced directly by the input). Therefore, we calculated the abrupt changes in $\dot{q}$ only. The RF of the short period example vs different sampling intervals is plotted in Fig. VII-3. In order to make the various RF plots independent of the initial values, the RF was normalized by the initial conditions as follows: for $\alpha_o = 0$

$$(RF)_1 = \frac{1}{\dot{q}_o^2} \sum_i^{\infty} \Delta\dot{q}^2 \qquad (7.23)$$

and for $q_o = 0$

$$(RF)_2 = \frac{1}{\alpha_o^2}\sum_i \Delta\dot{q}^2 \quad . \tag{7.24}$$

Note: (a) For different weighting matrices, W, the plots of RF in Fig. VII-3 will have exactly the same form and only the scale of the vertical axis will be multiplied by some constant. (b) Although we are dealing with a linear system, the superposition principle does not hold for the RF, i.e., the RF for combined initial conditions is a quadratic form of the initial conditions.

Without a proper simulation, it will be difficult to explain the behavior of the RF for different sampling intervals. Therefore a complete digital simulation has been done and the simulation results are plotted in Figs VII-4 through VII-7. The simulation scheme is described in Appendix B. The different plots are organized by the following order:

T = 0.02 sec, T = 0.05 sec	Fig. VII-4	$q_0 \neq 0$, $\alpha_0 = 0$
T = 0.08 sec, T = 0.12 sec	Fig. VII-5	$q_0 \neq 0$, $\alpha_0 = 0$
T = 0.02 sec, T = 0.05 sec	Fig. VII-6	$q_0 = 0$, $\alpha_0 \neq 0$
T = 0.08 sec, T = 0.12 sec	Fig. VII-7	$q_0 = 0$, $\alpha_0 \neq 0$

By inspecting these plots we can see the following properties.

(a) For $\alpha_o = 0$ (Figs. VII-4, 5), as the sampling interval T increases, the initial input u_o decreases. This behavior stems from the fact that the optimal gain c_q decreases for larger sampling intervals (see Table VI-1). That change in c_q is easily explained by using the fundamentals of the optimal

control theory: the optimal control gain minimizes the quadratic cost function. By keeping the weights in the quadratic cost function constant, the squared area under the u/q_o curve should be approximately constant. For longer sampling intervals, the first input acts on the system longer; therefore, its amplitude has to be smaller.

(b) The optimal design essentially generates a damping augmentation (see Table VII-1). Thus if $q = 0$ and $\alpha_o = 0$, the input builds slowly until q reaches maximum (Fig. VI-6). But for longer sampling intervals, the optimal control doesn't have the time to wait for larger q. Therefore it predicts the larger q and generates feedback by increasing c_α (see Table VII-1 and Fig. VII-7).

(c) The fact that the RF is lower for sampling intervals and

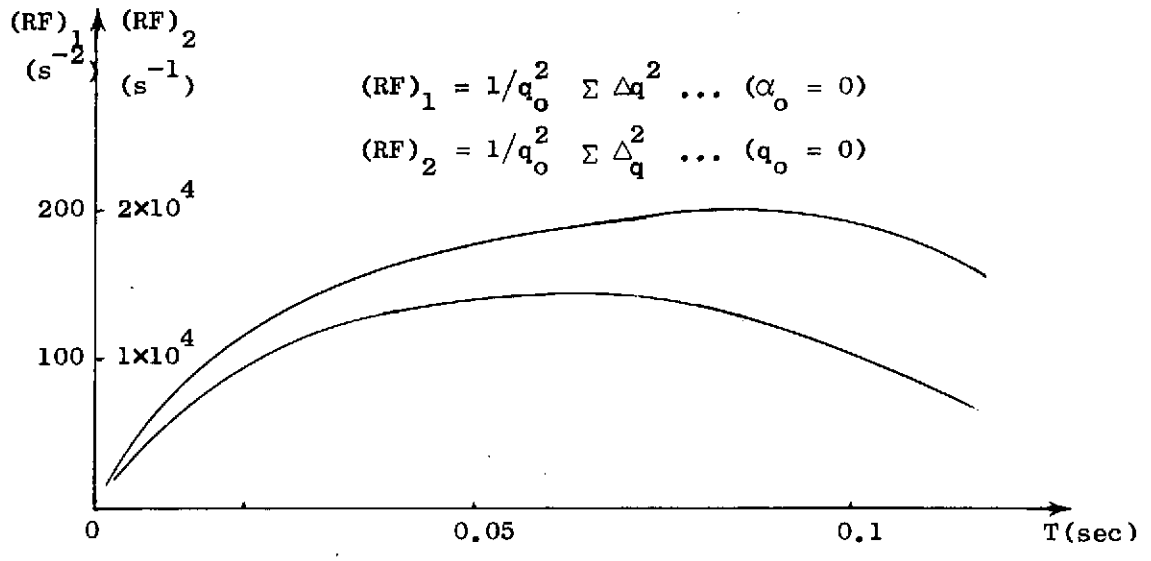

FIG. VII-3 THE ROUGHNESS FUNCTION OF THE SHORT PERIOD EXAMPLE VS DIFFERENT SAMPLING INTERVALS.

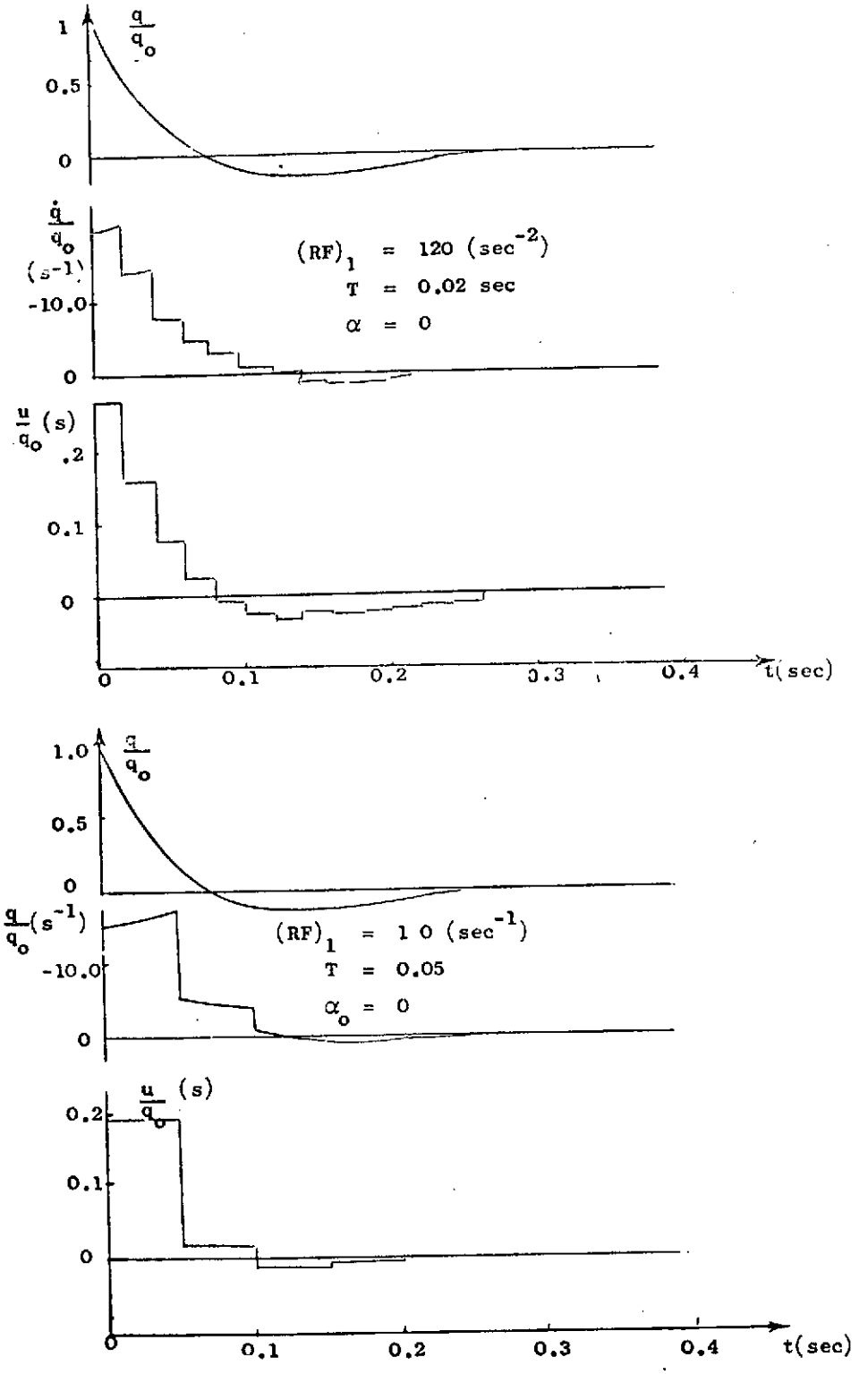

FIG. VII-4 TIME HISTORY OF THE SHORT PERIOD MODE.

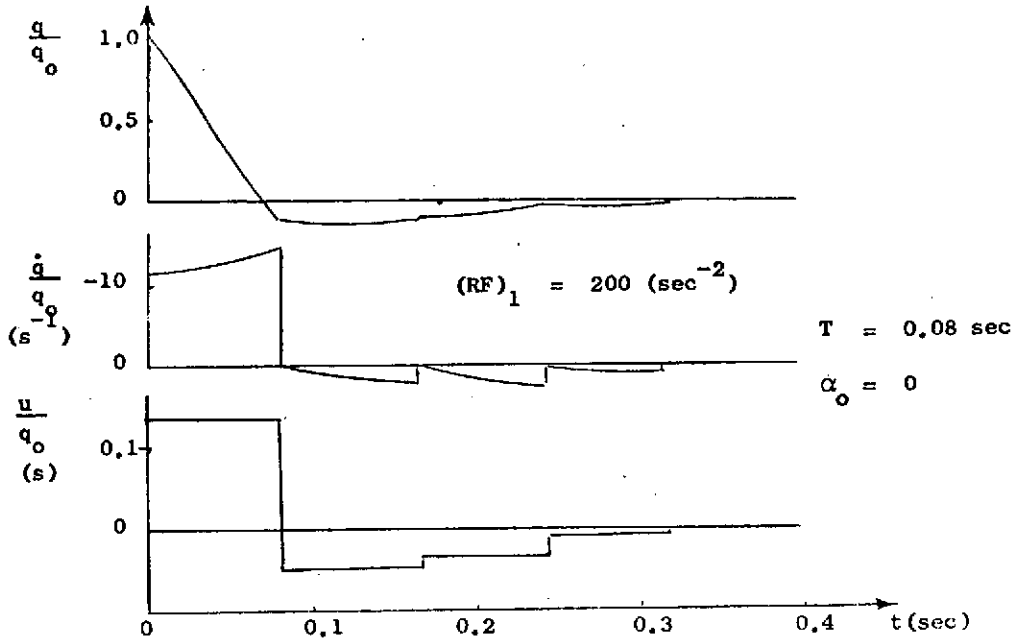

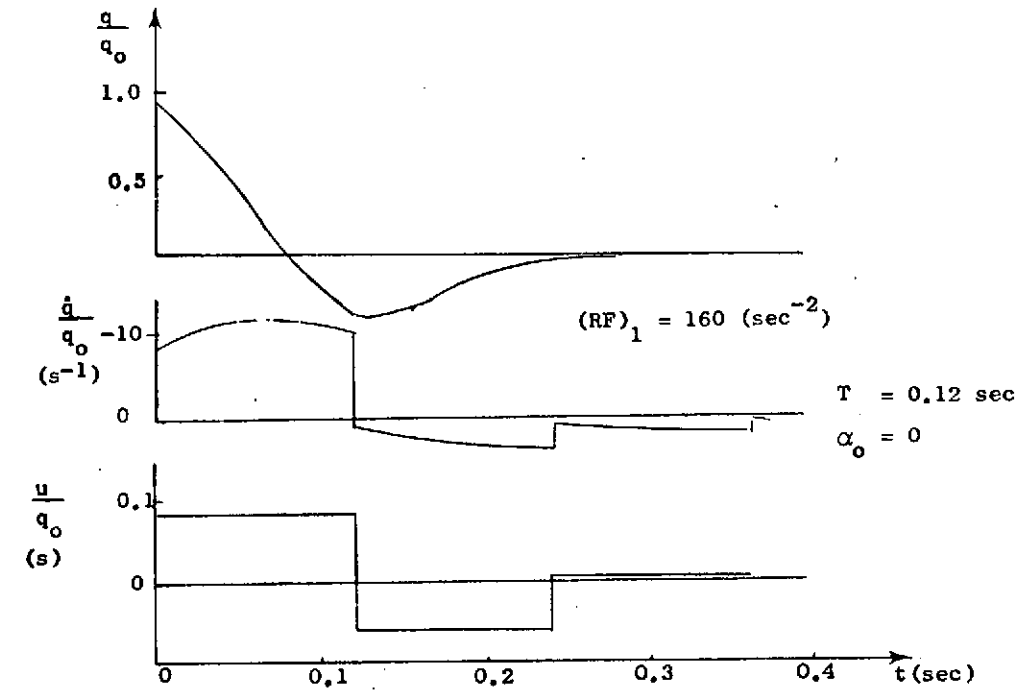

FIG. VII-5 TIME HISTORY OF THE SHORT PERIOD MODE.

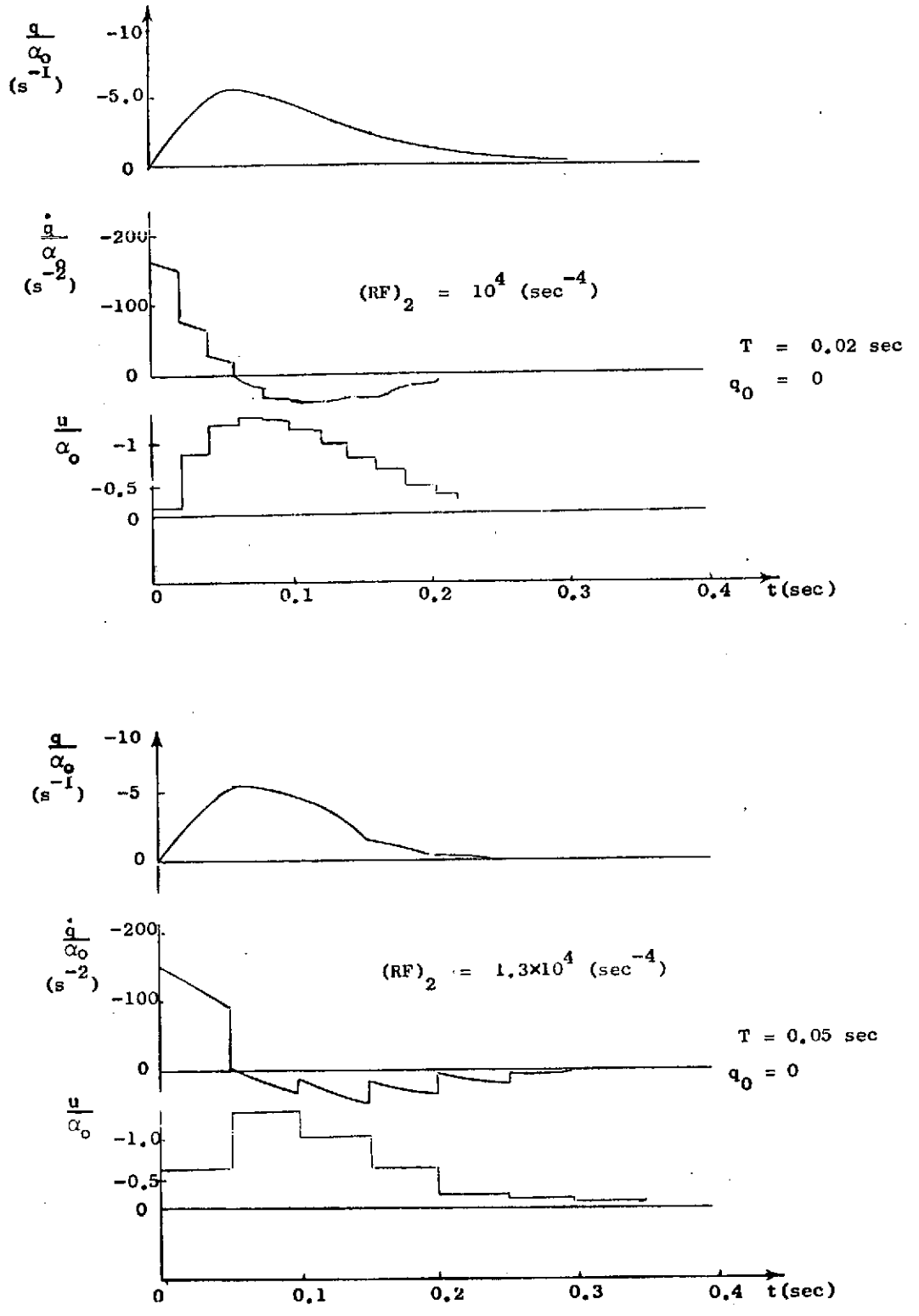

FIG. VII-6 TIME HISTORY OF THE SHORT PERIOD MODE.

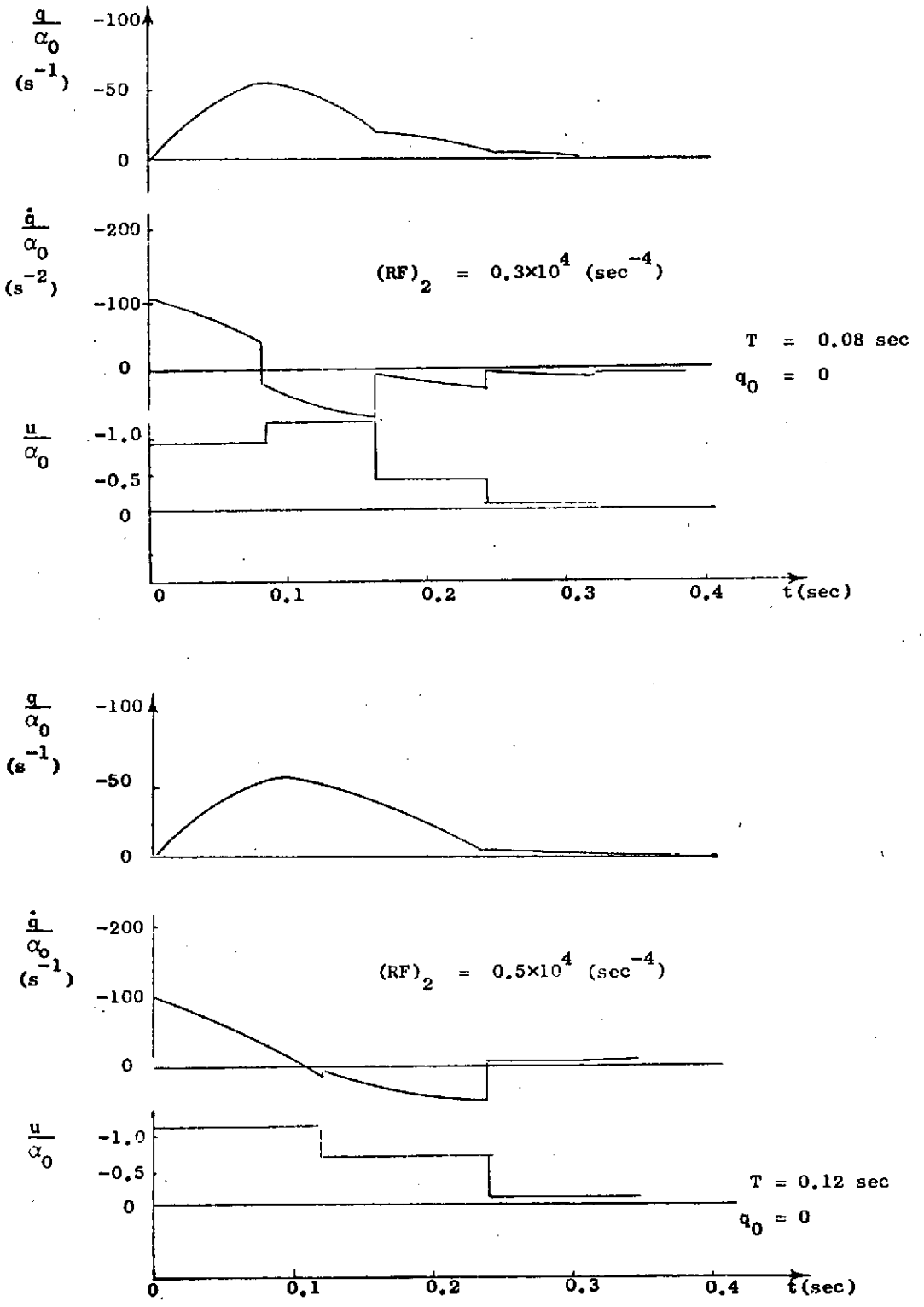

FIG. VII-7 TIME HISTORY OF THE SHORT PERIOD MODE.

longer than 0.1 sec does not mean that we are going to recommend the use of this low sampling rate (Fig. VII-3). There are other considerations in the selection of sampling rate, e.g., the time response.

B. THE MEAN ROUGHNESS FUNCTION OF A CLOSED LOOP SYSTEM DISTURBED BY AN EXTERNAL NOISE

We are also interested in estimating the average roughness of a continuous system controlled discretely and disturbed by a random noise

B-1 Definition of RF_m

The disturbed system is

$$\begin{aligned} \dot{x} &= Fx + Gu + w \qquad w \to N(0, Q) \\ x_{i+1} &= \Phi_c x_i + w_i \qquad w_i \to N(0, Q_d) \ . \end{aligned} \tag{7.25}$$

Φ_c is the closed loop transition matrix. Q_d is the covariance matrix of the discretized white noise with a power spectral density matrix Q.

The mean roughness function, RF_m, of this system will be defined as

$$RF_m = \mathrm{Tr}\, E\left\{(\dot{x}_{+i} - \dot{x}_{-i})(\dot{x}_{+i} - x_{-i})^T W\right\} \qquad i \to \infty \tag{7.26}$$

where $W \geq 0$. Using relation (7.6), we have (repeat)

$$\Delta\dot{x}_{i+1} \triangleq \dot{x}_{+i+1} - \dot{x}_{-i+1} = G(u_{i+1} - u_i) \ .$$

Therefore,

$$E\{\Delta\dot{x}_{i+1}\} = E\{GC(x_{i+1} - x_i)\} \ . \tag{7.27}$$

Combining (7.25) and (7.27, we get

$$E\{\Delta\dot{x}_{i+1}\} = E\{GC(\Phi_c x_i - x_i + w_i)\}, \qquad w_i \rightarrow N(0, Q_d)$$

where E is a linear operator. Furthermore, x_i and w_i are uncorrelated by definition. Therefore

$$E\{\Delta\dot{x}_{i+1}\} = E\{GC(\Phi_c - I)x_i\} \tag{7.28}$$

where x_i is a Gauss-Markov random process with a covariance matrix X_i. $\Delta\dot{x}_i$ is a linear combination of x_i, thus, $\Delta\dot{x}_i$ is also a Gaussian-Markov process with a covariance matrix, X_{r_i} given by

$$X_{r_i} = GC(\Phi_c - I)X_i(\Phi_c - I)^T C^T G^T + GCQ_d C^T G^T \tag{7.29}$$

where $X_i = E\{x_i x_i^T\}$. The steady state value of the covariance matrix X_i is the solution of

$$X = \Phi_c X \Phi_c^T + Q_d \, . \tag{7.30}$$

(see Chapter II). By combining (7.26) and (7.29) we have the final expression for RF_m

$$RF_m = Tr(X_r W) \tag{7.31}$$

where

$$X_r = GC(\Phi_c - I)X(\Phi_c - I)^T C^T G^T + GCQ_d C^T G^T. \tag{7.32}$$

Similar to the RF for an impulse response, the RF_m involves the solution of a matrix linear equation, (7.30).

B-2 RF_m of the Controlled Short Period Mode

In this section we will investigate the RF_m for the short period example described in Chapter IV. The only difference between this model

and the one used in Section VI-A-3 is in the augmentation of the states by the wind model as we will now describe.

The system:

$$\begin{bmatrix} \dot{q} \\ \dot{\alpha}_T \\ \dot{w}_g \end{bmatrix} = \begin{bmatrix} \Phi & \Gamma_w \\ 0 & \Phi_w \end{bmatrix} \begin{bmatrix} q \\ \alpha_T \\ w_g \end{bmatrix} + \Gamma_1 u + \Gamma_2 w, \qquad w \to N(0, Q) . \tag{7.33}$$

The open loop poles were located at $s = -2.6 \pm j13.5$ and the nominal weights (Ch. VI-C) relocated the closed loop poles to $s \cong 10 \pm 15$. As in Section VII-A-3, we are also assuming perfect measurements of the states. This is done for simplicity of calculation as we are interested in the behavior of the RF_m for different weights ($A_{a/B}$, $A_{\alpha/B}$) rather than in its absolute value. The wind gusts model used in this example is the model of flight condition No. 8 (σ_N = 12 ft/sec, τ_w = 0.5). All the calculations were made for one sampling rate (T = 0.05 sec).

By varying the values of $A_{q/B}$ and $A_{\alpha_T/B}$ we will consider the behavior of the following quantities: (1) $\bar{q}^2$, covariance of the state q; (2) $\bar{\alpha}_T^2$, covariance of the state α_T; (3) $\bar{u}^2$, covariance of the control u. Furthermore, the weighting matrix W in the RF_m criteria (6.26) will have the form

$$W = \begin{bmatrix} 1 & 0 & 0 \\ 0 & 1 & 0 \\ 0 & 0 & 0 \end{bmatrix} . \tag{7.34}$$

and we will consider the two components of RF_m: (repeat of Eq. 7.31)

$$RF_m = T_r(X_r W)$$

namely, RF_q, component of RF_m, corresponding to $(\bar{\Delta q})^2$; RF_{α},

component of RF_m corresponding to $(\overline{\Delta\alpha})^2$. The RF_m calculations are as follows:

The closed loop pole location as a function of different weight is plotted in Fig. VII-8. The nominal design was chosen in Ch. IV. The behavior of the above listed quantities as a function of $A_{q/B}$ is plotted in Fig. VII-9. The covariance of q ($\bar{q}2$) decreases for larger weights $A_{q/B}$. But this cannot be done without a penalty, which (a) an increase in RF_q, (b) an increase in $\bar{u}^2$.

The behavior of the system as a function of $A_{\alpha/B}$ is more complicated. As seen in Fig. VII-10, only $\bar{q}^2$ increases as $A_{\alpha/B}$ increases. The physical explanation is given in Fig. VII-8 where the increase in $A_{\alpha/B}$ keeps nearly the same damping but decreases the natural frequency; this means that the systems reponds slowly and there are less abrupt actions in the control. As a conclusion of this section, we may say that the RF_m provides us with additional insight into the system.

C. ROUGHNESS FUNCTIONS FOR FIRST ORDER HOLD, TRIANGULAR HOLD, AND PLANTS WITH FILTERED INPUT

The object of this section will be to suggest and investigate different functional forms which will enable us to compare roughness of control for different reconstruction holds and for plants which include actuators or filtered inputs.

The properties we expect from a roughness function are:

(a) The RF should be related to the difference of numbers in the discrete input sequence;

(b) For $T = 0$, the RF is zero;

(c) In order to establish experimentally a relationship between the RF and the pilot's evaluation, the RF should be represented by a positive function;

Pole No.	$\frac{A_q}{B}$	$\frac{A_{\alpha_T}}{B}$
1	0	10.0
2	1.0	10.0
3	2.0	10.0
4	1.0	0
5	1.0	30.0

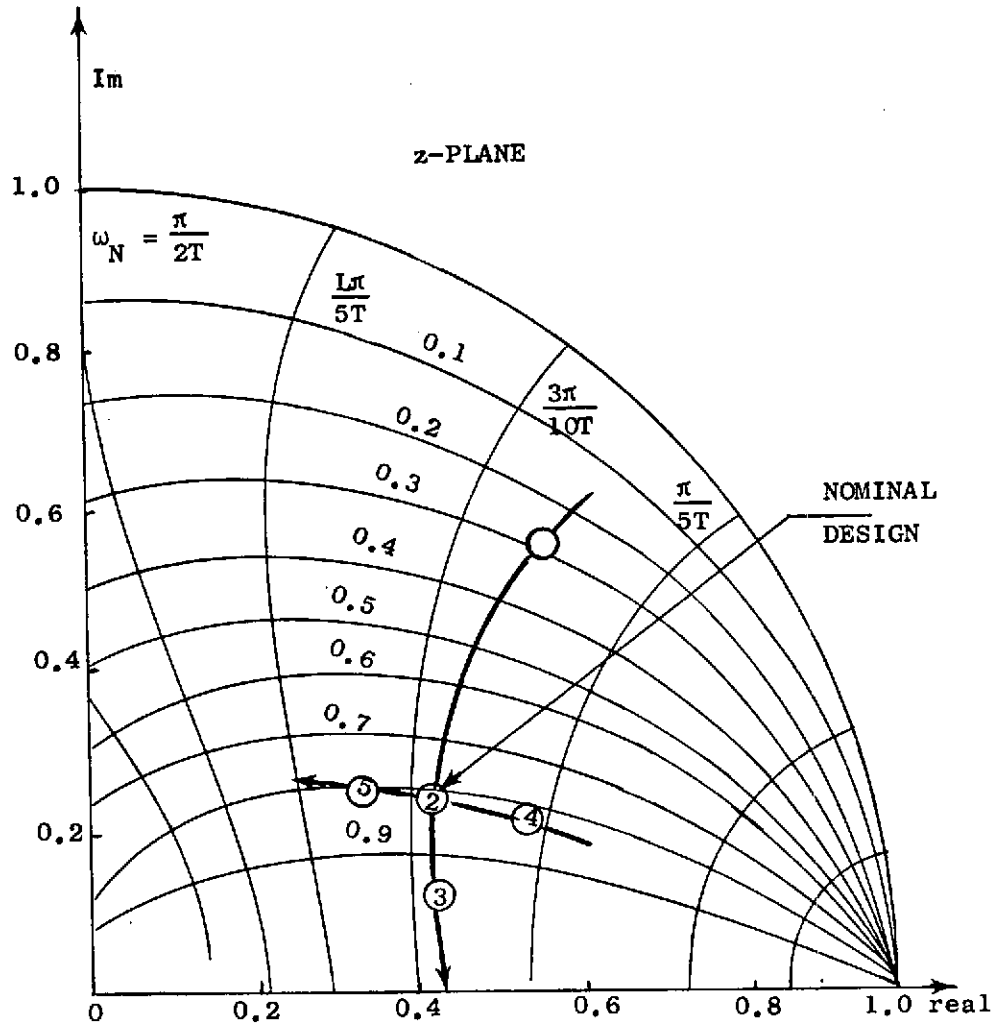

FIG. VII-8 SHORT PERIOD MODE. Pole locations as a function of weights on q and α_T. Flight Condition No. 8. T = 0.05 sec.

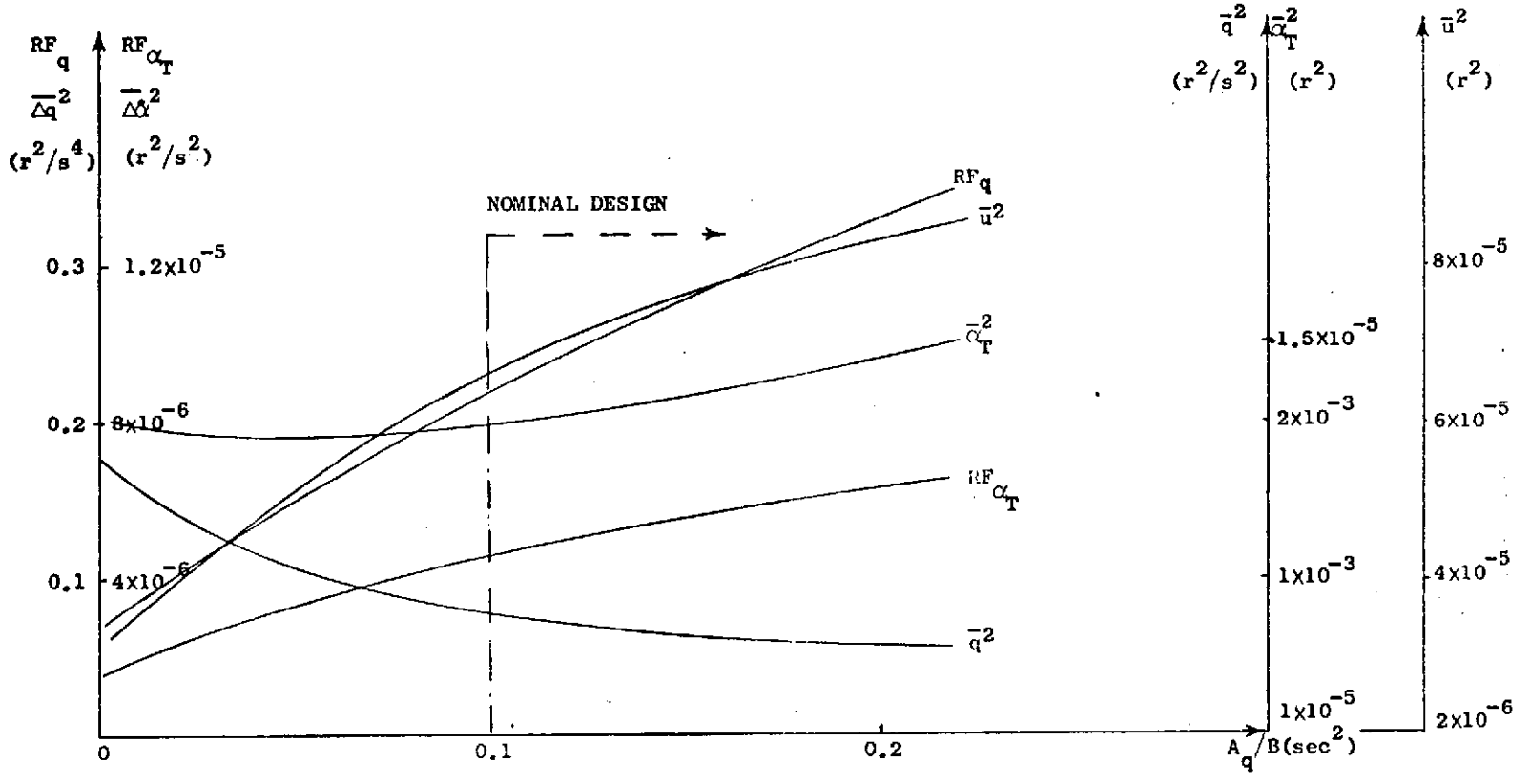

FIG. VII-9 RF_n AS A FUNCTION OF WEIGHT ON q, $\bar{u}^2$, $\bar{\alpha}_T^2$, and $\bar{q}^2$.

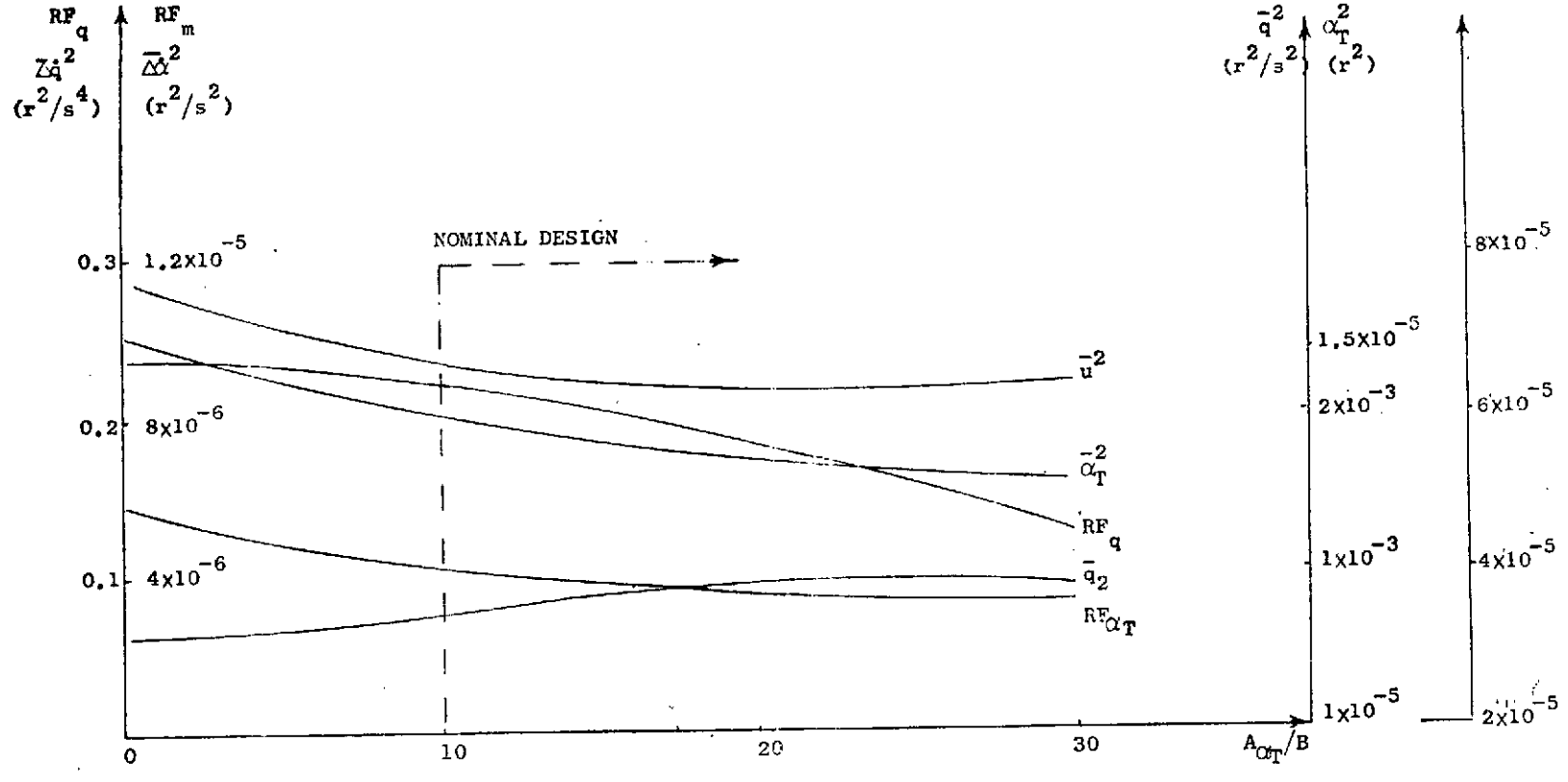

FIG. VII-10 RF_n AS A FUNCTION OF WEIGHT ON α_T, $\bar{u}^2$, $\bar{\alpha}_T^2$ and $\bar{q}^2$.

(d) The RF has to be user-oriented and it should have a convenient computer program form.

We will investigate the RF for four different control configurations: (a) zero order hold/ZOH; (b) first order hold/FOH; (c) triangular hold; (d) filtered input (or actuator lag). The block diagrams of the system and their schematical time responses are plotted in Figs. VII-11 and VII-12. It should be noted that in the classical sample data

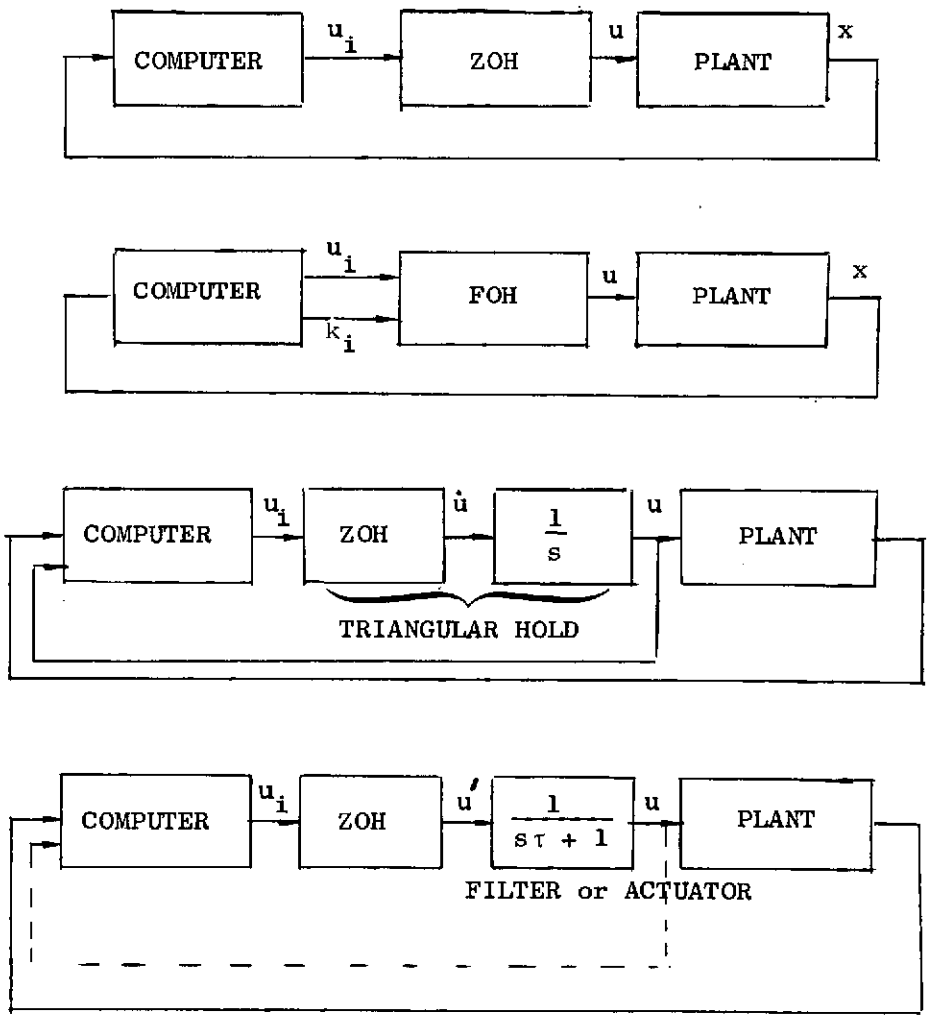

FIG. VII-11 DIFFERENT RECONSTRUCTION HOLD CONFIGURATIONS

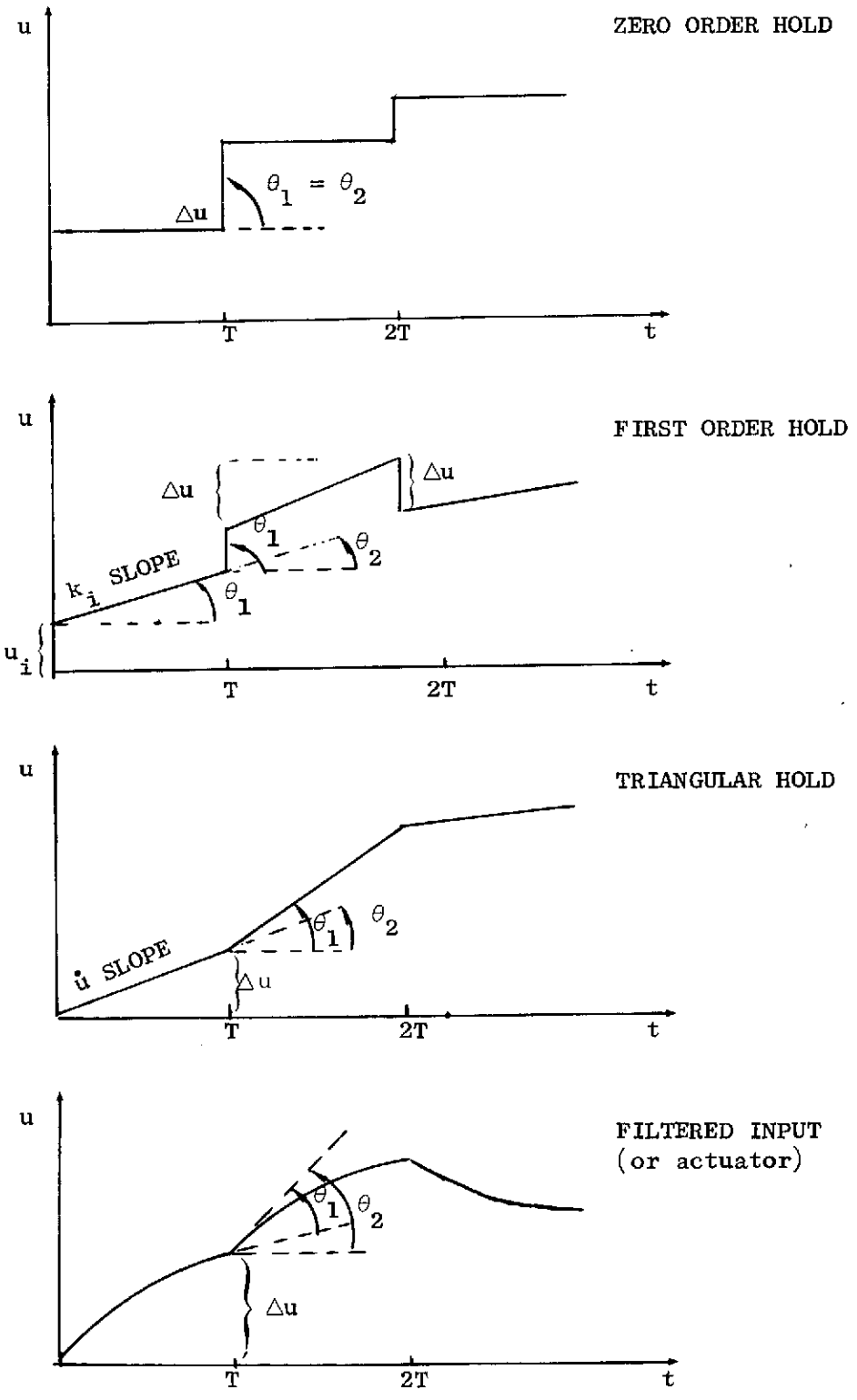

FIG. VII-12 THE SCHEMATIC BEHAVIOR OF DIFFERENT RECONSTRUCTION HOLDS AND THE PARAMETER DEFINITIONS FOR THE RF CALCULATIONS.

theory, the triangular hold is an unrealizable reconstruction hold and is used only for non-real time integration. However, if optimal control is used, the input u is actually a part of the state vector and is fed back (see Fig. VII-11). Therefore the triangular hold is realizable in this formulation.

The proposed RFs are:

$$RF_1 = \sum_{i=o}^{N} \left(\frac{\theta_1}{\pi/2}\right)^2 \Delta u^2$$

$$RF_2 = \sum_{i=o}^{N} \left(\frac{\theta_2}{\pi/2}\right)^2 \Delta u^2$$

$$RF_3 = \max\left|\frac{\theta_2}{\pi/2} \Delta u\right|$$

$$RF_4 = \max\left|\frac{\theta_1}{\pi/2} \Delta u\right| .$$

These four RFs can be calculated by simulation only. RF_1 and RF_2 are actually identical to the RF which was defined in Section A for a zero order hold. Only for this case does RF_1 and RF_2 have an analytical solution.

D. COMPARISON OF ROUGHNESS OF THE F-H MODEL FOR DIFFERENT RECONSTRUCTION HOLDS

Each of the four RFs will be demonstrated for the F-H short period mode (Flight Condition No. 8, $T = 0.05s$) using different reconstruction holds and actuator. The optimal feedback gains and the digital simulation was done by the Program DISC and by the simulation program described in Appendices A and B. Since the two programs are constructed for a ZOH (zero order hold), the FOH (first order hold)--the triangular hold--and the filtered input were reformulated to a ZOH equation: (repeat)

$$\dot{x} = Fx + Gu$$

where u is constant for $0 \leq \tau < T$. For the FOH:

$$\begin{bmatrix} x \\ \dot{u}_1' \end{bmatrix} = \begin{bmatrix} F & G \\ 0 & 0 \end{bmatrix} \begin{bmatrix} x \\ \acute{u}_1 \end{bmatrix} + \begin{bmatrix} G & 0 \\ 0 & I \end{bmatrix} \begin{bmatrix} \acute{u}_2 \\ k \end{bmatrix} \tag{7.35}$$

where

$$\left.\begin{aligned} \acute{u}_2 &= \text{constant} \\ k &= \text{constant} \\ u &= \acute{u}_1 + \acute{u}_2 \end{aligned}\right\} 0 \leq \tau < T .$$

The triangular hold:

$$\begin{bmatrix} x \\ \dot{u} \end{bmatrix} = \begin{bmatrix} F & G \\ 0 & 0 \end{bmatrix} \begin{bmatrix} x \\ u \end{bmatrix} + \begin{bmatrix} 0 \\ I \end{bmatrix} \acute{u} \tag{7.36}$$

where $\acute{u}$ = constant, $0 \leq \tau \leq T$.

The filtered input:

$$\begin{bmatrix} \dot{x} \\ \dot{u} \end{bmatrix} = \begin{bmatrix} F & G \\ 0 & -\frac{1}{\tau} \end{bmatrix} \begin{bmatrix} x \\ u \end{bmatrix} + \begin{bmatrix} 0 \\ \frac{1}{\tau} \end{bmatrix} \acute{u}$$

where $\acute{u}$ = constant, $0 \leq \tau \leq T$.

The feedback gains (weighting matrices) were so chosen that the closed loop poles of the short period mode were placed in identical positions for all the four control configurations $(z = 0.44 \pm j0.22)$.

To obtain a visual impression of the roughness, the behavior of the input u is plotted in Fig. VII-13 (for an initial condition in α). However, from visual inspection, we cannot definitely conclude which hold is 'better'. The pilot's rating is necessary to evaluate the roughness and to relate it to the proposed roughness functions. The numerical

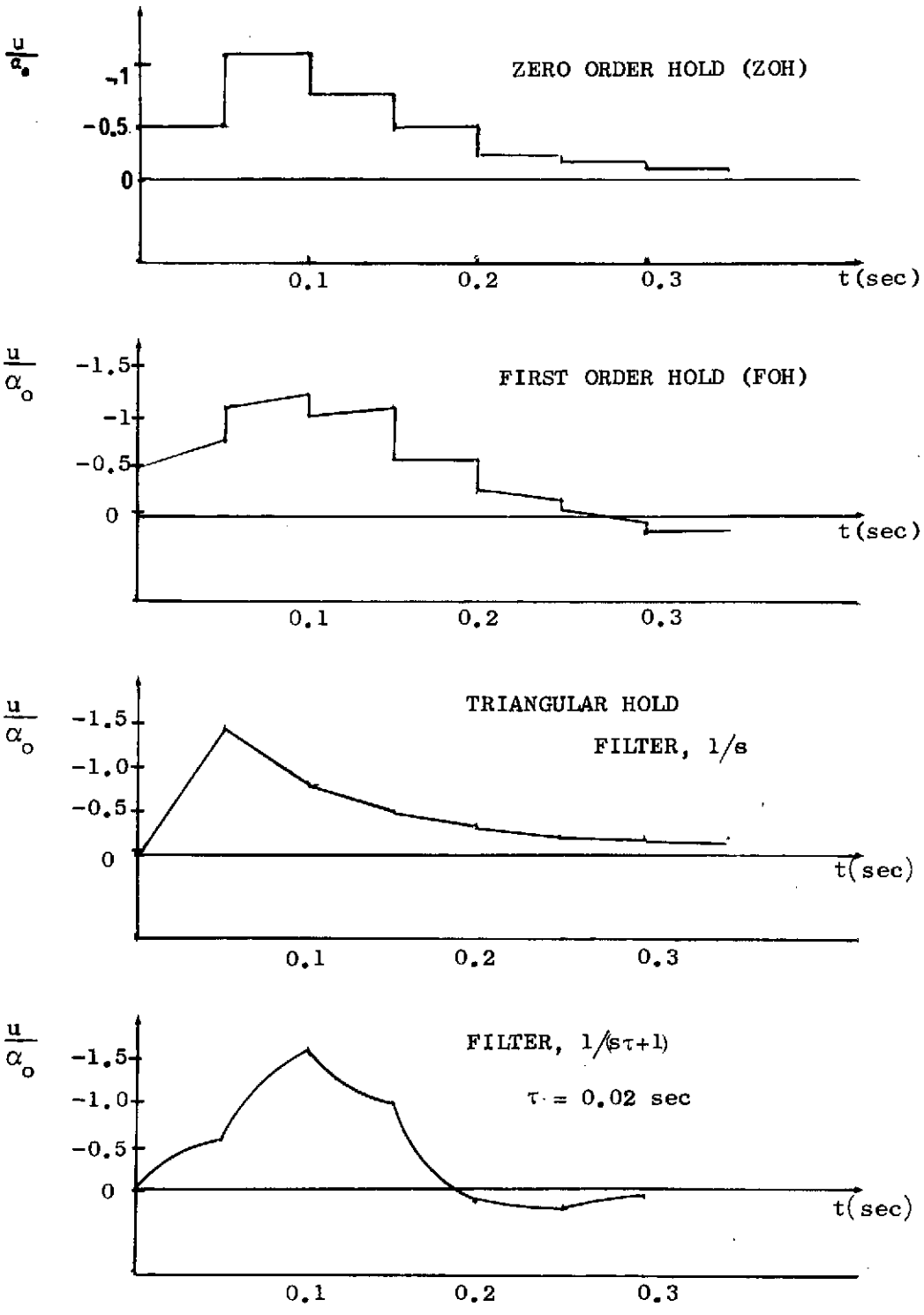

FIG. VII-13 TIME HISTORY OF THE CONTROL INPUT OF THE DIFFERENT RECONSTRUCTION HOLDS OF THE F-H. Flight Condition No. 8, T = 0.05s

values of the proposed roughness functions are summarized in Table VII-2.

Table VII-2

THE ROUGHNESS FUNCTIONS VALUES FOR THE F-H SHORT PERIOD MODE OF THE DIFFERENT RECONSTRUCTION HOLDS

	ZOH	FOH	Triangular Hold	Filtered Input
RF_1	1.42	0.95	0.16	1.1
RF_2	1.42	0.9	0.36	1.0
RF_3	0.9	0.6	0.3	0.9
RF_4	0.9	0.62	0.6	0.8

From Table VII-2 we may conclude that for the four proposed RFs, the triangular hold has the lowest value.

E. SUMMARY

1. The experimental results of Mathew for the digital autopilot of the Saab Wiggen airplane [MA-1] indicates the need for some measure of roughness as a design tool.

2. We have defined such a measure, calling it the "roughness function" (RF), which can be calculated by relatively simple algorithms.

VIII. CONCLUSIONS AND RECOMMENDATIONS

A. CONCLUSIONS

A-1 Selection of Sample Rate

Four principal factors influence the selection of the sample rate for the discrete control of a continuous system. These factors are:

a. the time response to control inputs,

b. the response to an external noise,

c. the sensitivity to variations of parameters,

d. the roughness of the response to control inputs.

Each of these factors and its relation to the sampling rate should be carefully investigated.

a. The time response.

The time response is directly related to the sampling interval. For future fly-by-wire controlled aircrafts, there is an inherent time lag between the pilot's decision and the execution of his command. This was discussed in Ch. III.

b. Response to an external noise.

The response to an external random disturbance is a function of the sampling rate. It was found that in discrete systems, there is a limit on noise alleviation. This limit is a function of the sampling rate.

c. Sensitivity to variations of parameters

The sensitivity to variation of parameters can be reduced by a modification of the discrete compensator. In the F-H short period example the bending mode frequency is one of the major uncertainties. It was found that the optimal compensator generates a narrow and sensitive notch filter which attenuates the bending frequency. For a 10 percent error in the bending frequency, the system is unstable for lower sampling rate (for $\omega_s/\omega_b < 2$). By modifying the compensator to broaden the notch, the bending mode was stabilized for much larger errors in bending frequency.

d. The roughness of response to control inputs

The roughness of response to control inputs is an inherent property of the zero order reconstruction hold. The roughness function defined in Ch. VI is used to give an analytical measure of the rough behavior of the system. This criterion, demonstrated on the F-H short period mode, will help designers to evaluate the behavior of a controlled system and select a suitable sampling rate.

A-2 Relationship Between Sensitivity and Compensator Poles

As is already known; the stability of a closed loop system is unrelated to the stability of the compensator. A stable system may have an unstable compensator but it has been found that if the compensator poles are more damped, the closed loop system has lower sensitivity to variation of parameters.

A-3 Filtering Property of the Zero Order Hold

The zero order hold has a well-known property: it filters all the frequencies which are integral multiples of the sampling rate. However, it has been found that if the system includes a subsystem

oscillating in the same frequency as the sampling rate, the whole system may be unstable in the intersample intervals. This instability cannot be detected by a discrete analysis. It is necessary to investigate the intersample behavior.

B. RECOMMENDATIONS

Further research is required on the following topics.

1. A theory and a computer algorithm for synthesis of an optimal discrete system which includes a sensitivity minimization.

2. An analysis of the behavior of a closed loop system which uses the modified first order reconstruction hold (proposed in Ch. II-A).

3. An experimental investigation of the relationship between both handling qualities and pilot comfort, and the numerical values of the roughness function.

4. An analysis of the reduction of roughness by filtering the reconstruction hold output, and of the resulting influence on the stability and complexity of the system.

5. A method which will help the designer decide on the minimal representation model of a given system. This representation should be sufficient to construct a control law for the actual plant. The behavior of this controlled plant will be unaffected by the unmodeled states.

Appendix A

PROGRAM DISC: OPTIMAL DISCRETE CONTROL AND FILTER SYNTHESIS BY EIGENVECTOR DECOMPOSITION

In this Program there are various options. The basic calculations are as follows. (a) For a system given as

$$x_{i+1} = \Phi x_i + \Gamma_1 u_i, \tag{A-1}$$

DISC calculates gain C, $u_i = Cx_i$ which minimizes the cost function J

$$J = \frac{1}{2} \sum_{i=0}^{\infty} x_i^T A x_i + u_i^T B u_i \qquad \begin{matrix} A > 0 \\ B > 0 \end{matrix} . \tag{A-2}$$

(b) For a system given as

$$\begin{aligned} x_{i+1} &= \Phi x_i + \Gamma_2 w_i & w_i &\to N(0, Q_d) \\ y_i &= H x_i + v_i & v_i &\to N(0, R) , \end{aligned} \tag{A-3}$$

DISC calculates the matrices M, P, K, where K represents the gains in the Kalman filter,

$$\begin{aligned} \bar{x}_{i+1} &= \hat{\Phi} x_i \\ \hat{x}_i &= \bar{x}_i + K(y_i - H\bar{x}_i) \end{aligned} \tag{A-4}$$

and M = the error covariance matrix before the measurements, and P = the error covariance matrix after the measurements.

(c) For a system combined from controller (a) and filter (b), DISC

calculates the covariance matrix X of the states, and the covariance matrix U of the control. X and U are the solution of

$$\begin{aligned} X - M &= (\Phi + \Gamma c)\,(X - P)\,(\Phi + \Gamma C)^T \\ U &= CXC^T \,. \end{aligned} \tag{A-5}$$

Various Options

The various options are (a) For

$$\dot{x} = Fx + G_1 u + G_2 w \qquad w \to N(O,\ Q),$$

and if the controls are reconstructed by a zero order hold, DISC calculates

$$\begin{aligned} \Phi &= e^{FT} \\ \Gamma_1 &= \int_o^T e^{F\tau} G_1 d\tau \end{aligned} \tag{A-6}$$

$$Q_D = \int_o^T \Phi(\tau) G_2 Q G_2^T \Phi(\tau)^T d\tau \tag{A-7}$$

and sets $\Gamma_2 = I$ (unity matrix). T is the sampling interval.

(b) If a continuous cost function,

$$J' = \frac{1}{2}\int_o^\infty (x^T A' x + u^T B' u)dt \tag{A-8}$$

is given, DISC calculates the control C, which minimizes the cost function J' by transforming J' to J by

$$J = \sum_{i=o}^{\infty} \begin{bmatrix} x_i^T & u_i^T \end{bmatrix} \begin{bmatrix} A_{11} & A_{12} \\ A_{21} & A_{22} \end{bmatrix} \begin{bmatrix} x_i \\ u_i \end{bmatrix} , \tag{A-9}$$

where

$$A_{11} = \int_o^T \Phi^T(\tau) A \Phi(\tau) d\tau$$

$$A_{12} = \int_o^T \Phi^T(\tau) A \Gamma(\tau) d\tau \qquad \text{(A-10)}$$

$$A_{22} = \int_o^T [\Gamma^T(\tau) A \Gamma(\rho) + B] d\tau$$

$$A_{21} = A_{12}^T ,$$

and transforms the system (A-1) into

$$x_{i+1} = (\Phi - \Gamma_1 A_{22}^{-1} A_{21}) x_i + \Gamma_1 u_i' \qquad \text{(A-11)}$$

$$u_1' = u_i + A_{22}^{-1} A_{21} x_i = C' x_i . \qquad \text{(A-12)}$$

After this transformation, (A-9) obtains the form of (A-2), i.e.,

$$J = \sum_{i=o}^{\infty} x_i^T (A_{11} - A_{12} A_{22}^{-1} A_{21}) x_i + u_i^T A_{22} u_i . \qquad \text{(A-13)}$$

DISC solves for C' (for A-11 and A-13) and calculates the desired C from

$$C = C' - A_{22}^{-1} A_{21} . \qquad \text{(A-14)}$$

(c) If perfect measurements are assumed, DISC calculates the covariance of the states, X, from

$$X = (\Phi + \Gamma c) X (\Phi + \Gamma c)^T + Q_d . \qquad \text{(A-15)}$$

(d) DISC calculates the open loop eigenvalues and eigenvectors. (The closed loop eigenvalues and eigenvectors, and the estimate error eigenvalues and eigenvectors, are always calculated and printed.) Using DISC

DATA			FORMAT
CARD	7	IOC/ IQ/ INQ/ ICC/	Format (4I2)
	8	NS/ NC/ NZ/ NG/ T	Format (4I3, F10.5)
	9	F or Φ	Format (6F12.5) row by row each row starts by new line
	•	G_1 or Γ_1	
	•	A	
	•	B	
	•	G_2 or Γ_2	
	•	Q or Q_d	
	•	R	
	•	H	
	/*	(last card)	

CARD 7: OPTIONS

IOC = 1 open loop eigenvalue and eigenvectors

IQ = 1 response for perfect measurements

INQ = 1 response for estimated measurements

ICC = 1 continuous cost function

If one or more of these options are not desired, set values to zero.

CARD 8

NS number of states

NC number of controls

NZ number of measurements

NG number of disturbances

T sampling interval

Important: In order to simplify the utilization of this program, all options are activated by necessary parameters and data. All unnecessary information should be deleted.

The various options and instruction for data input are summarized in Table A-1.

Table A-1

INPUT TO DISC

	CARD	CONTINUOUS SYSTEM PLUS ZOH					DISCRETE SYSTEM				
REGULATOR ONLY	7	x	0	0	x		x	0	0	0	
	8	NS	NC	0	0	T	NS	NC	0	0	0
	9	F G_1 A B					Φ Γ_1 A B				
REGULATOR PLUS RESPONSE TO EXTERNAL DISTURBANCE	7	x	1	0	x		x	1	0	0	
	8	NS	NC	0	NG	T	NS	NC	0	NG	0
	9	F G_1 A B G_2 Q					Φ Γ_1 A B Γ_2 Q_d				
FILTER	7	x	0	0	x		x	0	0	0	
	8	NS	0	NZ	NG	T	NS	0	NZ	NG	0
	9	F G_2 R H					Φ Γ_2 R H				
REGULATOR PLUS FILTER	7	x	x	x	x		x	x	x	0	
	8	NS	NC	NZ	NG	T	NS	NC	NZ	NG	0
	9	F G_1 A B G_2 Q R H					Φ Γ_1 A B $_2$ Q_d R H				

x → 0, 1 ... different options; 9 → order of reading matrices in.

Note: If more than the minimal amount of necessary parameters and data are read in, the program execution will fail. For example, you cannot:

(a) set ICC = 1. for pure discrete system
(b) set IQ = 1. and INQ = 1. simultaneously
(c) set NC $\neq$ 0 if you are asking for filter only.

The following is the computer program for DISC.

```
1.      //DISC JOB '5270,202,2.,10',KATZ,MSGLEVEL=1
2.      //  EXEC FORTHCL,LEVEL=G
3.      //FORT.SYSIN DD *
4.            IMPLICIT REAL*8(A-H,O-Z)
5.      C THE FOLLOWING ARE DIMENSIONED SO THAT AN  16  ORDER OR SMALLER SYSTEM
6.      C  WITH UP TO 16 CONTROLS CAN RUN
7.            DIMENSION A(32,32),RM(32,32),WR(32),WI(32),X(32,32),PRO(32,32),
8.           1CWR(16),CWI(16),ICNT(32),D(32),INT(32),BA(16,16),ACL(16,16),
9.           2GN(16,16), Q(16,16),RVEC(16,16),VECRN(16,16),VECIN(16,16),
10.          8VECI(16,16),VRV(16),VIV(16),VRRV(16),VRIV(16),W11(16,16),C(16),
11.          9LT(256),MT(256),B(16,16),GM(16,16),
12.          3W21(16,16),TCB(32,16),AT(256),CI(16),CT(16,16),BI(16,16),
13.          5Y(16,16),FT(16,16),FTIA(16,16),FTIY(16,16),FTIYA(16,16),
14.          7SC(16,16),VECR(16,16),
15.          4G(16,16),FBGC(16,16),VEC(16,16),VF(32,32),H(16,16),
16.          1AQ(20,20),W1Q(20,20),W3Q(20,20),CQ(20,20),
17.          1FTQ(20,20),Q21(16,16),AQ21(16,16),GA(16,16),QD(16,16),
18.          1R(16,16),RI(16,16),BAK(16,16),GL(16,16),GAT(16,16),
19.          1GAT1(16,16),GI(16,16),FBGCK(16,16),QDQ(20,20)
20.           REAL*4 FMT(16)
21.           CALL ERRSET(207,256,-1,1,1,215)
22.     C
22.1    C
22.2    C  THE 'MAIN ' PROGRAM READS THE DIMENSION , THE OPTION CARD
22.3    C  AND CALLS FOR EXECUTION SUBROUTINE.
22.4    C
22.5    C
22.6    21       READ(5,7432,END=10) NS,NC,NZ,NG,T
23.           NC1=NC
24.           IF(NC.GT.0) GO TO 1
25.           NC=NC+1
26.        1   NG1=NG
27.           IF (NG.GT.0) GO TO 2
28.           NG=NG+1
29.        2  NZ1=NZ
30.
```

```
      IF (NZ.GT.0) GO TO 3
      NZ= NZ+1
    3  READ(5,51)IOL,IQ,INQ,ICC
   51  FORMAT(4I2)
 7432  FORMAT(4I3,F10.5)
      N2=2*NS
      MHS=NS*NS
      NNC=NS+NC
      CALL EXEC(NS,NC,N2,A,RM,WR,WI,X,PRO,CWR,CWI,ICNT,D,INT,
     1ACL,SC,GN,Q,B,BI,G,FBGC,GM,BA,C,CI,CT,MT,LT,AT,W21,TCB,W11,VF,
     3NC1,NG1,NZ1,Y,FT,FTIA,FTIY,FTIYA,H,NZ,
     2VEC,RVEC,VECRN,VECIN,VECR,VECI,VRV,VIV,VRRV,VRIV,MHS,IA,
     4AQ,W1Q,W3Q,CQ,QDQ,FTQ,NNC,Q21,AQ21,NG,T,GA,QD,R,RI,BAK,
     4FBGCK,GL,GAT,GAT1,GI,IOL,IQ,INQ,ICC)
      GO TO 21
   10  RETURN
      END
      SUBROUTINE EXEC(NS,NC,N2,A,RM,WR,WI,X,PRO,CWR,CWI,ICNT,D,INT,
     1ACL,SC,GN,Q,B,BI,G,FBGC,GM,BA,C,CI,CT,MT,LT,AT,W21,TCB,W11,VF,
     3NC1,NG1,NZ1,Y,FT,FTIA,FTIY,FTIYA,H,NZ,
     2VEC,RVEC,VECRN,VECIN,VECR,VECI,VRV,VIV,VRRV,VRIV,MHS,IA,
     4AQ,W1Q,W3Q,CQ,QDQ,FTQ,NNC,Q21,AQ21,NG,T,GA,QD,R,RI,BAK,
     4FBGCK,GL,GAT,GAT1,GI,IOL,IQ,INQ,ICC)
C
C
C  'EXEC' READS ALL THE MATRICES FIRST...
C
C
      IMPLICIT REAL*8(A-H,O-Z)
      DIMENSION A(N2,N2),RM(N2,N2),WR(N2),WI(N2),X(N2,N2),PRO(N2,N2),
     1CWR(NS),CWI(NS),ICNT(N2),D(N2),INT(N2),BA(NS,NS),ACL(NS,NS),
     2GN(NS,NS), Q(NG,NG),RVEC(NS,NS),VECRN(NS,NS),VECIN(NS,NS),VECR(NS,
     7NS),
     8VECI(NS,NS),VRV(NS),VIV(NS),VRRV(NS),VRIV(NS),W11(NS,NS),C(NS),
     9LT(MHS),MT(MHS),B(NC,NC),GM(NS,NS),
     3W21(NS,NS),TCB(N2,NS),AT(MHS),CI(NS),CT(NS,NS),BI(NC,NC),
```

```
      5Y(NS,NS),FT(NS,NS),FTIA(NS,NS),FTIY(NS,NS),FTIYA(NS,NS),H(NZ,NS),
     4G(NS,NC),FBGC(NC,NS),VEC(NS,NS),VF(N2,N2),SC(NS,NS),
     1AQ(NNC,NNC),W1Q(NNC,NNC),W3C(NNC,NNC),CQ(NNC,NNC),
     1FTQ(NNC,NNC),Q21(NC,NS),AQ21(NC,NS),GA(NS,NG),QD(NS,NS),
     1R(NZ,NZ),RI(NZ,NZ),BAK(NS,NS),GL(NS,NC),GAT(NG,NS),
     1GAT1(NG,NS),GI(NS,NS),FBGCK(NS,NZ),QDQ(NNC,NNC)
      REAL*4 FMT(20)
C READ ALL MATRICES
C
C
      IGN=0
      NC=NC1
      NG=NG1
      NZ=NZ1
      DO 61 I=1,NS
   61 READ(5,7433)(BA(I,J),J=1,NS)
      IF (NC.EQ.0) GO TO 10
      DO 62 I=1,NS
   62 READ(5,7433)(G(I,J),J=1,NC)
      CALL MAKE(GL,G,NS,NC)
      DO 63 I=1,NS
   63 READ(5,7433)(SC(I,J),J=1,NS)
      DO 64 I=1,NC
   64 READ(5,7433)(B(I,J),J=1,NC)
 7433 FORMAT(6G12.5)
    3 FORMAT(' ','OPEN LOOP DYNAMICS MATRIX....')
    4 FORMAT(8(2X,1PD13.6))
      WRITE(6,1)
    1 FORMAT('1',' ----------   N E W   C A S E ----  ')
      WRITE(6,6666) NS,NC,T
 6666 FORMAT('1',' THE ORDER OF THE SYSTEM =', I2,',    NUMBER OF CONTRO
     1LS=', I2,',     SAMPLING TIME=',F10.5)
      IF (ICC.EQ.0) GO TO 45
      WRITE(6,111)
  111 FORMAT('0',' YOU ARE USING THE CONT. COST FUNCTION ',//)
   45   WRITE(6,3)
```

```
      DO 5001 NI=1,NS
 5001 WRITE(6,4) (BA(NI,NJ),NJ=1,NS)
      WRITE(6,7004)
7004  FORMAT('0','THE CONTROL DISTRIBUTION MATRIX IS...',//)
      DO 7005 NI=1,NS
 7005 WRITE(6,4)    (G(NI,NJ),NJ=1,NC)
      WRITE(6,3041)
 3041 FORMAT('0','THE STATE COST MATRIX IS....',//)
      DO 7007 NI=1,NS
 7007 WRITE(6,4)   (SC(NI,NJ),NJ=1,NS)
      WRITE(6,3042)
 3042 FORMAT('0','THE CONTROL COST MATRIX IS....',//)
      DO 7009 NI=1,NC
 7009 WRITE(6,4)    (B(NI,NJ),NJ=1,NC)
  10  IF (NG.EQ.0) GO TO 15
      DO 72 I=1,NS
  72  READ(5,7433)(GA(I,J),J=1,NG)
      DO 73 I=1,NG
  73  READ(5,7433)(Q(I,J),J=1,NG)
      IF (NZ.EQ.0) GO TO 11
      DO 74 I=1,NZ
  74  READ(5,7433)(R(I,J),J=1,NZ)
      DO 65 I=1,NZ
  65  READ(5,7433)(H(I,J),J=1,NS)
11      WRITE(6,6667) NS,NG,NZ,T
6667  FORMAT('1',' THE ORDER OF THE SYSTEM =', I2, ',   NUMBER OF PROCES
     1S  DIST.=', I2,', NUM. OF MEASUR.=',I2,',  SAMPL. TIME = ',F10.5)
      IF (NC.GT.0) GO TO 12
      WRITE(6,3)
      DO 8001 NI=1,NS
8001  WRITE(6,4) (BA(NI,NJ),NJ=1,NS)
  12          WRITE(6,8004)
8004  FORMAT('0','THE STATE  NOISE   DISTRIBUTION MATRIX IS....',//)
           DO 8005 NI=1,NS
8005  WRITE(6,4)    (GA(NI,NJ),NJ=1,NG)
      WRITE(6,8041)
```

```
132.       8041 FORMAT('0','THE STATE NOISE POW. S. DEN.  MATRIX IS....',//)
133.                 DO 8007 NI=1,NG
134.       8007 WRITE(6,4)   (Q(NI,NJ),NJ=1,NG)
135.            IF (NZ.EQ.0) GO TO 15
136.            WRITE(6,8042)
137.       8042 FORMAT('0','THE MEASUR. NOISE POW. S. DEN. MATRIX IS....',//)
138.                 DO 8009 NI=1,NZ
139.       8009 WRITE(6,4)    (R(NI,NJ),NJ=1,NZ)
140.            IF (T.EQ.0) GO TO 68
143.       68     WRITE(6,3043)
144.       3043 FORMAT('0','THE MEASURMENT MATRIX H IS...',//)
145.            DO 7010 NI=1,NZ
146.       7010 WRITE(6,4)   (H(NI,NJ),NJ=1,NS)
147.         15 CONTINUE
148.            IF (NC.GT.0) GO TO 6
149.            NC=NC1+1
150.          6 IF (NG.GT.0) GO TO 7
151.            NG=NG1+1
152.         7   NCNC=NC*NC
152.1      C
152.2      C
152.3      C  HERE (OPTION) EXEC CALCULATES EIGEN VALUES
152.4      C
152.5      C
153.            IF (IOL.EQ.0) GO TO 501
154.            DO 53 I = 1,NS
155.            DO 53 J = 1,NS
156.         53 GN(I,J) = BA(I,J)
157.       C*****************************************
158.            CALL BALANC (NS,NS,GN,LOW,IHIGH,D)
159.            CALL ELMHES (NS,NS,LOW,IHIGH,GN,INT)
160.            CALL HQR2 (NS,NS,LOW,IHIGH,GN,WR,WI,ACL,ICNT,&46)
161.            CALL ELMBAK (NS,LOW,IHIGH,NS,GN,INT,ACL)
162.            CALL BALBAK (NS,NS,LOW,IHIGH,NS,D,ACL)
163.       C*****************************************
164.            WRITE(6,2030)
```

```
      2030 FORMAT('1','OPEN LOOP EIGENVALUES AND EIGENVECTORS.....')
           IF(IOL.NE.0)
          1      CALL CNORM(CWR,CWI,ACL,NS,EVEC,VECRN,VECIN,VECR,VECI,VRV,
          1VIV,VRRV,VRIV)
            GO TO 501
        46 WRITE(6,1060)
      1060 FORMAT('0FAILURE IN HQR2')
       501   IF(T.EQ.0) GO TO 16
C
C
C     IF THE SYSTEM IS CONTIN.  PROGRAM 'CONV' WILL
C      DISCRETIZE IT.
C
C
     5         CALL CONV(BAK,GA,Q,NG,GAT,GAT1,GL,T,NC1,NG1,
          1BA,G,SC,B,AQ,W1Q,W3Q,CQ,QDC,FTQ,Q21,NS,NC,NNC,
          2NCNC,AT,LT,MT,BI,FBGC,Y,FT,W21,FTIA,FTIY,CT,QD,ICC)
           GO TO 18
        16  CALL MAKE(BAK,BA,NS,NS)
     18       NC=NC1
           NG=NG1
           CALL ZOT1(GI,NS,NS)
           DO 17 I=1,NS
        17  GI(I,I)=1.
           IF (NC.EQ.0) GO TO 30
C
C
C      PROGRAM 'INNER' CALCULATES THE OPTIMAL REGULATOR,
C      PROGRAM 'INNEK'CALCULATES THE S.S. KALMAN FILTER
C
C
        20  CALL INNER(NS,NC,N2,A,RM,WR,WI,X,PRO,CWR,CWI,ICNT,D,INT,
          1ACL,SC,GN,B,BI,GL,FBGC,GM,BA,C,CI,CT,MT,LT,AT,W21,TCB,W11,VF,
          3Y,FT,FTIA,FTIY,FTIYA,Q21,AQ21,ICC,
          2VEC,RVEC,VECRN,VECIN,VECR,VECI,VPV,VIV,VRRV,VRIV,MHS,IA)
           IF (NZ.EQ.0) GO TO 40
```

```
      30  IF(IT.EQ.0) GO TO 33
          CALL INNEK(NS,NS,N2,A,RM,WR,WI,X,PRO,CWR,CWI,ICNT,D,INT,
     1QD,GN,P,RI,GI,FBGCK,GM,BAK,C,CI,CT,MT,LT,AT,W21,TCB,W11,VF,
     3IQ,IQN,Y,FT,FTIA,FTIY,FTIYA,H,NZ,
     2VEC,RVEC,VECRN,VECIN,VECR,VECI,VRV,VIV,VRRV,VRIV,MHS,IA)
          GO TO 39
      33  CALL INNEK(NS,NG,N2,A,RM,WR,WI,X,PRO,CWR,CWI,ICNT,D,INT,
     1Q,GN,R,RI,GA,FBGCK,GM,BAK,C,CI,CT,MT,LT,AT,W21,TCB,W11,VF,
     3IG,IQN,Y,FT,FTIA,FTIY,FTIYA,H,NZ,
     2VEC,RVEC,VECRN,VECIN,VECR,VECI,VRV,VIV,VRRV,VRIV,MHS,IA)
      39  IF(INC.EQ.1) GO TO 51
      40  IF (IQ.EQ.1) GO TC 51
          GO TO 60
      51  CONTINUE
C
C
C  FROM HERE TO 60  CALCUL. OF CLCSED LOOP RESPCNSE
C   WILL BE DCNE (COV.  MATRIX  OF THE STATES.)
C
C
C     (X-P) = ACL*(X-P)*ACLT +(M-P)
C  M IS BAK    ,  P IS FT  , H  SHOULD BE  ZERO (LATER)
C   ACL  IS CLOSED LOOP TRANS. MATRIX,   T IS TRANS.
C   FOR RESP.OF CLOSED LCOP ONLY (NO PRCCESS NOISE) ....M-P=Q CR CD
C
C
          IQN=1
          IF (NZ.GT.0) GO TC 105
          NZ=NZ+1
  105        CALL ZOT1(H,NZ,AS)
          DO 106 I=1,NZ
   106    R(I,I)=1.
          IF (INC.EQ.0) GO TC 200
          ONE=1.
          CALL ADD(ONE,BAK,-CNE,FT,QD,NS,NS)
          CALL MAKE(SC,FT,NS,NS)
```

```
      CALL INNEK(NS,NS,N2,A,RM,WR,WI,X,PRO,CWR,CWI,ICNT,D,INT,
     1QD,GN,R,RI,GI,FBGCK,GM,ACL,C,CI,CT,MT,LT,AT,W21,TCB,W11,VF,
     3IQ,IQN,Y,FT,FTIA,FTIY,FTIYA,H,NZ,
     2VEC,RVEC,VECRN,VECIN,VECR,VECI,VRV,VIV,VRRV,VRIV,MHS,IA)
  300 CALL ADD(ONE,ACL,ONE,SC,ACL,NS,NS)
      GO TO 400
  200 IF(T.EQ.0) GO TO 500
      CALL INNEK(NS,NS,N2,A,RM,WR,WI,X,PRO,CWR,CWI,ICNT,D,INT,
     1QD,GN,R,RI,GI,FBGCK,GM,ACL,C,CI,CT,MT,LT,AT,W21,TCB,W11,VF,
     3IQ,IQN,Y,FT,FTIA,FTIY,FTIYA,H,NZ,
     2VEC,RVEC,VECRN,VECIN,VECR,VECI,VRV,VIV,VRRV,VRIV,MHS,IA)
      GO TO 400
  500 CALL INNEK(NS,NG,N2,A,RM,WR,WI,X,PRO,CWR,CWI,ICNT,D,INT,
     1Q,GN,R,RI,GA,FBGCK,GM,ACL,C,CI,CT,MT,LT,AT,W21,TCB,W11,VF,
     3IQ,IQN,Y,FT,FTIA,FTIY,FTIYA,H,NZ,
     2VEC,RVEC,VECRN,VECIN,VECR,VECI,VRV,VIV,VRRV,VRIV,MHS,IA)
  400 WRITE(6,401)
  401 FORMAT('0',' THE CLOSED LOOP STATE COV. MATRIX IS ',//)
      CALL SPIT1(ACL,NS,NS)
C
C      E(U,UT)=C(X-P)CT
C             =C(X)CT    ...FOR EXACT MEAS.
C
C       (    C=FBGC   )
C
      DO 81 I=1,NS
      DO 81 J=1,NC
   81 G(I,J)=FBGC(J,I)
      IF (INQ.EQ.0) GO TO 82
      CALL ADD(ONE,ACL,-ONE,SC,ACL,NS,NS)
   82 CALL MULT(FBGC,ACL,Q21,NC,NS,NS)
      CALL MULT(Q21,G,B,NC,NS,NC)
      WRITE(6,83)
   83 FORMAT('0',' THE CONTROL COV. MATRIX IS    ',//)
      CALL SPIT1(B,NC,NC)
   50 RETURN
```

```
      END
      SUBROUTINE CONV(BAK,GA,C,NG,GAT,GAT1,GL,T,NC1,NG1,
     1BA,G,SC,B,AQ,W1Q,W3Q,CQ,QDQ,FTQ,Q21,NS,NC,NNC,
     2NCNC,AT,LT,MT,BI,FBGC,Y,FT,W21,FTIA,FTIY,CT,QD,ICC)
      IMPLICIT REAL*8(A-H,O-Z)
      DIMENSION FT(NS,NS),W21(NS,NS),FTIA(NS,NS),FTIY(NS,NS),
     1AQ(NNC,NNC),W1Q(NNC,NNC),W3Q(NNC,NNC),CQ(NNC,NNC),
     1FTQ(NNC,NNC),Q21(NC,NS),GA(NS,NG),CD(NS,NS),
     1CT(NS,NS),BAK(NS,NS),GL(NS,NC),GAT(NG,NS),
     1GAT1(NG,NS),Q(NG,NG),BA(NS,NS),G(NS,NC),SC(NS,NS),
     1AT(NCNC),LT(NCNC),MT(NCNC),
     1B(NC,NC),QDQ(NNC,NNC),BI(NC,NC),FBGC(NC,NS),Y(NS,NS)
      NC=NC1
      NG=NG1
      CALL MAKE(BAK,BA,NS,NS)
      IF(ICC.EQ.0) GO TO 110
C
C
CPREPARE NEW MATRICES
C
C
      CALL ZOT1(AQ,NNC,NNC)
      DO 21 I=1,NS
      DO 21 J=1,NS
   21 AQ(I,J)=BA(I,J)
      DO 22 I=1,NS
      DO 22 J=1,NC
   22 AQ(I,J+NS)=G(I,J)
      CALL ZOT1(QDQ,NNC,NNC)
      DO 23 I=1,NS
      DO 23 J=1,NS
   23 QDQ(I,J)=SC(I,J)
      DO 24 I=1,NC
      DO 24 J=1,NC
   24 QDQ(NS+I,NS+J)=B(I,J)
      CALL FATQ(T,AQ,W1Q,W3Q,CQ,NNC,QDQ,FTQ)
```

```
296.            DO 25 I=1,NS
297.            DO 25 J=1,NS
298.         25 BA(I,J)=W1Q(I,J)
299.            DO 26 I=1,NS
300.            DO 26 J=1,NC
301.         26 G(I,J)=QDQ(I,NS+J)
302.       C CALCULATE BI= INV. OF QDQ(NS+I,NS+J)
303.       C
304.            DO 27 J=1,NC
305.            DO 27 K=1,NC
306.            I=(J-1)*NC+K
307.         27 AT(I)=QDQ(NS+K,NS+J)
308.            CALL MINV(NCNC,AT,NC,DE,LT,MT)
309.            DO 31 J=1,NC
310.            DO 31 K=1,NC
311.            I=(J-1)*NC+K
312.         31 BI(K,J)=AT(I)
313.            DO 28 I=1,NC
314.            DO 28 J=1,NS
315.         28 Q21(I,J)=QDQ(NS+I,J)
316.            CALL MULT(BI,Q21,FBGC,NC,NC,NS)
317.            CALL MULT(G,FBGC,Y,NS,NC,NS)
318.            DO 29 I=1,NS
319.            DO 29 J=1,NC
320.         29 GL(I,J)=W1Q(I,NS+J)
321.            CALL MULT(GL,FBGC,FT,NS,NC,NS)
322.            DO 30 I=1,NS
323.            DO 30 J=1,NS
324.         30 SC(I,J)=QDQ(I,J)
325.            ONE=1.
326.            CALL ADD(ONE,SC,-ONE,Y,SC,NS,NS)
327.            CALL ADD(ONE,BA,-ONE,FT,BA,NS,NS)
328.            IF (NG.EQ.0) GO TO 140
329.        110 IF (NG.EQ.0) GO TO 120
330.            DO 60 I=1,NS
331.            DO 60 J=1,NG
```

```
      GAT(J,I)=GA(I,J)
   60 CONTINUE
      CALL MULT(Q,GAT,GAT1,NG,NG,NS)
      CALL MULT(GA,GAT1,QD,NS,NG,NS)
      GO TO 130
  120 CALL ZOT1(QD,NS,NS)
  130 CALL EAT(ICC,T,BAK,Y,W21,FTIA,FTIY,CT,NS,QD,FT)
      IF (NG.EQ.0) GO TO 131
      WRITE(6,720)
  720 FORMAT('0',' THE DISCRETE  PROCESS NOISE COVARIANCE MATRIX :  '//)
      CALL SPIT1(QD,NS,NS)
  131     CALL MAKE(BAK,Y,NS,NS)
       IF (NC.EQ.0) GO TO 140
      IF (ICC.EQ.1) GO TO 140
      CALL MAKE(BA,Y,NS,NS)
      CALL MULT(W21,G,GL,NS,NS,NC)
      WRITE (6,81)
   81 FORMAT ('0',' THE DISCRETE CONTROL  DISTR. MATRIX IS... ',//)
      CALL SPIT1(GL,NS,NC)
  140 RETURN
      END
      SUBROUTINE  INNEK(NS,NC,N2,A,RM,WR,WI,X,PRO,CWR,CWI,ICNT,D,INT,
     1SC,GN,B,BI,G,FBGC,GM,BA,C,CI,CT,MT,LT,AT,W21,TCB,W11,VF,
     3IQ,IQN,Y,FT,FTIA,FTIY,FTIYA,H,NZ,
     2VEC,RVEC,VECRN,VECIN,VECR,VECI,VRV,VIV,VRRV,VRIV,MHS,IA)
      IMPLICIT REAL*8(A-H,O-Z)
      DIMENSION A(N2,N2),RM(N2,N2),WR(N2),WI(N2),X(N2,N2),PRO(N2,N2),
     1CWR(NS),CWI(NS),ICNT(N2),D(N2),INT(N2),BA(NS,NS),
     2GN(NS,NS), RVEC(NS,NS),VECRN(NS,NS),VECIN(NS,NS),VECR(NS,
     7NS),
     8VECI(NS,NS),VRV(NS),VIV(NS),VRRV(NS),VRIV(NS),W11(NS,NS),C(NS),
     9LT(MHS),MT(MHS),B(NZ,NZ),GM(NS,NS),
     3W21(NS,NS),TCB(N2,NS),AT(MHS),CI(NS),CT(NS,NS),BI(NZ,NZ),
     5Y(NS,NS),FT(NS,NS),FTIA(NS,NS),FTIY(NS,NS),FTIYA(NS,NS),H(NZ,NS),
     4G(NS,NC),FBGC(NS,NZ),VEC(NS,NS),VF(N2,N2),SC(NC,NC)
      REAL*4 FMT(20)
```

```
C
C***OUTPUT OPTIONS
C---IOL=1 IF THE OPEN LOOP EIGENSYSTEM IS DESIRED--TOTHERWISE IOL=0
      IOL  =  0
C*** ORDER OF THE SYSTEM DYNAMICS
C     (NOTE:THE DIMENSIONS OF THE SYSTEM DYNAMICS,CONTROL,
C           MEASUREMENT,AND COST MATRICES MUST BE SPECIFIED
C           IN THE DIMENSION STATEMENTS ABOVE)
      M = 2*NS
      MH = NS
      N  = M
C***ORDER OF THE CONTROL SYSTEM
C----NC = NUMBER OF SEPARATE CONTROLS
      NCC = NC
C***ORDER OF THE MEASUREMENT SYSTEM
C     (NOTE:IF ONLY THE CONTROL PROBLEM IS TO BE SOLVED THEN NO=0)
      NO = 0
      NG=1
C*****************************************
      CALL ZOT1(BI,NZ,NZ)
      DO 23 I = 1,NZ
   23 BI(I,I) = 1/B(I,I)
C***CALCULATION OF KALMAN GAINS:FORMATION OF THE HAMILTONIAN
C
C    **                        **          ***F IS BA NSXNS OPEN LOOP STATE
C    **                        **          ***G IS NSXNC STATE DISTR. MTRX.
C    * FTI          FTI*A      *          ***B IS R NZXNZ MEASUR. NOISE MTR
C    *                         *          ***SC IS Q NCXNC STATE NOISE MTR
C    *                         *          ***H IS NZXNS MEASUR.,T IS TRANS.
C    *                         *          ***I IS INV,A=HT*RI*H   Y=C*Q*CT
C    *  Y*FTI    F+Y*FTI*A     *          ***THE EQ. ARE: X(N+1)=F*X(N)+G*K
C    **                        **          Z(N)=H*X(N)+L,Q=E(K*KT),(AVERAGE)
C                                          R=E(L*LT)
C*****************************************************************
  500 CONTINUE
      DO 24 I = 1,NC
```

```
      DO 24 J = 1,MH
      PRO(I,J) = 0.DO
      DO 24 K = 1,NC
   24 PRO(I,J) = PRO(I,J) + SC(I,K)*G(J,K)
      DO 25 I = 1,MH
      DO 25 J = 1,MH
      Y(I,J)=0.DO
      DO 25 K = 1,NC
   25 Y(I,J)=Y(I,J)+G(I,K)*PRO(K,J)
C     CALCUL. A , A=HT*BI*H (BI=BI) SORRY TEMP REP A BY FTIY
      DO 26 I=1,NZ
      DO 26 J=1,MH
      PRO(I,J)=0.DO
      DO 26 K=1,NZ
   26 PRO(I,J)=PRO(I,J)+BI(I,K)*H(K,J)
      DO 27 I=1,MH
      DO 27 J=1,MH
      FTIY(I,J)=0.DO
      DO 27 K=1,NZ
   27 FTIY(I,J)=FTIY(I,J)+H(K,I)*PRO(K,J)
C     CALCULATE FT
      DO 3001 I=1,MH
       DO 3001 J=1,MH
 3001 FT(I,J)=0.DO
      DO 3002 I=1,MH
      DO 3002 J=1,MH
 3002 FT(I,J)=BA(J,I)
C     CALCULATE FTINV
      DO 327 J=1,NS
      DO 327 K=1,NS
      I=(J-1)*NS+K
  327 AT(I)=FT(K,J)
      CALL MINV(MHS,AT,MH,DE,LT,NT)
      DO 328 J=1,NS
      DO 328 K=1,NS
      I=(J-1)*NS+K
```

```
      328  FT(K,J)=AT(I)
C     MINV REPLACE FT BY FTINV, SO FROM HERE ON : FT=FTINV
C     CALCULATE FTINV*A=FTIIA,A=HT*RI*H
      DO 3003 I=1,MH
      DO 3003 J=1,MH
 3003 FTIA(I,J)=0.DO
      CALL GMPRD(MHS,MHS,MHS,FT,FTIY,FTIA,MH,MH,MH)
C     CALCULATE Y*FTINV=FTIY
      CALL GMPRD(MHS,MHS,MHS,Y,FT,FTIY,MH,MH,MH)
C     CALCULATE  Y*FTIA=FTIYA
      CALL  GMPRD(MHS,MHS,MHS,Y,FTIA,FTIYA,MH,MH,MH)
C     DETERMINE THE SUBBLOCK RM22
      DO 3004 I=1,MH
      DO 3004 J=1,MH
 3004 RM(I+MH,J+MH)=BA(I,J)+FTIYA(I,J)
C     CALCULAE SUBBLOCK RM21
      DO 3005 I=1,MH
      DO 3005 J=1,MH
 3005 RM(I+MH,J)=FTIY(I,J)
C     CALCULATE SUBBLOCK RM12
      DO 3006 I=1,MH
      DO 3006 J=1,MH
 3006 RM(I,J+MH)=FTIA(I,J)
C     CALCULATE SUBBLOCK RM11
      DO 3007 I=1,MH
      DO 3007 J=1,MH
 3007 RM(I,J)=+FT(I,J)
      DO 3008 J=1,M
      DO 3008 I=1,M
 3008 A(I,J)=RM(I,J)
C*************************************
      CALL BALANC (M,N,A,LOW,IHIGH,D)
      CALL ELMHES (M,N,LOW,IHIGH,A,INT)
      CALL HQR2 (M,N,LOW,IHIGH,A,WR,WI,X,ICNT,&46)
      CALL ELMBAK (M,LOW,IHIGH,N,A,INT,X)
      CALL BALBAK (M,N,LOW,IHIGH,N,D,X)
```

```
C*****************************************
             CALL  GAIN(M,NS,NC,RM,WR,WI,X,GN,W11,TCB,
     1W21,AT,LT,C,CI,CT,MHS,MT)
      CALL MAKE(BA,GN,NS,NS)
      IF (IQN.EQ.1) GO TO 389
      WRITE(6,1401)
 1401 FORMAT('0','THE MATRIX M (THE COV. OF EST.ERROR  BEFORE MEASUR.)
     1 IS  ',//)
      CALL RAPRNT(MH,MH,MH,8,GN,4,'(8(1X,1PD13.6))')
C CALCULATION OF P , P=FINV(M-Y)FTINV  ,  FINV=FTINVT
      DO 650 I=1,MH
      DO 650 J=1,MH
 650  GN(I,J)=GN(I,J)-Y(I,J)
      DO 651 I=1,MH
      DO 651 J=1,MH
      PRO(I,J)=0.DO
      DO 651 K=1,MH
 651  PRO(I,J)=PRO(I,J)+GN(I,K)*FT(K,J)
      DO 652 I=1,MH
      DO 652 J=1,MH
      GN(I,J)=0.DO
      DO 652 K=1,MH
 652  GN(I,J)=GN(I,J)+FT(K,I)*PRO(K,J)
      WRITE(6,1402)
      CALL MAKE(FT,GN,NS,NS)
 1402 FORMAT(' ',' THE MATRIX P (THE COV. OF EST. ERROR AFTER MEASUR.)
     1 IS  ',//)
      CALL RAPRNT(MH,MH,MH,8,GN,4,'(8(1X,1PD13.6))')
C
C  CALCULATION OF FILTER GAIN
C
C     CALCUL. FILTER GAIN  K=GN*HT*RI
 4    FORMAT(8(2X,1PD13.6))
      DO 800 I = 1,MH
      DO 800 J = 1,NZ
      PRO(I,J) = 0.DO
```

```
      DO 800 K = 1,NZ
  800 PRO(I,J) = PRO(I,J) +H(K,I)*BI(K,J)
C     FBGC=KALMAN=K=GN*PRO
      DO 801 I = 1,NS
      DO 801 J = 1,NZ
      FBGC(I,J) = 0.DO
      DO 801 K = 1,NS
  801 FBGC(I,J) = FBGC(I,J) +GN(I,K)*PRO(K,J)
      WRITE(6,977)
  977 FORMAT(' ','THE FILTER  GAINS K=P*HT*RINV ARE:',//)
      DO 968 I = 1,NS
  968 WRITE(6,4)   (FBGC(I,J),J = 1,NZ)
      WRITE(6,5998)
            CALL RGAIN(M,NS,NC,RM,WR,WI,X,GN,W11,TCB,
     1W21,AT,LT,C,CI,CT,MHS,MT)
 5998 FORMAT('1',' ESTIMATOR  EIGENVALUES AND EIGENVECTORS...')
            CALL CNORM( C,CI,CT ,NS,RVEC,VECRN,VECIN,VECR,VECI,VRV,
     1VIV,VRRV,VRIV)
 1400 CONTINUE
      GO TO 389
   46 WRITE(6,1060)
 1060 FORMAT('0FAILURE IN HQR2')
  389 RETURN
      END
      SUBROUTINE INNER(NS,NC,N2,A,RM,WR,WI,X,PRO,CWR,CWI,ICNT,D,INT,
     1ACL,SC,GN,B,BI,G,FBGC,GM,BA,C,CI,CT,MT,LT,AT,W21,TCB,W11,VF,
     3Y,FT,FTIA,FTIY,FTIYA,Q21,AQ21,ICC,
     2VEC,RVEC,VECRN,VECIN,VECR,VECI,VRV,VIV,VRRV,VRIV,MHS,IA)
      IMPLICIT REAL*8(A-H,O-Z)
      DIMENSION A(N2,N2),RM(N2,N2),WR(N2),WI(N2),X(N2,N2),PRO(N2,N2),
     1CWR(NS),CWI(NS),ICNT(N2),D(N2),INT(N2),BA(NS,NS),ACL(NS,NS),
     2GN(NS,NS),RVEC(NS,NS),VECRN(NS,NS),VECIN(NS,NS),VECR(NS,
     7NS),Q21(NC,NS),AQ21(NC,NS),
     8VECI(NS,NS),VRV(NS),VIV(NS),VRRV(NS),VRIV(NS),W11(NS,NS),C(NS),
     9LT(MHS),MT(MHS),B(NC,NC),GM(NS,NS),
     3W21(NS,NS),TCB(N2,NS),AT(MHS),CI(NS),CT(NS,NS),BI(NC,NC),
```

```
      5Y(NS,NS),FT(NS,NS),FTIA(NS,NS),FTIY(NS,NS),FTIYA(NS,NS),
      4G(NS,NC),FBGC(NC,NS),VEC(NS,NS),VF(N2,N2),SC(NS,NS)
       REAL*4 FMT(20)
C
C***OUTPUT OPTIONS
C---IOL=1 IF THE OPEN LOOP EIGENSYSTEM IS DESIRED--OTHERWISE IOL=0
       IOL   =  0
C*** ORDER OF THE SYSTEM DYNAMICS
C      (NOTE:THE DIMENSIONS OF THE SYSTEM DYNAMICS,CONTROL,
C            MEASUREMENT,AND COST MATRICES MUST BE SPECIFIED
C            IN THE DIMENSION STATEMENTS ABOVE)
       M = 2*NS
       MH = NS
       N  = M
C***ORDER OF THE CONTROL SYSTEM
C----NC = NUMBER OF SEPARATE CONTROLS
       NCC = NC
       NO = 0
       NG=1
C*****************************************
C***INITALIZATION OF MATRICES
       IF (ICC.EQ.1) GO TO 500
       DO 7 I= 1,NC
       DO 7 J = 1,NC
```

```
      7 BI(I,J) = 0.DO
        DO 23 I = 1,NC
     23 BI(I,I) = 1/B(I,I)
C***CALCULATION OF CONTROL GAINS:FORMATION OF CONTROL HAMILTONIAN
C
C    **                          **          ***F AND FT ARE THE OPEN LOOP
C    *                            *             DYNAMICS MATRIX AND TRANSPOSE
C    * F+Y*FTI*A        -Y*FTI    *          ***B IS NCXNC CONTROL WEIGHTING
C    *                            *             MATRIX
C    *                            *          ***A IS THE NSXNS STATE WEIGHTING
C    *                            *             MATRIX
C     *  -FTI*A           FTI     *          ***FTI =FTINVERSE,  Y=GM*BI*GM
```

```
C    **                          **          ***GM IS THE NSXNC CONTROL
C                                              DISTRIBUTION MATRIX
C*****************************************************************
  500 CONTINUE
      DO 24 I = 1,NC
      DO 24 J = 1,MH
      PRO(I,J) = 0.DO
      DO 24 K = 1,NC
   24 PRO(I,J) = PRO(I,J) + BI(I,K)*G(J,K)
      DO 25 I = 1,MH
      DO 25 J = 1,MH
      Y(I,J)=0.DO
      DO 25 K = 1,NC
   25 Y(I,J)=Y(I,J)+G(I,K)*PRC(K,J)
C     CALCULATE FT
      DO 3001 I=1,MH
       DO 3001 J=1,MH
 3001 FT(I,J)=0.DO
      DO 3002 I=1,MH
      DO 3002 J=1,MH
 3002 FT(I,J)=BA(J,I)
C     CALCULATE FTINV
      DO 327 J=1,NS
      DO 327 K=1,NS
      I=(J-1)*NS+K
  327 AT(I)=FT(K,J)
      CALL MINV(MHS,AT,MH,DE,LT,MT)
      DO 328 J=1,NS
      DO 328 K=1,NS
      I=(J-1)*NS+K
  328 FT(K,J)=AT(I)
C     MINV REPLACE FT BY FTINV, SC FROM HERE ON : FT=FTINV
C     CALCULATR FTINV*A=FTIIA,A=SC
      DO 3003 I=1,MH
      DO 3003 J=1,MH
 3003 FTIA(I,J)=0.DO
```

```
      CALL GMPRD(MHS,MHS,MHS,FT,SC,FTIA,MH,MH,MH)
C     CALCULATE Y*FTINV=FTIY
      CALL GMPRD(MHS,MHS,MHS,Y,FT,FTIY,MH,MH,MH)
C     CALCULATE  Y*FTIA=FTIYA
      CALL  GMPRD(MHS,MHS,MHS,Y,FTIA,FTIYA,MH,MH,MH)
C     DETERMINE THE SUBBLOCK RM11
      DO 3004 I=1,MH
      DO 3004 J=1,MH
 3004 RM(I,J)=-BA(I,J)-FTIYA(I,J)
C     CALCULAE SUBBLOCK RM12
      DO 3005 I=1,MH
      DO 3005 J=1,MH
 3005 RM(I,J+MH)=FTIY(I,J)
C     CALCULATE SUBBLOCK RM21
      DO 3006 I=1,MH
      DO 3006 J=1,MH
 3006 RM(I+MH,J)=FTIA(I,J)
C     CALCULATE SUBBLOCK RM22
      DO 3007 I=1,MH
      DO 3007 J=1,MH
 3007 RM(I+MH,J+MH)=-FT(I,J)
      DO 3008 J=1,M
      DO 3008 I=1,M
 3008 A(I,J)=-RM(I,J)
C*****************************************
      CALL BALANC (M,N,A,LOW,IHIGH,D)
      CALL ELMHES (M,N,LOW,IHIGH,A,INT)
      CALL HQR2 (M,N,LOW,IHIGH,A,WR,WI,X,ICNT,&46)
      CALL ELMBAK (M,LOW,IHIGH,N,A,INT,X)
      CALL BALBAK (M,N,LOW,IHIGH,N,D,X)
C*****************************************
            CALL RGAIN(M,NS,NC,RM,WR,WI,X,GN,W11,TCB,
     1W21,AT,LT,C,CI,CT,MHS,MT)
      WRITE(6,1401)
 1401 FORMAT('0','THE RICATTI GAIN MATRIX',//)
      CALL RAPRNT(MH,MH,MH,5,GN,4,'(5(1X,1PD13.6))')
```

```
C  CALCULATION OF FEEDBACK GAIN
C
C     CALC. FEEDBACK GAIN  U=-BINV*GT*FTINV(GN-A), A=SC
 4    FORMAT(8(2X,1PD13.6))
C---CALCULATE GT
      DO 810 I=1,MH
      DO 810 J=1,MH
  810 PRO(I,J)=GN(I,J)-SC(I,J)
       DO 811 I = 1,MH
       DO 811 J = 1,MH
      GN(I,J) =0.DO
      DO  811 K = 1,MH
  811 GN(I,J) = GN(I,J) +  FT(I,K)*PRO(K,J)
      DO 800 I = 1,NC
      DO 800 J = 1,MH
      PRO(I,J) = 0.DO
      DO 800 K = 1,MH
  800 PRO(I,J) = PRO(I,J) +G(K,I)*GN(K,J)
      DO 801 I = 1,NC
      DO 801 J = 1,NS
      FBGC(I,J) = 0.DO
      DO 801 K = 1,NC
  801 FBGC(I,J) = FBGC(I,J) +BI(I,K)*PRO(K,J)
C***THE OPTIMUM FEEDBACK CONTROL GAINS
      DO 802 I = 1,NC
      DO 802 J = 1,NS
  802 FBGC(I,J) = -FBGC(I,J)
      IF (ICC.EQ.1) GO TO 145
      WRITE(6,977)
  977 FORMAT(' ','THE CONTROL GAINS ARE:',//)
      DO 968 I = 1,NC
  968 WRITE(6,4)   (FBGC(I,J),J = 1,NS)
C***THE CLOSED LOOP DYNAMICS MATRIX
  145 CONTINUE
      DO 150 I = 1,NS
      DO 150 J = 1,NS
```

```
      PRO(I,J) = 0.D0
      DO 150 K = 1,NC
  150 PRO(I,J) = PRO(I,J)+G(I,K)*FBGC(K,J)
      DO 160 I = 1,NS
      DO 160 J = 1,NS
  160 ACL(I,J)=BA(I,J)+PRO(I,J)
      IF (ICC.EQ.0) GO TO 803
C     C=CPRIME-BI*Q21
      CALL MULT(BI,Q21,AQ21,NC,NC,NS)
      ONE=1.
      CALL ADD(ONE,FBGC,-ONE,AQ21,FBGC,NC,NS)
      WRITE(6,987)
  987 FORMAT(' ','THE CONTROL GAINS ARE:',//)
      DO 988 I = 1,NC
  988 WRITE(6,4)   (FBGC(I,J),J = 1,NS)
  803    WRITE(6,170)
  170 FORMAT('0','THE CLOSED LOOP DYNAMICS MATRIX IS..',//)
      DO 180 I = 1,NS
  180 WRITE(6,4) (ACL(I,J),J = 1,NS)
      WRITE(6,5998)
 5998 FORMAT('1','CLOSED LOOP EIGENVALUES AND EIGENVECTORS...')
           CALL CNORM( C,CI,CT ,NS,RVEC,VECRN,VECIN,VECR,VECI,VRV,
     1VIV,VRRV,VRIV)
 1400 CONTINUE
      GO TO 389
   46 WRITE(6,1060)
 1060 FORMAT('0FAILURE IN HQR2')
  389    RETURN
      END
      SUBROUTINE EATQ (T,A,W1,W3,C,N,QD,FT)
C
C     THIS SUBROUTINE COMPUTES THE TRANSITION MATRIX AND IT'S INTEGRAL.
C     THE SERIES IS TRUNCATED WHEN THE LARGEST ELEMENT OF THE LAST TERM
C     THE SERIES IS LESS THAN 1.E-03 TIMES THE SMALLEST ELEMENT OF THE S
C     SERIES.  WRITTEN BY R. MAINE  8/17/71
C
```

```
C
C     COMPUTES PHI(T/8)=EXP(A*T/8) AND ITS INTEGRAL
C     USES FOLLOWING RELATIONS 3 TIMES TO OBTAIN PHI(T) AND ITS INTEGRAL
C        PHI(2T)=PHI(T)**2
C        INTEGRAL(PHI(2T))=INTEGRAL(PHI(T))*(I+PHI(T))
C
C    INTEGRAL(PHI(2T)*2T)=INTEGRAL(PHI(T)*T)*(I+PHI(T)+
C                         +INTEGRAL(PHI(T))*PHI(T)*T
      IMPLICIT REAL*8(A-H,O-Z)
      DIMENSION A(N,N),W1(N,N),W3(N,N),C(N,N),
     1QD(N,N),FT(N,N)
      DO 5 I=1,N
      DO 5 J=1,N
    5 FT(I,J)=A(J,I)
      Z=T/8.
      CALL MULT(QD,A,C,N,N,N)
      CALL MULT(FT,C,W1,N,N,N)
      CALL MULT(FT,QD,W3,N,N,N)
      Z2=Z*Z/2.
      CALL ADD(Z,QD,Z2,C,QD,N,N)
      ONE=1.
      CALL ADD(ONE,QD,Z2,W3,QD,N,N)
      Z3=Z2*Z*2./3.
      CALL ADD(ONE,QD,Z3,W1,QD,N,N)
       NX=N
      NT=24
      CALL ZOT1(W1,N,N)
      DO 1 I=1,N
    1 W1(I,I)=1.0
      CALL MAKE (W3,W1,N,N)
      G=1.0
      W3MAX=1.E+50
      T=T/8.
      DO 7 I=1,NT
      BB=I
      G=G*T/BB
```

```
      W1MIN=1.E+50
      DO 30 J=1,NX
      DO 30 K=1,NX
      IF(W1(J,K).NE.0. .AND. DABS(W1(J,K)) .LT.W1MIN)W1MIN=DABS(W1(J,K))
   30 CONTINUE
      W3MAX1=W3MAX*T/BB
      CALL MULT (A,W3,C,N,N,N)
      CALL MAKE (W3,C,N,N)
      W3MAX=0.
      DO 40 J=1,NX
      DO 40 K=1,NX
      IF (DABS(W3(J,K)) .GT. W3MAX) W3MAX=DABS(W3(J,K))
   40 CONTINUE
      W3MAX=W3MAX*G
      CALL ADD (ONE,W1,C,W3,W1,N,N)
      IF( W3MAX .LT. W1MIN*1.E-03)GO TO 70
    7 CONTINUE
      WRITE (6,1000) W1MIN,W3MAX,W3MAX1
 1000 FORMAT('0ERROR IN EAT',5X,'W1MIN =',E15.6,5X,'W3MAX  =',E15.6/' ',
     117X,'W3MAX1 =',E15.6)
   70 CONTINUE
      DO 90 K=1,3
      DO 71 L=1,N
      DO 71 J=1,N
   71 FT(L,J)=W1(J,L)
      CALL MULT(QD,W1,W3,N,N,N)
      CALL MULT(FT,W3,C,N,N,N)
      CALL ADD(ONE,QD,ONE,C,QD,N,N)
      CALL MAKE (W3,W1,N,N)
      CALL MULT (W1,W3,C,N,N,N)
      CALL MAKE (W1,C,N,N)
      T=T*2.
   90 CONTINUE
      WRITE (6,51) I
   51 FORMAT('0','THE EXTENDED TRANSITION MATRIX',I5,' TERMS'/)
      CALL SPIT1 (W1,NX,NX)
```

```
      RETURN
      END
      SUBROUTINE EAT (ICC,T,A,W1,W2,W3,W4,C,N,QD,FT)
C
C     THIS SUBROUTINE COMPUTES THE TRANSITION MATRIX AND IT'S INTEGRAL.
C     THE SERIES IS TRUNCATED WHEN THE LARGEST ELEMENT OF THE LAST TERM
C     THE SERIES IS LESS THAN 1.E-03 TIMES THE SMALLEST ELEMENT OF THE S
C     SERIES.
C
C
C     COMPUTES PHI(T/8)=EXP(A*T/8) AND ITS INTEGRAL
C     USES FOLLOWING RELATIONS 3 TIMES TO OBTAIN PHI(T) AND ITS INTEGRAL
C
C        PHI(2T)=PHI(T)**2
C        INTEGRAL(PHI(2T))=INTEGRAL(PHI(T))*(I+PHI(T)).
C
C    INTEGRAL(PHI(2T)*2T)=INTEGRAL(PHI(T)*T)*(I+PHI(T)+
C                         +INTEGRAL(PHI(T))*PHI(T)*T
      IMPLICIT REAL*8(A-H,O-Z)
      DIMENSION A(N,N),W1(N,N),W2(N,N),W3(N,N),W4(N,N),C(N,N),
     1QD(N,N),FT(N,N)
      DO 5 I=1,N
      DO 5 J=1,N
    5 W1(I,J)=A(J,I)
      Z=T/8.
      CALL MULT(QD,W1,W2,N,N,N)
      CALL MULT(A,W2,W1,N,N,N)
      CALL MULT(A,QD,W3,N,N,N)
      Z2=Z*Z/2.
      CALL ADD(Z,QD,Z2,W2,QD,N,N)
      ONE=1.
      CALL ADD(ONE,QD,Z2,W3,QD,N,N)
      Z3=Z2*Z*2./3.
      CALL ADD(ONE,QD,Z3,W1,QD,N,N)
       NX=N
      NT=24
      CALL ZCT1(W1,N,N)
```

```
      CALL MAKE (W2,W1,N,N)
      DO 1 I=1,N
    1 W1(I,I)=1.0
      CALL MAKE (W3,W1,N,N)
      G=1.0
      W3MAX=1.E+50
      T=T/8.
      DO 7 I=1,NT
      BB=I
      G=G*T/BB
      W1MIN=1.E+50
      W2MIN=1.E+50
      DO 30 J=1,NX
      DO 30 K=1,NX
      IF(W1(J,K).NE.0. .AND. CABS(W1(J,K)) .LT.W1MIN)W1MIN=DABS(W1(J,K))
      IF(W2(J,K).NE.0. .AND. CABS(W2(J,K)) .LT.W2MIN)W2MIN=DABS(W2(J,K))
   30 CONTINUE
      W3MAX1=W3MAX*T/BB
      CALL ADD (ONE,W2,G,W3,W2,N,N)
      CALL MULT (A,W3,C,N,N,N)
      CALL MAKE (W3,C,N,N)
      W3MAX=0.
      DO 40 J=1,NX
      DO 40 K=1,NX
      IF (DABS(W3(J,K)) .GT. W3MAX) W3MAX=DABS(W3(J,K))
   40 CONTINUE
      W3MAX=W3MAX*G
      CALL ADD (ONE,W1,G,W3,W1,N,N)
      IF(W3MAX1 .LT. W2MIN*1.E-03 .AND. W3MAX .LT. W1MIN*1.E-03)GO TO 70
    7 CONTINUE
      WRITE (3,1000) W1MIN,W3MAX,W2MIN,W3MAX1
 1000 FORMAT('0ERROR IN EAT',5X,'W1MIN =',E15.6,5X,'W3MAX  =',E15.6/' ',
     117X,'W2MIN =',E15.6,5X,'W3MAX1 =',E15.6)
   70 CONTINUE
      DO 90 K=1,3
      DO 71 L=1,N
```

```
      DO 71 J=1,N
   71 FT(L,J)=W1(J,L)
      CALL MULT(QD,FT,W3,N,N,N)
      CALL MULT(W1,W3,FT,N,N,N)
      CALL ADD(ONE,QD,ONE,FT,CD,N,N)
      CALL MAKE (W3,W1,N,N)
      CALL MULT (W1,W3,C,N,N,N)
      CALL MAKE (W1,C,N,N)
      CALL MULT(W2,W3,A,N,N,N)
      DO 80 J=1,N
   80 W3(J,J)=W3(J,J)+1.
      CALL MULT(W2,W3,C,N,N,N)
      CALL MAKE (W2,C,N,N)
      T=T*2.
   90 CONTINUE
      IF (ICC.EQ.1) GO TO 91
      WRITE (6,51) I
   51 FORMAT('1','THE TRANSITION MATRIX',I5,' TERMS'/)
      CALL SPIT1 (W1,NX,NX)
91      RETURN
      END
      SUBROUTINE MULT(A,B,C,N,M,K)
      IMPLICIT REAL*8(A-H,O-Z)
      DIMENSION A(N,M),B(M,K),C(N,K)
      DO 10 I=1,N
      DO 10 L=1,K
      XX=0.DO
      DO 11 J=1,M
   11 XX=XX+A(I,J)*B(J,L)
   10 C(I,L)=XX
      RETURN
      END
      SUBROUTINE SPIT1(A,N,M)
      IMPLICIT REAL*8(A-H,O-Z)
      DIMENSION A(N,M)
      DO 10 NI=1,N
```

```
      10 WRITE(6,20) (A(NI,NJ),NJ=1,M)
      20 FORMAT (8(1X,1PD13.6))
         RETURN
         END
         SUBROUTINE ZOT1(A,N,M)
         IMPLICIT REAL*8(A-H,O-Z)
         DIMENSION A(N,M)
         DO 10 I=1,N
         DO 10 J=1,M
      10 A(I,J)=0.DO
         RETURN
         END
         SUBROUTINE MAKE(A,B,N,M)
         IMPLICIT REAL*8(A-H,O-Z)
         DIMENSICN A(N,M),B(N,M)
         DO 10 I=1,N
         DO 10 J=1,M
      10 A(I,J)=B(I,J)
         RETURN
         END
          SUBROUTINE ADD(X,A,Y,B,C,N,M)
         IMPLICIT REAL*8(A-H,O-Z)
         DIMENSION A(N,M),B(N,M),C(N,M)
         DO 10 I=1,N
         DO 10 J=1,M
      10 C(I,J)=X*A(I,J)+Y*B(I,J)
         RETURN
         END
         SUBROUTINE RAPRNT(NMAX,M,N,L,A,IDIM,FMT)
         REAL*8 A(NMAX,N)
         DIMENSION FMT(IDIM)
         NU=L
         DO 20 NL=1,N,L
         IF (NU.GT.N) NU=N
         DO 10 I=1,M
      10 WRITE(6,FMT)(A(I,J),J=NL,NU)
```

```
953.            WRITE(6,100)
954.          100 FORMAT(' ')
955.           20 NU=NU+L
956.            RETURN
957.            END
958.            SUBROUTINE CDIV (A,B,C,D,E,F)
959.            IMPLICIT REAL*8 (A-H,C-Z)
960.      C
961.      C     THIS SUBROUTINE COMPUTES THE COMPLEX DIVISION
962.      C
963.      C              E + F*I = (A + B*I)/(C + D*I)
964.      C
965.            T=C*C+D*D
966.            E=(A*C+B*D)/T
967.            F=(B*C-A*D)/T
968.      C
969.            RETURN
970.            END
971.            SUBROUTINE HQR2 (NM,N,LOW,HI,H,WR,WI,F,ICNT,*)
972.      C
973.            IMPLICIT REAL*8 (A-H,O-Z)
974.            DIMENSION H(NM,NM),WR(NM),WI(NM),F(NM,NM),ICNT(NM)
975.            INTEGER HI, HI1, EN, EL
976.            REAL*8 IM,IV,MA(50),MB(50)
977.            DATA EPSM / Z3410000000000000 /
978.            LOGICAL LAST
979.      C
980.            DO 101 I=1,N
981.            DO 9101 J=I,N
982.            F(I,J)=0.0D0
983.         9101 F(J,I)=0.0D0
984.          101 F(I,I)=1.0D0
985.      C
986.            IF (N.GT.2)MA(3)=H(3,1)
987.            IF (N.LT.4) GO TO 9102
988.            DO 102 I=4,N
```

```
      MA(I)=H(I,I-2)
  102 MB(I)=H(I,I-3)
C
 9102 LOWM1=LOW-1
      HI1=HI+1
C
C     ----- STORE KNOWN EIGENVALUES
C
      IF (LOWM1.LT.1) GO TO 9103
      DO 103 I=1,LOWM1
      WR(I)=H(I,I)
      WI(I)=0.0D0
  103 ICNT(I)=0
C
 9103 IF (HI1.GT.N) GO TO 9104
      DO 104 I=HI1,N
      WR(I)=H(I,I)
      WI(I)=0.0D0
  104 ICNT(I)=0
C
 9104 EN=HI
      T=0.0D0
C
C     ----- DETERMINE EIGENVALUE EN
C
  105 IF (EN.LT.LOW) GO TO 100
C
          ITS=0
          NA=EN-1
C
C         ----- SEARCH FOR SPLIT
C
  200     L=EN
  106     IF (L.EQ.LOW) GO TO 109
          IF (DABS(H(L,L-1)).LE.EPSM*(DABS(H(L-1,L-1))
     X    +DABS(H(L,L)))) GO TO 109
```

```
1025.                 L=L-1
1026.                 GO TO 106
1027.       C
1028.       C         ----- TEST FOR CONVERGENCE
1029.       C
1030.          109    X=H(EN,EN)
1031.                 IF (L.EQ.EN) GO TO 110
1032.                 Y=H(NA,NA)
1033.                 W=H(EN,NA)*H(NA,EN)
1034.                 IF (L.EQ.NA) GO TO 111
1035.                 IF (ITS.EQ.30)RETURN1
1036.       C
1037.       C         ----- COMPUTE SHIFT
1038.       C
1039.                 IF (ITS.NE.10.AND.ITS.NE.20) GO TO 113
1040.                 T=T+X
1041.                 DO 112 I=LOW,EN
1042.          112    H(I,I)=H(I,I)-X
1043.                 S=DABS(H(EN,NA))+DABS(H(NA,EN-2))
1044.                 Y=.75D0*S
1045.                 X=Y
1046.                 W=-0.4375D0*S*S
1047.       C
1048.       C         ----- QR ROTATION
1049.       C
1050.          113    ITS=ITS+1
1051.                 EL=NA-L
1052.                 DO 114 MM=1,EL
1053.                    M=NA-MM
1054.                    Z=H(M,M)
1055.                    R=X-Z
1056.                    S=Y-Z
1057.                    P=(R*S-W)/H(M+1,M)+H(M,M+1)
1058.                    Q=H(M+1,M+1)-Z-R-S
1059.                    R=H(M+2,M+1)
1060.                    S=DABS(P)+DABS(Q)+DABS(R)
```

```
1061.                  P=P/S
1062.                  Q=Q/S
1063.                  R=R/S
1064.                  IF (M.EQ.L) GO TO 115
1065.                  IF (DABS(H(M,M-1))*(DABS(Q)+DABS(R)).LE.EPSM*DABS(P)
1066.            X     *(DABS(H(M-1,M-1))+DABS(Z)+DABS(H(M+1,M+1))))
1067.            X     GO TO 115
1068.      114         CONTINUE
1069.      C
1070.      115   MP2=M+2
1071.            DO 116 I=MP2,EN
1072.      116   H(I,I-2)=0.0D0
1073.            MP3=M+3
1074.            IF (EN.LT.MP3) GO TO 9117
1075.            DO 117 I=MP3,EN
1076.      117   H(I,I-3)=0.0D0
1077.     9117   CONTINUE
1078.      C
1079.            DO 118 K=M,NA
1080.               LAST=K.EQ.NA
1081.               IF (K.EQ.M) GO TO 119
1082.               P=H(K,K-1)
1083.               Q=H(K+1,K-1)
1084.               R=0.0D0
1085.               IF (.NOT.LAST)R=H(K+2,K-1)
1086.               X=DABS(P)+DABS(Q)+DABS(R)
1087.               IF (X.EQ.0.0D0) GO TO 118
1088.               P=P/X
1089.               Q=Q/X
1090.               R=R/X
1091.      119      S=0.0D0
1092.               IF (P.EQ.0.0D0) GO TO 1119
1093.               IF (DLOG10(DABS(P)).GE.-38.0D0) S=P*P
1094.      1119     IF (Q.EQ.0.0D0) GO TO 2119
1095.               IF (DLOG10(DABS(Q)).GE.-38.0D0) S=S+Q*Q
1096.      2119     IF (R.EQ.0.0D0) GO TO 3119
```

```
1097.                IF (DLOG10(DABS(R)).GE.-38.0D0) S=S+R*R
1098.      3119      S=DSQRT(S)
1099.                IF (P.LT.0)S=-S
1100.                IF (K.EQ.M) GO TO 120
1101.                H(K,K-1)=-S*X
1102.                GO TO 9121
1103.       120      IF (L.NE.M)H(K,K-1)=-H(K,K-1)
1104.      9121      P=P+S
1105.                X=P/S
1106.                Y=Q/S
1107.                Z=R/S
1108.                Q=Q/P
1109.                R=R/P
1110.                DO 121 J=K,N
1111.                   P=H(K,J)+Q*H(K+1,J)
1112.                   IF (LAST) GO TO 122
1113.                   P=P+R*H(K+2,J)
1114.                   H(K+2,J)=H(K+2,J)-P*Z
1115.       122         H(K+1,J)=H(K+1,J)-P*Y
1116.       121         H(K,J)=H(K,J)-P*X
1117.                J=MINO(EN,K+3)
1118.                DO 123 I=1,J
1119.                   P=X*H(I,K)+Y*H(I,K+1)
1120.                   IF (LAST) GO TO 124
1121.                   P=P+Z*H(I,K+2)
1122.                   H(I,K+2)=H(I,K+2)-P*R
1123.       124         H(I,K+1)=H(I,K+1)-P*Q
1124.       123         H(I,K)=H(I,K)-P
1125.                DO 125 I=LOW,HI
1126.                   P=X*F(I,K)+Y*F(I,K+1)
1127.                   IF (LAST) GO TO 126
1128.                   P=P+Z*F(I,K+2)
1129.                   F(I,K+2)=F(I,K+2)-P*R
1130.       126         F(I,K+1)=F(I,K+1)-P*Q
1131.       125         F(I,K)=F(I,K)-P
1132.       118      CONTINUE
```

```
C
C          ----- END OF QR ROTATICN
C
           GO TO 200
C
C          ----- CNE REAL ROOT IS CETERMINED
C
  110      H(EN,EN)=X+T
           WR(EN)=H(EN,EN)
           WI(EN)=0.0D0
           IF (EN.NE.1)H(EN,NA)=0.0D0
           ICNT(EN)=ITS
           EN=NA
           GO TO 105
C
C          ----- TWO ROOTS ARE CETERMINED
C
  111      P=(Y-X)/2.0D0
           Q=P*P+W
           Z=DSQRT(DABS(Q))
           X=X+T
           H(EN,EN)=X
           H(NA,NA)=Y+T
           IF (NA.NE.1)H(NA,NA-1)=0.0D0
           ICNT(EN)=-ITS
           ICNT(NA)=ITS
C
           IF (Q.LE.0.0D0) GO TO 201
C
C          ----- TWO REAL ROOTS
C
           IF (P.LT.0.0D0)Z=-Z
           Z=P+Z
           WR(NA)=X+Z
           S=X-W/Z
           WR(EN)=S
```

```
1169.                 WI(NA)=0.0D0
1170.                 WI(EN)=0.0D0
1171.                 X=H(EN,NA)
1172.                 R=DSQRT(X*X+Z*Z)
1173.                 P=X/R
1174.                 Q=Z/R
1175.                 DO 203 J=NA,N
1176.                    Z=H(NA,J)
1177.                    H(NA,J)=Q*Z+P*H(EN,J)
1178.       203          H(EN,J)=Q*H(EN,J)-P*Z
1179.                 DO 204 I=1,EN
1180.                    Z=H(I,NA)
1181.                    H(I,NA)=Q*Z+P*H(I,EN)
1182.       204          H(I,EN)=Q*H(I,EN)-P*Z
1183.                 DO 205 I=LOW,HI
1184.                    Z=F(I,NA)
1185.                    F(I,NA)=Q*Z+P*F(I,EN)
1186.       205          F(I,EN)=Q*F(I,EN)-P*Z
1187.                 H(EN,NA)=0.0D0
1188.                 GO TO 202
1189.           C
1190.           C
1191.           C        ----- TWO COMPLEX ROOTS
1192.           C
1193.              201  WR(NA)=X+P
1194.                   WR(EN)=X+P
1195.                   WI(NA)=Z
1196.                   WI(EN)=-Z
1197.           C
1198.              202  EN=EN-2
1199.                   GO TO 105
1200.           C       ----- END OF EIGENVALUE ITERATION
1201.              100 RNRM=0.0D0
1202.                  K=1
1203.                  DO 210 I=1,N
1204.                  DO 209 J=K,N
```

```
      209 RNRM=RNRM+DABS(H(I,J))
      210 K=I
C
C     ----- DETERMINE THE EIGENVECTORS OF THE TRIANGULAR MATRIX STORED
C     ----- IN H AND OVERWRITE THEM ON H
C
      EN=N
  400 IF (EN.LT.2) GO TO 401
C
         P=WR(EN)
         Q=WI(EN)
         NA=EN-1
C
         IF (Q.NE.0.0D0) GO TO 212
C
C        ----- REAL EIGENVECTOR CORRESPONDING TO REAL EIGENVALUE
C
         I=NA
  206    IF (I.LT.1) GO TO 220
C
            S=H(I,EN)
            IP1=I+1
            IF (NA.LT.IP1) GO TO 9214
            DO 214 J=IP1,NA
  214       S=S+H(I,J)*H(J,EN)
 9214       Y=0.0D0
            IF (I.NE.1)Y=H(I,I-1)
  215       Z=P-H(I,I)
            IF (Z.EQ.0.0D0)Z=EPSM*RNRM
            IF (Y.NE.0.0D0) GO TO 9213
C
            H(I,EN)=S/Z
            GO TO 213
C
 9213       I=I-1
            P=H(I,EN)
```

```
                    IP2=I+2
                    IF (NA.LT.IP2) GO TO 9216
                    DO 216 J=IP2,NA
      216           R=R+H(I,J)*H(J,EN)
     9216           W=H(I,I)-P
                    X=H(I,I+1)
                    IF (DABS(W).LE.DABS(Y)) GO TO 217
C
                    RM=Y/W
                    Z=(S-RM*R)/(Z+RM*X)
                    H(I+1,EN)=Z
                    H(I,EN)=(-R-X*Z)/W
                    GO TO 213
C
      217           RM=W/Y
                    X=(RM*S-R)/(X+RM*Z)
                    H(I+1,EN)=X
                    H(I,EN)=(-S+X*Z)/Y
C
C
      213       I=I-1
                GO TO 206
C
      220       H(EN,EN)=1.0D0
                GO TO 211
C
C           ----- COMPLEX EIGENVECTOR CORRESPONDING TO COMPLEX EIGENVALUE
C
      212       I=NA
      299       IF (I.LT.1) GO TO 350
C
                   R=H(I,EN)
                   S=0.0D0
                   IP1=I+1
                   IF (IP1.GT.NA) GO TO 9301
                   DO 301 J=IP1,NA
```

```
1277.                   R=R+H(I,J)*H(J,NA)
1278.        301        S=S+H(I,J)*H(J,EN)
1279.       9301        CONTINUE
1280.                   Y=0.0D0
1281.                   IF (I.NE.1)Y=H(I,I-1)
1282.        302        Z=H(I,I)-P
1283.       C
1284.                   IF (Y.NE.0.0D0) GO TO 9303
1285.       C
1286.                   CALL CDIV(-R,-S,Z,Q,H(I,NA),H(I,EN))
1287.                   GO TO 303
1288.       C
1289.       9303        I=I-1
1290.                   RA=H(I,EN)
1291.                   SA=0.0D0
1292.                   IP2=I+2
1293.                   IF (NA.LT.IP2) GO TO 9304
1294.                   DO 304 J=IP2,NA
1295.                   RA=RA+H(I,J)*H(J,NA)
1296.        304        SA=SA+H(I,J)*H(J,EN)
1297.       9304        CONTINUE
1298.                   W=H(I,I)-P
1299.                   X=H(I,I+1)
1300.                   IF (DABS(W)+DABS(Q).LE.DABS(Y)) GO TO 305
1301.       C
1302.                    CALL CDIV(Y,0.0D0,W,Q,RM,IM)
1303.                    R=R-RM*RA+IM*SA
1304.                    S=S-RM*SA-IM*RA
1305.                    T1=RM*X-Z
1306.                    T2=IM*X-Q
1307.                    CALL CDIV(R,S,T1,T2,RV,IV)
1308.                    T1=-RA-X*RV
1309.                    T2=-SA-X*IV
1310.                    CALL CDIV(T1,T2,W,Q,H(I,NA),H(I,EN))
1311.                    GO TO 306
1312.       C
```

```
      305         RM=W/Y
                  IM=Q/Y
                  RA=RA-RM*R+IM*S
                  SA=SA-RM*S-IM*R
                  T1=RM*Z-IM*Q-X
                  T2=IM*Z+RM*Q
                  CALL CDIV(RA,SA,T1,T2,RV,IV)
                  H(I,NA)=(IV*Q-RV*Z-R)/Y
                  H(I,EN)=-(S+IV*Z+RV*Q)/Y
C
      306         H(I+1,NA)=RV
                  H(I+1,EN)=IV
C
C
      363       I=I-1
                GO TO 299
C
      350       H(EN,NA)=1.0D0
                H(EN,EN)=0.0D0
                EN=NA
C
      211   EN=EN-1
            GO TO 400
C
C     ----- END EIGENVECTORS OF TRIANGULAR MATRIX
C
C
      401   IF (WI(1).EQ.0.0D0)H(1,1)=1.0D0
            IF (LOWM1.LT.1) GO TO 9402
            DO 402 I=1,LOWM1
               IP1=I+1
               DO 402 J=IP1,N
      402      F(I,J)=H(I,J)
C
     9402   IF (HI1.GT.N) GO TO 404
            DO 403 I=HI1,N
```

```
1349.                IF (I.EQ.N) GO TO 9403
1350.                IP1=I+1
1351.                DO 403 J=IP1,N
1352.          403   F(I,J)=H(I,J)
1353.          C
1354.           9403 IF (LOW.GT.HI) GO TO 404
1355.                DO 416 J=HI1,N
1356.                DO 416 I=LOW,HI
1357.                   Z=0.0D0
1358.                   DO 405 K=LOW,HI
1359.          405      Z=Z+F(I,K)*H(K,J)
1360.          416      F(I,J)=Z
1361.          C
1362.           404 J=HI
1363.           9404 IF (J.LT.LOW) GO TO 413
1364.          C
1365.                IF (WI(J).EQ.0.0D0) GO TO 407
1366.          C
1367.                IP=J-1
1368.                DO 408 I=LOW,HI
1369.                   Y=0.0D0
1370.                   Z=0.0D0
1371.                   DO 409 K=LOW,J
1372.                   Y=Y+F(I,K)*H(K,IP)
1373.          409      Z=Z+F(I,K)*H(K,J)
1374.                   F(I,IP)=Y
1375.          408      F(I,J)=Z
1376.                J=IP
1377.                GO TO 406
1378.          C
1379.          407   DO 410 I=LOW,HI
1380.                   Z=0.0D0
1381.                   DO 411 K=LOW,J
1382.          411      Z=Z+F(I,K)*H(K,J)
1383.          410      F(I,J)=Z
1384.          C
```

```
      406 J=J-1
          GO TO 9404
C
C         ----- END EIGENVECTOR DETERMINATION
C
      413 IF (N.GT.2)H(3,1)=MA(3)
          IF (N.LT.4)RETURN
          DO 415 I=4,N
          H(I,I-2)=MA(I)
      415 H(I,I-3)=MB(I)
C
          RETURN
          END
          SUBROUTINE BALANC (NM,N,A,LOW,HI,D)
C
          IMPLICIT REAL*8 (A-H,C-Z)
          DIMENSION A(NM,NM),D(NM)
          INTEGER HI
          LOGICAL NOCONV
          DATA B,B2 / 16.0D0, 256.0D0 /
C
          L = 1
          K = N
C
C         SEARCH FOR ROWS ISOLATING AN EIGENVALUE AND PUSH THEM DOWN
C
      100 J = K
      101 IF (J.LT.1) GO TO 110
          R = 0.0D0
          DO 102 I = 1,K
      102 R = R+DABS(A(J,I))
          R = R-DABS(A(J,J))
          IF (R.NE.0.0D0) GO TO 103
          D(K) = J
          IF (J.EQ.K) GO TO 203
          DO 201 I = 1,K
```

```
1421.                F = A(I,J)
1422.                A(I,J) = A(I,K)
1423.        201     A(I,K) = F
1424.            DO 202 I = L,N
1425.                F = A(J,I)
1426.                A(J,I) = A(K,I)
1427.        202     A(K,I) = F
1428.        203 K = K-1
1429.            GO TO 100
1430.        103 J = J-1
1431.            GO TO 101
1432.      C
1433.      C     SEARCH FOR COLUMNS ISOLATING AN EIGENVALUE AND PUSH THEM LEFT
1434.      C
1435.        110 J = L
1436.        109 IF (J.GT.K) GO TO 113
1437.            C = 0.0D0
1438.            DO 112 I = L,K
1439.        112 C = C+DABS(A(I,J))
1440.            C = C-DABS(A(J,J))
1441.            IF (C.NE.0.0D0) GO TO 111
1442.            D(L) = J
1443.            IF (J.EQ.L) GO TO 213
1444.            DO 211 I = 1,K
1445.                F = A(I,J)
1446.                A(I,J) = A(I,L)
1447.        211     A(I,L) = F
1448.            DO 212 I = L,N
1449.                F = A(J,I)
1450.                A(J,I) = A(L,I)
1451.        212     A(L,I) = F
1452.        213 L = L+1
1453.            GO TO 110
1454.        111 J = J+1
1455.            GO TO 109
1456.      C
```

```
      113 LOW = L
          HI = K
          IF (L.GT.K)RETURN
          DO 300 I = L,K
      300 D(I) = 1.0D0
C
C     NOW BALANCE THE MATRIX IN ROWS L THROUGH K
C
      302 NOCONV = .FALSE.
          DO 301 I = L,K
C
              C = 0.0D0
              R = 0.0D0
              DO 303 J = L,K
              IF (J.EQ.I) GO TO 303
              C = C+DABS(A(J,I))
              R = R+DABS(A(I,J))
      303     CONTINUE
C
              F = 1.0D0
              S = C+R
C
              G = R/B
      304     IF (C.GE.G) GO TO 305
              F = F*B
              C = C*B2
              GO TO 304
C
      305     G = R*B
      306     IF (C.LT.G) GO TO 307
              F = F/B
              C = C/B2
              GO TO 306
C
      307     IF ((C+R)/F.GE.0.95D0*S) GO TO 301
C
```

```
1493.                 G = 1.0D0/F
1494.                 D(I) = D(I)*F
1495.                 NOCONV = .TRUE.
1496.                 DO 311 J = L,N
1497.           311   A(I,J) = A(I,J)*G
1498.                 DO 312 J = 1,K
1499.           312   A(J,I) = A(J,I)*F
1500.           C
1501.           301   CONTINUE
1502.           C
1503.                 IF (NOCONV) GO TO 302
1504.                 RETURN
1505.           C
1506.                 END
1507.                 SUBROUTINE BALBAK(NM,N,LOW,HI,M,D,Z)
1508.           C
1509.                 IMPLICIT REAL*8 (A-H,C-Z)
1510.                 INTEGER HI
1511.                 DIMENSION D(NM),Z(NM,NM)
1512.                 IF (LOW.GT.HI) GO TO 107
1513.                 DO 101 I=LOW,HI
1514.                    S=D(I)
1515.                    DO 102 J=1,M
1516.           102      Z(I,J)=Z(I,J)*S
1517.           101      CONTINUE
1518.           C
1519.           107   IF (LOW.LE.1) GO TO 108
1520.                 LOWM1=LOW-1
1521.                 DO 103 II=1,LOWM1
1522.                    I=LOW-II
1523.                    K=D(I)
1524.                    IF (K.EQ.I) GO TO 103
1525.                    DO 104 J=1,M
1526.                       S=Z(I,J)
1527.                       Z(I,J)=Z(K,J)
1528.           104         Z(K,J)=S
```

```
      103    CONTINUE
C
      108 IF (HI.GE.N)RETURN
          IH=HI+1
          DO 105 I=IH,N
             K=D(I)
             IF (K.EQ.I) GO TO 105
             DO 106 J=1,M
                S=Z(I,J)
                Z(I,J)=Z(K,J)
      106       Z(K,J)=S
      105    CONTINUE
C
          RETURN
          END
          SUBROUTINE ELMHES(NM,N,K,L,A,INT)
C
          IMPLICIT REAL*8 (A-H,C-Z)
          DIMENSION INT(NM),A(NM,NM)
          LM1=L-1
          KP1=K+1
          IF (LM1.LT.KP1) RETURN
C
          DO 101 M=KP1,LM1
             I=M
             X=0.0D0
             DO 102 J=M,L
                IF (DABS(A(J,M-1)).LE.DABS(X)) GO TO 102
                X=A(J,M-1)
                I=J
      102       CONTINUE
             INT(M)=I
             IF (I.EQ.M) GO TO 103
C
             MM1=M-1
             DO 104 J=MM1,N
```

```
1565.                  Y=A(I,J)
1566.                  A(I,J)=A(M,J)
1567.      104         A(M,J)=Y
1568.                  DO 105 J=1,L
1569.                  Y=A(J,I)
1570.                  A(J,I)=A(J,M)
1571.      105         A(J,M)=Y
1572.      C
1573.      103     IF (X.EQ.0) GO TO 101
1574.              MP1=M+1
1575.              DO 106 I=MP1,L
1576.                  Y=A(I,M-1)
1577.                  IF (Y.EQ.0) GO TO 106
1578.                  Y=Y/X
1579.                  A(I,M-1)=Y
1580.                  DO 107 J=M,N
1581.      107         A(I,J)=A(I,J)-Y*A(M,J)
1582.                  DO 108 J=1,L
1583.      108         A(J,M)=A(J,M)+Y*A(J,I)
1584.      106         CONTINUE
1585.      101     CONTINUE
1586.      C
1587.          RETURN
1588.          END
1589.          SUBROUTINE ELMBAK (NM,K,L,R,A,INT,Z)
1590.      C
1591.          IMPLICIT REAL*8 (A-H,O-Z)
1592.          DIMENSION A(NM,NM),INT(NM),Z(NM,NM)
1593.          INTEGER R
1594.          LMK=L-K-1
1595.          IF (LMK.LT.1)RETURN
1596.          DO 101 MM=1,LMK
1597.              M=L-MM
1598.              MP1=M+1
1599.              DO 102 I=MP1,L
1600.                  X=A(I,M-1)
```

```
1601.                IF (X.EQ.0) GO TO 102
1602.                DO 103 J=1,R
1603.          103   Z(I,J)=Z(I,J)+X*Z(M,J)
1604.          102   CONTINUE
1605.              I=INT(M)
1606.              IF (I.EQ.M) GO TO 101
1607.              DO 104 J=1,R
1608.                X=Z(I,J)
1609.                Z(I,J)=Z(M,J)
1610.          104   Z(M,J)=X
1611.          101 CONTINUE
1612.            RETURN
1613.            END
1614.            SUBROUTINE RGAIN(M,NS,NC,RM,WR,WI,VF,GN,W11,TCB,
1615.           1W21,AT,LT,C,CI,CT,MHS,MT)
1616.            IMPLICIT REAL*8 (A-H,O-Z)
1617.            DIMENSION WR(M),WI(M),VF(M,M),GN(NS,NS),RM(M,M)
1618.            DIMENSION  W11(NS,NS),TCB(M,NS),W21(NS,NS),LT(MHS),MT(MHS)
1619.            DIMENSION AT(MHS)
1620.            DIMENSION C(NS),CI(NS),CT(NS,NS)
1621.            MH = NS
1622.            K = 1
1623.            KP = 1
1624.            KN = 1
1625.           10 IF(K.GT.M) GO TO 200
1626.            WZ=WR(K)**2+WI(K)**2-1.
1627.            IF(WZ) 100,5000,50
1628.           50 IF(WI(K)) 80,75,80
1629.        C  ----------EIGENVECTOR FOR REAL EIGENVALUE,POSITIVE
1630.           75 CONTINUE
1631.            KP = KP+1
1632.            K=K+1
1633.            GO TO 10
1634.        C  ----------EIGENVECTOR FOR COMPLEX EIGENVALUE,POSITIVE REAL PART
1635.           80 CONTINUE
1636.            KP = KP+2
```

```
      K = K+2
      GO TO 10
  100 IF(WI(K)) 120,110,120
C  ----------EIGENVECTOR FOR REAL EIGENVALUE,NEGATIVE REAL PART
  110 C(KN) = WR(K)
      CI(KN) = WI(K)
      DO 95 J= 1,M
   95 TCB(J,KN) = VF(J,K)
      KN = KN+1
      K=K+1
      GO TO 10
C  ----------EIGENVECTOR FOR COMPLEX EIGENVALUE,NEGATIVE REAL PART
  120 RR = WR(K)
      RI = WI(K)
      C(KN) = RR
      C(KN+1) = RR
      CI(KN) = RI
      CI(KN+1) = - RI
      DO 121 J = 1,M
      FR = VF(J,K)
      FI = VF(J,K+1)
      TCB(J,KN) = FR+FI
  121 TCB(J,KN+1) = FR-FI
      KN = KN+2
      K = K+2
      GO TO 10
  200 CONTINUE
      DO 299 I = 1,NS
      DO 299 J = 1,NS
  299 CT(I,J) = TCB(I,J)
C  FORMATION OF W11
      DO 300 I = 1,MH
      DO 300 J = 1,MH
  300 W11(I,J) = TCB(I,J)
      KNS = NS+1
C  FORMATION OF W21
```

```
      DO 320  I=1,MH
      DO 320  J=1,MH
  320 W21(I,J)= TCB(I+MH,J)
  322 CONTINUE
      MHS=MH*MH
C   INVERT W11
      DO 327 J=1,NS
      DO 327 K=1,NS
      I=(J-1)*NS +K
  327 AT(I)=W11(K,J)
      CALL MINV(MHS, AT,MH,DETC,LT,MT)
      DO 328 J=1,NS
      DO 328 K=1,NS
      I=(J-1)*NS +K
  328 W11(K,J)=AT(I)
C
C   CALCULATE THE PGAIN MATRIX
      DO 325 IL=1,MH
      DO 325 JL=1,MH
      GN(IL,JL) = 0.D0
      DO 325 KL=1,MH
  325 GN(IL,JL)=GN(IL,JL)+W21(IL,KL)*W11(KL,JL)
      GO TO 6000
 5000 WRITE(6,1)
    1 FORMAT('1','ZERO EIGENVALUE-RICATTI EQUATION HAS NO SS')
 6000 RETURN
      END
      SUBROUTINE MINV(NM,A,N,D,L,M)
      IMPLICIT REAL*8 (A-H,O-Z)
      DIMENSION A(NM),L(NM),M(NM)
      DOUBLE PRECISION A,D,BIGA,HOLD
      D=1.0D0
      NK=-N
      DO 80 K=1,N
      NK=NK+N
      L(K)=K
```

```
1709.            M(K)=K
1710.            KK=NK+K
1711.            BIGA=A(KK)
1712.            DO 20 J=K,N
1713.            IZ=N*(J-1)
1714.            DO 20 I=K,N
1715.            IJ=IZ+I
1716.         10 IF( DABS(BIGA)- DABS(A(IJ))) 15,20,20
1717.         15 BIGA=A(IJ)
1718.            L(K)=I
1719.            M(K)=J
1720.         20 CONTINUE
1721.      C
1722.      C           INTERCHANGE ROWS
1723.      C
1724.            J=L(K)
1725.            IF(J-K) 35,35,25
1726.         25 KI=K-N
1727.            DO 30 I=1,N
1728.            KI=KI+N
1729.            HOLD=-A(KI)
1730.            JI=KI-K+J
1731.            A(KI)=A(JI)
1732.         30 A(JI) =HOLD
1733.      C
1734.      C           INTERCHANGE COLUMNS
1735.      C
1736.         35 I=M(K)
1737.            IF(I-K) 45,45,38
1738.         38 JP=N*(I-1)
1739.            DO 40 J=1,N
1740.            JK=NK+J
1741.            JI=JP+J
1742.            HOLD=-A(JK)
1743.            A(JK)=A(JI)
1744.         40 A(JI) =HOLD
```

```
1745.      C
1746.      C         DIVIDE COLUMN BY MINUS PIVOT (VALUE OF PIVOT ELEMENT IS
1747.      C         CONTAINED IN BIGA)
1748.      C
1749.           45 IF(BIGA) 48,46,48
1750.           46 D=0.0D0
1751.              RETURN
1752.           48 DO 55 I=1,N
1753.              IF(I-K) 50,55,50
1754.           50 IK=NK+I
1755.              A(IK)=A(IK)/(-BIGA)
1756.           55 CONTINUE
1757.      C
1758.      C         REDUCE MATRIX
1759.      C
1760.              DO 65 I=1,N
1761.              IK=NK+I
1762.              HOLD=A(IK)
1763.              IJ=I-N
1764.              DO 65 J=1,N
1765.              IJ=IJ+N
1766.              IF(I-K) 60,65,60
1767.           60 IF(J-K) 62,65,62
1768.           62 KJ=IJ-I+K
1769.              A(IJ)=HOLD*A(KJ)+A(IJ)
1770.           65 CONTINUE
1771.      C
1772.      C         DIVIDE ROW BY PIVOT
1773.      C
1774.              KJ=K-N
1775.              DO 75 J=1,N
1776.              KJ=KJ+N
1777.              IF(J-K) 70,75,70
1778.           70 A(KJ)=A(KJ)/BIGA
1779.           75 CONTINUE
1780.      C
```

```
C          PRODUCT OF PIVOTS
C
      D=D*BIGA
C
C          REPLACE PIVOT BY RECIPROCAL
C
      A(KK)=(1.0D0)/BIGA
   80 CONTINUE
C
C          FINAL ROW AND COLUMN INTERCHANGE
C
      K=N
  100 K=(K-1)
      IF(K) 150,150,105
  105 I=L(K)
      IF(I-K) 120,120,108
  108 JQ=N*(K-1)
      JR=N*(I-1)
      DO 110 J=1,N
      JK=JQ+J
      HOLD=A(JK)
      JI=JR+J
      A(JK)=-A(JI)
  110 A(JI) =HOLD
  120 J=M(K)
      IF(J-K) 100,100,125
  125 KI=K-N
      DO 130 I=1,N
      KI=KI+N
      HOLD=A(KI)
      JI=KI-K+J
      A(KI)=-A(JI)
  130 A(JI) =HOLD
      GO TO 100
  150 RETURN
      END
```

```
      SUBROUTINE CNORM(WZ,WY,VEC,NS,RVEC,VECRN,VECIN,VECR,VECI,VRV,
     1VIV,VRRV,VRIV)
      IMPLICIT REAL*8 (A-H,O-Z)
      DOUBLE PRECISION  WZ,WY,VEC
      DIMENSION WZ(NS),WY(NS),VEC(NS,NS)
      DIMENSION RVEC(NS,NS),VECRN(NS,NS),VECIN(NS,NS),VECR(NS,NS),
     1          VECI(NS,NS),VRV(NS),VIV(NS),VRRV(NS),VRIV(NS)
    7 FORMAT(' ')
    8 FORMAT('0REAL EIGENVALUE   (',I2,').......',14X,'REAL EIGENVECTOR
     1(',I2,').......'//1X,'(',F15.8,')+J(',F15.8,')',13X,'(',F15.8,')'
     2)
    9 FORMAT(44X,'(',F15.8,')')
   10 FORMAT('0COMPLEX EIGENVALUE(',I2,').......',14X,'COMPLEX EIGENVEC
     1TOR(',I2,').......'//1X,'(',F15.8,')+J(',F15.8,')',13X,'(',F15.8
     2,')+J(',F15.8,')')
   11 FORMAT(44X,'(',F15.8,')+J(',F15.8,')')
C
      LM=0
      LR=0
      LC=0
      DO 999 K =1,NS
      LK =K+1
      REMOD = 0.DO
      IF (DABS(WY(K)).LT.1.D-10) GO TO 998
      IF (LM.EQ.1.AND.K.EQ.NS) GO TO 1000
      IF (LM.EQ.1) GO TO 992
      LC=LC+1
      EMAX = 0.DO
      DO 997 I = 1,NS
      VECR(I,LC)=VEC(I,K)
      VECI(I,LC)=VEC(I,LK)
      CMOD=VECR(I,LC)**2+VECI(I,LC)**2
      IF (CMOD-EMAX)997,990,990
  990 EMAX = CMOD
      M=I
  997 CONTINUE
```

```
      VMR = VECR(M,LC)
      VMI = VECI(M,LC)
      EMXIN=1.D0/EMAX
      DO 980 I=1,NS
      VR = VECR(I,LC)
      VI = VECI(I,LC)
      VECRN(I,LC)=EMXIN*(VR*VMR+VI*VMI)
  980 VECIN(I,LC)=EMXIN*(-VR*VMI+VI*VMR)
      VRV(LC)=WZ(K)
      VIV(LC)=WY(K)
  992 LM=0
      IF(DABS(WY(K)+WY(LK)).LT.1.D-10) LM=1
      GO TO 999
  998 LR=LR+1
      DO 996 I=1,NS
      RVEC(I,LR)=VEC(I,K)
  996 REMOD=RVEC(I,LR)**2+REMOD
      RMOD=DSQRT(REMOD)
      DO 995 I=1,NS
  995 RVEC(I,LR)=RVEC(I,LR)/RMOD
      VRRV(LR)=WZ(K)
      VRIV(LR)=WY(K)
      IF(K.EQ.NS) GO TO 1000
  999 CONTINUE
C1000 WRITE(6,7)
 1000 CONTINUE
      IF (LC .EQ. 0) GO TO 961
      DO 960 J=1,LC
      WRITE(6,10) J,J,VRV(J),VIV(J),VECRN(1,J),VECIN(1,J)
  960 WRITE(6,11) (VECRN(K,J),VECIN(K,J),K=2,NS)
  961 IF (LR.EQ.0) GO TO 1005
      WRITE(6,7)
      DO 965 J=1,LR
      WRITE(6,8) J,J,VRRV(J),VRIV(J),RVEC(1,J)
  965 WRITE(6,9) (RVEC(K,J),K=2,NS)
 1005 RETURN
```

```
      END
      SUBROUTINE GMADD(NM,A,B,R,N,M)
      REAL*8 A,B,R
      DIMENSION A(NM),B(NM),R(NM)
      DO 10 I=1,NM
   10 R(I)=A(I)+B(I)
      RETURN
      END
      SUBROUTINE GMPRD(NM,ML,NL,A,B,R,N,M,L)
      REAL*8 A,B,R
      DIMENSION A(NM),B(ML),R(NL)
      IR=0
      IK=-M
      DO 10 K=1,L
      IK=IK+M
      DO 10 J=1,N
      IR=IR+1
      JI=J-N
      IB=IK
      R(IR)=0.
      DO 10 I=1,M
      JI=JI+N
      IB=IB+1
   10 R(IR)=R(IR)+A(JI)*B(IB)
      RETURN
      END
      SUBROUTINE  GAIN(M,NS,NC,RM,WR,WI,VF,GN,W11,TCB,
     1W21,AT,LT,C,CI,CT,MHS,MT)
      IMPLICIT REAL*8 (A-H,C-Z)
      DIMENSION WR(M),WI(M),VF(M,M),GN(NS,NS),RM(M,M)
      DIMENSION  W11(NS,NS),TCB(M,NS),W21(NS,NS),LT(MHS),MT(MHS)
      DIMENSION AT(MHS)
      DIMENSION C(NS),CI(NS),CT(NS,NS)
      MH = NS
      K = 1
      KP = 1
```

```
      KN = 1
   10 IF(K.GT.M) GO TO 200
      WZ=-WR(K)**2-WI(K)**2+1.
      IF(WZ) 100,5000,50
   50 IF(WI(K)) 80,75,80
C  ----------EIGENVECTOR FOR REAL EIGENVALUE,POSITIVE
   75 CONTINUE
      KP = KP+1
      K=K+1
      GO TO 10
C  ----------EIGENVECTOR FOR COMPLEX EIGENVALUE,POSITIVE REAL PART
   80 CONTINUE
      KP = KP+2
      K = K+2
      GO TO 10
  100 IF(WI(K)) 120,110,120
C  ----------EIGENVECTOR FOR REAL EIGENVALUE,NEGATIVE REAL PART
  110 C(KN) = WR(K)
      CI(KN) = WI(K)
      DO 95 J= 1,M
   95 TCB(J,KN) = VF(J,K)
      KN = KN+1
      K=K+1
      GO TO 10
C  ----------EIGENVECTOR FOR COMPLEX EIGENVALUE,NEGATIVE REAL PART
  120 RR = WR(K)
      RI = WI(K)
      C(KN) = RR
      C(KN+1) = RR
      CI(KN) = RI
      CI(KN+1) = - RI
      DO 121 J = 1,M
      FR = VF(J,K)
      FI = VF(J,K+1)
      TCB(J,KN) = FR+FI
  121 TCB(J,KN+1) = FR-FI
```

```
1961.            KN = KN+2
1962.            K = K+2
1963.            GO TO 10
1964.          200 CONTINUE
1965.            DO 299 I = 1,NS
1966.            DO 299 J = 1,NS
1967.          299 CT(I,J) = TCB(I,J)
1968.        C  FORMATION OF W11
1969.            DO 300 I = 1,MH
1970.            DO 300 J = 1,MH
1971.          300 W11(I,J) = TCB(I,J)
1972.            KNS = NS+1
1973.        C  FORMATION OF W21
1974.            DO 320 I=1,MH
1975.            DO 320 J=1,MH
1976.          320 W21(I,J)= TCB(I+MH,J)
1977.          322 CONTINUE
1978.            MHS=MH*MH
1979.        C  INVERT W11
1980.            DO 327 J=1,NS
1981.            DO 327 K=1,NS
1982.            I=(J-1)*NS +K
1983.           327  AT(I)=W11(K,J)
1984.            CALL MINV(MHS, AT,MH,DETC,LT,MT)
1985.            DO 328 J=1,NS
1986.            DO 328 K=1,NS
1987.            I=(J-1)*NS +K
1988.           328  W11(K,J)=AT(I)
1989.        C
1990.        C  CALCULATE THE RGAIN MATRIX
1991.            DO 325 IL=1,MH
1992.            DO 325 JL=1,MH
1993.            GN(IL,JL) = 0.DO
1994.            DO 325 KL=1,MH
1995.          325 GN(IL,JL)=GN(IL,JL)+W21(IL,KL)*W11(KL,JL)
1996.            GO TO 6000
```

```
1997.          6000 WRITE(6,1)
1998.             1 FORMAT('1','ZERO EIGENVALUE-RICATTI EQUATION HAS NO SS')
1999.          6000 RETURN
2000.               END
2001.       /*
2002.       //LKED.SYSLMOD DD DSN=S270.ERAN(DISC),
2003.       // UNIT=2314,VOL=SER=SYS14,DISP=(,KEEP),
2004.       // SPACE=(TRK,(5,5,1),RLSE)
2005.       /*
```

Appendix B

THE SIMULATION SCHEME: A SIMULATION ALGORITHM FOR A DISCRETELY CONTROLLED, LINEAR, CONTINUOUS, TIME INVARIANT SYSTEM

If one is interested in investigating the behavior between the samplings, say, n_s times during the interval, T, the basic integration step will be $T_s (T_s = T/n_s)$. The integration algorithm solves, step by step, the following equations.

$$x_{i+1} = \Phi_p(T_s)x_i + \Gamma_p(T_s)u_j. \tag{B-1}$$

The control u_j is constant during n_s iterations. Φ_p and Γ_p are calculated a priori from

$$\begin{aligned} \phi_p(T_s) &= e^{-F_p T_s} \\ \Gamma_p(T_s) &= \left[\int_o^{T_s} e^{-F_p \tau}\, d\tau\right] G_p \,. \end{aligned} \tag{B-2}$$

u_j is calculated every T (after n_s iterations of Eq. B-1) from:

$$\begin{aligned} u_j &= C\hat{x}_j + u_o(T) \\ \hat{x}_{j+1} &= (I - KH)[(\Phi(T) + \Gamma(T)*C)\hat{x}_j + u_o(T)] + Ky_{i+1} \\ y_{j+1} &= H\, x_{j+1} \,. \end{aligned} \tag{B-3}$$

Equations B-3 are the compensator equations. Φ and Γ are calculated similarly to (B-2). Equations B-3 are mechanized in the discrete compensator, the derivation of the equations having been given in Chapter VI.

All the matrices of (B-3) are calculated by our discrete synthesis program, DISC. Φ and Γ represent the assumed system, while Φ_p and Γ_p belong to the actual real plant. The distinction between these two systems is necessary in order to investigate the sensitivity (Ch. VI).

The relation between T, T_s, and n_s is described in Fig. B-1.

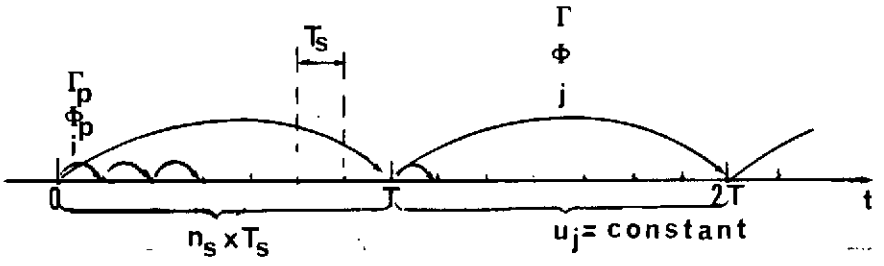

FIG. B-1 THE SIMULATION TIMING.
T = sampling time of the plant.
T_s = sampling step in the simulation.

REFERENCES

AS-1 Åstrom, K.J., "On The Choice of Sampling Rates in Optimal Linear System," IBM Research Report, R-J-243, IBM, San Jose, Calif., Apr 1963.

BA-1 Baechler, D.O., "Aerospace Computer Characteristics," IEEE Computer, Jan-Feb 1971.

BE-1 Berman, H., and R. Gran, "An Organized Approach to the Digital Autopilot Design Problem," AIAA Guidance & Control Conf., Key Biscayne, Fla., Paper No. 73-848, Aug 1973.

BER-1 Berger, C.S., "A Numerical Solution of the Matrix Equation $P = \phi P \phi' + S$," IEEE Trans. On Automatic Control, Aug 1971.

BL-1 Blakelock, J.H., Automatic Control of Aircrafts and Missiles, J. Wiley & Sons, New York, 1965.

BO-1 Borow, M.S., et al, "Navy Digital Flight Control System Development," Honeywell Document No. 21857-FR, Honeywell, Inc., Minneapolis, Minn., Dec 1972.

BR-1 Bryson, A.E., and Y.C. Ho, Applied Optimal Control, Ginn-Blaisdell, Waltham, Mass., 1969.

BR-2 Bryson, A.E., and W.E. Hall, "Optimal Control and Filter Synthesis by Eigenvector Decomposition," SUDAAR Report No. 436, Stanford University, Dept. Aeronautics & Astronautics, Stanford, Calif., Nov 1971.

BR-3 Bryson, A.E., and D.G. Luenberger, "The Synthesis of Regulator Logic Using State Variable Concepts," IEEE Proc., Vol. 58, No. 11, pp. 1803-1811, Nov 1970.

BR-4 Bryson, A.E., "Control Theory for Random Systems," SUDAAR Report No. 447, Stanford University, Dept. Aeronautics and Astronautics, Stanford, Calif., Sept 1972

BRE-1 Breza, M., and A.E. Bryson, "Minimum Variance Filter with Eigenvalue Constraints," Ph.D. Dissertation, Dept. Aeronautics and Astronautics, Stanford, University, Stanford, Cal., Fall 1974.

BU-1 Bucy, R.S., and P.D. Joseph, Filtering for Stochastic Processes with Application to Guidance, Interscienc Publishers, Divsn of Wiley and Sons, 1968.

CA-1 Cadzow, J.A. and H.R. Martens, Discrete-Time and Computer Control Systems, Prentice-Hall Inc., Englewood Cliffs, N.J., 1970.

CA-2 Cadzow, J.A., Discrete-Time Systems, Prentice-Hall, Inc., New Jersey, 1973.

CH-1 Chen, C.T., Introduction to Linear System Theory, Holt, Rinehart and Winston, Inc., N.Y., 1970.

DE-1 Deets, D.A., and K.J. Szalai, "Design and Flight Experience With a Digital Fly-By-Wire Control System Using Apollo Guidance System Hardware on an F-8 Aircraft," AIAA Guidance & Control Conf., Paper No. 72-881, Aug 1972.

ED-1 Edwards, J.W., "Flight Test Experience in Digital Control of a Remotely Piloted Vehicle," AIAA Guidance & Control Conf., Paper No. 72-883, Aug 1972.

ET-1 Etkin, B., Dynamics of Flight, J. Wiley & Sons, N.Y., 1967.

FR-1 Francis, J.G., "The QR Transformation, Parts I and II," Computer J., Vol. 4, No. 3, Nov 1961.

FRA-1 Frame, J.S., "A Simple Recursion Formula for Inverting a Matrix," Bulletin Amer. Math Soc., Vol. 55, pp. 1045, 1949.

GU-1 Gunckel, T.F., and G.F. Franklin, "A General Solution for Linear Sampled-Data Control Systems," Trans. ASME, Vol. 85D, 1963.

HA-1 Hansen, R., "Transforming Differential Domains Into Sampled Representations," IEEE Trans on Automatic Control, Feb. 1974.

HAD-1 Hadass, Z., and J.D. Powell, "A Design Method for Minimization Sensitivity to Plant Parameters Variations," AIAA Mechanics and Control of Flight Conf., Anaheim, Calif., Aug 1974.

HA-1 Hall, W.E., "Synthesis of Hover Autopilot for Rotrary-Wing VTOL Aircraft," SUDAAR Report No. 446, Stanford University, Dept. Aeronautics and Astronautics, Stanford, Calif., Jun 1972.

HE-1 Hewer, G.A., "An Iterative Technique for the Computation of the Steady State Gains for the Discrete Optimal Regulator," IEEE Trans. on Automatic Control, Aug. 1971.

HO-1 Howerton, R.D., "A New Solution of the Discrete Algebraic Riccati Equation," IEEE Trans. on Automatic Control, Feb. 1974.

HOL-1 Holley, W.E., and A.E. Bryson, Jr., "Multi-Input, Multi-Output Regulator Design for Constant Disturbances and Non-Zero Set Points," SUDAAR Rept. No. 465, Stanford University, Dept. Aeronautics and Astronautics, Stanford, Calif., Aug 1973.

JO-1 Johnson, J.M., "The Application of Digital Filters Using Observers to the Design of an ICBM Flight Control System," AIAA Guidance & Control Conf., Key Biscayne, Fla., AIAA Paper No. 73-845, Aug 1973.

JOH-1 Johnson, J.C., and C.L. Phillips, "An Algorithm for the Computation of the Integral of the State Transition Matrix," IEEE Trans. on Automatic Control, Apr 1971.

KA-1 Kalman, R.E., "A New Approach to Linear Filtering and Prediction Problems," Trans. ASME, J. Basic Eng., Mar 1960.

KI-1 Kisslinger, R.L., and G.J. Vetsch, "Synthesis of a Fly-By-Wire System for an F-4," J. Aircraft, Jul 1973.

KO-1 Kolk, R., Modern Flight Dynamics," Prentice-Hall, Inc., Englewood Cliffs, New Jersey, 1961.

KU-1 Kuo, B.C., and D.W. Peterson, "Optimal Discretization of Continuous Data Control System," Automatica, Vol. 9, 1973.

KW-1 Kwakernaak, H., and R. Sivan, Linear Optimal Control Systems, Wiley-Interscience, New York, 1972.

LE-1 Lee, J.F.L., "A Digital Flight Control System Design Approach for a Space Shuttle Booster Type Vehicle," AIAA Paper No. 74-20, Jan 1974.

LEW-1 Lewis, A.H., et al, "On the Behavior of Optimal Linear Regulators," Int. J. of Control, Vol. 13, Feb 1971.

MA-1 Mathews, M.A., "Saab Digital Flight Control," AIAA 12th Aerospace Sciences Meeting, Washington, D.C., Paper No. 74-26, Jan 1974.

McG McGough, J.G., "The Effects of Sampling Rate in Digital Flight Control Systems," Proc. of the Nat. Aerospace Electr. Conf., NAECON 1974 Record, May 1973.

ME-1 Melzer, S.M., and B.C. Kuo, "Sampling Period Sensitivity of the Optimal Sampled Data Linear Regulator," Automatica, Vol. 7, 1971.

MR-1 Mrazek, J.G., "Consideration in the Design of a Digital Flight Function for a High Performance Aircraft," NAECON 1974 Record, May 1974.

OS-1 Osder, S., et al, "Digital Autopilots: Design Considerations and Simulator Evaluations," NASA Ames Res Center, Pub. No. 70-1364-00-00, NASA Ames, Moffett Field, Calif., Oct 1971.

PA-1 Palson, T., "Parameter Uncertainties in Control System Design," Ph.D. Dissertation, Mass. Insti. of Technology, Measurement Systems Lab., Cambridge, Mass, May 1971.

PO-1 Potter, J.E., "Matrix Quadratic Solutions," SIAM J. Applied Math., Vol. 14, No. 3, May 1966.

RA-1 Ragazzini, S.P., and G.F. Franklin, Sampled Data Control Systems, McGraw-Hill, 1958.

SI-1 Simmons, J.C., and B.M. Hall, "Digital Control System Development for the Delta Launch Vehicle," AIAA Guidance & Control Conf., Key Biscayne, Fla., AIAA Paper No. 73-847, Aug 1973.

SL-1 Slater, G.L., "A Unified Approach to Digital Flight Control Algorithms," AIAA Mechanics and Control of Flight Conference, Anaheim, Calif., Aug 5-9, 1974, Paper No. 74-884.

ST-1 Stubbs, G.S., et al, "Digital Autopilots for Thrust Vector Control of the Apollo CSM/LM Vehicles," AIAA Guidance & Control Conf., Aug 1969, AIAA Paper No. 69-847.

STA-1 Stapleford, R., unpublished report, Systems Technology, Inc., Mountain View, Calif., Sept. 1974.

SU-1 Sutton, M.L., et al, "Feasibility Study for an Advanced Digital Flight Control System," LSI Tech Rept No. ADR-773, Lear Siegler, Inc., Santa Monica, Calif., Oct 1972.

SW-1 Swaim, R.L., "Aircraft Elastic Mode Control," J. Of Aircraft, Feb 1971.

VA-1 Vaughan, D.R., "A Non-Recursive Solution of the Discrete Matrix Riccati Equation," IEEE Trans. on Automatic Control, Oct 1970.

WI-1 Widnall, W.S., "Lunar Module Digital Autopilot," J. of Spacecraft and Rockets, Jan 1971.

YA-1 Yackel, R.A., B.C. Kuo, and G. Singh, "Digital Redesign of Continuous Systems by Matching of States at Multiple Sampling Periods," Automatica, Vol. 10, 1974.